Dipartimento di Scienze della Vita

## Dottorato in Scienze della Vita-Life Sciences

38° Ciclo

Coordinatrice: Prof.ssa Simona Maccherini

# Spatial analysis of plant diversity and habitats in Italian coastal dune ecosystems to identify conservation priorities

Settore scientifico disciplinare: BIOS-01/C

*Candidata*
Emilia Pafumi
Università di Siena

*Firma digitale della candidata*

Firmato digitalmente da Emilia Pafumi
Data: 23.02.2026 08:26:07 CET

*Supervisore*
Prof.ssa Simona Maccherini
Università di Siena

*Co-supervisori*
Prof. Giovanni Bacaro
Università di Trieste

Prof. Duccio Rocchini
Università di Bologna

Anno accademico di conseguimento del titolo di Dottore di ricerca
2024/25

# Table of Contents

# Abstract

Coastal sand dune ecosystems support unique plant diversity and provide essential ecosystem services, yet they are among the most threatened ecosystems worldwide due to pressures from urbanization, tourism, invasive alien species and coastal erosion. Thus, effective prioritization of conservation efforts and robust monitoring methods are urgently needed. This thesis investigates patterns of plant diversity and habitat distribution on coastal dunes by integrating different approaches, from the analysis of field-collected vegetation data to remote sensing techniques, with the goal of supporting coastal dune conservation.

In the first part of the thesis (Chapter 1), I aimed to identify conservation priority hotspots in relation to an existing network of protected areas, focusing on the coastal dunes of Tuscany. The analysis of $\alpha$-, $\beta$-, and $\gamma$-diversity based on field-collected plant community data revealed compositionally unique sites as priority sites for conservation. However, they were only partially included within protected areas.

The second part of the thesis examined the potential of remote sensing techniques for coastal dune habitat monitoring. Although these techniques provide broad spatial and temporal coverage, their application to coastal dunes is challenged by the small and fragmented nature of habitat patches relative to the spatial resolution of available imagery. To address this challenge, I first aimed to provide an effective technique for habitat monitoring from satellite data, by testing fuzzy approaches to image classification (Chapter 2). These approaches, which assign pixels probabilities of belonging to multiple habitats, provided a more realistic representation of vegetation patterns than traditional crisp approaches.

Subsequently, I explored the use of Convolutional Neural Networks (CNNs), a promising technique that leverages both spectral and spatial information contained in images but still has limited application in habitat mapping. In a pilot study (Chapter 3), I evaluated CNN performance using spectral datasets with varying spatial resolutions, including Unmanned Aerial Vehicles (UAV), airborne, Google Earth and WorldView-3 imagery. High spatial resolution proved crucial for accurate habitat mapping, while additional spectral bands were beneficial only for coarser data.

Finally, I extended the application of CNNs to multiple dune systems (Chapter 4). While UAV-based models showed promising generalization between two pilot sites, the broad-scale

application of CNNs to a large set of sites along the Italian coastline showed that the high heterogeneity both in vegetation and imagery can limit transferability.

In conclusion, the integration of approaches based on field data and remote sensing proved valuable for analyzing plant diversity patterns on coastal dunes, identifying conservation priorities and providing effective monitoring methods. Future progress toward broad-scale assessments will require further integration of multi-source, multi-scale and multi-temporal datasets with advanced methodologies, to support the conservation of these fragile ecosystems.

# Riassunto

Gli ecosistemi delle dune costiere supportano una diversità vegetale unica e forniscono servizi ecosistemici essenziali; tuttavia, sono tra gli ecosistemi più minacciati a livello globale, a causa delle pressioni derivanti da urbanizzazione, turismo, specie aliene invasive ed erosione costiera. Per tali motivi, sono urgentemente necessarie delle strategie efficaci per la prioritizzazione degli interventi di conservazione e dei metodi di monitoraggio robusti. Questa tesi indaga i pattern di diversità vegetale e la distribuzione degli habitat nelle dune costiere integrando diversi approcci, dall'analisi di dati di vegetazione raccolti in campo a tecniche di telerilevamento, con l'obiettivo di supportare la conservazione delle dune costiere.

Nella prima parte della tesi (Capitolo 1), l'obiettivo è stato quello di identificare gli hotspot di priorità per la conservazione in relazione a una rete esistente di aree protette, concentrandosi in particolare sulle dune costiere della Toscana. L'analisi di $\alpha$-, $\beta$-, e $\gamma$-diversità, basata su dati sulle comunità vegetali raccolti in campo, ha permesso di individuare i siti unici dal punto di vista composizionale come siti prioritari per la conservazione. Tali siti, tuttavia, risultavano solo parzialmente inclusi all'interno di aree protette.

La seconda parte della tesi ha valutato il potenziale delle tecniche di telerilevamento per il monitoraggio degli habitat delle dune costiere. Nonostante queste tecniche offrano un'ampia copertura spaziale e temporale, la loro applicazione alle dune costiere è ostacolata dalla natura ridotta e frammentata delle patch di habitat rispetto alla risoluzione spaziale delle immagini disponibili. Per affrontare questa sfida, ho innanzitutto puntato a sviluppare una tecnica efficace per il monitoraggio degli habitat a partire da dati satellitari, testando approcci *fuzzy* alla classificazione delle immagini (Capitolo 2). Questi approcci, che assegnano a singoli pixel una probabilità di appartenenza a più habitat, hanno fornito una rappresentazione più realistica

dei pattern di vegetazione rispetto agli approcci tradizionali.

Successivamente, ho esplorato l'uso delle reti neurali convoluzionali (Convolutional Neural Networks, CNNs), strumenti promettenti che sfruttano sia l'informazione spettrale sia l'informazione spaziale contenute nelle immagini, ma che hanno ancora applicazioni limitate nella mappatura di habitat. In uno studio pilota (Capitolo 3), ho valutato le prestazioni delle CNN utilizzando dataset spettrali con diversa risoluzione spaziale, tra cui immagini da droni (UAV), Google Earth e WorldView-3. Un'alta risoluzione spaziale si è rivelata cruciale per una mappatura degli habitat accurata, mentre l'utilizzo di bande spettrali aggiuntive ha prodotto miglioramenti solo per i dati a risoluzione minore.

Infine, l'applicazione delle CNN è stata estesa a diversi sistemi dunali (Capitolo 4). I modelli basati su dati da drone hanno mostrato capacità di generalizzazione promettenti in due siti pilota, mentre l'applicazione su larga scala delle CNN a un ampio insieme di siti lungo la costa italiana ha evidenziato come l'elevata eterogeneità sia nella vegetazione che nelle immagini possa limitare la generalizzazione dei modelli.

In conclusione, l'integrazione di approcci basati su dati di campo e di telerilevamento si è dimostrata efficace per analizzare pattern di diversità sulle dune costiere, identificare le priorità di conservazione e fornire metodi di monitoraggio robusti. I futuri avanzamenti verso valutazioni su più ampia scala richiederanno un'integrazione ancora maggiore di dati multi-sorgente, multi-scala e multi-temporali con metodologie di analisi avanzate, al fine di supportare la conservazione di questi ecosistemi fragili.

# Preface

This thesis investigates spatial patterns of plant diversity and habitats in the coastal sand dunes of Italy, adopting different approaches, from the analysis of plant community data to the application of remote sensing methods, with the ultimate aim of supporting the monitoring and conservation of these ecosystems.

In the introduction, I provide an overview of coastal dune ecosystems in terms of their ecology and main conservation issues. Then, I discuss two key research priorities for their conservation: prioritizing conservation actions based on diversity patterns, and improving the effectiveness of habitat monitoring, considering the opportunities and challenges posed by remote sensing techniques in this context.

In the first chapter of the thesis, I focus on field-collected plant community data, carrying out an analysis of $\alpha$, $\beta$, and $\gamma$-diversity at the regional scale, to identify compositionally unique sites located both inside and outside protected areas.

In the second chapter, I explore the potential of satellite remote sensing for habitat mapping on coastal dunes, testing whether non-traditional image classification approaches, in particular fuzzy approaches, could better represent the variability in coastal dune vegetation.

In the third chapter, I further address the challenge of mapping the small and fragmented coastal dune habitats by exploring the use of Convolutional Neural Networks (CNNs). As a pilot study, I compare CNN performance across remote sensing imagery with varying spatial and spectral resolutions.

In the fourth chapter, I expand on the previous work by assessing the applicability of CNNs across multiple sites, first focusing on two pilot areas and then performing a test on the national scale, assessing feasibility and limitations of this approach.

In the conclusions section, I synthesize the main findings of the thesis and outline future research perspectives.

**Author contributions per chapter**

*Chapter 1* – Emilia Pafumi: Conceptualization, Formal analysis, Writing – Original Draft; Claudia Angiolini: Conceptualization, Investigation, Supervision, Writing – Review & Editing; Simona Sarmati: Investigation, Writing – Review & Editing; Giovanni Bacaro: Conceptualization, Supervision, Writing – Review & Editing; Emanuele Fanfarillo: Conceptualization, Investigation, Writing – Review & Editing; Tiberio Fiaschi: Investigation, Writing – Review & Editing; Bruno Foggi: Investigation, Writing – Review & Editing; Matilde Gennai: Investigation, Writing – Review & Editing; Simona Maccherini: Conceptualization, Investigation, Supervision, Writing – Review & Editing.

*Chapter 2* – Emilia Pafumi: Conceptualization, Investigation, Writing – original draft; Claudia Angiolini: Conceptualization, Investigation, Funding acquisition, Supervision, Writing – review & editing; Giovanni Bacaro: Conceptualization, Investigation, Methodology, Supervision, Writing – review & editing; Emanuele Fanfarillo: Conceptualization, Investigation, Supervision, Writing – review & editing; Tiberio Fiaschi: Investigation, Writing – review & editing; Duccio Rocchini: Conceptualization, Investigation, Methodology, Supervision, Writing – review & editing; Simona Sarmati: Investigation, Writing – review & editing; Michele Torresani: Methodology, Writing – review & editing; Hannes Feilhauer: Methodology, Writing – review & editing; Simona Maccherini: Conceptualization, Funding acquisition, Investigation, Supervision, Writing – review & editing.

*Chapter 3* – Emilia Pafumi: Conceptualization, Formal analysis, Investigation, Methodology, Writing – original draft; Claudia Angiolini: Funding acquisition, Investigation, Writing – review & editing; Giovanni Bacaro: Conceptualization, Investigation, Methodology, Supervision, Writing – review & editing; Leopoldo de Simone: Data curation, Formal analysis, Investigation, Methodology, Writing – review & editing; Emanuele Fanfarillo: Investigation, Writing – review & editing; Tiberio Fiaschi: Investigation, Writing – review & editing; Duccio Rocchini: Conceptualization, Investigation, Methodology, Supervision, Writing – review & editing; Elisa Thouverai: Formal analysis, Investigation, Methodology, Writing – review & editing; Simona Maccherini: Conceptualization, Funding acquisition, Investigation, Supervision, Writing – review & editing.

# General introduction

## Coastal sand dune ecosystems

At the interface between terrestrial and marine environments lies the coastal area, a narrow strip influenced by factors from both domains. Globally, over one third of the coastline is represented by sandy beaches (Luijendijk et al., 2018). In conditions where there is a prevailing onshore wind, a continuous supply of sand, and an obstacle such as vegetation to capture the sand load, the beach can develop a dune system, which is highly dynamic and can have a variety of shapes and sizes (Maun, 2009). Coastal sand dunes occur in almost all latitudes, in a variety of climates and biomes (Martínez et al., 2008). In Europe, over 5,300 $km^2$ are covered by coastal dunes (Delbaere, 1998).

Regardless of their location, coastal dune systems are characterized by harsh environmental conditions in terms of soil moisture, salt spray, solar radiation, temperatures, organic matter content (Maun, 2009). To cope with these natural environmental stressors, dune plant species have developed unique physiological and morphological adaptations, such as salt resistance, increased shoot and rhizome/stolon development to contrast sand burial, leaf hairiness, succulence, C4 and CAM photosynthesis, fruit buoyancy (Hesp, 1991).

However, the intensity of environmental stressors changes markedly along the sea-inland gradient, creating a high heterogeneity in micro-environmental conditions (Maun, 2009). For this reason, sand dune vegetation tends to exhibit a zonation pattern, characterized by the occurrence of discrete belt-like communities from the sea to the inland (Maun, 2009; Tordoni et al., 2021). Indeed, plant communities change along the sea-inland gradient, both in terms of species richness (Sperandii et al., 2019) and of species composition (Tordoni et al., 2018; Torca et al., 2019). The main factors affecting this variation in the Mediterranean area are soil parameters, which vary substantially along the gradient (Fenu et al., 2013) and are strongly correlated to the distribution of plant species and communities (Angiolini et al., 2013, 2018).

Empirical evidence suggests that fine-scale ecological gradients are more important for plant diversity patterns in coastal dunes rather than broad geographical ones. For instance, Torca et al. (2019) found that dune vegetation along the Atlantic European coast primarily varies along the sea-inland gradient, with embryo dunes hosting azonal vegetation, while mobile and fixed

dunes are also differentiated into biogeographical groups. Similarly, Honrado et al. (2010) found that most variation in dune vegetation profiles in Portugal was due to ecological conditions, rather than biogeographical gradients. Nonetheless, European coastal dune vegetation shows differences between the Mediterranean region and the Atlantic-Baltic region (Marcenò et al., 2018).

This unique mosaic of plant communities within a limited space holds a significant conservation value (Acosta et al., 2009). In addition, dune vegetation provides habitats for multiple animal communities, such as butterflies (Rasino et al., 2024) and hymenopterans (Koyama & Ide, 2020). Moreover, coastal dunes provide essential ecosystem services (Drius et al., 2019), such as coastal defense from storms and erosion (Arkema et al., 2013), carbon sequestration (Drius et al., 2016), and cultural services (Everard et al., 2010).

## Threats to coastal dune ecosystems

The combined impacts of urbanization, tourism, invasive alien species and coastal erosion make coastal dunes some of the most threatened ecosystems in Europe (Janssen et al., 2016). In Italy, 88% of coastal sand dunes habitats are in a bad conservation status, while the remaining 12% is in inadequate conditions, and the trend is deteriorating for almost 70% of them (Prisco et al., 2020).

In the context of climate change, sea level rise is predicted to cause major shoreline retreats worldwide, and almost half of the global sandy coastline could face severe erosion > 100 m by the end of the 21$^{st}$ century under a high emission scenario (Vousdoukas et al., 2020). At the same time, over 30% of the global sandy coastline (and 65% of the Mediterranean) is "hardened", i.e. greatly affected by the presence of anthropogenic structures, which limit the natural dynamism and landward migration of beaches (Nawarat et al., 2024). The resulting effect is the so-called "coastal squeeze" between the sea level rise and the expansion of anthropized areas (Defeo et al., 2009).

Coastal dunes are also directly affected by coastal tourism, also in relation to big events (Andriolo & Gonçalves, 2023). Even if dune plants can tolerate a medium level of disturbance (Pinna et al., 2019), indeed, a strong human trampling can reduce the diversity of dune plant communities (Santoro, Jucker, Prisco, et al., 2012), while the presence of plastic litter on the beach can affect the phenology of dune plants (Menicagli et al., 2019).

Moreover, coastal dunes are highly susceptible to plant invasions (Lozano et al., 2023), especially in sites close to human activities (Tordoni et al., 2021). Invasive alien species can directly affect soil chemistry (Novoa et al., 2013) and locally alter the microclimate (Kozhoridze et al., 2025), ultimately causing functional homogenization in dune plant communities (Tordoni et al., 2019).

## Research priorities for the conservation of coastal dune biodiversity

Considering the high rate of global biodiversity decline (Pimm et al., 2014), the conservation of biodiversity meets multiple urgent challenges. These challenges can only be faced through integrated strategies, by enhancing biodiversity data availability, improving the modelling of environmental and biological processes, integrating management into conservation planning, and setting conservation priorities (Wang et al., 2024). Moreover, analyzing the ecosystem processes that support biodiversity rather than focusing on single species or habitats is increasingly recognized as beneficial in spatial planning (Van Der Biest et al., 2020).

An important step in conserving biodiversity is considering the scale at which it is analyzed. Biodiversity can be observed at multiple spatial scales, as patterns of species diversity from the local ($\alpha$-diversity) to the regional scale ($\gamma$-diversity), and as the variation in species composition among sites within a region ($\beta$-diversity) (Whittaker, 1960, 1972). Analyzing all the three components is necessary to understand where species occur, whether regional species pools are represented, and which sites should be prioritized (Belote et al., 2021), i.e. either those with high species richness or those with high complementarity (Socolar et al., 2016).

One of the main instruments for conservation are protected areas, which should be designed to ensure representativeness and persistence in order to promote the long-term survival of the full variety of biodiversity (Margules & Pressey, 2000). However, protected areas are not always effective (Watson et al., 2016), especially because climate change can cause shifts in species distribution (Bellard et al., 2012).

In Europe, conservation efforts are mainly focused on guaranteeing biological diversity through the preservation of habitats, flora and fauna. The key instrument to achieve this objective is the Council Directive 92/43/EEC, hereafter Habitats Directive, which defines habitats as “terrestrial or aquatic areas distinguished by geographic, abiotic and biotic features, whether entirely natural or semi-natural”. The priority habitats at risk of disappearance are

listed in Annex I and are required to be conserved across Member States. For this, protected areas are established, creating the Natura 2000 network. Moreover, the Habitats Directive mandates the monitoring (Art. 11) and regular reporting every six years (Art. 17) of the conservation status of habitats, in terms of four main parameters, i.e., range, area, structure and functions, and future prospects. Since most habitats are described based on vegetation, this component is the main focus of conservation status assessments (Gigante et al., 2016).

Around 35% of coastal dune area in Europe is now protected by the Natura 2000 network (European Commission, 2022), and more than 170 LIFE projects have targeted coastal dune habitats from 1992 to 2015 (Silva et al., 2017). However, some critical issues in the effectiveness of protected areas have been pointed out in particular in Italy, both in the present state (Prisco et al., 2012; Sperandii et al., 2020) and in future projections (Prisco et al., 2013).

Since most conservation measures are based on *in situ* protection and are implemented through spatial planning and site-based actions (Pressey et al., 1996), they require spatially explicit information. Therefore, biodiversity maps have high practical value for monitoring, assessing biodiversity policy targets, and guiding conservation efforts (Margules & Pressey, 2000). However, it is important to note that maps are always selective and can never fully represent the real world (Malavasi, 2020).

Mapping and monitoring methods for coastal dune habitats are not homogeneous across Europe and often rely on expert assessments, jeopardizing the effective implementation of EU policy (Delbosc et al., 2021). Traditional field-based mapping, in particular, is generally very accurate at a small scale, but it is highly time-consuming and can be prone to inconsistencies (Naas et al., 2023). Thus, it is important to develop methods that can be applied to greater spatial and temporal scales.

## Opportunities and challenges of remote sensing

Over the last four decades, remote sensing has become one of the most cost- and time-effective tools to study biodiversity and ecosystems across space and time (Vanden Borre et al., 2011; Torresani et al., 2024; Álvarez-Martínez et al., 2026). Remote sensing broadly refers to the acquisition of information about objects through the measurement of emitted or reflected electromagnetic energy. In ecological applications, passive remote sensing is most commonly used and is mainly based on the differential absorption and reflection of solar radiation by

surface materials across wavelengths (Richards, 2013).

The increasing availability of a variety of sensors and platforms, combined with the development of image analysis techniques and machine learning, has opened new possibilities in ecology and biodiversity conservation (Kerry et al., 2022). However, the application of these tools remains constrained by sensor characteristics and data resolution (Corbane et al., 2015; Kerry et al., 2022), as well as by the amount and quality of ground truth data (Álvarez-Martínez et al., 2026).

Habitat mapping on coastal dunes presents specific challenges. First, habitat patches are generally small and fragmented, requiring very high-resolution images so that pixel size is smaller than the objects to map (Nagendra, 2001; Gamon et al., 2020). Second, vegetation cover is often sparse, making the contribution of sandy soil background an important source of interference with vegetation signal (Trotta et al., 2025). Ideally, remote sensing data for dune habitat mapping should combine broad spatial and temporal cover, very high spatial resolution, multiple spectral bands and free availability. In reality, such data do not exist, making trade-offs unavoidable.

Satellite platforms offer the highest potential for broad-scale monitoring, for their regular coverage of large areas over time (Mairota et al., 2015). However, most studies involving satellite images on coastal dunes rely on free datasets such as Landsat and Sentinel missions, which have global coverage but a medium spatial resolution which only allows coarse analyses (Martín-Gallego et al., 2025). Indeed, these studies on coastal dunes mainly focused on land cover (Timm & McGarigal, 2012; Latella et al., 2021), vegetation physiognomic formations (Rapinel et al., 2014), or broad vegetation classes (Marzialetti et al., 2019, 2020). Commercial very high-resolution satellites, such as QuickBird or WorldView, provide higher spatial detail (up to a maximum of 0.30 m) and enable finer spatial analyses also on coastal dunes but are constrained by high acquisition costs (De Giglio et al., 2017; Martín-Gallego et al., 2025). A particular case is represented by Google Earth, as it provides free images from different commercial satellites. Despite their spectral content being limited to RGB bands, these data have been successfully used in combination with advanced image analysis methods in some environments (Guirado et al., 2017; Watanabe et al., 2020).

Airborne platforms and, more recently, Unmanned Aerial Vehicles (UAVs) provide very high spatial resolution data suitable for studying coastal dune ecosystems (Klemas, 2015). For

instance, airborne data have been used for habitat mapping in England (Shanmugam et al., 2003; Brownett & Mills, 2017), Denmark (Juel et al., 2013), and Italy (Bertacchi, 2017), while UAV data have been used for land cover mapping (Suo et al., 2019), monitoring of disturbances through spectral vegetation indices (Andriolo & Gonçalves, 2023), mapping of plant communities (De Giglio et al., 2019; Agrillo et al., 2023; Cruz et al., 2023; Innangi et al., 2025), mapping of typical dune species (Belcore et al., 2024) or detection of invasive alien species such as *Acacia saligna* (Marzialetti et al., 2021) and *Carpobrotus* sp. (Innangi et al., 2023). However, both airborne and UAV data are typically limited in spatial extent and temporal continuity.

Concurrently with the increase in data availability, since the 2010s there has been a rapid advancement in automated image analysis tools for the production of habitat maps (Álvarez-Martínez et al., 2026). Machine learning algorithms, which are able to learn patterns from data, are increasingly used in multiple ecological research fields, including species distribution modelling, management optimization and image-based tasks such as habitat mapping and species monitoring (Cipriano et al., 2025). In general, mapping methods can be broadly divided in two groups: pixel-based approaches, which are suitable also for medium-resolution imagery, and approaches that exploit the spatial context, which are only applicable to very high-resolution data. In the first case, each pixel is generally assigned to a corresponding class, indicating a specific land cover or vegetation type, through the classification process. However, when pixel size exceeds the size of the class to map, alternative approaches that assign each pixel to multiple classes can be more appropriate. This is the case of fuzzy classifications, which are based on the long-known fuzzy set theory (Zadeh, 1965) and have been proposed also for the study of landscape patterns (Rocchini, 2010), but are still rarely applied (Feilhauer et al., 2021).

In the second case, when pixels are much smaller than habitat patches, it becomes useful to consider also the spatial context. Convolutional Neural Networks (CNNs) are designed to exploit such information by extracting high-level features, such as patterns and edges, from low-level inputs, such as pixel intensity values (LeCun et al., 2015). CNNs have been shown to improve classification accuracy for very high-spatial resolution data, even if the spectral content is limited to RGB bands (Kattenborn et al., 2019). However, the application of CNNs to habitat mapping is still at an early stage, requiring investigation of suitable spatial scales and types of data to use (Álvarez-Martínez et al., 2026).

## General aims

Since coastal dunes are highly valuable yet threatened ecosystems, and multiple research gaps exist in support of their monitoring and conservation, this PhD project aims to investigate spatial patterns of plant diversity and habitats on coastal dunes by integrating complementary approaches, from the analysis of field-collected plant community data to remote sensing techniques, with three general aims.

The first aim is to identify conservation priority areas and assess the effectiveness of an existing network of protected areas focusing on the coastal dunes of Tuscany (Chapter 1). Specifically, I will analyze a large set of coastal dune vegetation data, with two objectives: 1) investigate the spatial patterns of regional plant community diversity in coastal dunes to identify conservation priority sites; and 2) assess the effectiveness of the existing network of protected areas through the spatial distribution of conservation priority hotspots. This study will provide an ecological baseline for the subsequent studies, shedding light on the main conservation issues of coastal dunes, which can inform the development of remote sensing approaches for identifying and monitoring hotspots of diversity and habitat distribution.

The second aim is to provide a novel and effective technique for remote habitat monitoring from satellite data, by testing a fuzzy approach to classification (Chapter 2). Specifically, I will use multispectral images from WorldView-3 satellite, to assess: 1) the efficiency of remote sensing-based mapping of habitats classified with different systems; and 2) whether employing a fuzzy approach improves the habitat mapping product compared to the traditional crisp approach. Thus, this study will investigate the potential of satellite remote sensing and explore whether its limitations, particularly in terms of spatial resolution, can be overcome through non-traditional image classification approaches, while laying the groundwork for applying more advanced techniques to higher-resolution data in subsequent studies.

The third aim is to assess the applicability of one of these advanced techniques, i.e., CNN-based habitat mapping in coastal dunes. As a pilot study, I will compare the effectiveness of CNNs across four remote sensing datasets with varying spatial resolutions and spectral bands (Chapter 3). Subsequently, to support broader-scale monitoring and simulate real-world applications, I will compare single-site and multi-site implementations of CNNs, first focusing on two study areas and then performing a test at the national scale (Chapter 4).

Overall, this PhD project provides an integrated framework in which field-based analyses of plant diversity and conservation priorities on coastal dunes progressively support the development, testing and scaling of remote sensing-based approaches, ultimately improving the spatial analysis of patterns of diversity and habitat distribution and the identification of conservation and monitoring priorities for coastal dune ecosystems.

# Chapter 1

## Spatial patterns of coastal dune plant diversity reveal conservation priority hotspots in and out a network of protected areas

Emilia Pafumi[1,2], Claudia Angiolini[1,2]*, Simona Sarmati[3], Giovanni Bacaro[4], Emanuele Fanfarillo[1,2], Tiberio Fiaschi[1], Bruno Foggi[5], Matilde Gennai[5], Simona Maccherini[1,2]

[1]Department of Life Sciences, University of Siena, 53100 Siena, Italy; [2]NBFC, National Biodiversity Future Center, 90133 Palermo, Italy; [3]Department of Sciences, University of Roma Tre, 00146 Rome, Italy; [4]Department of Life Sciences, University of Trieste, 34127 Trieste, Italy; [5]Department of Biology, University of Florence, 50121 Florence, Italy

*Corresponding author

*Published as:*

Pafumi E, Angiolini C, Sarmati S, Bacaro G, Fanfarillo E, Fiaschi T, Foggi B, Gennai M, Maccherini S (2024) Spatial patterns of coastal dune plant diversity reveal conservation priority hotspots in and out a network of protected areas. *Global Ecology and Conservation* 54, e03085 https://doi.org/10.1016/j.gecco.2024.e03085

## Abstract

Effective conservation planning requires identifying priority hotspots to allocate resources. To preserve biodiversity, it is crucial to consider $\alpha$, $\beta$ and $\gamma$-diversity and protect the irreplaceable sites with high ecological uniqueness, which can host uncommon species assemblages that would be lost if only species-rich sites were protected. Coastal dunes, hosting highly specialized plant communities, are among the most threatened ecosystems worldwide. In this study, we identified conservation priority hotspots to assess the effectiveness of the network of protected areas in coastal dunes of Tuscany (central Italy), using data on plant communities collected in 506 plots. We additively partitioned $\gamma$-diversity in its $\alpha$ and $\beta$ components, observing a significant variation at all spatial levels only for dune species. In terms of $\alpha$-diversity, we found that Northern protected sites were richer in dune species, while synanthropic and alien species were equally present inside and outside protected areas of the region. By partitioning the total $\beta$-diversity into its components (replacement and richness difference), we found a prevalence of replacement for dune species, indicating the most unique sites as the ones to favor for conservation. Unique sites were identified through Local Contributions to Beta Diversity and their conservation value was determined by their species composition and the relationship with landscape variables. Unique sites with high conservation value were only partly protected, while some protected sites were altered and required restoration. Our approach proved effective for identifying the most unique sites, indicating some issues in the existing protected network, while providing valuable information on sites to prioritize for future conservation actions.

**Keywords:** Beta-diversity, Biodiversity conservation, LCBD, Natura2000, Prioritization of conservation, Replacement

# 1. Introduction

Identifying conservation priority hotspots is fundamental for the maintenance of biodiversity in an era of unprecedented global biodiversity decline (Pimm et al., 2014). The definition of priorities allows to allocate the limited resources available in the most effective way and is a key component of systematic conservation planning (Margules & Pressey, 2000), the most influential paradigm in conservation (Kukkala & Moilanen, 2013), which overcomes the opportunistic approaches that in the past led to uneven representations of natural features (Pressey et al., 1996). However, multiple priority criteria can be adopted and can lead to different results (Dubois et al., 2020; Belote et al., 2021).

Biodiversity can be measured at different spatial scales: $\alpha$-diversity is the variation at the local scale within a community, $\gamma$-diversity is the overall variation at the regional scale, while $\beta$-diversity is the variation among communities within a region (Whittaker, 1960, 1972). Effective conservation strategies should extend beyond the conventional methodologies centered on prioritizing biodiversity hotspots characterized by elevated species richness ($\alpha$-diversity). As elucidated by Socolar et al. (2016), it becomes imperative to embrace the guiding principle of complementarity for the preservation of diversity at the regional scale: to prioritize sites with complementary species compositions, a concept related to $\beta$-diversity. Hotspots of species richness, indeed, do not necessarily host species with conservation priorities (Orme et al., 2005), while some species-poor areas host species with high conservation value (Harper et al., 2022). However, a certain degree of redundancy in the protected network is also necessary for the persistence of biodiversity over time, to maintain species even in case of local extinctions (Walker, 1995).

The analysis of $\beta$-diversity allows to understand the phenomena generating the patterns of diversity and has significant implications in conservation planning (Legendre, 2014). Following the approach developed by Legendre and De Cáceres (2013), the total $\beta$-diversity of a region can be estimated as the total variance of the community data and can be partitioned into two components, namely species replacement and richness difference, which are respectively described as the substitution of species in one site by different species in another site, and the loss of species from one site to another. From the relative importance of the two components in a region, indications for conservation planning can be derived: in landscapes where richness difference is the dominant component of $\beta$-diversity, it is preferable to prioritize

the most species-rich sites, while in the other case it is better to prioritize the most unique ones (Socolar et al., 2016). The most ecologically unique sites in a region can be identified by computing the Local Contributions to Beta Diversity (LCBD; Legendre and De Cáceres, 2013), and this approach has been recently adopted by some authors to select priority sites for conservation, mainly for animals in freshwater habitats (Hill et al., 2021; Iacarella, 2022), but to a lesser extent also for plant communities, in wetlands (Dubois et al., 2020), lakes (Heino et al., 2022), forests (Tan et al., 2019), high-latitude ecosystems (Niskanen et al., 2017), and agroecosystems (Fanfarillo et al., 2023). Understanding the drivers of site uniqueness is important to plan conservation actions. However, the same drivers can affect site uniqueness in different ways according to which ecosystem is studied and to which taxonomic group is used to compute LCBDs. For instance, local environmental variables effectively explained the variation in site ecological uniqueness using plant communities in forests (Tan et al., 2019; Yao et al., 2021) and bird communities in agroecosystems (García-Navas et al., 2022) but they were weak predictors of LCBD variation using insect communities in streams (Heino & Grönroos, 2017).

Coastal sand dunes are ecosystems of high conservation value (Acosta et al., 2009), located on the narrow band at the interface between land and sea, where a strong environmental gradient determines the presence of unique plant communities (Torca et al., 2019; Tordoni et al., 2019, 2021). Coastal dunes support highly specialized plant species, which are often rare or endangered (Acosta et al., 2009), and provide fundamental ecosystem services (Drius et al., 2019), including coastal defense (Arkema et al., 2013), carbon storage (Drius et al., 2016), and recreation (Everard et al., 2010). However, they are nowadays among the most threatened ecosystems in Europe, due to the impacts of urbanization, touristic pressure, spread of invasive alien species and coastal erosion (Janssen et al., 2016). In Italy, 88% of coastal sand dunes habitats are in a bad conservation status, while the remaining 12% is in inadequate conditions, and the trend is deteriorating for almost 70% of them (Prisco et al., 2020).

Protected areas are essential tools for the maintenance of biodiversity, but their efficacy in terms of habitat and species conservation is being questioned (Watson et al., 2016). A protected area should meet two objectives: representativeness, as it should represent the full variety of biodiversity, and persistence, as it should promote the long-term survival of biodiversity (Margules & Pressey, 2000), which will be increasingly jeopardized by the effects of climate changes (Bellard et al., 2012).

In Italy, the network of protected areas along sandy coasts has been described as fairly representative of the current distribution of dune habitats, and its efficacy has been predicted to drop in the near future due to climate change, especially for the most vulnerable habitats in mobile and fixed dunes (Prisco et al., 2013). Moreover, in a recent resurvey of the coastal dunes of central Italy, the protection status showed no positive effect on habitat loss or trends of focal and alien species over a period of 10 years (Sperandii et al., 2020). However, knowledge about the role of protected areas at the Italian level is fragmented (Prisco et al., 2012), and recent studies found substantial differences in the conservation status of dune ecosystems within the protected areas of southern Tuscany (Landi et al., 2012; Sarmati et al., 2019; Bonari et al., 2021).

To assess the role of protected areas in conservation, a common approach is to compare biodiversity inside and outside protected areas (Gray et al., 2016). In coastal dunes, however, the conservation value is not necessarily related to species richness: species richness varies along the coastal zonation and even species-poor habitats can host endangered or rare elements (Acosta et al., 2009). Moreover, plant richness and cover tend to be highest in sites with medium disturbance, as was observed in a recent study in Sardinian dunes (Pinna et al., 2019). Thus, in these ecosystems $\beta$-diversity could be a more useful criterion for the prioritization of conservation. However, the approach based on $\beta$-diversity and LCBD has never been applied on coastal dune plant communities to identify conservation priorities.

As pointed out by several authors, a complete understanding of the conservation status of coastal dunes can only be obtained if the identity of species is taken into account and different groups of species are analyzed separately, in addition to the overall pool (Del Vecchio et al., 2016; Prisco et al., 2016). In particular, dune species, which are stenoecious species often restricted to a specific zone of the dune (Angiolini et al., 2018), can serve as indicators of good conservation status (Santoro, Carboni, et al., 2012). On the other hand, synanthropic species, which are generally favored by anthropic disturbance, are generalist species that do not perform the same functions of dune species, and thus can indicate a degradation of the dune systems (Biondi et al., 2012). Similarly, alien species can directly affect dune habitats through modifications of soil properties (Novoa et al., 2013) and functional homogenization (Tordoni et al., 2019).

The aim of this study is to identify conservation priority areas and to assess the effectiveness

of the existing network of protected areas in coastal dune ecosystems of Tuscany (central Italy). Specifically, we will analyze a large set of coastal dune vegetation data collected in the region, with the following main objectives: i) analyze the spatial patterns of regional plant community diversity in coastal dunes to identify conservation priority sites; ii) assess the effectiveness of the existing network of protected areas through the distribution of conservation priority hotspots. These steps are of fundamental importance to search new areas to reach the objectives of the 2030 European Strategy of Biodiversity that plans to arrive at the 30% of protected territory in each country (*EU Biodiversity Strategy for 2030. Bringing nature back into our lives*, 2020).

## 2. Methods

### 2.1. Study area

The study was carried out along the c. 200 km of sandy coasts of Tuscany (central Italy). The climate is Mediterranean, with upper meso-mediterranean thermotype and ombrotype ranging from lower humid in the North to upper dry in the South (Pesaresi et al., 2017). In this region, coastal dunes are composed of Late Quaternary sand (Carmignani et al., 2013) and generally occupy a narrow stripe, with a maximum extent of 300 m and a height < 10 m (Bertacchi, 2017). Different plant communities usually occur along a well-defined zonation, typical of coastal dune systems, ranging from the annual vegetation of drift lines, through embryonic shifting dunes, to white dunes, stable dune grasslands, coastal dune scrubs, and coastal dune woods (Acosta et al., 2007). The anthropic pressure is uneven in the region: the Northern part is highly frequented by tourists and urbanized, while the Southern part is generally better preserved (Ciccarelli et al., 2014). The study area includes different protected areas, which are partly overlapping (Fig. 1). In particular, there are eight Special Areas for Conservation (SACs) included in the Natura 2000 network, namely “Dune Litoranee di Torre del Lago” (IT5170001, 43.828611 N, 10.253889E), “Selva Pisana” (IT5170002, 43.710278 N, 10.306389E), “Padule di Bolgheri” (IT5160004, 43.224167 N, 10.544722E), “Tombolo da Castiglion della Pescaia a Marina di Grosseto” (IT51A0012, 42.743611 N, 10.942222E), “Dune costiere del Parco dell’Uccellina” (IT51A0015, 42.636100 N, 11.073600E), “Pineta Granducale dell’Uccellina” (IT51A0014, 42.653600 N, 11.048300E), “Laguna di Orbetello” (IT51A0026, 42.459722 N, 11.222500E), and “Duna del Lago di Burano” (IT51A0032, 42.398056 N, 11.372222E). Moreover, there are two Regional Parks (the Migliarino-San Rossore-Massaciuccoli Park -

provinces of Pisa and Lucca, and the Maremma Park - province of Grosseto), which partly include some SACs within their boundaries, and three State Nature Reserves: “Tombolo di Cecina”, “Tomboli di Follonica e Scarlino”, and “Duna Feniglia”.

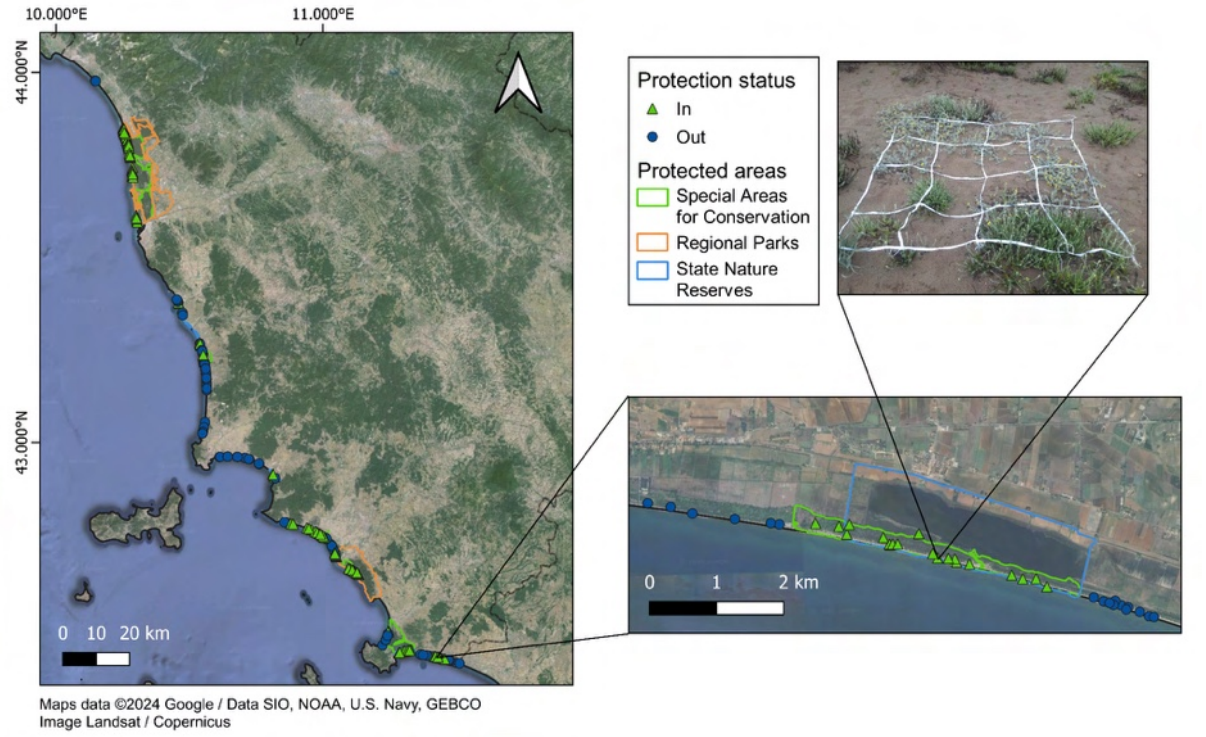


**Fig. 1.** Location of the surveyed sites in the study area. Image source: Google Earth 2024. Figure adapted from the published version of Chapter 1 (colors modified).

### 2.2. Sampling design and data collection

Vegetation data were collected between 2018 and 2021 according to a stratified random sampling design. Two bands were mapped along the Tuscan coast: band AB, including shifting dunes (EUNIS habitat N14; Chytrý et al., 2020) and stable dune grasslands (EUNIS habitat N16), that could not be separated as they occurred in a fine-grained mosaic, and band C, corresponding to coastal dune scrub (EUNIS habitat N1B). For each band, a number of squared plots of 4 $m^2$ proportional to the surface was randomly launched (c. 0.7 plots/ha). Ad hoc plots were added on the field to cover the community of sand beach drift lines (EUNIS habitat N12), for a total of 506 plots (Table 1). In each plot, vascular plant species occurrence and abundance (% cover) were recorded. Nomenclature follows the Portal to the Flora of Italy (2023). Plant species were then classified into three classes according to FloraVeg.EU database (www.floraveg.eu): dune species (i.e., occurring in the broad habitat “Coastal beach, dune or

shingle"), synanthropic, and alien species.

### 2.3. Landscape metrics

To obtain a set of landscape metrics to use for assessing what drives the ecological uniqueness of the communities, a landcover map was produced by photointerpretation of 20 cm resolution orthophotos (GEOSCOPIO, 2022). A total of 11 landcover classes were mapped based on the CORINE Land Cover nomenclature extended to the fourth level of detail: (1) artificial areas (including urban fabrics, industrial units, roads); (2) beach resort facilities and camping; (3) agricultural areas; (4) afforestation (coniferous reforestation with *Pinus* spp.); (5) mixed coniferous-broadleaved forests; (6) Mediterranean maquis (woody dune vegetation); (7) semi-natural woody vegetation (bushy vegetation with scattered trees represented by foredune woodland degradation or forest regeneration/recolonization); (8) semi-natural herbaceous vegetation (grasslands and meadows); (9) open sand (beach pioneer vegetation); (10) herbaceous dune vegetation; (11) wetlands. Note that two of these classes correspond to the bands used for vegetation sampling: herbaceous dune vegetation (EUNIS habitat N14 and N16) and woody dune vegetation (EUNIS habitat N1B). Around each plot, a rectangular buffer of 300 m x 50 m, orthogonal to the coastline, was generated as in Malavasi et al. (2018). For each rectangular buffer, a set of landscape metrics was computed: proportion of artificial landcover (%ART), proportion of bathing facilities (%ARV), proportion of agricultural land (%AGR), proportion of coastal wetlands (%WTC), minimum distance to the centroid of an artificial patch (distART), minimum distance to the centroid of a bathing facility (distARV), Shannon index of diversity of landcover types (LandShan), distance to the shoreline, dune width. Moreover, slope was measured for each plot in the field. Landscape metrics were computed using QGIS 3.28.7 software (QGIS Development Team, 2022) and the R package `landscapemetrics` (Hesselbarth et al., 2019).

### 2.4. Statistical analyses

To account for the different levels of anthropic pressure present in the region, the analysis was conducted independently for the Northern and Southern sites. The promontory of Piombino, situated midway along the coast of Tuscany, was delineated as the demarcation point.

For each plot the value of species richness was computed, and differences in mean species richness between protected and non-protected areas were assessed through a Wilcoxon test,

considering first the complete set of species and then the individual species groups (dune, synanthropic, alien) separately.

The total $\beta$-diversity of the region was computed as the total variance of the community data matrix, which can reach a maximum value of 1 (Legendre & De Cáceres, 2013), and it was partitioned into its two components, replacement and richness difference (Legendre, 2014), both for the complete set of species and for the individual groups, using *beta.div.comp* function in the R package `adespatial` (Dray et al., 2023). The significance of the three $\beta$-diversity components (Total $\beta$-diversity, Richness difference, and Replacement) was tested against a null model based on 1000 simulations. This model was obtained through non-sequential swapping and shuffling of the real data matrix to preserve fill, column and row frequencies, as well as either row or column sums. The *commsim* function (*swsh_samp* method) from the R package `vegan` (Oksanen et al., 2022) was utilized for this purpose. p-values were then calculated under the null hypothesis of no difference between the observed $\beta$-diversity component value and values obtained randomly.

To get a deeper insight into the role of single sites in regional diversity, subsequent analyses have focused on the complete set of species. The Local Contributions to Beta Diversity (LCBD) were computed for each site and were tested for significance by 999 random permutations, while Species Contributions to Beta Diversity (SCBD) were computed for each species, using *beta.div* function in the R package `adespatial` (Dray et al., 2023). The relationship of LCBD with landscape variables was investigated through a beta regression, which is a modelling tool suitable for variables that assume values between 0 and 1, using the R package `betareg` (Cribari-Neto & Zeileis, 2010). We used beta regression with logit link function to model the relation between LCBD (response variable) and landscape metrics (predictors). Correlation among predictors was checked through Spearman's correlation, and a subset of landscape variables was selected through a forward selection procedure, using function *forward.sel* in the R package `adespatial` (Dray et al., 2023). This function performs a forward selection by permutation of residuals under reduced model, which stops when either the selected variables reach a set value (number of rows – 1 by default), the R2 or the adjusted-R2 of the model exceed a threshold (0.99 by default), the p-value of a variable is higher than alpha (0.05 by default), or the difference in model R2 with the previous step is lower than a threshold (0.001 by default; Dray et al., 2023). Through this procedure, we selected three

variables as predictors for the beta regression: distance from the sea, slope, and distance from artificial surfaces. The variation explained by the beta regression model is measured through the pseudo-R2, which assumes values between 0 and 1, and is defined as the squared correlation coefficient between the linear predictor and the link-transformed response (Cribari-Neto & Zeileis, 2010).

To understand the reasons why sites with significant LCBD (i.e., unique sites) were different from the others, we analyzed the species composition of sites with significantly different LCBD values through a Nonmetric Multidimensional Scaling (NMDS), based on a Bray-Curtis similarity matrix derived from log-transformed species abundances. Landscape variables having a significant correlation with NMDS axes were overlaid to the ordination plot using the *envfit* function in the R package `vegan` (Oksanen et al., 2022). A NMDS with all sites was also performed to understand the difference in species composition between the significant LCBD sites and the others (Supplementary Materials, Fig. S2).

The total $\gamma$-diversity of the region was partitioned across the spatial scales of analysis following the additive partitioning approach (Lande, 1996; Gering et al., 2003; Crist et al., 2003), taking into account first the complete set of species and then the individual groups of species. The levels considered were: diversity within plot ($\alpha_{plot}$), between plots ($\beta_{plot}$), between localities ($\beta_{site}$), and between zones of the region ($\beta_{North/South}$). The significance of each level was tested by 999 permutations, using the function *adipart* in the R package `vegan` (Oksanen et al., 2022).

All analyses were performed using R 4.3.0 (R Core Team, 2023).

**Table 1.** Number of surveyed plots for each zone of the region inside and outside protected areas.

| Zone | Protection status | Surface (ha) | N° plots |
|---|---|---|---|
| North | In | 284.48 | 202 |
| | Out | 134.28 | 97 |
| South | In | 195.43 | 127 |
| | Out | 112.99 | 80 |

## 3. Results

A total of 192 plant species were found in the study area, of which 73 were classified as dune species, 56 as synanthropic and 14 as alien. The most frequent species were *Thinopyrum junceum* (occurring in 42.68% of the plots), *Juniperus macrocarpa* (34.78%) and *Helichrysum stoechas* (34.38%), which are all dune species. Among synanthropic species, the most frequent were *Cerastium glomeratum* (12.25%), *Anisantha sterilis* (3.75%) and *Dittrichia viscosa* (3.75%), while the most frequent alien species were *Xanthium orientale* (11.66%), *Oenothera* sp. (3.75%) and *Ambrosia psilostachya* (2.37%).

Species richness was significantly higher inside protected areas than outside only in the Northern part of the region (Fig. 2). In particular, this pattern emerged for the whole set of species and for the dune species group, while no significant differences were found for the other groups.

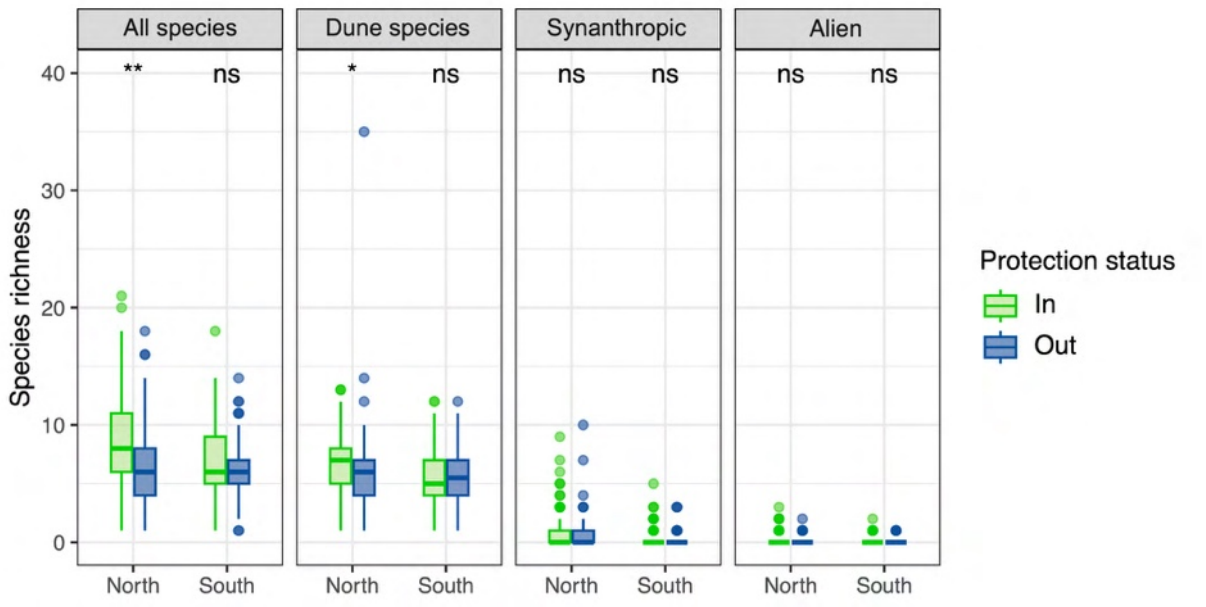


**Fig. 2.** Values of species richness inside and outside of protected areas. Mean values were compared with a Wilcoxon test (** $p < 0.01$; * $p < 0.05$; ns = non-significant). Figure adapted from the published version of Chapter 1 (colors modified).

The total $\beta$-diversity in the region was 0.47. For the whole set of species and for the dune species group, the replacement was more prevalent (> 85%). Protected and non-protected areas showed a similar pattern, while Northern and Southern sites differed only in terms of total $\beta$-

diversity of synanthropic species, which was higher in the North (Fig. 3).

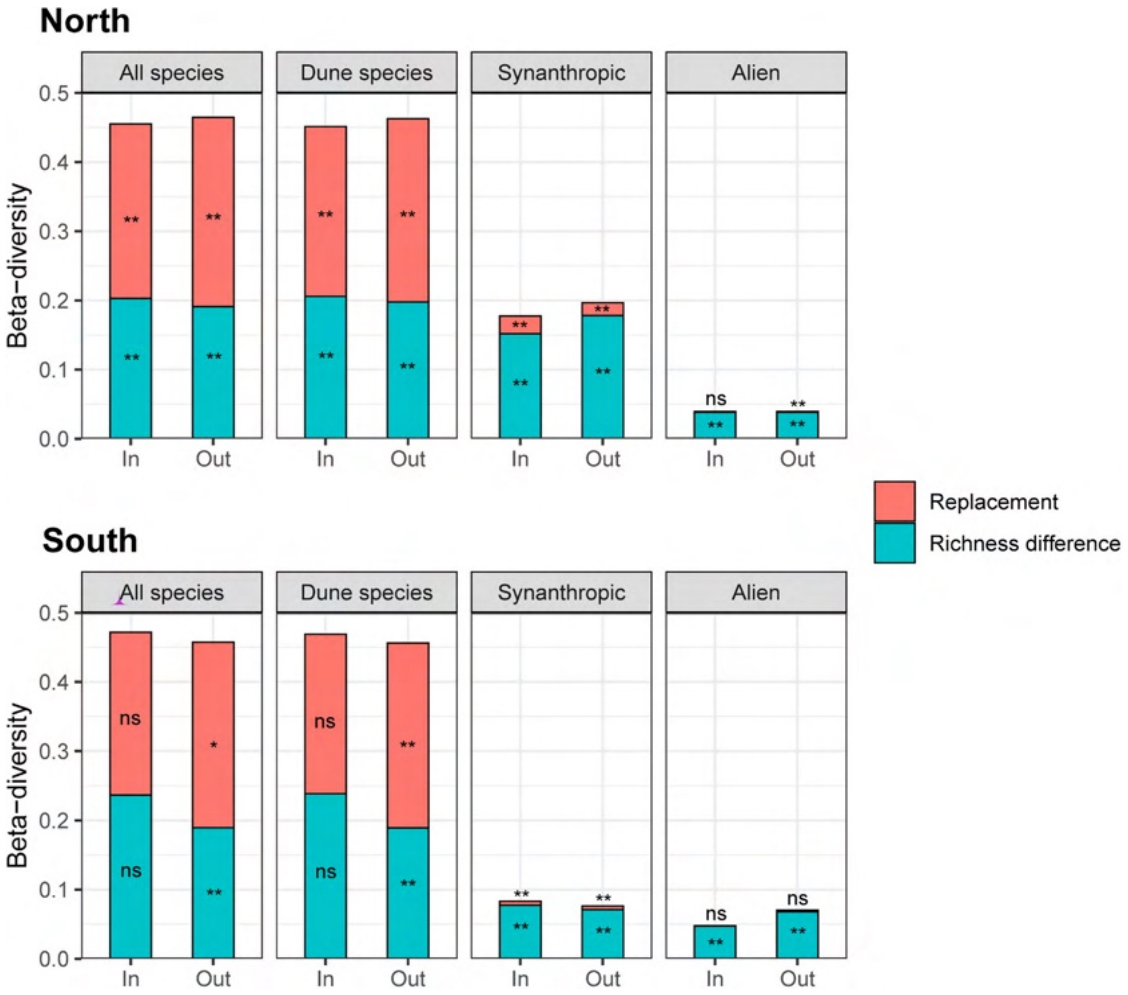


**Fig. 3.** Partitioning of total $\beta$-diversity into replacement and richness difference, computed for the North (a) and South (b) of Tuscany, considering all species together and the single groups of species separately, and distinguishing sites inside and outside protected areas. Significance of $\beta$-diversity components was tested against a null model (** $p < 0.01$; * $p < 0.05$; ns = non-significant).

Through the analysis of LCBD, a total of 42 sites with a significant contribution to the $\beta$-diversity of the region were highlighted, of which 30 were located inside protected areas (Fig. 4). Generally, highest LCBD values were given by plots with low species richness (LCBD *vs.* species richness: Spearman's cor = –0.45, $p < 0.05$) mostly located in the herbaceous band. The landscape variables computed to assess the relation with LCBD are reported in Table 2. The beta regression explained a low proportion of the variation of LCBD (pseudo-R2 = 0.15), but revealed a significant negative relation of LCBD with the distance from the shoreline and the slope, and a positive relation with the distance to artificial surfaces (Table 3).

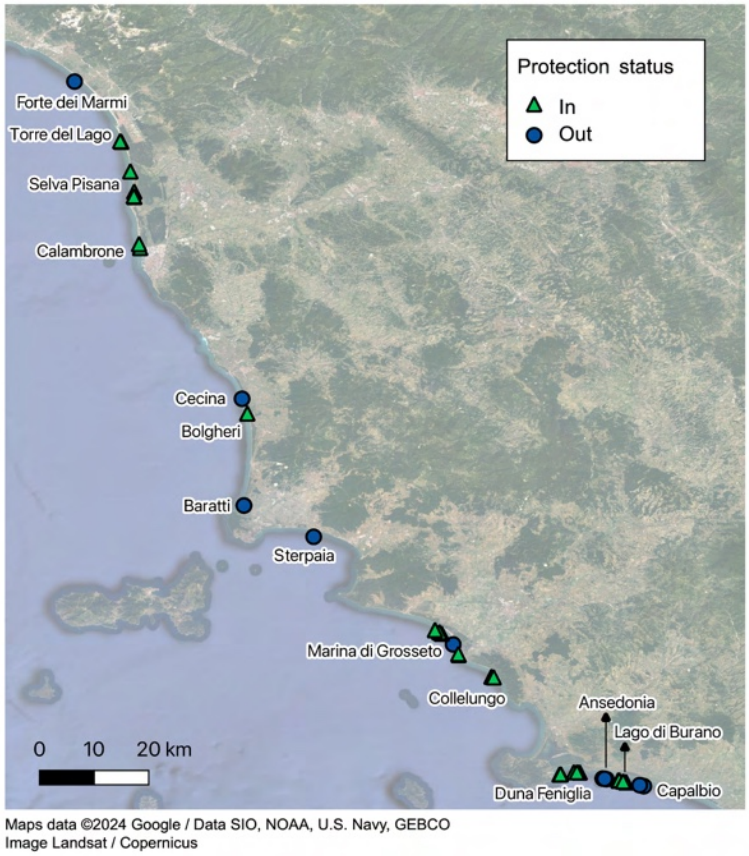


**Fig. 4.** Local Contributions to Beta Diversity for the plots in the study area, calculated considering all species together. Only the 42 plots with a significant LCBD value ($p < 0.05$) are shown, of which 30 are located inside protected areas and 12 outside. Image source: Google Earth 2024. Figure adapted from the published version of Chapter 1 (colors modified).

**Table 2.** Summary statistics of the environmental and landscape variables computed for each plot.

| Variable | Mean | Min-Max | SD |
|---|---|---|---|
| Sea distance (m) | 93.19 | 5.91-398.64 | 71.28 |
| Dune width (m) | 120.74 | 2.81-467.31 | 82.38 |
| Slope (%) | 2.94 | 0.00-25.00 | 7.90 |
| %ART | 0.35 | 0.00-32.75 | 2.47 |
| %ARV | 0.11 | 0.00-28.23 | 1.37 |
| %AGR | 0.32 | 0.00-36.32 | 2.39 |
| %WTC | 0.22 | 0.00-25.75 | 1.87 |
| Distance to ART (m) | 221.90 | 0.00-4143.70 | 468.17 |
| Landscape Shannon | 1.16 | 0.00-1.97 | 0.32 |

**Table 3.** Results of beta regression analysis of LCBD with landscape variables (pseudo-$R^2$ = 0.15).

| | Estimate | Std. Error | z value | Pr(>\|z\|) |
|---|---|---|---|---|
| (Intercept) | -6.17 | 0.01 | -570.26 | < 0.01 |
| Sea distance | -0.01 | 0.01 | -7.51 | < 0.01 |
| Slope | -0.01 | 0.01 | -3.75 | < 0.01 |
| Distance to ART | 0.01 | 0.01 | 4.08 | < 0.01 |

The NMDS ordination of the sites with significant LCBD (Fig. 5; stress = 0.04) showed that species composition in these sites mainly vary along the sea-inland gradient, represented by the first axis of the ordination, ranging from sites with salt-tolerant species of the drift lines on the right (e.g. *Cakile maritima, Salsola tragus, Convolvulus soldanella*), to sites with scrub species on the left (e.g. *Pistacia lentiscus, Smilax aspera, Juniperus turbinata*). The second gradient in species composition is a gradient of anthropic disturbance: in the lower portion of the ordination plot, where there is a higher proportion of artificial surface, sites are richer in synanthropic species (e.g. *Papaver rhoeas, Avena barbata, Anisantha sterilis*). The analysis of differences in LCBD between the North and the South of the region gave only slightly different results, which are reported in Supplementary Materials (Fig. S3).

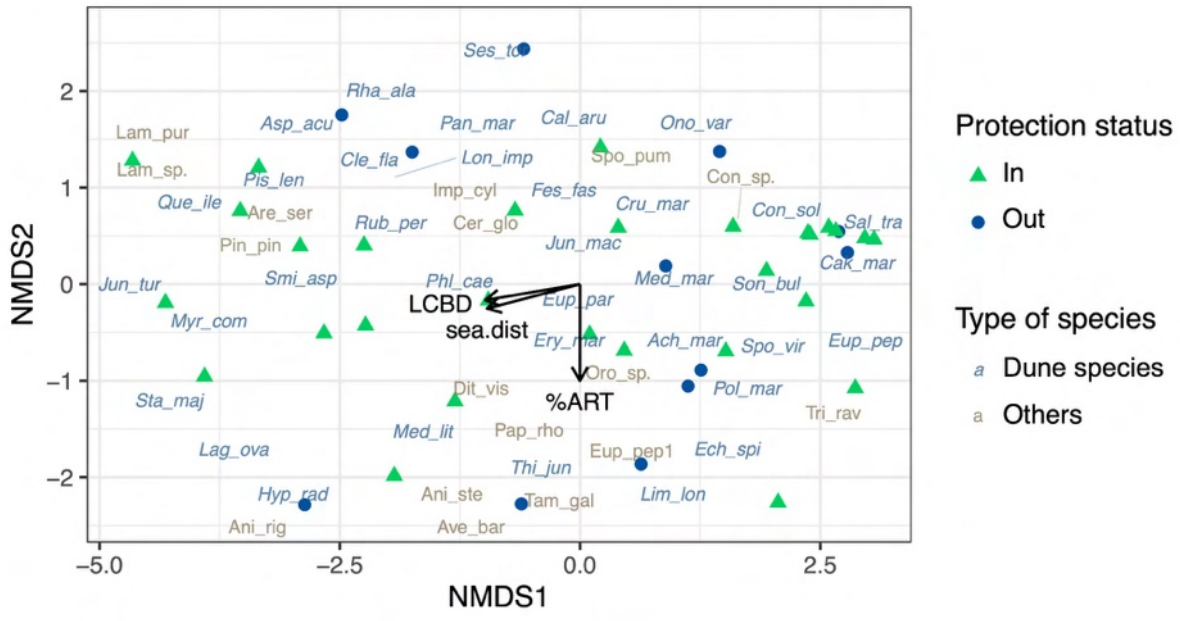


**Fig. 5.** Output of NMDS ordination, derived from Bray-Curtis similarity matrix based on log-transformed species abundances, for the plots with significant LCBD values (stress = 0.04). Species

names (reported in Table S1) were abbreviated as follows: *Achillea maritima* (Ach_mar), *Anisantha rigida* (Ani_rig), *Anisantha sterilis* (Ani_ste), *Arenaria serpyllifolia* (Are_ser), *Asparagus acutifolius* (Asp_acu), *Avena barbata* (Ave_bar), *Cakile maritima* (Cak_mar), *Calamagrostis arenaria* subsp. *arundinacea* (Cal_aru), *Cerastium glomeratum* (Cer_glo), *Clematis flammula* (Cle_fla), *Convolvulus soldanella* (Con_sol), *Convolvulus* sp. (Con_sp.), *Crucianella maritima* (Cru_mar), *Dittrichia viscosa* (Dit_vis), *Echinophora spinosa* (Ech_spi), *Eryngium maritimum* (Ery_mar), *Euphorbia paralias* (Eup_par), *Euphorbia peplis* (Eup_pep), *Euphorbia peplus* (Eup_pep1), *Festuca fasciculata* (Fes_fas), *Hypochaeris radicata* (Hyp_rad), *Imperata cylindrica* (Imp_cyl), *Juniperus macrocarpa* (Jun_mac), *Juniperus turbinata* (Jun_tur), *Lagurus ovatus* (Lag_ova), *Lamium purpureum* (Lam_pur), *Lamium* sp. (Lam_sp.), *Limbarda crithmoides* subsp. *longifolia* (Lim_lon), *Lonicera implexa* (Lon_imp), *Medicago littoralis* (Med_lit), *Medicago marina* (Med_mar), *Myrtus communis* (Myr_com), *Ononis variegata* (Ono_var), *Orobanche* sp. (Oro_sp.), *Pancratium maritimum* (Pan_mar), *Papaver rhoeas* (Pap_rho), *Phleum arenarium* subsp. *caesium* (Phl_cae), *Pinus pinea* (Pin_pin), *Pistacia lentiscus* (Pis_len), *Polygonum maritimum* (Pol_mar), *Quercus ilex* (Que_ile), *Rhamnus alaternus* (Rha_ala), *Rubia peregrina* (Rub_per), *Salsola tragus* (Sal_tra), *Seseli tortuosum* (Ses_tor), *Smilax aspera* (Smi_asp), *Sonchus bulbosus* (Son_bul), *Sporobolus pumilus* (Spo_pum), *Sporobolus virginicus* (Spo_vir), *Stachys major* (Sta_maj), *Tamarix gallica* (Tam_gal), *Thinopyrum junceum* (Thi_jun), *Tripidium ravennae* (Tri_rav). Landscape variables having a significant correlation with NMDS axes, namely sea distance (sea.dist) and proportion of artificial landcover (%ART), along with LCBD, were overlaid to the ordination plot. Figure adapted from the published version of Chapter 1 (colors modified).

Values of SCBD are reported in Table 4. The species with the highest contributions to *β*-diversity were *Juniperus macrocarpa* (0.14), *Calamagrostis arenaria* subsp. *arundinacea* (0.09) and *Thinopyrum junceum* (0.06), which were also among the most frequent ones (SCBD *vs*. species frequency: Spearman's cor = 0.89, $p < 0.05$). Similar results were also obtained when the analysis was performed separately for Northern and Southern sites (highest SCBD in the North: *J. macrocarpa* 0.16, *C. arenaria* subsp. *arundinacea* 0.10*, Pancratium maritimum* 0.06; in the South: *J. macrocarpa* 0.14, *C. arenaria* subsp. *arundinacea* 0.08, *T. junceum* 0.07).

**Table 4.** Species contributions to $\beta$-diversity (SCBD) and species frequencies (%) in the Tuscany dataset, and SCBD values computed separately for the Northern and Southern parts of the region. The species are ordered according to decreasing SCBD values and only the species with SCBD values higher than the mean are reported.

| **Species** | **SCBD** | **Frequency (%)** | **SCBD (North)** | **SCBD (South)** |
|---|---|---|---|---|
| *Juniperus macrocarpa* | 0.14 | 34.78 | 0.16 | 0.14 |
| *Calamagrostis arenaria* subsp. *arundinacea* | 0.09 | 22.33 | 0.10 | 0.08 |
| *Thinopyrum junceum* | 0.06 | 42.69 | 0.06 | 0.07 |
| *Helichrysum stoechas* | 0.05 | 34.39 | 0.05 | 0.06 |
| *Pancratium maritimum* | 0.05 | 25.30 | 0.06 | 0.02 |
| *Cakile maritima* | 0.04 | 16.80 | 0.01 | 0.07 |
| *Eryngium maritimum* | 0.04 | 18.18 | 0.05 | 0.02 |
| *Anthemis maritima* | 0.03 | 15.02 | 0.01 | 0.06 |
| *Euphorbia paralias* | 0.03 | 20.55 | 0.04 | 0.01 |
| *Festuca fasciculata* | 0.03 | 32.21 | 0.03 | 0.01 |
| *Echinophora spinosa* | 0.03 | 19.96 | 0.03 | 0.02 |
| *Medicago marina* | 0.02 | 10.87 | 0.01 | 0.04 |
| *Achillea maritima* | 0.02 | 4.74 | 0.01 | 0.03 |
| *Medicago littoralis* | 0.02 | 32.41 | 0.03 | 0.01 |
| *Seseli tortuosum* | 0.02 | 18.97 | 0.03 | 0.00 |
| *Lomelosia rutifolia* | 0.02 | 11.26 | 0.03 | 0.00 |
| *Crucianella maritima* | 0.02 | 7.71 | 0.02 | 0.02 |
| *Ononis variegata* | 0.02 | 10.08 | 0.02 | 0.01 |
| *Pistacia lentiscus* | 0.02 | 9.09 | 0.00 | 0.03 |
| *Salsola tragus* | 0.02 | 16.01 | 0.01 | 0.03 |
| *Smilax aspera* | 0.01 | 16.80 | 0.01 | 0.02 |
| *Pinus pinaster* | 0.01 | 5.53 | 0.00 | 0.02 |
| *Sporobolus virginicus* | 0.01 | 12.06 | 0.00 | 0.02 |
| *Phillyrea angustifolia* | 0.01 | 8.10 | 0.00 | 0.02 |
| *Phleum arenarium* subsp. *caesium* | 0.01 | 13.44 | 0.01 | 0.00 |

| | | | | |
|---|---|---|---|---|
| *Lagurus ovatus* | 0.01 | 18.18 | 0.01 | 0.01 |
| *Convolvulus soldanella* | 0.01 | 10.08 | 0.01 | 0.00 |
| *Erica multiflora* | 0.01 | 4.15 | 0.00 | 0.02 |
| *Salvia rosmarinus* | 0.01 | 2.77 | 0.00 | 0.01 |
| *Silene canescens* | 0.01 | 15.22 | 0.01 | 0.00 |
| *Cerastium glomeratum* | 0.01 | 12.25 | 0.01 | 0.00 |
| *Hypochaeris radicata* | 0.01 | 6.92 | 0.01 | 0.00 |
| *Euphorbia peplis* | 0.01 | 7.31 | 0.01 | 0.00 |
| *Sporobolus pumilus* | 0.01 | 2.37 | 0.01 | 0.00 |
| *Silene otites* | 0.01 | 11.46 | 0.01 | 0.00 |

Finally, the results of the additive partitioning of $\gamma$-diversity are represented in Fig. 6: for dune species, all levels of analysis are significant, while for synanthropic and alien species only the plot level is significant.

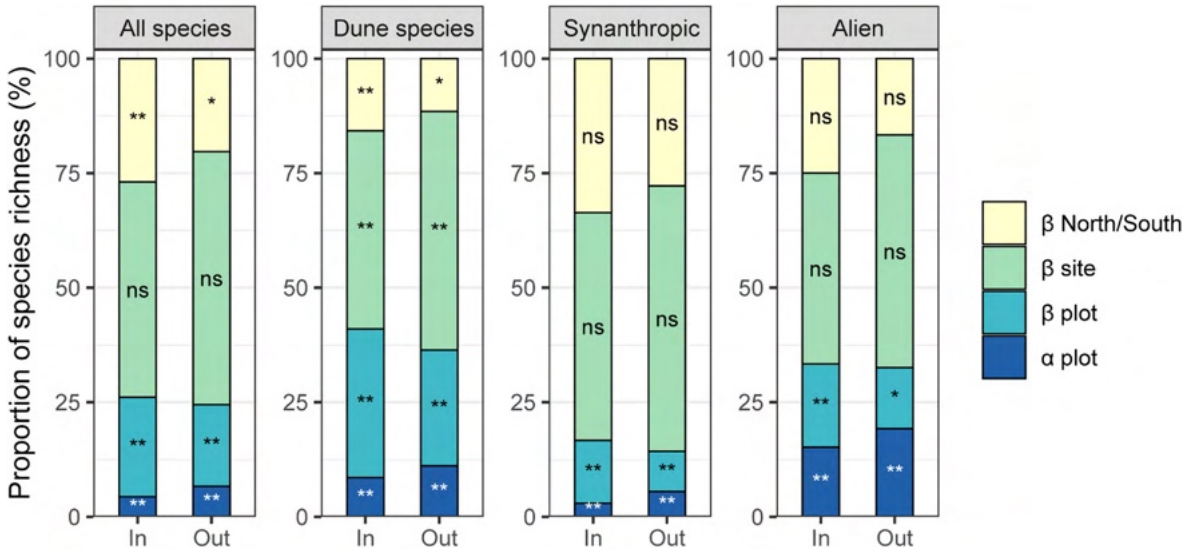


**Fig. 6.** Contributions (%) of the $\alpha$ and $\beta$-diversity components to the total species richness of the study area, for each protection status (inside/ outside protected areas) and each species group. Contributions were determined through the additive partitioning approach (** $p < 0.01$; * $p < 0.05$; ns = non-significant).

## 4. Discussion

Our approach has proved effective for identifying the most unique sites on a regional scale relying on the analysis of $\beta$-diversity (Dubois et al., 2020; Hill et al., 2021; Heino et al., 2022). By analyzing species composition and exploring the relationship between community uniqueness and landscape variables, we were able to distinguish sites with a high conservation value and prioritize them for protection. Moreover, analyzing the patterns of $\alpha$-diversity and $\beta$-diversity at the different scales, with different groups of species separately, we got a valuable insight on the distribution of dune plant diversity with respect to protected areas, contributing to the assessment of their efficacy in the conservation of coastal dunes of Tuscany.

In terms of species richness, in the North of the region protected sites are richer in dune species than non-protected ones, while in the South the two areas show similar data. Touristic and recreational activities, indeed, are particularly intense in the North, and are known to cause a reduction of species richness in coastal dunes, especially where there is no protection (Santoro, Jucker, Carboni, et al., 2012; Prisco et al., 2021).

Remarkably, the richness of synanthropic and alien species inside and outside protected areas is similar. The synanthropic species tend to be more resistant to human-induced alterations than dune plants, and in some cases they increase in altered sites occupying gaps unexploited by dune species (Del Vecchio et al., 2015). The absence of a positive effect of anthropic disturbance on the species richness of synanthropic and alien species could be due to the extreme abiotic conditions of the coastal environment that limit non-specialized species, as observed in other studies (Carboni et al., 2010; Malavasi et al., 2016). Moreover, this result suggests that protection measures do not stop the entrance of species related to anthropic disturbance in protected areas. Protected areas, indeed, are connected to their surroundings by multiple ecological processes (Hansen & DeFries, 2007; Holenstein et al., 2021). In coastal dunes, the surroundings can act as an introduction source for synanthropic species (Carboni et al., 2011; Bazzichetto et al., 2018), and coastal dunes are indeed particularly prone to invasions (Lozano et al., 2023). Thus, for conservation it is crucial to manage these ecosystems as a whole, paying attention also to the surrounding landscape (Cox & Underwood, 2011).

Nonetheless, the total number of alien species found in Tuscany is low, in line with other studies (Ciccarelli et al., 2014), and notably, some of the most widespread and harmful invasive species, as *Carpobrotus* spp. (Carboni et al., 2010), were not found in the surveyed plots.

The analysis of $\beta$-diversity can provide deeper information on the processes structuring plant communities (Legendre & De Cáceres, 2013). In this study, different patterns emerge according to the group of species under investigation, independently of the protection status of the areas. For dune species, the most important component of $\beta$-diversity is the replacement. This result can be explained as the gain and loss of species occurring among the different habitats of dune ecosystems (Legendre, 2014). Dune species generally have narrow ecological ranges and particular ecophysiological adaptations (Angiolini et al., 2018). On the contrary, the dominant component of $\beta$-diversity of synanthropic and alien species is richness difference, suggesting that there is a limited pool of these species and that the differences among sites are mainly determined by the loss of species, as was found also in other studies (e.g. Tordoni et al., 2018).

The spatially hierarchical partitioning of $\gamma$-diversity points out a similar situation: the diversity of dune species is significant at all levels, indicating that there are ecological processes shaping this community at different scales. On the other hand, for synanthropic and alien species, only the plot level is significant, suggesting that their species pool is limited, and $\beta$-diversity can be captured just by the variability between plots.

The prevalence of replacement for focal species has a consequence for conservation: it means that for the conservation of this group of species it is preferable to protect multiple areas, preferring the ones with the most unique sites, rather than to protect only the sites with the highest species richness (Socolar et al., 2016; Carlos-Júnior et al., 2019; Hill et al., 2021). High LCBD values generically indicate sites with a high uniqueness with respect to the overall status of the study area (Legendre & De Cáceres, 2013), and therefore can indicate also sites subjected to disturbance or characterized by peculiar ecological conditions (Dubois et al., 2020; Perez Rocha et al., 2023).

In our study, high contributions to $\beta$-diversity were given by sites with low species richness, as observed in many other studies (Heino & Grönroos, 2017; Dubois et al., 2020; Hill et al., 2021; Perez Rocha et al., 2023). Moreover, LCBD had a complex relation with environmental factors: it increased with increasing proximity to the shoreline, indicating that sites closer to the sea are highly unique, but it also increased with decreasing slopes, which are generally characteristic of the communities located at both extremes of the coastal zonation (Acosta et al., 2007). Also, the positive relation between LCBD and distance to artificial surfaces suggests that ecological

uniqueness can be reduced by anthropic disturbance, as observed also in other works (García-Navas et al., 2022). The low proportion of variation of LCBD explained by local environmental variables is consistent with findings for stream insect assemblages (Heino & Grönroos, 2017) and agricultural landscapes (García-Navas et al., 2022), and could be due to the fact that ecological uniqueness is linked to multiple communities across the coastal zonation rather than specific environmental conditions. However, it is necessary to take into account the species composition of the unique sites before drawing conclusions on their conservation value.

In this study, the ordination of the sites with significant LCBD showed that their uniqueness is due to various reasons. Most of the unique sites are well-preserved aspects of coastal dune vegetation, corresponding to different habitats along the sea-inland zonation. As these sites are exceptions, the overall status of coastal dunes in Tuscany appears to be degraded, and synanthropic species are indeed widespread throughout our study area. Interestingly, several unique sites are covered by the pioneer vegetation of drift lines, a naturally species-poor habitat characterized by highly specialized species like *Cakile maritima*, *Salsola tragus*, *Convolvulus soldanella* (Prisco et al., 2012). As emerged from other works, this habitat is often in an unfavorable conservation status (Bertacchi, 2017; Sperandii et al., 2019; Sarmati et al., 2019), because it is highly vulnerable to tourism and mechanical cleaning (Attorre et al., 2013), while being also sensitive to erosion (Bazzichetto et al., 2020). Nonetheless, our analysis also revealed the presence of unique sites characterized by *Calamagrostis arenaria* subsp. *arundinacea*, by *Crucianella maritima*, by dune grasslands, and by dune scrubs, suggesting that there is not a single habitat to give priority to, and stressing the importance of conserving the complete coastal vegetation mosaic (Acosta et al., 2009).

A similar indication emerges from the analysis of the SCBD. Indeed, the species contributing the most to the regional $\beta$-diversity are *Juniperus macrocarpa, Calamagrostis arenaria* subsp. *arundinacea*, *Thinopyrum junceum,* and *Cakile maritima,* which are the most representative and the structural species of the main communities occurring in the coastal zonation (Acosta et al., 2007). In addition, many of these species have high frequency in our dataset, and thus are the ones varying the most in occurrence and abundance, as observed in previous studies (Heino & Grönroos, 2017; Fanfarillo et al., 2023). Such results underline the importance of conserving the whole dune zonation (Acosta et al., 2009).

Notably, some of the unique sites are not protected and thus particularly vulnerable, so these

results can serve as a base to choose what areas should be included in the network of protection (Dubois et al., 2020). The expansion of the network, however, would also require assessing the current and future distribution of threats like urbanization, as was done recently by Doxa et al. (2017). At the same time, our results also highlighted the importance of considering species composition alongside LCBD analysis, separating dune species from synanthropic and alien species. Indeed, high value of LCBD may indicate also sites rich in synanthropic species and surrounded by a high proportion of artificial land, or altered in other ways, as two sites particularly rich in *Achillea maritima*, a sub-nitrophilous species that is an indicator of dune degradation when present with high coverage (Acosta et al., 2007). Remarkably, when these sites are located inside protected areas, high value of LCBD can be also an indication on where to address restoration efforts (Legendre & De Cáceres, 2013).

## 5. Conclusions

Our approach proved to be effective for prioritizing coastal dune sites based on their ecological uniqueness. The analysis of $\beta$-diversity allowed to identify new sites for conservation on a regional scale and to assess the effectiveness of the existing network of protected areas by analyzing their distribution. We observed some differences between protected and non-protected areas, but these differences changed according to which type of diversity metric was considered and which group of species was analyzed, suggesting that it is essential to consider different groups of species separately and indicating the dune species group as the most interesting to explore.

In the North of Tuscany, protected areas appear to be richer in dune species, while in the South the overall situation seems more homogeneous. Definitive conclusions on the effectiveness of protected areas for the conservation of coastal dune diversity cannot be drawn, also because much depends on the initial state of the protected area (Sperandii et al., 2020), however our results suggest that there are some unique sites with high conservation value which are not protected and some protected sites with low level of conservation, raising the question of whether the existing network of protected areas should be better assessed.

Potential future steps include extending the analysis to other aspects of diversity, such as functional, phylogenetic or spectral diversity, to assess how appropriate the current network is for the protection of them. Moreover, the scale of analysis could be expanded to include larger areas, and, finally, the outputs of these analyses can be gathered to suggest new relevant sites

to prioritize for protection giving an important contribution to the 2030 Conservation Strategy of European Commission (2020).

## Acknowledgements

We are thankful to Manuele Bazzichetto and Vojta Bartak for the production of the landcover map and the computation of the landscape metrics. The research was partially funded by the Ministry of University and Research (MUR), PRIN Project 2022FCAAA4 Prioritisation of coastal areas for plant diversity conservation through a multidisciplinary approach (PRIORCOAST), and by Regione Toscana - Project "NaTNet" – Natural Tuscany Network CUP D54I19001090002. E. Pafumi, C. Angiolini, S. Sarmati, E. Fanfarillo, and S. Maccherini were funded under the National Recovery and Resilience Plan (NRRP), Mission 4 Component 2 Investment 1.4 - Call for tender No. 3138 of 16 December 2021, rectified by Decree n.3175 of 18 December 2021 of Italian Ministry of University and Research funded by the European Union – NextGenerationEU; Award Number: Project code CN_00000033, Concession Decree No. 1034 of 17 June 2022 adopted by the Italian Ministry of University and Research, CUP B63C22000650007, Project title "National Biodiversity Future Center - NBFC".

# Chapter 2

## Fuzzy approaches provide improved spatial detection of coastal dune EU habitats

Emilia Pafumi[1,2]*, Claudia Angiolini[1,2], Giovanni Bacaro[3], Emanuele Fanfarillo[1,2], Tiberio Fiaschi[1], Duccio Rocchini[4,5], Simona Sarmati[6,2], Michele Torresani[7], Hannes Feilhauer[8,9,10], Simona Maccherini[1,2]

[1]Department of Life Sciences, University of Siena, 53100 Siena, Italy; [2]NBFC, National Biodiversity Future Center, 90133 Palermo, Italy; [3]Department of Life Sciences, University of Trieste, 34127 Trieste, Italy; [4]BIOME Lab, Department of Biological, Geological and Environmental Sciences, Alma Mater Studiorum University of Bologna, 40126 Bologna, Italy; [5]Czech University of Life Sciences Prague, Faculty of Environmental Sciences, Department of Spatial Sciences, Praha - Suchdol, 16500, Czech Republic; [6]Department of Sciences, University of Roma Tre, 00146 Rome, Italy; [7]Free University of Bolzano/Bozen, Faculty of Agricultural, Environmental and Food Sciences, 39100 Bolzano/Bozen, Italy; [8]Institute for Earth System Science and Remote Sensing, Leipzig University, Leipzig, Germany; [9]German Centre for Integrative Biodiversity Research (iDiv), Halle-Jena-Leipzig, Germany; [10]Helmholtz Centre for Environmental Research – UFZ, Leipzig, Germany

*Corresponding author

*Published as:*

Pafumi E, Angiolini C, Bacaro G, Fanfarillo E, Fiaschi T, Rocchini D, Sarmati S, Torresani M, Feilhauer H, Maccherini S (2025) Fuzzy approaches provide improved spatial detection of coastal dune EU habitats. *Ecological Informatics* 86, 103059 https://doi.org/10.1016/j.ecoinf.2025.103059

## Abstract

Mapping habitats on coastal dunes, crucial yet highly vulnerable ecosystems, requires objectivity and repeatability, which are still lacking in the implementation of the Habitats Directive. Although remote sensing offers promising solutions, the effectiveness of distinguishing habitats on coastal dunes from satellite imagery remains uncertain. In this study, we compare crisp and fuzzy classification approaches using WorldView-3 imagery to map coastal dune habitats in two Natural Parks of Tuscany (Italy).

Field-collected vegetation data were classified into Annex I habitats of Habitats Directive and EUNIS habitats. Using field data as reference, we performed image classifications with a crisp method (Random Forests) and three fuzzy methods, namely Random Forests, Spectral Angle Mapper and Multiple Endmember Spectral Mixture Analysis. Metrics of overall accuracy and Mantel tests were used to compare the results.

EUNIS habitats exhibited the best performance in terms of classification accuracy, likely due to the simpler classification system. We observed a great disparity among habitats, with coastal dune scrubs and white dunes generally achieving the highest accuracy. Fuzzy classifications, despite yielding lower overall accuracy than crisp classification, provided a more realistic representation of vegetation patterns, highlighting the inherent fuzziness of vegetation in coastal dunes. Despite challenges related to image resolution and habitat heterogeneity, combining satellite imagery with field surveys proved valuable for mapping coastal dune habitats, contributing essential data to the conservation of these fragile ecosystems. We provide a novel and effective tool, which will reduce the economic and physical efforts needed for habitat search and sampling in the field.

**Keywords:** Coastal dunes, Fuzzy classification, Habitats Directive, Habitat mapping, Machine learning, Remote sensing

# 1. Introduction

Vegetation mapping and monitoring are essential for the study and conservation of biodiversity (Reddy, 2021). In Europe, conservation efforts primarily focus on habitats, which in the Habitats Directive are defined as "terrestrial or aquatic areas distinguished by geographic, abiotic and biotic features, whether entirely natural or semi-natural" (Council Directive 92/43/EEC, hereafter HD). The HD lists priority habitats at risk of disappearance in Annex I (hereafter Annex I habitats) and mandates their conservation across Member States, requiring their conservation status to be monitored (Art. 11) and reported every six years (Art. 17). Since the description of these habitats is predominantly vegetation-based, their conservation status is typically assessed through vegetation features (Gigante et al., 2016). Specifically, maps of habitat distribution are fundamental for monitoring the "area" parameter, which is necessary for assessing conservation status according to the HD. However, the lack of clarity and homogeneity in monitoring methods, which mainly rely on expert assessments, poses challenges to the effective implementation of the HD (Delbosc et al., 2021).

The implementation of conservation measures is complicated by the existence and use of several habitat classification systems (European Environment Agency, 2014). One of the most widely used systems in Europe is the European Nature Information System (EUNIS), which hierarchically classifies terrestrial and marine habitats (Davies & Moss, 1998), and serves as the foundation for the European Red List of Habitats (Janssen et al., 2016). Since HD and EUNIS are the two main habitat classification systems in Europe, we will refer to habitats from both systems collectively as "EU habitats" hereafter. In recent years, the EUNIS system has been revised, incorporating updated criteria for habitat identification, so that it has become a reference for harmonizing datasets and linking networks of experts (Chytrý et al., 2020).

Coastal sand dunes are among the most threatened ecosystems in Europe (Janssen et al., 2016). The ongoing pressures of urbanization, tourism and coastal erosion are increasingly compressing dunes between the sea and human settlements (Defeo et al., 2009; Tordoni et al., 2021). Invasive alien species pose a further threat to the integrity of these ecosystems (Tordoni et al., 2019). These pressures have resulted in the poor conservation status of most dune habitats (Prisco et al., 2020). Consequently, there is an urgent need for effective tools to monitor and map these fragile habitats (Delbosc et al., 2021).

The mapping of coastal dune habitats presents significant challenges, primarily because these

habitats occur in small patches, often with sparse vegetation cover (Prisco et al., 2012) and are highly dynamic (Sperandii et al., 2018; Chelli et al., 2022). The poor conservation status of coastal dunes can hamper habitat identification (Sarmati et al., 2019). In this context, remote sensing techniques offer several advantages over field mapping for the realization of habitat maps, including the capacity to cover large, even inaccessible areas in a cost-effective and highly time-efficient manner (Vanden Borre et al., 2011) and to reduce the trampling produced during field surveys, to which some dune species are sensitive (Santoro, Jucker, Prisco, et al., 2012). Moreover, remote sensing techniques provide high objectivity and repeatability, key features required for habitat conservation assessment (Delbosc et al., 2021).

In recent years, several studies have demonstrated the potential of remote sensing for the detailed mapping of coastal dune habitats, primarily using data from aerial orthophotos (Juel et al., 2013; Bertacchi, 2017), airborne spectrometers (Shanmugam et al., 2003; Brownett & Mills, 2017), and unmanned aerial vehicles (Agrillo et al., 2023; Cruz et al., 2023). Satellite sensors would also be well-suited for monitoring highly dynamic habitats such as coastal dunes, thanks to their regular coverage of large areas over time (Mairota et al., 2015). However, they pose greater challenges to their use due to their lower spatial resolution (Nagendra et al., 2013; Bhatt & Maclean, 2023), so that there is still a knowledge gap in their effectiveness for such purposes. The small size of habitat patches on coastal dunes constrains the grain of the imagery used for mapping, as the pixel resolution of the images should ideally be smaller than the objects being mapped (Nagendra, 2001; Gamon et al., 2020; Torresani et al., 2024). Moreover, due to the low vegetation cover, variations in soil background interfere with the vegetation signal (Prudnikova et al., 2019). In coastal dunes, the use of satellite data has been predominantly focused on mapping study-specific typologies, such as land cover (Timm & McGarigal, 2012), vegetation formations defined by physiognomy (Rapinel et al., 2014), or broad vegetation classes (Marzialetti et al., 2019, 2020), while the extent to which EU habitats can be distinguished remains uncertain.

Typically, mapping techniques rely on defining crisp classes and attributing individual objects (pixels) to those classes. However, these crisp classification systems have notable limitations in certain situations. One is when vegetation is better described by a continuum rather than by discrete classes, as in ecotones (Rocchini et al., 2013). A second one is when, even if vegetation classes are discrete, the map grain is so coarse that each object is a mixture of multiple classes (Foody, 1996). In both cases, more realistic descriptions can be provided by fuzzy

classifications (Shanmugam et al., 2006; Rocchini & Ricotta, 2007; Rocchini, 2010). Within the framework of the fuzzy set theory, each object is assigned a probability of membership to multiple classes (Zadeh, 1965), thereby enabling the representation of gradual transitions between discrete classes and intermediate situations, phenomena that are common both in real landscapes and in remotely sensed images (Lucas et al., 2002). Despite these advantages, fuzzy classifications are seldom employed in vegetation mapping (Feilhauer et al., 2021).

Considering the high potential of satellite images for large-scale habitat mapping, in this study we tested a fuzzy approach to classification for mapping coastal dune habitats using high resolution satellite imagery, aiming at providing a novel and effective technique for remote habitat monitoring. We compare the results of habitat mapping obtained using the HD (11 habitats for Italian dunes; Biondi et al., 2009) and level 3 EUNIS (5 habitats for Italian dunes; Chytrý et al., 2020) classifications. Specifically, we use ~1 m multispectral images from WorldView-3, selected because dune habitats often occur in patches too small to be captured by freely available, lower-resolution data like 10 m Sentinel-2, to assess: 1) the efficiency of remote-sensing based mapping of habitats classified with different systems (HD and EUNIS); 2) whether employing a fuzzy approach improves the habitat mapping product compared to the traditional crisp approach.

## 2. Materials and methods

### 2.1. Study area

The study was carried out in two Regional Parks along the coast of Tuscany (central Italy; Fig. 1): the Migliarino-San Rossore-Massaciuccoli Park (MSRM, centroid coordinates: 43.732968°N, 10.312429°E), in the north, and the Maremma Park (42.641538°N, 11.087048°E), in the south. The first study area partially overlaps with the Special Areas of Conservation (SACs) “Dune Litoranee di Torre del Lago” (IT5170001) and “Selva Pisana” (IT5170002), while the second study area partially overlaps with the SAC “Dune costiere del Parco dell'Uccellina” (IT51A0015).

The climate is Mediterranean, with an upper meso-mediterranean thermotype and an ombrotype ranging from lower humid in the North to upper dry in the South (Pesaresi et al., 2017). In the region, coastal dunes occupy a narrow stripe, up to 300 m wide and 10 m high (Bertacchi, 2017) and are primarily composed of Late Quaternary sand (Carmignani et al.,

2013). Coastal dune systems support various plant communities arranged in a well-defined zonation, ranging from annual vegetation of drift lines to embryonic shifting dunes, white dunes, stable dune grasslands, and coastal dune scrubs and woods (Acosta et al., 2007). The anthropogenic pressure is higher in the MSRM Park (mean population density = 66.28 people/km$^2$) compared to the Maremma Park (41.89 people/km$^2$; EUROSTAT, 2021).

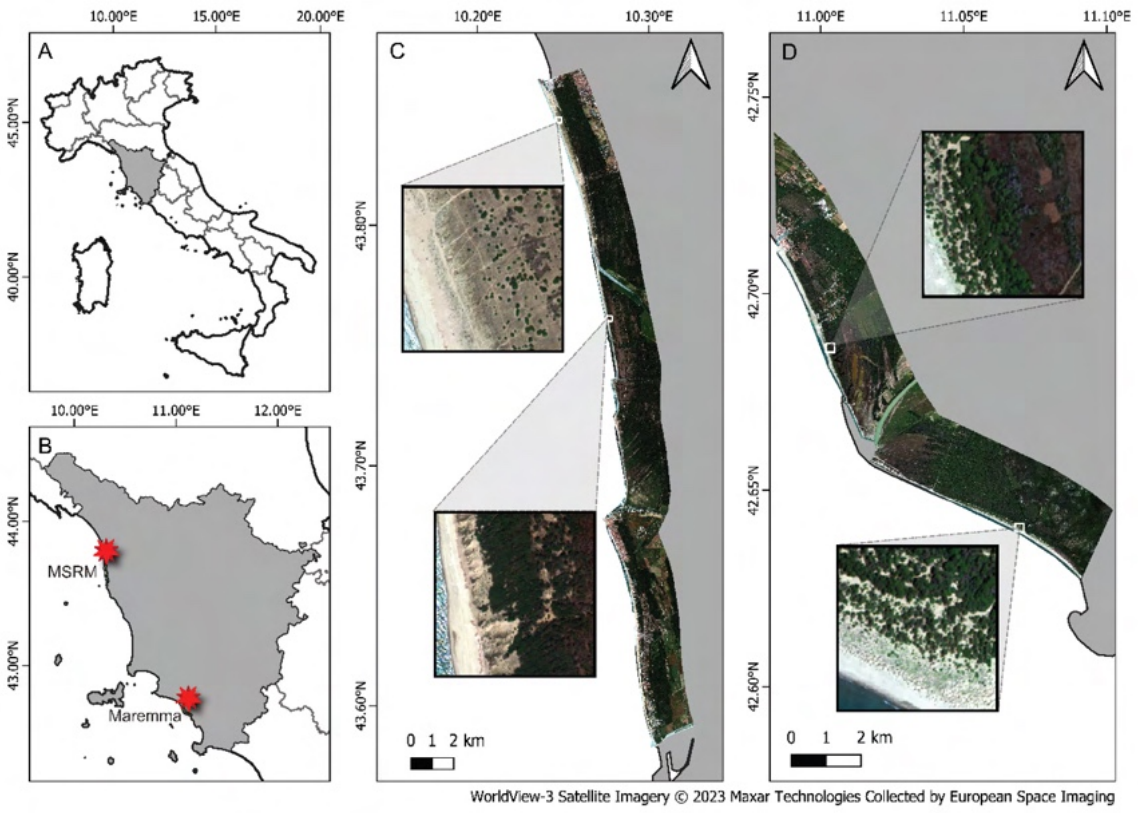


**Fig. 1.** Location of the study area in Italy (A), with indication of the two sites in Tuscany: Migliarino-San Rossore-Massaciuccoli (MSRM) and Maremma Park (B). WorldView-3 true color composites for the MSRM Park (C) and for the Maremma Park (D), including close-up views on some areas for example.

### 2.2. Vegetation sampling

Field surveys were conducted between 2018 and 2021 using a stratified random sampling design. The regional coast was divided into two bands: one encompassing shifting dunes and stable dune grasslands, which occurred in a fine-grained mosaic, and the other representing coastal dune scrub. Within each band, 4 m$^2$ squared plots were randomly selected in proportion to the surface area (approximately 0.8 plots/ha). The plot size was selected in accordance with other studies conducted on these vegetation types (Carboni et al., 2011; Sperandii et al., 2018).

Ad hoc plots were established on the field to sample the annual vegetation of drift lines, which was sporadic and thus barely detectable with the random plots. In total, we sampled 244 plots, 173 in MSRM Park and 71 in Maremma Park. Vascular plant species occurrence and abundance (visually assessed percentage cover) were recorded in each plot. Species nomenclature follows the Portal to the Flora of Italy (2023), containing updated data from Bartolucci et al. (2018) and Galasso et al. (2018). The field data accuracy, influenced by GPS precision (approximately 4 m), was improved by verifying plot positions on a 20 cm orthophoto from the year 2019 (GEOSCOPIO, 2022). Plot data are included in the SALTISH dataset (Gholizadeh et al., under review).

### 2.3. Habitat classification

The workflow followed to generate the habitat classification maps starting from field vegetation data is illustrated in Figure 2.

Vegetation plots were classified into EU habitats using three independent approaches:

1. Expert classification: vegetation plots were classified into the habitats present in the Annex I of the HD, based on an expert assessment of the habitats species composition as indicated in the Interpretation Manual of European Union Habitats (European Commission, 2013) and its Italian version (Biondi et al., 2009).

2. Unsupervised classification of the plots on the Chord-transformed species abundance matrix using noise clustering. Noise clustering is a non-hierarchical clustering method that assigns a cluster membership probability to each object based on its Euclidean distance to cluster centroids, while also considering a *noise* cluster, which captures objects beyond a certain distance from all other clusters (De Cáceres et al., 2010). A tuning procedure was applied to optimize three parameters: the number of clusters (nC), the fuzziness coefficient (m; the smaller its value, the closer the classification will approximate crispness), and the distance to the noise cluster (**δ**). The noise clustering procedure was performed with the *vegclust* function from the R package `vegclust` (De Cáceres et al., 2010) and repeated with various combinations of the parameter values, following Rapinel et al. (2018). After determining the optimal parameter values (nC = 6, m = 1.6, **δ** = 1.5), noise clustering was performed to obtain the final clusters. Each cluster and the plots therein included that were assigned only to that cluster were classified into one habitat following the HD system.

3. Vegetation plots were classified into EUNIS habitats at level 3 following the EUNIS Expert System (Chytrý et al., 2020), using the R code implemented by Bruelheide et al. (2021).

In all the three cases, plots that could not be attributed to a single habitat were considered mixed and excluded from the reference dataset for image classifications. Finally, for the groups derived from each classification, we detected indicator species computing the Indicator Value (IndVal) of each species, which is a measure of the association between a species and a group of sites (Dufrêne & Legendre, 1997), using the *multipatt* function from the R package `indicspecies` (De Cáceres & Legendre, 2009).

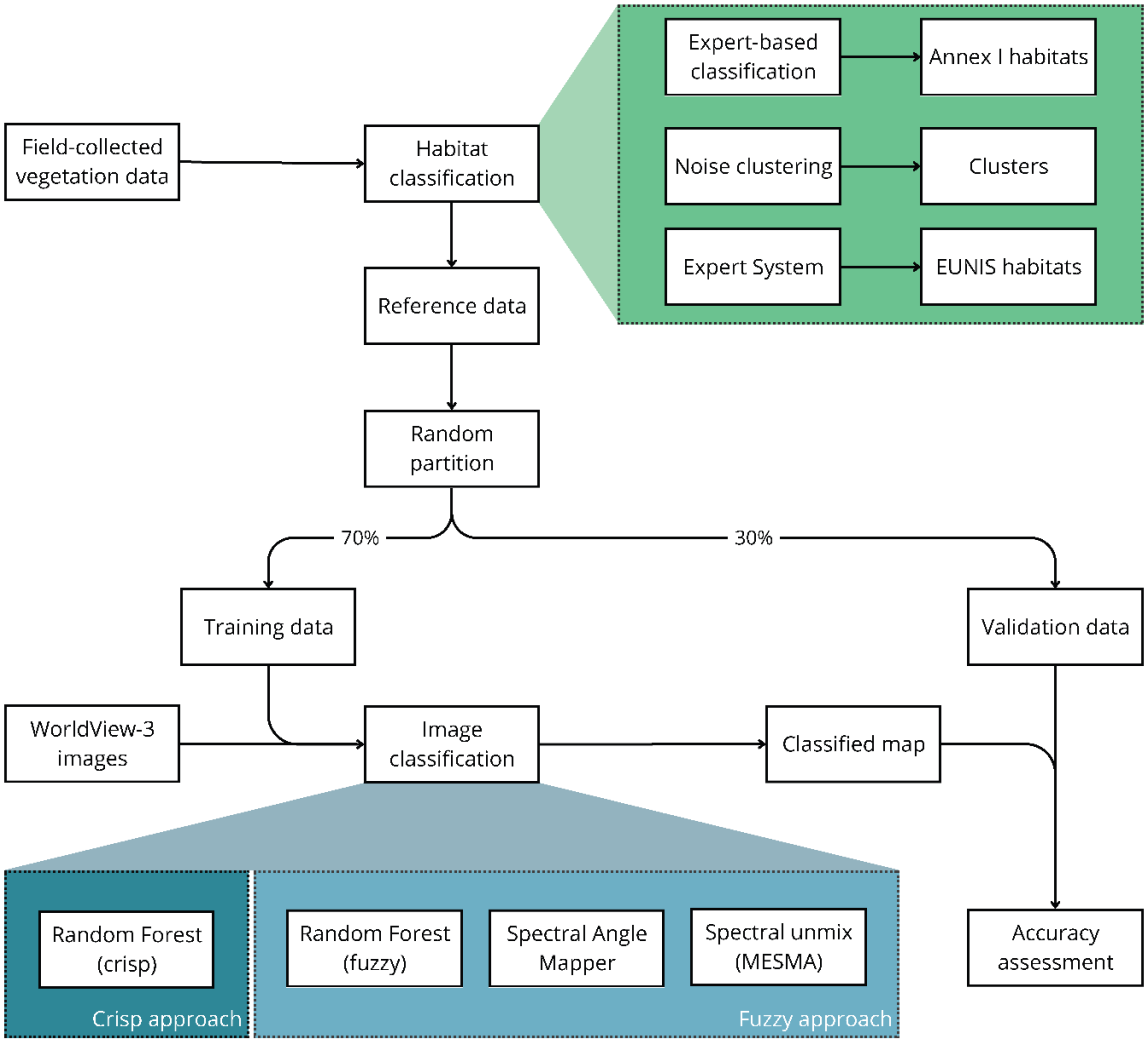


**Fig. 2.** Workflow of the analyses.

### 2.4. Remote sensing images

Two multispectral WorldView-3 images were acquired: one on 26 May 2017 for the MSRM Park and one on 16 May 2019 for the Maremma Park. Since no significant changes in vegetation were observed within the area during the relevant timeframe, the temporal mismatch between image acquisitions and field surveys was not expected to affect the results. WorldView-3 data include one panchromatic band (center wavelength: 649 nm) bundled with a multispectral image comprising eight spectral bands: coastal blue (427 nm), blue (482 nm), green (547 nm), yellow (604 nm), red (660 nm), red-edge (723 nm), near-infrared 1 (824 nm), and near-infrared 2 (914 nm). The images were delivered at the 3D-level of processing, i.e. orthorectified, sensor-corrected and radiometrically corrected through dark offset subtraction and non-uniformity correction (Kuester, 2016). The reported geolocation accuracy was < 3.0 m CE90, and the spatial resolution was 1.2 m for MSRM Park and 1.6 m for Maremma Park. Due to these differences, the analyses were performed separately for the two images. For each image, water bodies, artificial structures and agricultural land were masked using a pre-existing land cover map produced by photointerpretation of a 20 cm orthophoto from 2019 (Sarmati et al., 2025).

### 2.5. Image classification

Image classification was executed through two different approaches: crisp, in which each pixel is assigned to a single class, and fuzzy, which produces a membership matrix for each pixel.

The crisp classification was performed using Random Forests, ensemble classifiers based on independent predictions made by decision trees on bootstrap subsamples of training data, which produce a final crisp assignment based on majority voting (Breiman, 2001). Random Forests were selected due to their robustness to small training datasets, ability to handle correlation among predictors and relatively low computational cost, making them one of the most powerful and widely applied algorithms for image classifications (Maxwell et al., 2018). To assess the generalization capacity, which can pose a challenge for machine learning classifiers, the field reference dataset was randomly split into 70% for training and 30% for testing, ensuring that testing data were not used in training. The number of trees was set to 500, while the *mtry* parameter (i.e., the number of randomly selected variables used at each node) was optimized through a 5-fold cross-validation.

For the fuzzy classification, three algorithms were compared: Random Forests, Spectral Angle

Mapper (SAM) and Multiple Endmembers Spectral Mixture Analysis (MESMA). Here, Random Forests were used in a fuzzy sense, by considering the proportion of trees predicting a specific class for the pixel as the probability of the pixel belonging to that class. SAM determines the spectral similarity between a pixel spectrum and a reference spectrum by treating them as vectors in a space with dimensions corresponding to the number of bands and calculating the angle between them, thus generating a fuzzy map where pixel values correspond to spectral angles in radians (Kruse et al., 1993). The reference spectrum for each class was obtained by averaging the spectral signatures of the plots assigned to that class. To convert the spectral angles into probability values, each pixel value was subtracted from the maximum value in the map and the resulting values were normalized, so that probabilities at each pixel sum up to 1. The last algorithm utilized was MESMA, which models a pixel spectrum as a linear combination of reference spectra (Roberts et al., 1998), producing a raster with one layer for each endmember, where each pixel represents the estimated presence probability of the endmember in that pixel.

The Random Forest crisp and fuzzy classifications were performed using the `caret` R package (Kuhn, 2021). The SAM and MESMA fuzzy classifications were performed using the *sam* and *mesma* functions from the R package `RStoolbox`, respectively (Leutner et al., 2024). The resulting maps were represented with a color scale from the `viridis` package (Garnier et al., 2023) to ensure their readability (Crameri et al., 2020).

### 2.6. Accuracy assessment

The accuracy of image classifications was assessed through the confusion matrix, from which overall accuracy (proportion of correctly classified pixels), producer's accuracy (proportion of pixels of a class that are correctly classified), and user's accuracy (proportion of pixels classified into a class that actually belong to that class) were derived. For fuzzy classifications, the fuzzy confusion matrix was constructed by extracting the probabilities of each reference pixel and computing the average probabilities for each class (Zlinszky & Kania, 2016).

We assessed the information loss from vegetation data to classified maps by using multiple Mantel tests (Mantel, 1967). For this analysis, we considered all 244 field-sampled plots, including those not attributed to a single habitat. We tested the correlation between the dissimilarity matrix of vegetation plots, computed using Euclidean distances on the Chord-transformed species abundance matrix, and the dissimilarity matrix derived from predicted

maps. To construct the latter matrix, we extracted the predicted class memberships for each plot and calculated Euclidean distances among them. Mantel tests were performed with the *mantel* function from the R package `vegan` (Oksanen et al., 2022), using 999 randomizations and the Pearson correlation coefficient. The resulting Mantel R value, which ranges from 0 to 1, reflects the correlation between vegetation data and classified maps, with higher values indicating a higher proportion of information preserved in the classification. A significance level of 0.05 was adopted.

To obtain a spatially explicit measure of accuracy, maps of uncertainty were generated. For the crisp classification, uncertainty was measured as the probability (number of votes) of the assigned class. For fuzzy Random Forests and SAM, the Probability Surplus Index was used to quantify the difference between the probability of the dominant and the second most probable class (Zlinszky & Kania, 2016). For MESMA, we used the Root Mean Square Error (RMSE), i.e., the difference between the original spectrum and the best-fit spectrum generated from unmixed endmember proportions. For subsequent steps, we focused on the map from fuzzy Random Forests. To investigate the drivers of spatial uncertainty, we compared this map with a spectral heterogeneity map. Spectral heterogeneity was quantified by deriving the first principal component from the original image and calculating the standard deviation in a moving window of 7 x 7 pixels, using the *focal* function from the `raster` R package (Hijmans, 2023). Additionally, we computed Rao's Q index using the function *paRao* from the R package `rasterdiv` (Thouverai et al., 2021), setting a moving window of 7 pixels and a "multidimension" method.

Finally, to explore the spectral characteristics of plots classified as mixed and excluded from the reference dataset, we performed a Principal Component Analysis on the spectral bands of the complete set of field-sampled plots, using the function *rda* from the R package `vegan` (Oksanen et al., 2022).

All analyses were carried out in R 4.3.2 (R Core Team, 2023).

# 3. Results

## 3.1. Habitat classification

A total of 142 species were found across the 244 surveyed plots, with the most frequent species being *Helichrysum stoechas*, *Festuca fasciculata* and *Medicago littoralis* (present, respectively, in 53%, 48% and 43% of the plots). The mean total vegetation cover was 19.07%, with the highest values observed in plots dominated by *Juniperus macrocarpa* (57.46%).

The classes resulting from the three types of habitat classification are reported in Table 1. The expert-based classification attributed the plots to six Annex I habitats of coastal dunes (i.e., habitat 1210, 2110, 2120, 2210, 2230, and 2250, whose definitions are provided in Table 1, with indicator species reported in Table S1 of the Supplementary Materials). Out of the 244 plots, 100 plots were considered as mixed (76 in MSRM Park and 23 in Maremma Park) and excluded from the reference dataset.

**Table 1.** Classes resulting from the three types of habitat classification, with the description of the class and the corresponding number of plots in the Migliarino-San Rossore-Massaciuccoli (MSRM) and the Maremma Park (Mar). The last column reports the mean total vegetation cover of the 4 m2 plots for each class.

| | Class | Description | # MSRM | # Mar | Cov (%) |
|---|---|---|---|---|---|
| Annex I | 1210 | Annual vegetation of drift lines | 0 | 4 | 8.61 |
| | 2110 | Embryonic shifting dunes | 12 | 6 | 21.46 |
| | 2120 | Shifting dunes along the shoreline with *Ammophila arenaria* (‘white dunes’) | 22 | 12 | 16.54 |
| | 2210 | Crucianellion maritimae fixed beach dunes | 15 | 6 | 15.48 |
| | 2230 | *Malcolmietalia* dune grasslands | 5 | 0 | 10.21 |
| | 2250 | * Coastal dunes with *Juniperus* spp. | 41 | 20 | 34.12 |
| | excluded | - | 77 | 23 | - |
| clusters | C1 | Community with *Cakile maritima* | 11 | 9 | 5.59 |
| | C2 | Community with *Thinopyrum junceum* | 14 | 9 | 24.97 |
| | C3 | Community with *Calamagrostis arenaria* subsp. *arundinacea* | 29 | 14 | 14.83 |
| | C4 | Community with *Helichrysum stoechas* | 22 | 9 | 10.88 |
| | C5 | Community with *Lomelosia rutifolia* | 31 | 0 | 9.85 |
| | C6 | Community with *Juniperus macrocarpa* | 52 | 24 | 30.41 |
| | excluded | - | 14 | 6 | - |

| | | | | | |
|---|---|---|---|---|---|
| EUNIS (level 3) | N12 | Mediterranean and Black Sea sand beach | 2 | 8 | 6.36 |
| | N14 | Mediterranean, Macaronesian and Black Sea shifting coastal dune | 40 | 23 | 18.59 |
| | N16 | Mediterranean and Macaronesian coastal dune grassland (grey dune) | 57 | 11 | 11.63 |
| | N1B | Mediterranean and Black Sea coastal dune scrub | 5 | 6 | 107.84 |
| | excluded | - | 68 | 23 | - |

Noise clustering resulted in six clusters, whose indicator species are in Table 2. A total of 20 plots (14 in MSRM Park and 6 in Maremma Park) were not assigned to a single cluster and were therefore excluded from the reference dataset.

**Table 2.** Indicator species for the six clusters obtained from noise clustering.

| **Cluster** | **Indicator Species** | **IndVal** | **p value** | |
|---|---|---|---|---|
| C1 | *Cakile maritima* | 0.63 | 0.01 | ** |
| | *Achillea maritima* | 0.40 | 0.01 | ** |
| C2 | *Thinopyrum junceum* | 0.82 | 0.01 | ** |
| | *Echinophora spinosa* | 0.76 | 0.01 | ** |
| | *Anthemis maritima* | 0.48 | 0.01 | ** |
| | *Pancratium maritimum* | 0.46 | 0.01 | ** |
| | *Convolvulus soldanella* | 0.40 | 0.03 | * |
| C3 | *Calamagrostis arenaria* subsp. *arundinacea* | 0.94 | 0.01 | ** |
| C4 | *Helichrysum stoechas* | 0.80 | 0.01 | ** |
| C5 | *Lomelosia rutifolia* | 0.81 | 0.01 | ** |
| | *Cerastium glomeratum* | 0.67 | 0.01 | ** |
| | *Marcus-kochia ramosissima* | 0.58 | 0.01 | ** |
| | *Anisantha tectorum* | 0.36 | 0.01 | ** |
| | *Ambrosia psilostachya* | 0.36 | 0.01 | ** |
| | *Equisetum ramosissimum* | 0.34 | 0.01 | ** |
| C6 | *Juniperus macrocarpa* | 0.99 | 0.01 | ** |
| | *Smilax aspera* | 0.65 | 0.01 | ** |
| | *Rubia peregrina* | 0.61 | 0.01 | ** |
| | *Pinus pinaster* | 0.41 | 0.01 | ** |
| | *Rubus ulmifolius* | 0.38 | 0.02 | * |
| | *Cistus creticus* subsp. *eriocephalus* | 0.32 | 0.02 | * |
| | *Quercus ilex* | 0.32 | 0.03 | * |
| | *Geranium purpureum* | 0.28 | 0.02 | * |

Finally, EUNIS classification through the Expert System allowed plots to be assigned to four coastal dune habitats (i.e., habitat N12, N14, N16, and N1B, whose definitions are reported in Table 1 and whose indicator species are reported in Table S2 of the Supplementary Materials). However, no attribution was possible for 91 plots (68 in MSRM Park and 23 in Maremma Park), which were excluded from the reference dataset.

### 3.2. Image classification

The maps resulting from crisp and fuzzy Random Forest classifications are shown in Fig. 3 and Fig. 4, respectively. The SAM and MESMA fuzzy classifications produced analogous results to the fuzzy Random Forests and the corresponding maps can be found in Supplementary Materials (Fig. S1 and S2).

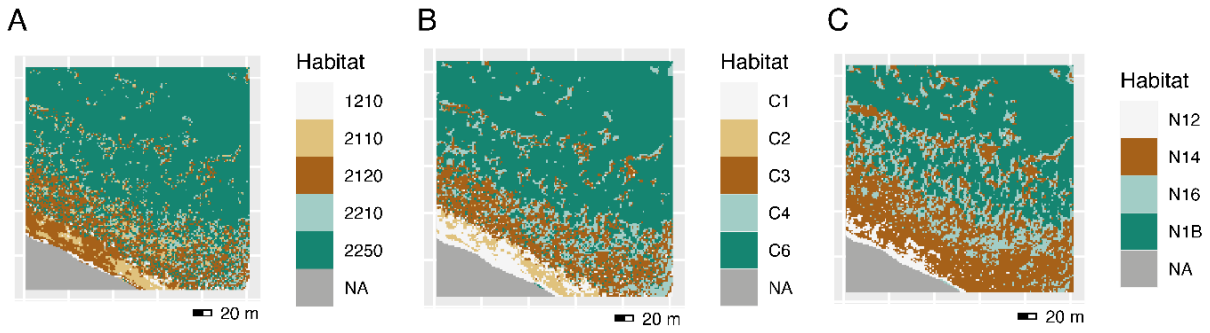


**Fig. 3.** Close-up of the crisp Random Forest classified maps in a portion of the Maremma Park. The represented classes correspond to expert-classified Annex I habitats (A), clusters obtained from noise clustering (B), and EUNIS habitats (C).

The results of classification accuracy assessment are in Fig. 5. In terms of overall accuracy (OA; Fig. 5A), the crisp approach produced higher values on average across the three habitat classifications (mean OA = 0.58) than all the fuzzy approaches, namely Random Forests (mean OA = 0.40), SAM (mean OA = 0.23), and MESMA (mean OA = 0.34). The only exception was the fuzzy Random Forest classification of EUNIS habitats in Maremma Park, which outperformed all other methods, achieving an accuracy rate of 0.90. Among the habitat classifications, EUNIS produced the highest accuracy (mean OA = 0.49), followed by HD (mean OA = 0.36) and noise clustering (mean OA = 0.32). Additionally, the Maremma Park generally achieved higher accuracy (mean OA = 0.43) than the MSRM Park (mean OA = 0.35).

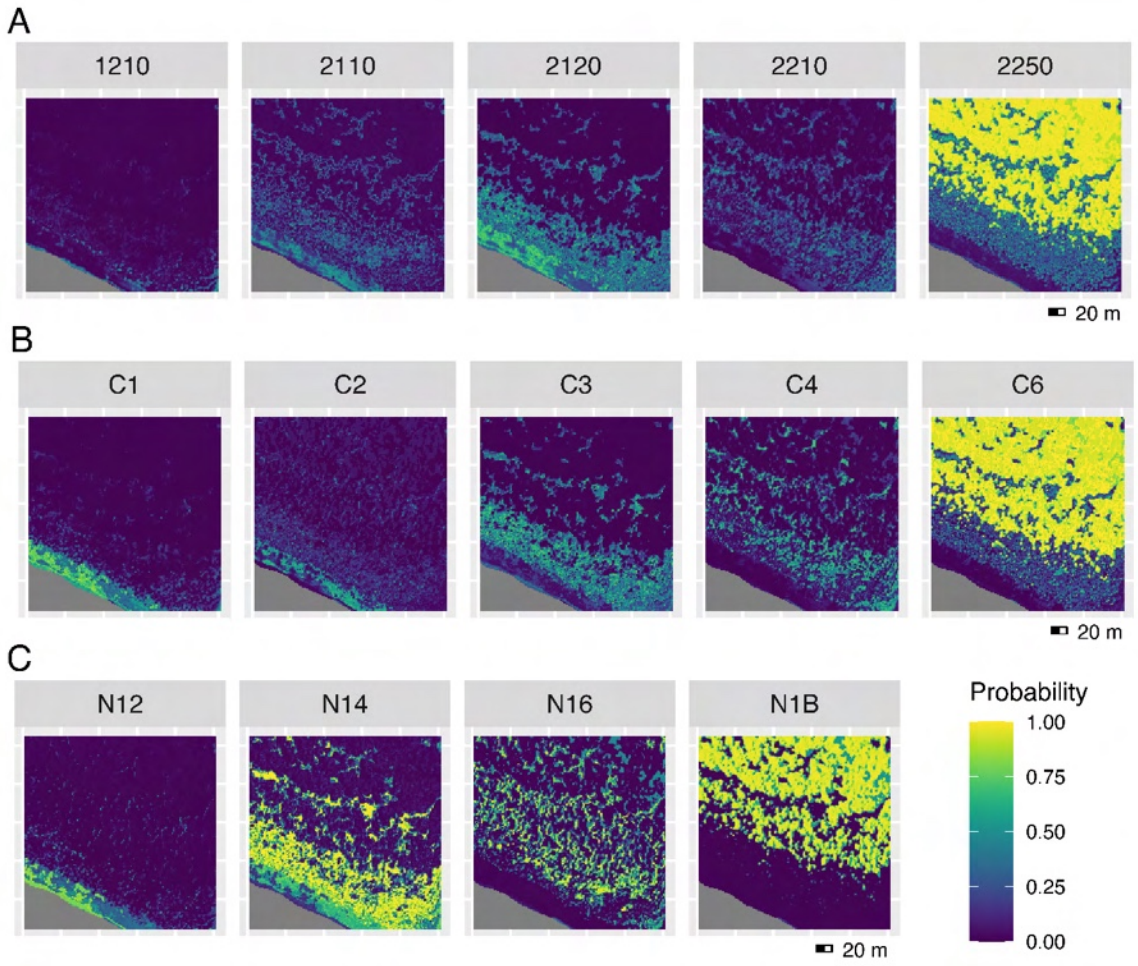


**Fig. 4.** Close-up of the fuzzy Random Forest classified maps in a portion of the Maremma Park. The represented classes correspond to expert-classified Annex I habitats (A), clusters obtained from noise clustering (B), and EUNIS habitats (C).

According to the Mantel R statistics (Fig. 5B), the biggest amount of information from the vegetation plots was retained by the fuzzy Random Forest classification (mean R = 0.38), followed by the crisp method (mean R = 0.36), and subordinately by SAM (mean R = 0.16) and MESMA (mean R = 0.02). The latter was the only method that consistently produced non-significant R values. The habitat classifications that preserved the highest degree of original information were noise clustering (mean R = 0.30) and expert-based HD classification (mean R = 0.26), while EUNIS had the biggest loss of information (mean R = 0.14).

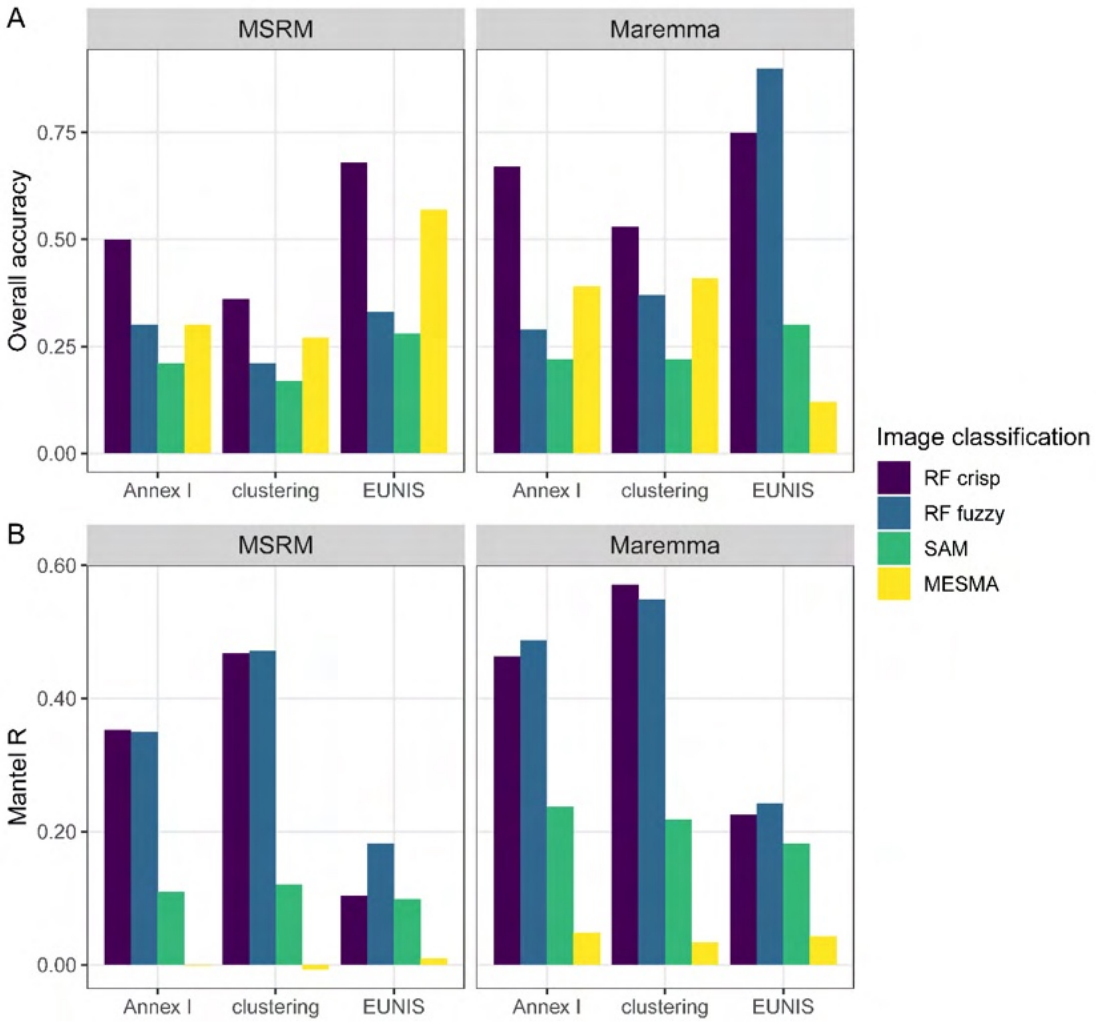


**Fig. 5.** Values of overall accuracy (A) and Mantel R statistic (B) for the classified maps obtained from different types of habitat classification and different methods of image classification, applied to the Migliarino-San Rossore-Massaciuccoli (MSRM) and Maremma Parks.

There was a marked difference in the accuracy associated with individual classes, and this also varied based on the classification method (Table 3). In most cases, the habitat of coastal dune scrubs (i.e., Annex I habitat 2250, cluster C6, EUNIS habitat N1B) reached the highest user's and producer's accuracy, followed by shifting dunes (i.e., Annex I habitat 2120, cluster C3, EUNIS habitat N14). Very low accuracy values were observed for the vegetation of drift lines (i.e., Annex I habitat 1210, cluster C1, EUNIS habitat N12), embryonic dunes (i.e., Annex I habitat 2110, cluster C2), and grasslands on fixed dunes (i.e., Annex I habitats 2210 and 2230, clusters C4 and C5, EUNIS habitat N16). Moreover, both user's and producer's accuracy were higher for each habitat in crisp compared to fuzzy classifications and were generally higher for EUNIS than for the other types of habitats.

**Table 3.** User's and producer's accuracy resulting for each class from each type of habitat classification and image classification, namely Random Forests (RF), Spectral Angle Mapper (SAM) and Multiple Endmember Spectral Mixture Analysis (MESMA), for the Migliarino-San Rossore-Massaciuccoli Park (MSRM) and for the Maremma Park (Mar).

User's accuracy

| | | RF crisp | | RF fuzzy | | SAM | | MESMA | |
|---|---|---|---|---|---|---|---|---|---|
| | Class | MSRM | Mar | MSRM | Mar | MSRM | Mar | MSRM | Mar |
| Annex I | 1210 | - | NA | - | 0.05 | - | 0.24 | - | 0.57 |
| | 2110 | 0.50 | 0.00 | 0.39 | 0.17 | 0.21 | 0.20 | 0.32 | 0.00 |
| | 2120 | 0.29 | 0.75 | 0.25 | 0.27 | 0.20 | 0.21 | 0.18 | 1.00 |
| | 2210 | 0.17 | 0.00 | 0.20 | 0.18 | 0.20 | 0.21 | 0.10 | 0.00 |
| | 2230 | NA | - | 0.16 | - | 0.21 | - | 0.43 | - |
| | 2250 | 0.82 | 0.83 | 0.45 | 0.42 | 0.22 | 0.24 | 0.33 | 0.37 |
| clusters | C1 | 0.00 | 1.00 | 0.20 | 0.75 | 0.18 | 0.25 | 0.32 | 0.67 |
| | C2 | 0.00 | 0.00 | 0.18 | 0.10 | 0.17 | 0.20 | 0.00 | 0.03 |
| | C3 | 0.22 | 1.00 | 0.15 | 0.47 | 0.17 | 0.21 | 0.12 | 0.51 |
| | C4 | 0.20 | 0.20 | 0.15 | 0.31 | 0.17 | 0.21 | 0.47 | 0.44 |
| | C5 | 0.42 | - | 0.29 | - | 0.17 | - | 0.61 | - |
| | C6 | 0.53 | 0.67 | 0.27 | 0.35 | 0.18 | 0.21 | 0.35 | 0.19 |
| EUNIS (level 3) | N12 | NA | 0.67 | 0.41 | 0.92 | 0.30 | 0.31 | 0.64 | 0.11 |
| | N14 | 0.67 | 0.80 | 0.24 | 0.79 | 0.26 | 0.28 | 0.40 | 0.11 |
| | N16 | 0.72 | 0.67 | 0.35 | 0.91 | 0.26 | 0.28 | 0.45 | 0.18 |
| | N1B | 0.00 | 1.00 | 0.80 | 1.00 | 0.30 | 0.34 | 0.54 | 0.03 |

Producer's accuracy

| | | RF crisp | | RF fuzzy | | SAM | | MESMA | |
|---|---|---|---|---|---|---|---|---|---|
| | Class | MSRM | Mar | MSRM | Mar | MSRM | Mar | MSRM | Mar |
| Annex I | 1210 | - | 0.00 | - | 0.01 | - | 0.23 | - | 1.00 |
| | 2110 | 0.33 | 0.00 | 0.25 | 0.15 | 0.21 | 0.21 | 0.64 | 0.00 |
| | 2120 | 0.33 | 1.00 | 0.35 | 0.39 | 0.20 | 0.21 | 0.07 | 0.06 |
| | 2210 | 0.25 | 0.00 | 0.25 | 0.10 | 0.20 | 0.21 | 0.05 | 0.00 |
| | 2230 | 0.00 | - | 0.06 | - | 0.21 | - | 0.03 | - |
| | 2250 | 0.75 | 0.83 | 0.60 | 0.79 | 0.21 | 0.24 | 0.69 | 1.00 |
| clusters | C1 | 0.00 | 0.50 | 0.11 | 0.40 | 0.18 | 0.23 | 0.66 | 0.86 |
| | C2 | 0.00 | 0.00 | 0.08 | 0.06 | 0.17 | 0.21 | 0.00 | 0.00 |
| | C3 | 0.25 | 0.75 | 0.21 | 0.39 | 0.17 | 0.21 | 0.25 | 0.37 |
| | C4 | 0.17 | 0.50 | 0.14 | 0.41 | 0.17 | 0.22 | 0.02 | 0.23 |
| | C5 | 0.56 | - | 0.31 | - | 0.17 | - | 0.21 | - |
| | C6 | 0.53 | 0.57 | 0.43 | 0.58 | 0.17 | 0.21 | 0.47 | 0.51 |
| EUNIS (level 3) | N12 | 0.00 | 1.00 | 0.02 | 0.84 | 0.30 | 0.30 | 1.00 | 0.14 |
| | N14 | 0.67 | 0.67 | 0.48 | 0.85 | 0.27 | 0.28 | 0.31 | 0.06 |
| | N16 | 0.76 | 0.67 | 0.58 | 0.96 | 0.27 | 0.29 | 0.09 | 0.23 |
| | N1B | 0.00 | 1.00 | 0.24 | 0.96 | 0.28 | 0.33 | 0.78 | 0.03 |

Maps of spatial uncertainty in the fuzzy Random Forest classifications for two sample areas are shown in Fig. 6, alongside maps of spectral heterogeneity computed as standard deviation. Since the other measures of uncertainty and heterogeneity produced similar results, the corresponding maps are provided in Supplementary materials (Fig. S3-S5). Generally, areas with higher spectral heterogeneity (typically located at the interfaces between herbaceous and shrub vegetation) exhibited a higher level of uncertainty in image classifications, and vice versa.

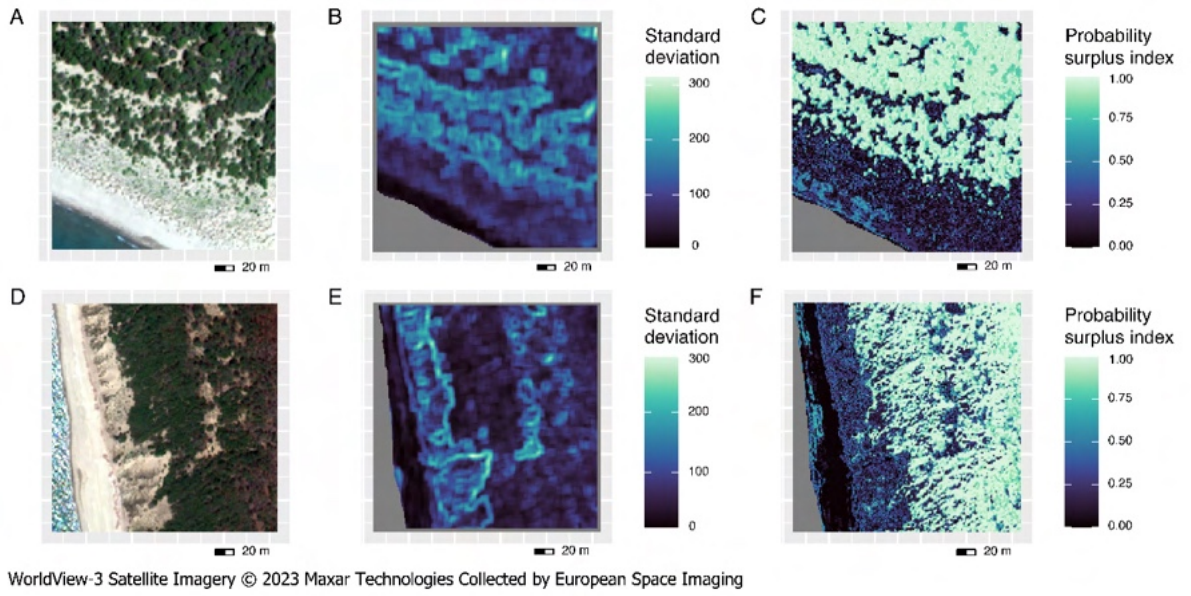


**Fig. 6.** Close-up of two areas: one more heterogeneous in the Maremma Park (A-C), and the other more homogeneous in the Migliarino-San Rossore-Massaciuccoli Park (D-F). For each area, a WorldView-3 true color composite is represented (A, D), along with a map of spectral heterogeneity (B, E) compared with a map of classification uncertainty (C, F). The former was calculated as the standard deviation of the first principal component of the image, while the latter was computed as the probability surplus index from the fuzzy Random Forest classification of Annex I habitats.

The results of the spectral PCA are shown in Fig. 7 for the Maremma Park and in Fig. S6 for the MSRM Park. Overall, plots assigned to different habitats based on vegetation data are grouped into distinct portions of the spectral PC space, although there is some overlap, especially between habitats of the embryonic and shifting dunes. Most plots designated as "mixed" based on vegetation data are situated in the central regions of the PC space and are assigned low habitat membership probabilities by the fuzzy classification.

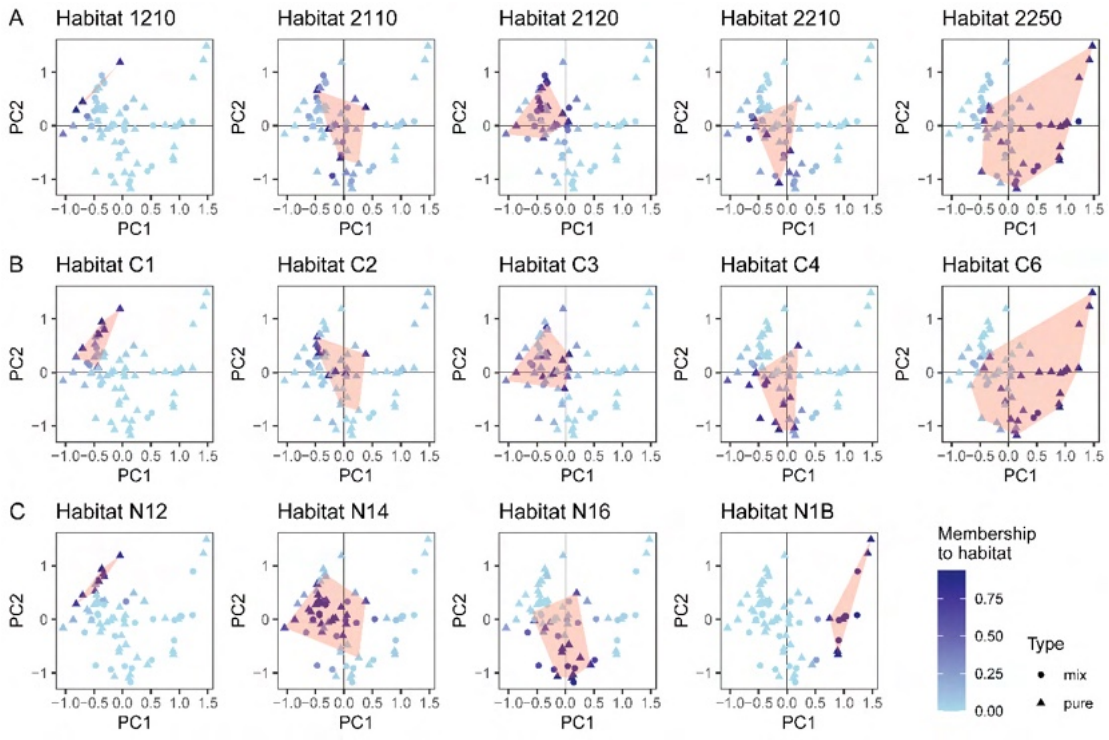


**Fig. 7.** Principal component analysis of the field-sampled plots on coastal dune habitats in the Maremma Park based on their spectral characteristics. Plots are represented with different shapes depending on whether they are identified as pure or mixed according to vegetation data, and are colored according to their probability of membership to each habitat as resulting from the fuzzy Random Forest classification for Annex I habitats (A), noise clusters (B) and EUNIS habitats (C). In each biplot, the red polygon indicates plots identified as belonging to a specific habitat based on vegetation data.

## 4. Discussion

Our study demonstrates for the first time the effectiveness of fuzzy classifications for mapping coastal dune habitats based on satellite imagery. We applied our approach to the two main habitat classification systems used in Europe for conservation purposes, i.e., HD and EUNIS, and found that EUNIS habitats can be mapped with greater accuracy. For the first time, we showed that fuzzy approaches to image classification are better suited to represent coastal dune habitats compared to the more common crisp approaches, as they account for the actual fuzziness of the vegetation mosaic.

### 4.1. Habitat classification: Habitats Directive and EUNIS

As expected, different habitat classification systems produced different results. Since the selection of a classification system influences the resulting map and any derived measures

(Tomaselli et al., 2016), it is important to understand the advantages and limitations of each classification. As it is known, there is no exact correspondence between Annex I and level 3 EUNIS habitats (Rodwell et al., 2018), with EUNIS habitats defining broader categories (Chytrý et al., 2020). In this study, the EUNIS system appeared more suitable for mapping coastal dune habitats since it resulted in a higher accuracy of image classification with respect to the HD system. This can be explained by the fact that the EUNIS system includes a smaller number of broader classes that are more easily identifiable since being more different between one another (Rapinel et al., 2014; Marzialetti et al., 2019). This was also confirmed by the higher spectral separability of EUNIS habitats, as revealed by the spectral PCA, which may also contribute to the higher accuracy of image classification. Few studies have directly compared the suitability of HD and EUNIS classification systems for habitat mapping: for example, Valentini et al. (2015) reported that habitats classified with the EUNIS system were more accurately mapped than those classified with the HD system in an estuarine area, because the latter included more and less well-defined classes.

Interestingly, a large portion of the reference data consisted of mixed plots that could not be assigned to a single Annex I or EUNIS habitat. This underscores the high heterogeneity of coastal dune vegetation and suggests that a fuzzy model may provide a more accurate representation compared to a crisp one even for habitat classification and description purposes. Notably, some studies have incorporated fuzziness into vegetation data by defining fuzzy communities (De Cáceres et al., 2010). For instance, this approach has been applied in wet grasslands (Rapinel et al., 2018), *Eucalyptus* woodlands (Duff et al., 2014), and peatlands (Räsänen et al., 2019). Mapping floristic gradients instead of communities can further improve the representation of vegetation patterns, as demonstrated in salt marshes (Unberath et al., 2019), urban forests (Gu et al., 2015), grasslands (Neumann et al., 2016), and peatlands (Räsänen et al., 2019). While these approaches enhanced vegetation mapping, they were not suitable for our study, which focused on specific habitat types of conservation interest.

As results from the spectral PCA, plots identified as mixed based on vegetation data generally also had an intermediate spectral response between multiple habitats. Conversely, some plots identified as pure showed spectral similarities with more than one habitat, resulting in a certain spectral overlap between habitats. As demonstrated by Amici (2011), crisp classes often have a high variability in fuzzy memberships. To overcome this issue, compromise vegetation typologies can be defined to improve spectral separability, but at the expense of the alignment

with HD or EUNIS habitat definitions (Rapinel et al., 2018).

### 4.2. Image classification: crisp and fuzzy

In this study, two main approaches for image classification were compared: a crisp approach and a fuzzy approach. As hypothesized, fuzzy maps captured a greater proportion of the variation in the original data, resulting in a more realistic representation of vegetation patterns compared to crisp maps. These approaches are better suited to capture the inherent fuzziness of landscapes (Rocchini et al., 2010; Triepke, 2017). Previous studies comparing crisp and fuzzy approaches have demonstrated the higher reliability of the latter, for example in coastal wetlands (Shanmugam et al., 2006) and grasslands (Rapinel et al., 2018).

Despite this, the overall accuracy of crisp classifications was higher. This counterintuitive result was also found by Feilhauer et al. (2021), who reported a 5% decrease in overall accuracy when transitioning from crisp to fuzzy Random Forests in an image classification of a mosaic of grasslands and bogs. It is important to note that comparing overall accuracy between crisp and fuzzy classifications might be misleading. The reference dataset used for measuring overall accuracy was formed by selecting only pure plots to adequately train the classification models, resulting in a reference dataset being crisper than the actual situation. In addition, accuracy metrics derived from a fuzzy confusion matrix are typically lower than crisp ones, because even slight levels of uncertainty for a reference pixel produce membership values lower than 1, thereby reducing the resulting accuracy metrics (Zlinszky & Kania, 2016).

Although fuzzy sets have been used for several decades in ecology (Roberts et al., 1986), including remote sensing studies (Foody, 1996), they remain underutilized for habitat mapping compared to crisp methods (Feilhauer et al., 2021). Recently, fuzzy classifications have been applied to represent vegetation ecotones in fynbos (De Klerk et al., 2018), wet grasslands (Rapinel et al., 2018) and peatlands (Räsänen et al., 2019). On coastal dunes, fuzzy approaches have been employed to map the relative proportions of sand and vegetation (Lucas et al., 2002; Shanmugam et al., 2003), monitor sand cover dynamics (Ettritch et al., 2018), map gradients of floristic composition (Unberath et al., 2019), and identify indicator species (Medina Machín et al., 2019; Durai et al., 2024). Building on this body of research, our study demonstrates for the first time the effectiveness of fuzzy classifications for mapping coastal dune habitats.

Among the fuzzy methods, Random Forests produced the best results, both in terms of overall

accuracy and proportion of information maintained by the classification. Random Forests are relatively robust to outliers and class imbalances (Kamusoko, 2019) and are currently one of the most powerful and most used machine learning classifiers (Maxwell et al., 2018; Listiani et al., 2022). Notably, most studies employing fuzzy approaches for habitat mapping have used spectral unmixing (Shanmugam et al., 2006; Dudley et al., 2015; Alvarez-Vanhard et al., 2020), convolutional neural networks (Carbonneau, Dugdale, et al., 2020), species distribution models incorporating environmental variables (Duff et al., 2014; Wiser et al., 2022), Bayesian-based probability algorithms (Amici, 2011; De Klerk et al., 2018) or unsupervised methods such as fuzzy k-means (Tapia et al., 2005). The usefulness of Random Forests has been highlighted in some studies (Räsänen et al., 2019; Feilhauer et al., 2021; Cruz et al., 2024), and our findings align with these results.

### 4.3. Applicability of the method

By using multispectral satellite imagery, our approach could be applied over broader spatial and temporal extents. The effectiveness of our method could also be tested with freely available, lower-resolution imagery like Sentinel-2 imagery. However, mapping small, fragmented habitats like those of coastal dunes would imply integrating higher-resolution data such as those collected with unmanned aerial vehicles (UAVs) to extract "pure" reference spectra (e.g. Alvarez-Vanhard et al., 2020). The fuzzy approach tested here for coastal dunes may also be applicable to other vegetation types characterized by environmental gradients or mosaics, such as riparian zones or grasslands, for which crisp approaches can be limiting (Rapinel et al., 2018).

A drawback of fuzzy approaches is that fuzzy maps can be more difficult to interpret for non-technical users compared to crisp maps (Duff et al., 2014). However, presenting fuzzy maps alongside crisp maps can help identify transitional areas and zones of uncertainty, providing a more comprehensive basis for management and decision-making (Feilhauer et al., 2021). Furthermore, because fuzzy maps represent probabilities, they can be easily interpreted as the percentage likelihood of a pixel belonging to a particular class (Rocchini, 2010). This makes them highly accessible and straightforward to understand, even for non-expert users.

In general, the overall accuracy for mapping coastal dune habitats in this study was high for EUNIS habitats (maximum value of 0.90) and moderate for Annex I and noise cluster habitats (maximum values of 0.67 and 0.53, respectively), with multiple classifications producing an

accuracy lower than 0.50. These findings are largely consistent with those of other studies using satellite data to classify broader vegetation classes. For instance, Marzialetti et al. (2019) used Sentinel-2 to map coarse physiognomic classes of dune vegetation with an accuracy of 0.79 assessed with visual checkpoints, which decreased to 0.53 when assessed with floristic data (similar to the reference data used in our study). They concluded that 10-m resolution images could only be used to distinguish herbaceous and woody vegetation. Rapinel et al. (2014) achieved an accuracy of 0.74 in mapping vegetation formations from WorldView-2 images. Timm and McGarigal (2012) mapped coastal land cover with an accuracy of 0.75. De Giglio et al. (2017) achieved an accuracy of 0.83 using WorldView-2 images to map large vegetation classes.

Our method provides a novel and effective approach to accurately map coastal dune habitats on a large scale. Due to the current limitations in imagery availability for large areas and the fine scale of coastal dune habitats, our sub-pixel approach can offer a valuable basis for monitoring and supporting conservation efforts (Delbosc et al., 2021). Technological advancements will likely enhance the accuracy of habitat mapping products with very high-resolution imagery. To date, this is enabling the application of deep learning models that extract multi-scale patterns, allowing even individual trees to be monitored (Beloiu et al., 2023; Brandt et al., 2025).

### 4.4. Limitations and uncertainties

Interestingly, we observed lower classification accuracy for the MSRM Park compared to the Maremma Park. This disparity may reflect an influence of anthropogenic pressure on habitat mapping: the generally worse conservation status of MSRM Park likely complicated habitat assignment based on vegetation data (Sarmati et al., 2019) and resulted in a higher proportion of mixed plots. Additionally, temporal differences in image acquisition could have played a role. Images were selected to align with the period of field surveys and to ensure consistent phenological phases, a critical factor to relate spectral reflectance to species composition (Feilhauer & Schmidtlein, 2011). However, it was not possible to retrieve two images from the same year. Thus, another reason for the worst performance of our method in the MSRM Park might have been a longer time lag between field sampling and image acquisition, so that this study area might have been affected by slightly faster transformation dynamics related to anthropogenic disturbance.

Errors in the georeferencing of reference data are another major source of error in remote sensing studies (Foody, 2009; Persson et al., 2022). Here, we minimized this error by verifying plot positions on an orthophoto after acquiring the GPS position in the field, although some emerging approaches also suggest the possibility to address imperfect training data (Meerdink et al., 2024). Moreover, we only tested our method using one plot size, which was selected based on previous research on coastal dunes (e.g. Carboni et al., 2011) and aligned with the resolution of satellite imagery. In the future, a multiscale analysis could be useful to detect the most appropriate plot and pixel sizes for these ecosystems (Wang et al., 2001).

We analyzed the spatial uncertainty of classifications in relation to spectral heterogeneity, finding that areas with higher heterogeneity tended to exhibit higher classification uncertainty. This observation aligns with prior research, which demonstrated the negative impact of spectral heterogeneity in training data on classification accuracy (Villoslada et al., 2020). This is especially the case where sand and vegetation pixels are mixed (Smyth et al., 2022). However, classification uncertainty may also arise from the presence of heterogeneous conditions in the field, where no single class is clearly predominant. In such cases, spectral heterogeneity can provide an insight into where the fuzziest situations occur and possibly guide sampling efforts to better understand them (Tapia et al., 2005; Zlinszky & Kania, 2016).

Class-specific accuracy metrics highlighted a large difference in classification performances for different habitats. Automatic classification methods are generally more effective for habitats with distinctively dominant species in terms of cover, and less for habitats characterized by a higher species equitability and species with low growth-form (Bell et al., 2015). In our case, coastal dune scrubs generally achieved the highest accuracy, likely because it is a shrubland with high vegetation cover dominated by *Juniperus* spp., clearly differentiated from herbaceous vegetation at both functional level (defined by functional traits such as specific leaf area, leaf dry matter content, and water potential at turgor loss point) and spectral level (defined by spectral bands) in coastal dunes (Beccari et al., 2024). Another habitat mapped with high accuracy was the shifting dunes with *Calamagrostis arenaria* subsp. *arundinacea*. This species forms large tussocks, taller than the other dune species (Torca et al., 2019), which exhibit distinct colors, particularly during the flowering season (Cruz et al., 2023). By contrast, habitats like vegetation of drift lines and fixed dunes grasslands were mapped with much lower accuracy. This is possibly due to their sparse vegetation cover, which increases the interference from bare soil (Prudnikova et al., 2019), or their generally smaller

extent. Moreover, these habitats are characterized by annual species with small size (Torca et al., 2019), which complicates their detection using remotely sensed data (Medina Machín et al., 2019).

## 5. Conclusion

Our work provides a novel and effective tool in the context of the conservation and monitoring of EU habitats, which will allow practitioners to improve habitat detection and identification while reducing the economic and physical efforts needed for their search and sampling in the field. We developed a useful technique to create high-resolution habitat maps on coastal dunes, some of the most highly threatened ecosystems worldwide, at a level of detail never achieved with satellite imagery. Our approach, which could be applied at any scale from local, to regional, national or beyond, addresses the pressing need to develop objective and repeatable tools for habitat monitoring. In this context, it will be especially useful to monitor the habitats area of occupancy, a crucial parameter for assessing habitat conservation status under the HD.

We further confirmed the effectiveness of fuzzy approaches in capturing ecological gradients and mixed vegetation types often overlooked by traditional crisp methods.

As a future research direction, these approaches can be compared with deep learning methods such as convolutional neural networks, to assess their potential for producing better results.

## Data availability

The data and code supporting this study are available at: https://doi.org/10.17632/b9vn8mvhk6.1. An example of code usage is provided at: https://github.com/emiliapafumi/fuzzy-dunes.git. Plot data are included in the SALTISH dataset (Gholizadeh et al., 2025). Due to specific license agreements, the WorldView-3 data are not available for sharing, but can be requested from https://earth.esa.int/eogateway/missions/worldview-3 after approval of a data request to the European Space Agency.

## Acknowledgements

E. Pafumi, C. Angiolini, E. Fanfarillo, S. Sarmati and S. Maccherini were funded under the National Recovery and Resilience Plan (NRRP), Mission 4 Component 2 Investment 1.4 - Call

for tender No. 3138 of 16 December 2021, rectified by Decree n.3175 of 18 December 2021 of Italian Ministry of University and Research funded by the European Union – NextGenerationEU; Award Number: Project code CN_00000033, Concession Decree No. 1034 of 17 June 2022 adopted by the Italian Ministry of University and Research, CUP B63C22000650007, Project title “National Biodiversity Future Center - NBFC”. The research was also supported by the Tuscany region - Project “NaTNet” – Natural Tuscany Network CUP D54I19001090002. WorldView-3 data were provided by the European Space Agency (ESA) within its Third Party Missions programme.

# Chapter 3

## Pixels and patterns in the sand: decoding coastal dune habitats with multi-resolution CNNs

Emilia Pafumi[1,2]*, Claudia Angiolini[1,2], Giovanni Bacaro[3], Leopoldo de Simone[1], Emanuele Fanfarillo[1,2], Tiberio Fiaschi[1], Duccio Rocchini[4,5], Elisa Thouverai[3], Simona Maccherini[1,2]

[1]Department of Life Sciences, University of Siena, Via P.A. Mattioli 4, 53100 Siena, Italy; [2]NBFC, National Biodiversity Future Center, 90133 Palermo, Italy; [3]Department of Life Sciences, University of Trieste, Via L. Giorgieri 10, 34127 Trieste, Italy; [4]BIOME Lab, Department of Biological, Geological and Environmental Sciences, Alma Mater Studiorum University of Bologna, Via Irnerio 42, 40126 Bologna, Italy; [5]Czech University of Life Sciences Prague, Faculty of Environmental Sciences, Department of Spatial Sciences, Kamýcka 129, Praha - Suchdol 16500, Czech Republic

*Corresponding author

*Under review as:*

Pafumi E, Angiolini C, Bacaro G, de Simone L, Fanfarillo E, Fiaschi T, Rocchini D, Thouverai E, Maccherini S. Pixels and patterns in the sand: decoding coastal dune habitats with multi-resolution CNNs.

## Abstract

Mapping coastal dune habitats through remote sensing is crucial for biodiversity conservation, but it is challenging due to the small and fragmented nature of habitat patches relative to the spatial resolution of available imagery. Convolutional Neural Networks (CNNs), by leveraging both spectral and spatial information, offer a promising solution, but their application to coastal dunes remains limited. This study evaluates CNN performance for coastal dune habitat mapping using spectral data with varying spatial resolutions: Unmanned Aerial Vehicle (UAV; 0.02 m), airborne (0.20 m), Google Earth (0.30 m), and WorldView-3 imagery (0.40 m). Ground truth data were collected in 4 $m^2$ plots in Tuscany (Italy) and supplemented with photo-interpreted points, representing five classes: shifting dunes (EUNIS habitat N14), dune grasslands (N16), dune scrubs (N1B), bare sand, and sea. For each remote sensing dataset, one CNN was trained on RGB imagery and another including additional spectral bands, where available. Most maps achieved high accuracy, confirming the effectiveness of CNNs for habitat mapping. Accuracy of RGB-derived maps declined with coarser resolution, from UAV (88%) to airborne (86%), Google Earth (80%) and WorldView-3 (38%). Including additional spectral bands had varying effects on accuracy (+6% for UAV, +7% for airborne, +25% for WorldView-3). Among habitats, dune scrubs were mapped most accurately, while shifting dunes were often confused with bare sand. These findings underscore the value of very high-resolution imagery for habitat mapping with CNNs, suggesting that even Google Earth imagery can support broader-scale applications when UAV or airborne data are unavailable.

**Keywords:** Biodiversity, Coastal dunes, Convolutional Neural Networks, Deep Learning, Habitat mapping, Remote sensing, Spatial resolution

# 1. Introduction

Biodiversity mapping is a crucial task: although maps cannot faithfully represent reality, they serve essential practical purposes, such as guiding conservation efforts (Malavasi, 2020). Habitat maps are particularly important in Europe, where many conservation policies, including the Habitats Directive (92/43/EEC), require the identification and mapping of habitats as key units for protection. Remote sensing, by providing quantitative data over large spatial and temporal scales, has significantly advanced habitat mapping (Kerry et al., 2022). However, the suitability of remote sensing data remains strongly dependent on spectral, spatial and temporal resolution: fine habitat differentiation generally requires multiple spectral bands to improve spectral separability, but this often comes at the expense of spatial detail or temporal frequency, which are relevant for complex landscapes (Corbane et al., 2015). In this study, we focus primarily on the issue of spatial resolution.

Coastal dune habitats are both highly threatened and challenging to map, due to their typically small and fragmented patches (Acosta et al., 2007). Recent studies have explored automatic approaches for dune habitat mapping, testing remote sensing data with varying spatial resolutions (Delbosc et al., 2021). The highest detail is currently provided by Unmanned Aerial Vehicles (UAVs), which have been used to map land cover (Suo et al., 2019), plant communities (De Giglio et al., 2019; Agrillo et al., 2023; Cruz et al., 2023; Innangi et al., 2025), and even single species (Marzialetti et al., 2021; Innangi et al., 2023; Belcore et al., 2024). However, these studies are limited to a local scale, and it remains critical to assess the trade-off between spatial resolution and broader-scale applicability. Free satellite data only allow to map broad land cover classes (Marzialetti et al., 2019; Latella et al., 2021), while commercial satellites often enable more accurate mapping but are constrained by high acquisition costs (De Giglio et al., 2017; Pafumi et al., 2025). Recently, free Google Earth imagery has also been tested for specific vegetation types, such as bamboo forests (Watanabe et al., 2020) or scrub habitats (Guirado et al., 2017). However, its limited spectral information (RGB only) necessitates advanced classification methods for distinguishing habitats.

In recent years, machine learning has opened new possibilities for ecological applications (Cipriano et al., 2025), especially in remote sensing (Cresson, 2020). Among these methods, deep learning stands out for its ability to automatically extract complex features from raw data (LeCun et al., 2015). Specifically, Convolutional Neural Networks (CNNs) are well suited for

image classification tasks, as they exploit the hierarchical structure of images to extract high-level features (e.g., edges and patterns) from low-level inputs (e.g., pixel intensities), thus leveraging both spectral information and spatial context and improving ecological mapping performance (Kattenborn et al., 2019). The effectiveness of CNNs has been demonstrated in various applications, especially with very high-resolution data, like UAV (Schiefer et al., 2020) or airborne imagery (Carbonneau, Dugdale, et al., 2020). Despite their growing use, CNNs remain poorly explored in the context of coastal dune habitats, and few studies have systematically assessed how their performance varies with spatial resolution.

This study addresses this gap by testing CNN-based habitat mapping in coastal dunes across four remote sensing datasets with decreasing spatial resolution: UAV imagery (0.02 m), airborne imagery (0.20 m), Google Earth imagery (0.30 m), and WorldView-3 satellite imagery (0.40 m). For each dataset, we assess CNN performance using RGB bands only and then test the added value of including additional spectral bands, where available.

## 2. Materials and methods

### 2.1. Study area

The study was carried out in the sandy beach of Collelungo in Tuscany (Italy; Fig. 1). The site is inside the Maremma Regional Park and the Special Area of Conservation “Dune costiere del Parco dell'Uccellina” (IT51A0015). The climate is Mediterranean, with an upper meso-mediterranean thermotype and an upper dry ombrotype (Pesaresi et al., 2017). Vegetation follows the typical coastal dune zonation, with annual vegetation of drift lines closer to the sea, followed by shifting dunes, stable dune grasslands and dune scrubs moving inland (Acosta et al., 2007; Tordoni et al., 2019, 2021; Beccari et al., 2024; Sarmati et al., 2025).

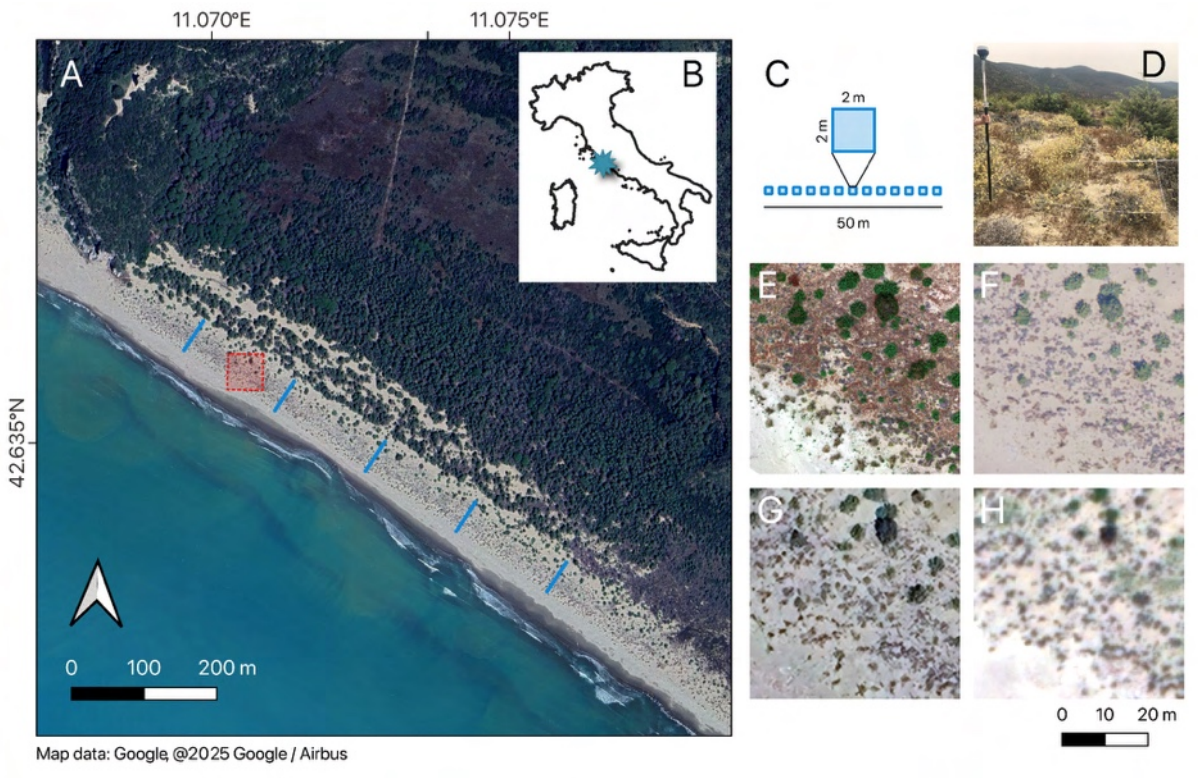


**Fig. 1.** Study area with field surveyed transects represented in blue (A), its position in Italy (B), a transect scheme (C), an example of surveyed plot (D) and close-up views of the remote sensing datasets used: UAV (E), airborne (F), Google Earth (G), and WorldView-3 (H). The area in the close-up views is indicated with a red square in A.

### 2.2. Ground truth data

Ground truth data were collected during vegetation surveys in June 2024 over an area of c. 4 ha. Five transects of fixed length (50 m) were placed perpendicularly to the coastline at 150 m from one another, with the first transect located 100 m from the beginning of the beach. Along each transect, 13 squared plots of 2 m x 2 m were placed, each at 4 m from the other, for a total of 65 plots. We measured coordinates at the top-left and bottom-right vertices of each plot along the sea-upland direction of each transect. Two EMLID Reach RS2 GNSS units were used for this purpose, one as a base station and one as a rover, connected for Real-Time Kinematic (RTK) survey with a local accuracy of 0.001 m. Since network communication in the area was insufficient, acquired coordinates were subsequently used for a Post-Processed Kinematic (PPK) survey using the EMLID Studio software. The coordinates were calculated in the WGS84 reference system (EPSG: 4326), with PPK processing based on RTCM3 positional data of the Leica SmartNet network of reference stations (GROK site, with a baseline

of approximately 18 km). After PPK corrections, plot coordinates had an RMS horizontal accuracy of less than 1 cm.

In each plot, vascular plant species occurrence and abundance (visually estimated % cover) were recorded. Plots were assigned to EUNIS habitats at the third level of detail based on their species composition using the EUNIS Expert System (Chytrý et al., 2020; Bruelheide et al., 2021). Three habitats were considered: “Mediterranean, Macaronesian and Black Sea shifting coastal dune” (N14), “Mediterranean and Macaronesian coastal dune grassland (grey dune)” (N16), and “Mediterranean and Black Sea coastal dune scrub” (N1B). Plots not assigned to any habitat or classified into other habitat types (specifically, N12 - “Mediterranean and Black Sea sand beach”, N1G - “Mediterranean coniferous coastal dune forest”, and “Sb - Dwarf-shrub vegetation”) were excluded from the reference dataset, as their number was too small to be considered in the analysis.

To improve the ground truth dataset and compensate for class imbalance, additional 2 m x 2 m squares were identified through photo interpretation of the highest-resolution image. The final dataset consisted of 500 squares assigned to five classes: habitat N14, N16, N1B, bare sand, and sea.

A workflow scheme of the analyses, from data collection to CNN segmentation, is in Fig. 2.

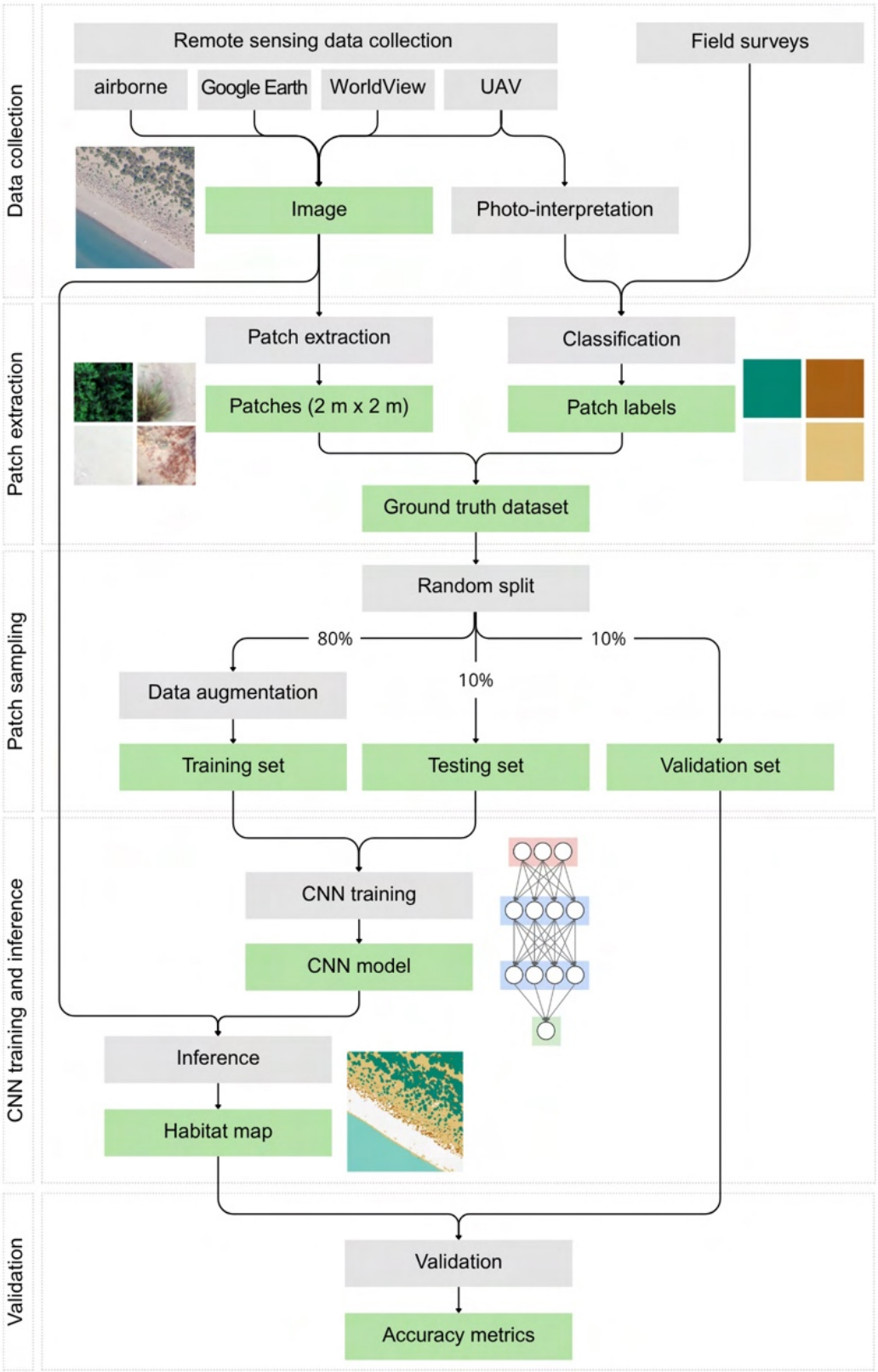


**Fig. 2.** Workflow scheme of the analyses.

## 2.3. Remote sensing data collection and pre-processing

### *2.3.1. UAV imagery*

The UAV photogrammetric survey was carried out on 20 June 2024, simultaneously with the vegetation surveys. This study adopted a low-altitude UAV, the DJI Matrice 300 RTK, equipped with the MicaSense Altum-PT multispectral camera (MicaSense Inc., Seattle, DC, USA). We used five out of seven sensors of the camera, each with a resolution of 2064 × 1544 pixels (≈ 3.2 MP per band), covering five discrete spectral bands: blue (center 475 nm, bandwidth ± 32 nm), green (560 ± 27 nm), red (668 ± 14 nm), red edge (717 ± 12 nm), and near-infrared (842 ± 57 nm). Prior to the flight, we placed the calibrated reflectance panel CRP2 on a flat, leveled surface within the mapping area. We used the Altum-PT to capture images of the panel under the same sunlight conditions as the planned survey, allowing radiometric calibration of multispectral data. Simultaneously, the downwelling light sensor DLS2 was used to record irradiance and sun-angle data for subsequent correction in processing. Flight observation was carried out between 13:00 and 14:00 (UTC+2). The flying height was set at 45 m, achieving a Ground Sampling Distance (GSD), or spatial resolution, of 1.94 cm/pixel. Both image frontal and side overlap were set at 75%, which is essential for the image matching algorithms in Structure-from-Motion software (Eltner et al., 2016). Before the acquisition of the images, six Ground Control Points (GCP), three of which were used afterwards as Check Points (CP), were distributed in the study area and surveyed. The center of each GCP coordinate was acquired using the same methodology of the vegetation plots (see 2.2. Ground truth data).

After the flight, UAV data were processed in Agisoft Metashape Professional v 2.1.0, applying radiometric corrections to all the 1,046 acquired images using both the reflectance panel and the DLS2 sensor data. After image alignment, a five-band orthomosaic was generated, with a final output size of 40,300 x 29,430 pixels. The orthomosaic was referenced in WGS84 / UTM Zone 32N (EPSG: 32632), with a CP horizontal Root Mean Square Error (RMSE) of 2.46 cm.

### *2.3.2. Airborne imagery*

An airborne orthophoto from 25 August 2023 was downloaded from the regional open dataset (Regione Toscana, 2023). The image was acquired using Leica DMC4 and DMC3 sensors with four spectral bands, i.e. red (580-660 nm), green (480-590 nm), blue (420-510 nm), and near-

infrared (720-850 nm), with a spatial resolution of 0.20 m.

#### *2.3.3. Google Earth imagery*

RGB imagery was downloaded from Google Earth Pro 7.3.6 (Google, 2025). Among the available images, the one with the closest date to the field surveys was chosen, i.e., a Pléiades Neo satellite image from 26 April 2023, with a spatial resolution of 0.30 m (Airbus, 2023). The image was downloaded from Google Earth Pro at an eye altitude of 1 km, corresponding to a pixel size of c. 0.14 m.

#### *2.3.4. WorldView-3 imagery*

A multispectral image from WorldView-3 satellite was acquired on 16 May 2019. The image includes one panchromatic band at 0.40 m spatial resolution (center wavelength: 649 nm) bundled with eight spectral bands at 1.60 m resolution: coastal blue (427 nm), blue (482 nm), green (547 nm), yellow (604 nm), red (660 nm), red-edge (723 nm), near-infrared 1 (824 nm), and near-infrared 2 (914 nm). Images were delivered at the 3D-level of processing, i.e. orthorectified, sensor-corrected and radiometrically corrected through dark offset subtraction and non-uniformity correction (Kuester, 2016), with a reported geolocation accuracy < 3.0 m CE90.

To improve spatial resolution of WorldView-3 images, multispectral bands were pansharpened using the cubic resampling algorithm. To correct for a slight misalignment between datasets, images were reprojected with UAV data as reference. These steps were carried out in QGIS 3.40.8 (QGIS Development Team, 2024).

### 2.4. Semantic segmentation using CNNs

For the semantic segmentation of images into dune habitats, we applied CNNs based on U-Net architecture, a widely used model, specifically developed to perform well with few training images (Cresson, 2020). U-Net is an encoder-decoder architecture which consists of a contracting path with convolutional layers, followed by a symmetric expanding path with transposed convolutions (Ronneberger et al., 2015). In this study, CNN architecture was optimized by testing different values of key parameters (i.e., number of layers, kernel sizes, stride). The final structure comprises three convolutional layers and three symmetric deconvolutional layers (Fig. S1). Convolutions use a 3x3 kernel with stride 1, padding “same”,

and HeNormal initialization to reduce the vanishing gradient and stabilize the network. To efficiently reduce and restore spatial dimensions in the UAV dataset, max pooling and transposed convolutions with a stride of 2 were employed. For the other datasets, we used a stride 1 throughout the network and omitted pooling layers to avoid excessive downsampling. After each (de)convolutional layer, a ReLu activation and a Batch Normalization layer are applied, respectively to compute the node output and reduce the internal covariate shift. A final argmax layer assigns each pixel to the most probable class.

To assess the effect of spatial resolution on classification accuracy, an independent CNN was trained for each remote sensing dataset using RGB images as input. Then, to assess the effect of adding spectral bands, additional CNNs were trained on multispectral images, for all datasets except Google Earth, which only includes RGB bands, for a total of seven CNN models (Table 1, Fig. S2).

Patches were extracted with the same size as the field sampled plots (2 m x 2 m), thus with a different number of pixels according to the resolution of the data used. In each case, patches were randomly split into 80% training, 10% testing and 10% validation. To artificially increase the training dataset, data augmentation was performed by adding two preprocessing layers (random flips and random rotations).

Training was performed using gradient descent on the loss function (categorical cross entropy) with Adam optimizer, setting 50 epochs, a batch size of 8 and a learning rate of 0.0002.

CNNs were built and trained using Orfeo ToolBox Tensor Flow (OTBTF; Cresson, 2019), a remote module of the Orfeo ToolBox open-source library (Grizonnet et al., 2017), that allows to integrate deep learning models into remote sensing workflows by using the TensorFlow platform for machine learning (Abadi et al., 2015) through its high-level Keras API (Chollet, 2015). The `pyotb` library was used as a Python wrapper for Orfeo ToolBox applications, enabling seamless integration of OTB's remote sensing processing capabilities within Python-based workflows.

**Table 1.** List of CNNs trained in this study with different types of remote sensing data.

| Data | Spatial resolution (m) | Input spectral bands | CNN |
|---|---|---|---|
| UAV | 0.02 | RGB | CNN-01 |
| | | multispectral | CNN-02 |
| airborne | 0.20 | RGB | CNN-03 |
| | | multispectral | CNN-04 |
| Google Earth | 0.30 | RGB | CNN-05 |
| WorldView-3 | 0.40 | RGB | CNN-06 |
| | | multispectral | CNN-07 |

### 2.5. Validation

The accuracy of the output maps was assessed using the validation ground truth dataset, computing the following validation metrics: 1) overall accuracy, i.e. the percentage of correctly classified pixels; 2) precision, i.e. the proportion of true positives over all classified positives, also known as user's accuracy in traditional remote sensing studies; 3) recall, i.e. the proportion of true positives over all actual positives, also known as producer's accuracy; and 4) F1-score, i.e. the harmonic mean of precision and recall (Maxwell et al., 2021).

To assess whether a post-processing step could improve output maps, we applied a sieve filter, which reduces the salt-and-pepper effect. We tested different sieve values on UAV-derived maps: 25 pixels (i.e., remove patches < 0.01 $m^2$ assigning those pixels to the neighboring class), 100 pixels (i.e., remove patches < 0.04 $m^2$), and 250 pixels (i.e. remove patches < 0.10 $m^2$), and compared the resulting map accuracy metrics.

## 3. Results and discussion

Habitat maps produced through segmentation of RGB imagery are in Fig. 3, while those derived from multispectral imagery are in Fig. S3. Despite visible differences in terms of resolution and noise, in most cases the typical sea-inland succession can be recognized (Fig. S4), with bare sand and shifting dunes closer to the sea, followed by stable dune grasslands intermixed with dune scrubs (Acosta et al., 2007), reflecting the typical changes in

environmental conditions and plant diversity along the sea-inland gradient (Torca et al., 2019; Tordoni et al., 2021).

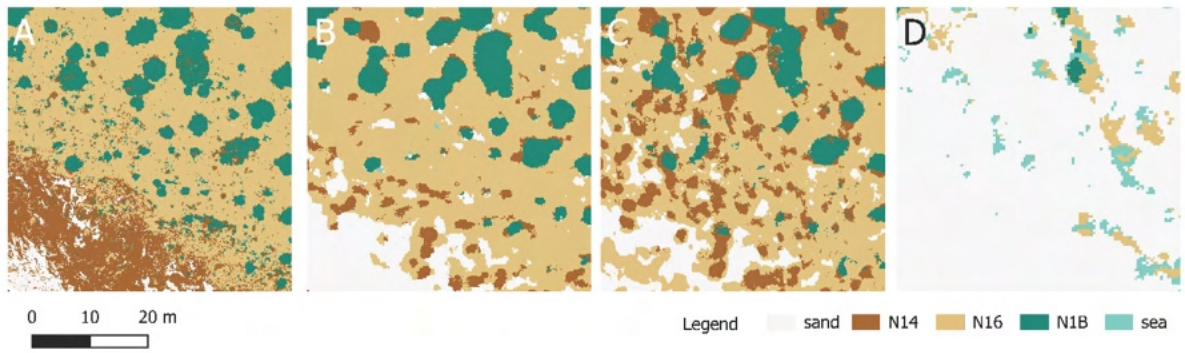


**Fig. 3.** Close-up views of the habitat maps produced through CNN segmentation of RGB imagery from four datasets: UAV (A), airborne (B), Google Earth (C), and WorldView-3 (D).

Overall, four out of seven maps had a high accuracy (>85%), confirming the potential of CNNs for habitat mapping (Fig. 4). To our knowledge, this is one of the first studies assessing CNNs to map habitats on coastal dunes. For comparison, Suo et al. (2019) mapped land cover with a maximum likelihood classifier achieving 69% accuracy with RGB and 78% with multispectral UAV imagery. Agrillo et al. (2023) reached 78% accuracy combining UAV data with environmental predictors in a Random Forest model. Similarly, Laporte-Fauret et al. (2020) applied Random Forest to hyperspectral data, producing vegetation maps with 83% accuracy.

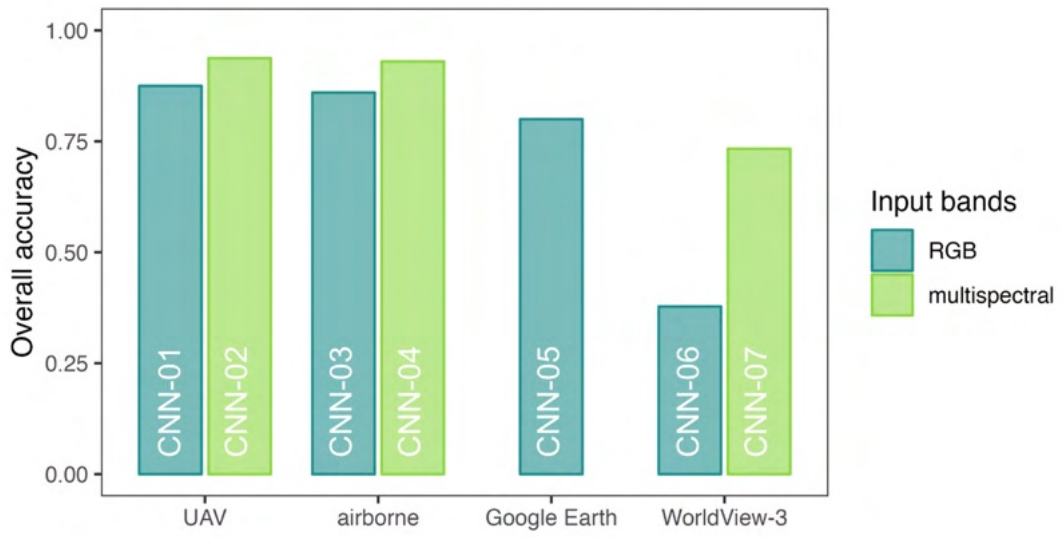


**Fig. 4.** Overall accuracy of the CNN-classified maps.

A key finding of this study is the consistent decline in CNN performance with decreasing spatial resolution: accuracy of RGB-based maps dropped from 88% (UAV) to 86% (airborne), 80% (Google Earth) and 38% (WorldView-3). This trend is in line with previous research on CNNs: for example, tree mapping accuracy in a temperate forest decreased from 89% at 0.02 m to 62% at 0.32 m (Schiefer et al., 2020), while in a bamboo forest from 93% at 0.13 m to 74% at 0.65 m (Watanabe et al., 2020).

This resolution effect suggests that only hyperspatial imagery, i.e., imagery with pixels much smaller than target objects, can reveal the fine-scale patterns that CNNs exploit to identify objects, such as branching structures for trees (Schiefer et al., 2020). Notably, the benefits of hyperspatial data do not apply to all methods. For example, conventional spectral-based classifiers may perform worse with higher-resolution data due to high intra-class spectral variability (e.g., sunlit and shaded leaves of the same tree having different reflectance), which reduces spectral separability (Nagendra & Rocchini, 2008). Conversely, their performance can improve as resolution decreases and spectral separability increases (De Giglio et al., 2017), until mixed pixels become prevalent, at which point pixel-based fuzzy classifications may be preferable (Pafumi et al., 2025).

Additionally, the negative impact of low spatial resolution on CNN performance may be amplified by an indirect effect: to match field plot sizes, patches extracted from lower-resolution imagery had a smaller number of pixels. Smaller tile sizes can increase the edge effect caused by the moving window approach of CNNs, as noted by Schiefer et al. (2020), although they reported only minor performance differences across tile sizes (128, 256, 512 pixels).

Interestingly, including additional spectral bands had only a minor positive effect on mapping accuracy at very high resolutions (+6% for UAV, +7% for airborne), while the effect was greater at coarser resolutions (+25% for WorldView-3). This suggests that spatial patterns may be more informative than spectral reflectance for mapping at very high resolutions, as previous research has found (e.g., Carbonneau, Dugdale, et al., 2020), highlighting the value of relatively inexpensive RGB sensors on UAVs.

We observed a marked difference in classification performance among habitats, especially at coarser resolutions (Appendix S5). Dune scrubs (habitat N1B) were mapped with the highest precision and recall, as in other studies (Marzialetti et al., 2019; Pafumi et al., 2025). Stable

dune grasslands (N16) also reached relatively high values, while shifting dunes (N14) often achieved a precision similar to N16 but a low recall, mostly due to confusion with bare sand (Appendix S6, S7). These two habitats showed the greatest decline in accuracy with decreasing resolution, probably because the fine-scale patterns exploited by CNNs were no longer discernible, also due to their lower vegetation cover (Appendix S8).

Furthermore, we found that a simple post-processing step reduced the salt-and-pepper effect in the highest-resolution maps, slightly improving accuracy (Appendix S9, S10). However, the advisability of applying this step, including the choice of optimal filter size, depends on the application, and more sophisticated methods could be explored (Chen et al., 2018).

Although this study focused on a single site, the findings have broader implications for large-scale applications. Ideally, extensive UAV surveys would provide the most accurate habitat maps for coastal dunes. Thanks to the high spatial detail of these images, field sampling efforts can also be reduced: we surveyed a relatively small number of plots (65 plots over 4 ha) and then expanded the ground truth dataset through photo interpretation. Notably, several studies have reported higher accuracy using visually delineated ground truth from imagery compared to field-based data, due to reduced spatial inaccuracy and sampling bias (Marzialetti et al., 2019; Kattenborn et al., 2019). However, field surveys remain necessary to relate vegetation features to their appearance in imagery, especially if plot locations are recorded with high precision simultaneously with UAV acquisition, as in this work, thus minimizing spatial misalignment.

Despite these advantages, UAVs are currently not appropriate for covering broad spatial extents, such as the whole Italian coastline, due to the required costs and expertise. Nonetheless, UAV-based research has been increasing in the last years (e.g., De Giglio et al., 2019; Malavasi et al., 2021; Marzialetti et al., 2021; Agrillo et al., 2023; Belcore et al., 2024; Innangi et al., 2025), and new possibilities could be opened in the future.

As an alternative, our study showed that airborne and Google Earth imagery can still offer reliable maps, though only the latter is currently available at the national level. Based on these results, a national-scale test of CNNs using these data will be the next step in research. It is important to note, however, that the transferability of CNNs across sites can vary, from low (Watanabe et al., 2020) to high (Carbonneau, Dugdale, et al., 2020; Schiefer et al., 2020), indicating the need for future studies to specifically assess CNN transferability in coastal dunes.

## 4. Conclusion

This study emphasizes the efficacy of CNNs for mapping coastal dune habitats and offers a pioneering analysis of the influence of remote sensing data's spatial resolution on CNN performance. Very high-resolution UAV imagery was confirmed as the most valuable data to produce accurate habitat maps, revealing fine-scale spatial patterns which are essential for CNNs. With coarser-resolution datasets, mapping accuracy clearly declined, while the inclusion of additional spectral bands became more beneficial. Despite not being the ideal solution, airborne and Google Earth data still supported high-accuracy maps (>80%), suggesting potential for cost-effective, broader-scale applications, once CNN transferability across dune systems has been further explored. By assessing CNN applicability across multiple remote sensing datasets, this study offers novel and practical insights which can support monitoring and conservation of the highly vulnerable coastal dune ecosystems.

## Data availability

The code and ground truth data used for the analyses is available at: https://github.com/emiliapafumi/deep-dunes.git. The airborne orthophoto is available from https://www.regione.toscana.it/geoscopio; Google Earth imagery can be downloaded from Google Earth Pro; WorldView-3 data can be requested from https://earth.esa.int/eogateway/missions/worldview-3 after approval of a data request to the European Space Agency.

## Acknowledgements

We thank the Maremma Regional Park for granting research permits and supporting fieldwork activities. We are grateful to Paul Toffoloni for his assistance with the code. EP, CA, EF and SM were funded under the National Recovery and Resilience Plan (NRRP), Mission 4 Component 2 Investment 1.4 - Call for tender No. 3138 of 16 December 2021, rectified by Decree n.3175 of 18 December 2021 of Italian Ministry of University and Research funded by the European Union – NextGenerationEU; Award Number: Project code CN_00000033, Concession Decree No. 1034 of 17 June 2022 adopted by the Italian Ministry of University and Research, CUP B63C22000650007, Project title "National Biodiversity Future Center - NBFC". WorldView-3 data were provided by the European Space Agency (ESA) within its Third Party Missions programme.

# Chapter 4

## Deep learning-based habitat mapping of Italian coastal dunes: a multi-scale and multi-site assessment

*Manuscript in preparation*

## Abstract

Coastal sand dunes are highly dynamic and ecologically valuable ecosystems, yet their strong environmental heterogeneity poses challenges for mapping habitats using remote sensing. Recently, Convolutional Neural Networks (CNNs) have shown potential for habitat mapping by exploiting both spectral and spatial information. However, their transferability across sites and data sources remains poorly understood, especially for coastal dunes. This study assessed the applicability and generalization capability of CNN-based mapping across multiple spatial scales and remote sensing datasets.

CNN performance was evaluated using imagery with different spectral and spatial resolutions, including images from Unmanned Aerial Vehicle (UAV), WorldView-3 satellite and Google Earth. Ground truth data consisted of vegetation plots classified into EUNIS habitats based on species composition. CNN models were trained for two pilot study sites using both site-specific and multi-site approaches, testing both RGB-only and multispectral inputs where available. Finally, CNN performance was further evaluated at the national scale along the Italian coastline using Google Earth imagery.

Spatial resolution of input imagery strongly influenced classification accuracy. UAV-based models achieved the highest overall accuracy (up to 0.95), while performance declined with coarser spatial resolutions. Adding spectral bands improved classification accuracy, particularly for WorldView-3 imagery, but had limited effects for UAV data. Generally, multi-site models were less accurate than site-specific models, though the difference depended on the data source. Model transferability was moderate for UAV and WorldView-3, but poor for Google Earth imagery, especially at the national scale, where ecological and radiometric heterogeneity strongly reduced CNN performance. Coastal dune scrubs were the habitats mapped most accurately, while shifting dunes and bare sand were often confused.

Overall, this study highlights the potential and current limitations of CNN-based habitat mapping for coastal dunes across multiple sites, underscoring the importance of very high-spatial resolution data for large-scale monitoring and conservation applications.

**Keywords:** Biodiversity, Coastal dunes, Convolutional Neural Networks, Deep Learning, Habitat mapping, Model transferability, Remote sensing

# 1. Introduction

Coastal dunes are highly dynamic systems, and their dynamism is at the basis of important ecosystem services (Van Der Biest et al., 2017). Over one third of the world shoreline is sandy, with varying trends of erosion and accretion over the last decades (Luijendijk et al., 2018). In Italy, coastal dunes host unique plant communities with high conservation value (Acosta et al., 2009; Tordoni et al., 2018). However, they have been subjected to strong anthropogenic pressures since the 20$^{th}$ century, with the increase of tourism and urbanization, and are now generally in a poor conservation status (Prisco et al., 2020). These pressures have caused, for example, changes at the landscape level, with a general increase in anthropogenic land cover and a reduction in natural land cover (Malavasi et al., 2013). Although effective protection measures can locally reverse the trend (Cini et al., 2025), the overall effectiveness of the European Natura 2000 network for coastal dune protection remains limited (Sperandii et al., 2020).

Coastal dunes are intensively studied ecosystems with respect to plant diversity, as their ease of access allows repeated field sampling across gradients (e.g., Sperandii et al., 2019; Tordoni et al., 2021). Nonetheless, their wide extension and intrinsic dynamism require continuous, fine-scale and up-to-date data to support effective monitoring and conservation actions (Delbosc et al., 2021).

Remote sensing represents an essential source of data for studying and monitoring natural habitats, although important trade-offs exist in terms of data availability, spatial resolution and spectral detail (Corbane et al., 2015). In particular, spatial resolution strongly influences the feasibility of habitat discrimination: habitats characterized by large and homogeneous patches, such as forests or grasslands, can easily be mapped also from low-resolution imagery (Rapinel et al., 2019; Mikula et al., 2021). In contrast, ecotones pose specific challenges, as they are characterized by high spatial heterogeneity within a limited space (Rocchini et al., 2013). Coastal areas represent an ecotone, characterized by strong gradients in environmental conditions (Tordoni et al., 2018). In particular, the variation in soil parameters along the sea-inland direction influences the distribution of plant species and communities (Angiolini et al., 2013, 2018; Bazzichetto et al., 2016).

Due to their ecotonal nature, coastal dune habitats require remote sensing data with adequate spatial detail. Satellite imagery is generally used for large-scale analyses, in particular

leveraging the accessibility of datasets as Sentinel-2 and Landsat-8 (Álvarez-Martínez et al., 2026). However, their relatively coarse spatial resolution generally limits outputs to coarse landcover maps (Latella et al., 2021). This limitation can be partly mitigated by exploiting high temporal resolution (Marzialetti et al., 2019, 2020) or spectral information, especially applying fuzzy classifications and spectral unmixing (Ettritch et al., 2018; Pafumi et al., 2025). In recent years, new instruments such as Unmanned Aerial Vehicles (UAVs) have enabled the acquisition of hyperspatial imagery, i.e. imagery with pixels much smaller than target objects, opening new possibilities for the analysis of coastal dune vegetation (Agrillo et al., 2023; Cruz et al., 2023).

Moreover, advancements in machine learning are greatly expanding ecological applications of remote sensing, especially through the increasing availability of open-source tools (Cresson, 2020; Cipriano et al., 2025). Among these approaches, Convolutional Neural Networks (CNNs) have demonstrated high effectiveness, even when applied to images with limited spectral content, such as RGB imagery from UAV sensors for tree species mapping (Schiefer et al., 2020) or from airborne sources for fluvial scenes classification (Carbonneau, Dugdale, et al., 2020). The effectiveness of CNNs is mainly due to their ability to exploit both spectral information and spatial context of an image by learning hierarchical features, from lower-level inputs such as pixel intensities to higher-level features, such as edges and patterns (Kattenborn et al., 2019). Nonetheless, many challenges remain in the application of deep learning to remote sensing, including the scarcity of high-quality ground truth datasets for training and the interpretability of these complex models (Ball et al., 2017).

In this context of unprecedented availability of remote sensing data and powerful open-source tools for image analysis based on machine learning, also plant community data are becoming increasingly accessible thanks, for example, to vegetation databases (Bruelheide et al., 2019). A clear need emerges to integrate these elements within a unique framework and assess the current limits in habitat mapping at spatial scales relevant for conservation, such as the national scale. Recently, some nationwide projects for dune habitat mapping have been carried out in areas where homogeneous and up-to-date airborne imagery is available, such as the Dutch coast (Lansu et al., 2025) and the New Zealand coast (Ryan et al., 2025). However, in many countries, including Italy, similar remote sensing datasets are not uniformly available at the national scale. Thus, it is important to explore alternative data sources and test how their characteristics (mainly spatial and spectral resolution) affect habitat detectability and model

transferability across environmentally heterogeneous areas.

Thus, the aim of this study is to assess the transferability of CNN-based coastal dune habitat mapping, building upon the framework developed in Chapter 3, with the ultimate objective of supporting large-scale monitoring of these vulnerable ecosystems. The first part of the study is focused on two pilot study areas, to perform a multi-scale assessment of CNN performance in habitat mapping, comparing results obtained from remote sensing imagery with varying spatial and spectral resolutions, namely UAV, Google Earth, and WorldView-3 imagery. The second part simulates a real-world application by training CNNs on a large set of sites along the Italian coasts using Google Earth imagery, which is currently the only freely available source of high-resolution imagery suitable for large-scale applications.

## 2. Materials and methods

### 2.1. Study area

The Italian sandy coastline extends for approximately 3,400 km, making up nearly half of the total 7,500 km coastline (ISPRA, 2025a). Sandy beaches are generally narrow, covering a total surface of 120 $km^2$, of which only 35% is represented by beaches wider than 50 m and longer than 1 km, and 15% by beaches narrower than 25 m (ISPRA, 2025a). Italian coastline is highly dynamic, with 27% beaches subjected to erosion and 28% subjected to accretion in the period 2006-2020 (ISPRA, 2025a). Due to sea level rise and increasing anthropogenic pressure, coastal erosion is predicted to affect 70% of beaches by 2050 (Celata & Gioia, 2024).

The climate on Italian coasts is mainly Mediterranean, except for the northern Adriatic coastline, extending from Friuli Venezia Giulia to Marche region, which has a Temperate climate (Pesaresi et al., 2017).

Coastal dune vegetation in undisturbed conditions is characterized by a typical sea-inland zonation, which ranges from annual beach communities, to perennial herbaceous communities of embryonic and shifting dunes, to stable dune grasslands and finally to dune scrubs with *Juniperus* spp. and other species of the evergreen Mediterranean macchia (Acosta et al., 2007; Tordoni et al., 2019, 2021; Beccari et al., 2024).

Overall, the Italian coastline is highly urbanized: 22.9% of the coastal area within 300 m of the shoreline has been transformed into artificial surfaces, and c. 50% of the space behind beaches

is artificial, with peaks in Liguria (90%), Marche (80%), Emilia-Romagna (71%), Abruzzo (70%) and Campania (70%) (ISPRA, 2025b). In Veneto, a complete dune zonation can be found only along 19 km coastline, out of the 59 km of coastal dunes present in the region (Bezzi et al., 2018).

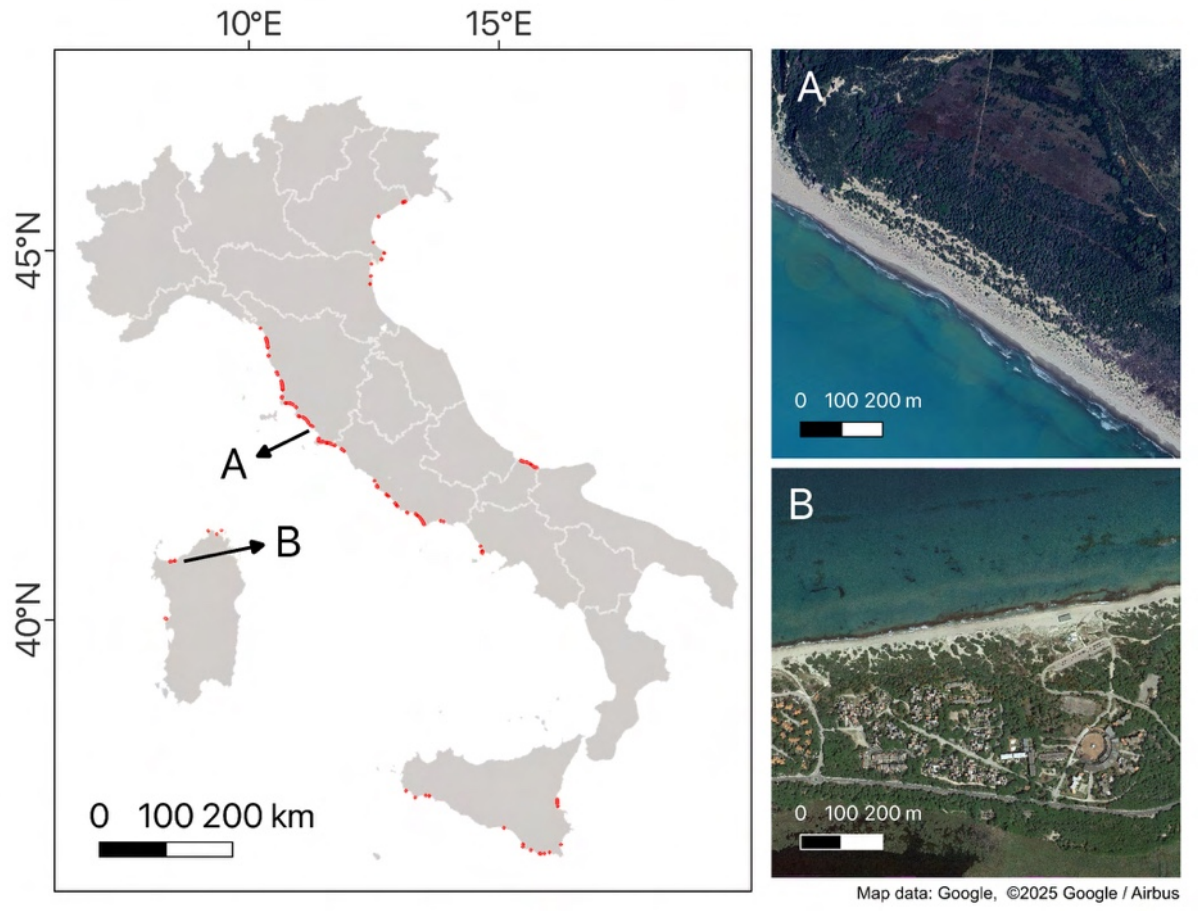


**Fig. 1.** Location of the 160 study areas in Italy, with a close-up view on the two pilot sites, in Tuscany (A) and in Sardinia (B).

The first part of this study was carried out on two pilot sites: the sandy beach of Collelungo in southern Tuscany (site A, centroid coordinates: 42.63581 N, 11.07292 E) and the sandy beach of Platamona in northern Sardinia (site B, centroid coordinates: 40.81996 N, 8.50067 E). Site A is located inside the Maremma Regional Park and included in the Special Area of Conservation “Dune costiere del Parco dell'Uccellina” (IT51A0015), thus having a low human pressure. On the other hand, site B is not protected and is part of a long sandy beach hosting multiple beach resorts, thus having a higher anthropogenic disturbance.

The second part of the study was carried out at the Italian level. A total of 160 areas of interest (AOIs) of 1 km x 1 km were placed along the Italian coasts in 8 administrative regions: three on the Tyrrhenian coast (Tuscany, Lazio, Campania), three on the Adriatic coast (Veneto, Emilia-Romagna, Molise), and two islands (Sardinia, Sicily). The complete set of AOIs is represented in Fig. 1 and listed in Table S1.

### 2.2. Ground truth data

The ground truth dataset includes vegetation plots sampled across Italy in the period 2017-2025. A total of 1,131 plots were collected from existing databases, specifically the SALTISH database of Tuscany (Gholizadeh et al., 2025), the RanVegDunes database (Sperandii et al., 2017), and the ReSurveyDunes database (Acosta et al., 2025), and from unpublished data. The plot sizes range from 1 $m^2$ to 25 $m^2$, with the majority (82.27%) being squared plots of 2 m × 2 m, as in most studies conducted on coastal dune vegetation (Carboni et al., 2011; Sperandii et al., 2018). To reduce heterogeneity in training data, only the 825 plots of 2 m × 2 m were used to extract patches for training CNNs. The other plots were nonetheless used in the validation steps for comparing predicted habitat labels with ground truth habitat assignments. Plot position was recorded in the field with standard GPS instruments, having a precision ranging from 1.8 m to 4 m.

In each plot, vascular plant species occurrence and abundance (visually estimated percentage cover) were recorded. Species names were standardized according to the EuroPlusMed database (Euro+Med, 2006).

On the basis of species composition, plots were classified into EUNIS habitats at the third level of detail using the EUNIS Expert System (Chytrý et al., 2020; Bruelheide et al., 2021). Plots not classified into any habitat, or classified into more than one habitat, or classified into a habitat not of interest for this study were excluded from the reference dataset (Table 1). The final reference dataset included 980 plots, assigned to three EUNIS habitats: “Mediterranean, Macaronesian and Black Sea shifting coastal dune” (N14), “Mediterranean and Macaronesian coastal dune grassland (grey dune)” (N16), and “Mediterranean and Black Sea coastal dune scrub” (N1B). To represent non-vegetated classes, an additional 632 squares of 2 m x 2 m corresponding to bare sand and sea were identified through photo interpretation.

**Table 1.** List of ground truth plots assigned to classes through the EUNIS Expert System.

| Code | Description | # plots |
|---|---|---|
| N14 | Mediterranean, Macaronesian and Black Sea shifting coastal dune | 241 |
| N16 | Mediterranean and Macaronesian coastal dune grassland (grey dune) | 527 |
| N1B | Mediterranean and Black Sea coastal dune scrub | 212 |
| MA253 | Mediterranean mid-low saltmarsh | 25 |
| N12 | Mediterranean and Black Sea sand beach | 74 |
| N1G | Mediterranean coniferous coastal dune forest | 9 |
| N1J | Mediterranean and Black Sea moist and wet dune slack | 7 |
| N22 | Mediterranean and Black Sea coastal shingle beach | 2 |
| T | Forest | 1 |
| T1H | Broadleaved deciduous plantation of non site-native trees | 2 |
| T21 | Mediterranean evergreen Quercus forest | 4 |
| ? | not assigned to any EUNIS habitat | 24 |
| + | assigned to more than one EUNIS habitat | 3 |

## 2.3. Remote sensing data collection and pre-processing

### *2.3.1. UAV imagery*

UAV flights were carried out for the two pilot sites in Tuscany and Sardinia.

For pilot site A (in Tuscany), the UAV photogrammetric survey was conducted on 20 June 2024, using a low-altitude UAV, the DJI Matrice 300 RTK, equipped with a MicaSense Altum-PT multispectral camera (MicaSense Inc., Seattle, DC, USA). Five of the seven sensors were used, each with a resolution of 2064 × 1544 pixels (≈ 3.2 MP per band), covering five discrete spectral bands: blue (center 475 nm, bandwidth ± 32 nm), green (560 ± 27 nm), red (668 ± 14 nm), red edge (717 ± 12 nm), and near-infrared (842 ± 57 nm). Before the flight, a calibrated reflectance panel (CRP2) was placed on a flat surface within the survey area. To enable radiometric calibration, the Altum-PT camera was used to capture images of the panel under the same sunlight conditions as the planned survey, while the downwelling light sensor (DLS2)

recorded irradiance and sun-angle data. The flight was carried out between 13:00 and 14:00 local time (UTC+2) at a flying altitude of 45 m, resulting in a Ground Sampling Distance (GSD), or spatial resolution, of 1.94 cm/pixel. Image overlap was set at 75% (both frontal and side), to ensure reliable image matching in Structure-from-Motion software (Eltner et al., 2016). Six Ground Control Points (GCP) were distributed across the site, and three of them were later used as Check Points (CP). GCP coordinates were acquired using two EMLID Reach RS2 GNSS units, one serving as a base station and the other one as a rover, connected for Real-Time Kinematic (RTK) survey with a local accuracy of 0.001 m. Due to insufficient network communication in the area, Post-Processed Kinematic (PPK) corrections were applied to the acquired coordinates in the EMLID Studio software, using RTCM3 positional data of the Leica SmartNet network of reference stations (GROK site, 18 km baseline). The final coordinates, calculated in the WGS84 reference system (EPSG: 4326), had an RMS accuracy < 1 cm in both Easting and Northing directions.

A total of 1,046 images were acquired. Image processing was performed in Agisoft Metashape Professional v 2.1.0. Radiometric corrections were applied to all images using the reflectance panel and the DLS2 data. After image alignment, a five-band orthomosaic was generated, with a size of 40,300 x 29,430 pixels. The orthomosaic was referenced in WGS84 / UTM Zone 32N (EPSG: 32632), with a horizontal Root Mean Square Error of 2.46 cm.

For pilot site B (in Sardinia), the UAV photogrammetric survey was carried out on 23 May 2025, using a DJI Mavic 3M, equipped with a RGB camera (sensor: CMOS 4/3, 20 MP, image size: 5280×3956) and a multispectral camera (sensor: CMOS 1/2.8", 5 MP, image size: 2592×1944). The multispectral camera included four spectral bands, i.e., green (560 ± 16 nm), red (650 ± 16 nm), red edge (730 ± 16 nm) and near-infrared (860 nm ± 26 nm). Reflectance was calibrated using the sunlight sensor. The flight resulted in a GSD of 1.99 cm/pixel.

To reduce inter-site heterogeneity, only the four common bands (i.e., green, red, red edge and near-infrared) were considered as multispectral images. Also, pixel values were scaled in the 0-255 interval and histogram matching was applied, i.e. an image transformation was performed so that the histogram of image B matches the histogram of image A (Sada et al., 2018).

### *2.3.2. WorldView-3 imagery*

One multispectral image from WorldView-3 satellite was retrieved for each pilot site. For pilot site A (in Tuscany), the image was acquired on 16 May 2019, while for pilot site B (in Sardinia) on 3 May 2024. The images include eight spectral bands: coastal blue (center wavelength: 427 nm), blue (482 nm), green (547 nm), yellow (604 nm), red (660 nm), red-edge (723 nm), near-infrared 1 (824 nm), and near-infrared 2 (914 nm). There is also a panchromatic band (649 nm) at a resolution of 0.40 m (site A) and 0.30 m (site B), which was used for pansharpening the multispectral image through a cubic resampling algorithm (QGIS Development Team, 2024). Images were orthorectified, sensor-corrected and radiometrically corrected through dark offset subtraction and non-uniformity correction, and delivered at 3D processing level, with geolocation accuracy < 3.0 m CE90 (Kuester, 2016).

### *2.3.3. Google Earth imagery*

RGB images were downloaded from Google Earth Pro 7.3.6 (Google, 2025) with a spatial resolution of c. 0.30 m. Google Earth images derive from a variety of remote sensing sources depending on availability and location, including Pléiades satellite (0.50 m resolution), Pléiades Neo satellite (0.30 m resolution), SPOT 6 and 7 satellites (1.5 m resolution). For each AOI, one image of 1 km x 1 km was downloaded at an eye altitude of 1 km, selecting in the Google Earth catalogue the image from the closest date to the field surveys, for a total of 160 images (Table S1). For site A, the selected image was from 26 April 2023, while for site B from 28 April 2022. For the other Italian sites, image dates are reported in Table S1.

Subsequently, each image was clipped on its corresponding AOI extent and georeferenced to EPSG 4326 using python `rasterio` and `numpy` libraries (Harris et al., 2020). To reduce heterogeneity among images, multiple pre-processing methods were tested: dark object subtraction, histogram matching and flat field correction. Dark object subtraction is based on the identification of a dark object (pixel) which should have a reflectance value equal to 0: if its value is higher than 0, then the offset can be attributed to atmospheric scattering and is subtracted from each spectral band (Chavez, 1988). In histogram matching, the input image is transformed so that its histogram matches the histogram of a reference image (Sada et al., 2018). Flat-field correction allows to reduce variations among pixels due to sensor or lighting by using a region of the image with little spectral variation (i.e., the flat field) and a dark image to normalize spectral values (Roberts et al., 1986). After visually comparing the results, flat-

field correction was chosen as a pre-processing method.

The surface of the AOIs with artificial land cover was excluded by applying a mask based on the "Carta Natura" produced by Italian regions (Papini et al., 2008; Capogrossi, Casella, et al., 2013; Capogrossi, Laureti, & Angelini, 2013; Capogrossi, Laureti, Augello, et al., 2013; Bagnaia et al., 2017; Casella et al., 2019; Cardillo et al., 2021; Ceralli, 2021).

### 2.4. Remote sensing data exploration

To explore the spectral separability of classes across the different remote sensing data sources, ridgeline plots from the `imageRy` R package were used (Rocchini et al., 2025). To summarize the information contained in the different spectral bands, for each remote sensing data source (UAV, Google Earth, WorldView-3) a Principal Component Analysis was carried out on scaled band values, selecting the first Principal Component (PC1) as the one explaining the highest proportion of variance. Then, ridgeline plots were produced based on PC1 values, plotting the distribution of pixel values for each class as represented in ground truth patches.

To better understand the performance of CNNs across sites and data sources, the relationship between spectral variability in ground truth patches and variability in species composition was explored. Spectral distance among vegetation plots was quantified by calculating the Euclidean distance on the matrix of mean spectral band values extracted from ground truth patches. Compositional similarity among plots was quantified using the Bray-Curtis similarity matrix computed from the log-transformed species abundance matrix. The relationship between spectral distance and species similarity was visualized using the `hexbin` R package (Carr et al., 2008). To examine the relationship across different quantiles rather than across the whole distribution, quantile regression was applied (Cade & Noon, 2003). Quantile regression allows to reveal patterns in spectral distance decay otherwise underestimated by ordinary least squares regression (Rocchini & Cade, 2008). Specifically, the `quantreg` R package was used (Koenker, 1999), selecting quantiles $\tau = 0.50, 0.75, 0.90, 0.99$.

All exploratory analyses on spectral and compositional datasets were carried out using R 4.5.1 (R Core Team, 2025).

## 2.5. Semantic segmentation using CNNs

### *2.5.1. CNN architecture*

In this study, CNNs were used to perform semantic segmentation, i.e., to return predicted labels for all pixels in the output map through a pixel-wise procedure. The CNN architecture used in this study was based on the U-Net structure, which is an encoder-decoder model optimized to perform well even with a low number of training images (Ronneberger et al., 2015). The U-Net model is appropriate for semantic segmentation because it includes a first part with convolutional layers, which reduce resolution (encoder), and a second part with transposed convolutions to restore the original resolution (decoder). Here, the structure was optimized based on preliminary experiments testing multiple numbers of layers, kernel sizes and strides. The final model includes three convolutions (3x3 kernel with stride 1, padding "same", and HeNormal initialization for reducing the vanishing gradient and stabilizing the network) and three transposed convolutions (again, using 3x3 kernel with stride 1, padding "same", and HeNormal initialization). Each layer was followed by a ReLu activation layer to compute the node output and a Batch Normalization layer to reduce the internal covariate shift. A final argmax layer assigns each pixel to the most probable class.

### *2.5.2. Patch extraction*

Ground truth patches were extracted from the input remote sensing images in correspondence to the field sampled plots (2 m × 2 m). Then, the patches were randomly partitioned into three groups: training (80%), testing (10%) and validation (10%). Data augmentation was applied to increase the training dataset, because the lack of training images is a major challenge in CNN models and can result in network overfitting (Lalitha & Latha, 2022; Hao et al., 2023). Specifically, two preprocessing layers were added to the training dataset, which respectively performed random flips (horizontal and vertical) and random rotations.

### *2.5.3. CNN model training*

Model training was performed separately for each remote sensing dataset and for each training site, for a total of ten CNNs (Table 2). Categorical cross entropy was selected as loss function, Adam as optimizer, the number of epochs was set to 50, the batch size to 8, and the learning rate to 0.0002. The training was carried out using the Orfeo ToolBox Tensor Flow (OTBTF) module (Cresson, 2019) of the Orfeo ToolBox (OTB) open-source library (Grizonnet et al.,

2017), which is based on the Tensor Flow platform for machine learning (Abadi et al., 2015) and on the Keras API (Chollet, 2015). To integrate the remote sensing processing capabilities of OTB within Python-based workflows, the `pyotb` library was used as a Python wrapper.

**Table 2.** List of CNNs trained in this study.

| RS data | Type of CNN | Training site | Input bands | # CNN |
|---|---|---|---|---|
| UAV | site-specific | A | RGB | CNN-01-rgb |
| | | | multi | CNN-01-multi |
| | | B | RGB | CNN-02-rgb |
| | | | multi | CNN-02-multi |
| | multi-site | AB | RGB | CNN-03-rgb |
| | | | multi | CNN-03-multi |
| WorldView-3 | site-specific | A | RGB | CNN-04-rgb |
| | | | multi | CNN-04-multi |
| | | B | RGB | CNN-05-rgb |
| | | | multi | CNN-05-multi |
| | multi-site | AB | RGB | CNN-06-rgb |
| | | | multi | CNN-06-multi |
| Google Earth | site-specific | A | RGB | CNN-07 |
| | | B | RGB | CNN-08 |
| | multi-site | AB | RGB | CNN-09 |
| | | Italy | RGB | CNN-10 |

### *2.5.4. Validation*

The accuracy of habitat maps was assessed using validation ground truth data not used for training. For each CNN, the following metrics were computed: overall accuracy, i.e. the proportion of correctly classified pixels; precision, i.e. the proportion of pixels classified as class *i* which actually belong to class *i*; recall, i.e. the proportion of pixels belonging to class *i* which are classified as class *i*; and F1-score, i.e. the harmonic mean of precision and recall. Notably, precision and recall correspond, respectively, to user's accuracy and producer's accuracy in traditional remote sensing studies not involving deep learning (Maxwell et al., 2021).

# 3. Results

## 3.1. Exploration of remote sensing datasets

The ridgeline plots representing the distribution of values of the first principal component (PC1) extracted from the different remote sensing datasets in the ground truth patches are in Fig. 2. In all datasets, the curves for the sand class and the N14 class partially overlap, although the curve for sand is narrower, while the curve for N14 has a peak similar to sand and a long asymmetrical tail. The curve for class N16, which is only present in pilot site A, is slightly shifted with respect to N14 and more symmetrical. The curve for class N1B is generally well separated from the other classes, while the sea class generally has a narrow curve, at the opposite extreme of the range of values compared to sand. Overall, class overlap is smaller in the UAV dataset and larger in the WorldView-3 and Google Earth datasets. Moreover, the overlap increases when multiple sites are considered rather than single sites, with the highest overlap being observed when considering all Italian patches.

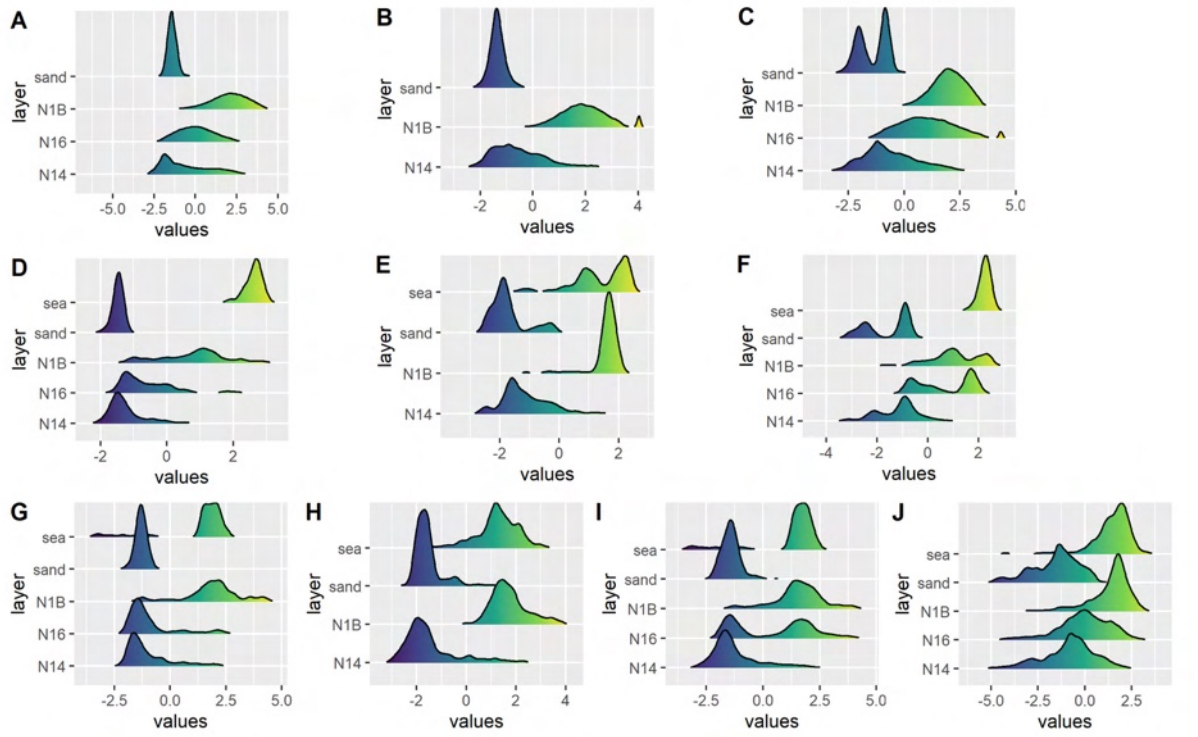


**Fig. 2.** Ridgeline plots representing the distribution of spectral values in ground truth patches in the different remote sensing datasets: UAV (A-C), WorldView-3 (D-F) and Google Earth (G-J), for the pilot site in Tuscany (A, D, G), the one in Sardinia (B, E, H), both pilot sites (C, F, I), and all Italian sites (J).

The relationship between spectral distance and compositional similarity between plots in the Italian dataset is represented in Fig. 3. Most plot pairs exhibited low compositional similarity. A negative relationship was observed particularly in the upper quantiles ($\tau = 0.75, 0.90, 0.99$): in these cases, high compositional similarity occurred mainly at small spectral distances and declined rapidly with increasing spectral distance.

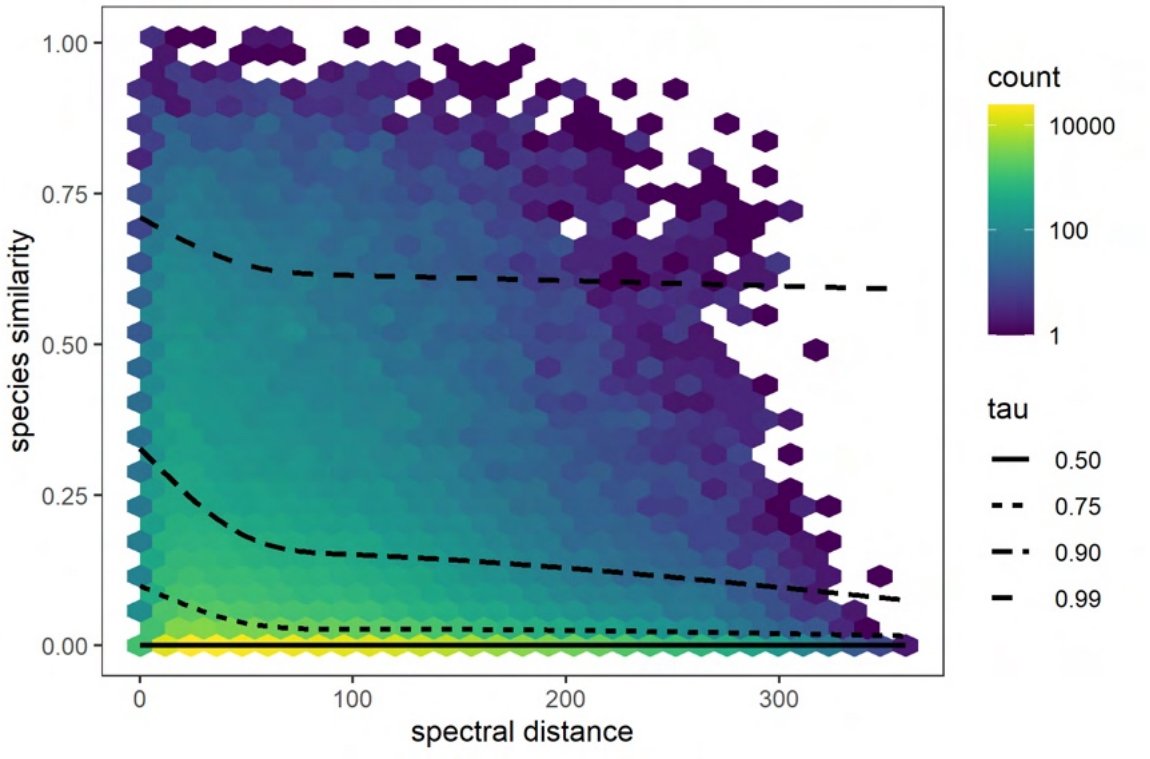


**Fig. 3.** Hexbin density plot of pairwise compositional similarity (calculated as 1 – Bray-Curtis dissimilarity) versus spectral Euclidean distance among ground truth plots. Dashed lines show quantile regression fits ($\tau = 0.50, 0.75, 0.90, 0.99$).

### 3.2. Accuracy of the habitat maps

Maps produced from the different CNN models are displayed in Fig. 4. The detail in habitat maps clearly decreases with coarser spatial resolutions (from UAV to WorldView-3 and Google Earth images), while the confusion among classes generally increases. This is particularly evident in the case of multi-site models trained on Google Earth data (i.e., CNN-09 and CNN-10).

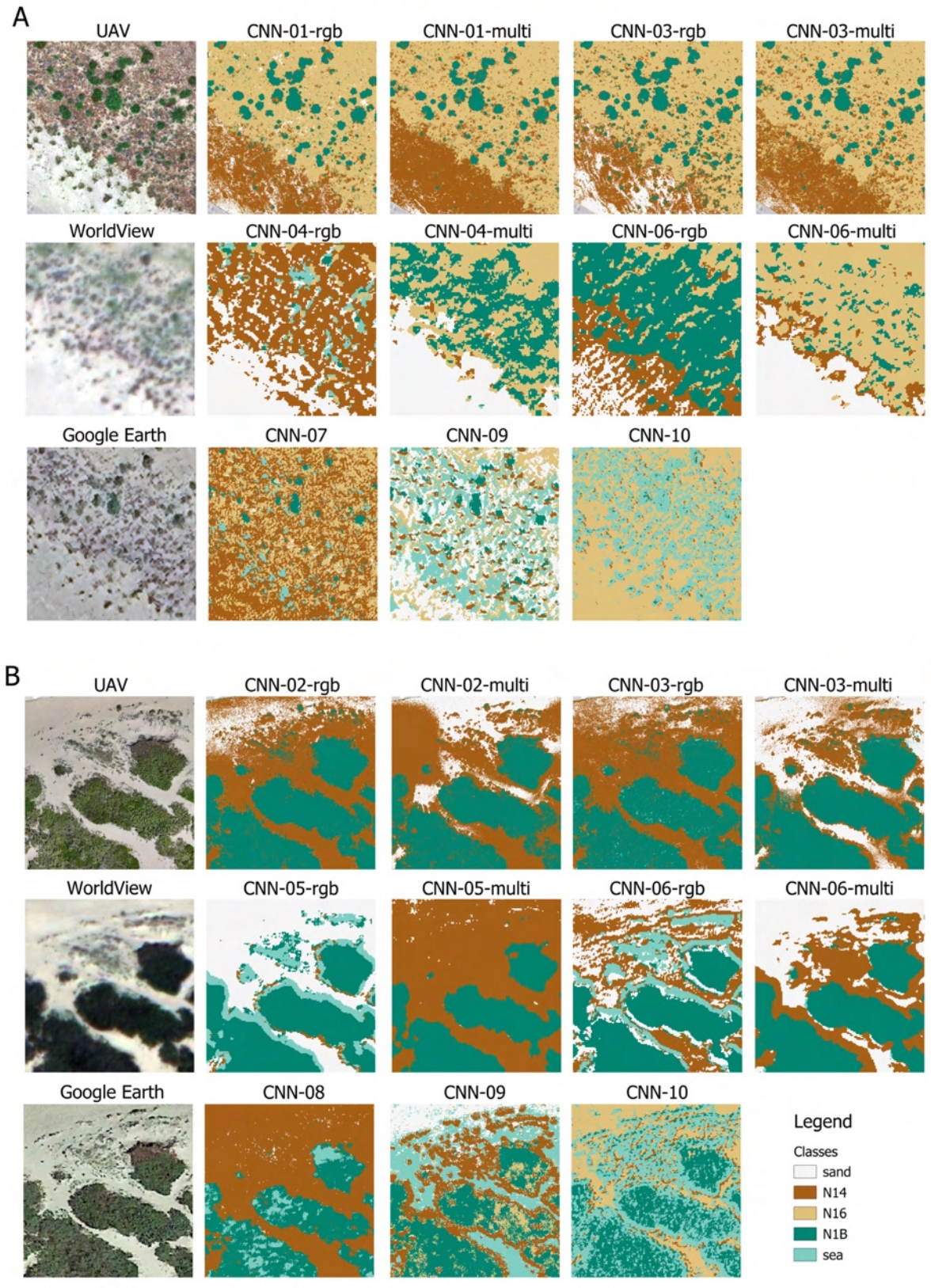


**Fig. 4.** Close-up views on the maps derived from segmentation using different CNN models for the pilot site in Tuscany (A) and Sardinia (B). See Table 2 for details on CNNs.

The accuracy of habitat maps changed according to the type of remote sensing data used, both in terms of spatial resolution and spectral bands, and according to the study area on which the CNN was trained (Fig. 5; Table S2). In the pilot study, the maximum overall accuracy was reached in site A using UAV data, especially when the single-site model was applied, either using multispectral images (overall accuracy = 0.95) or only RGB bands (OA = 0.90). In general, the inclusion of additional bands besides RGB improved classification performance, for both UAV data (+0.05 in site A, +0.14 in site B, +0.08 in both sites) and WorldView-3 data (+ 0.05 in site B).

Multi-site models were generally less accurate than single-site models, but with some differences: for UAV data, multi-site models achieved intermediate accuracy (OA = 0.89) between single-site models trained on site A (OA = 0.93) and site B (OA = 0.77). In contrast, for Google Earth imagery, multi-site models trained on the two pilot sites (OA = 0.56) or on all Italian sites (OA = 0.39) performed substantially worse than single-site models for both site A (OA = 0.64) and site B (OA = 0.70).

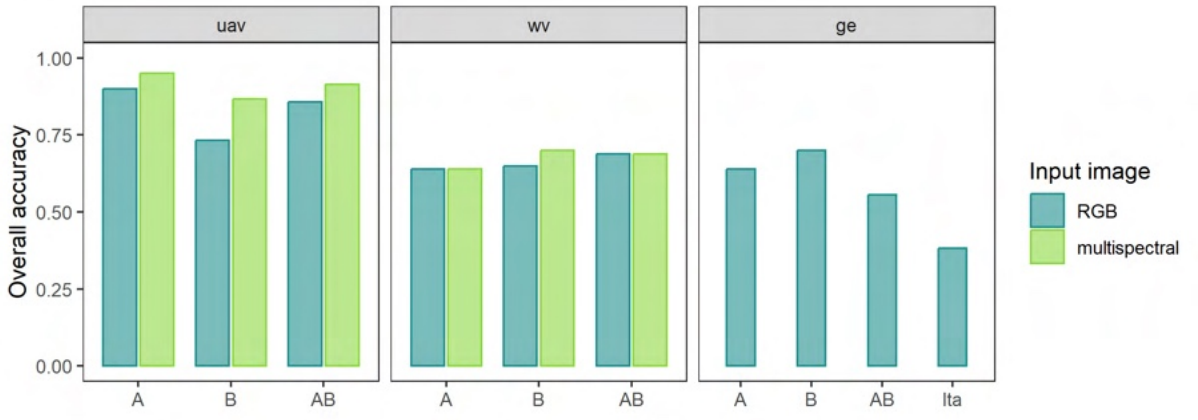


**Fig. 5.** Overall accuracy of the habitat maps produced from CNNs trained on different sources of remote sensing data and sites (pilot site A, pilot site B, both, all Italian sites). See Table 2 for details on CNNs.

As for class-specific accuracy values, there was a large difference among classes in terms of F1-Score (Fig. 6), precision and recall (Table S3). In most cases, coastal dune scrub (habitat N1B) was the habitat mapped with the highest accuracy. The sea class was also well distinguished. In contrast, both sand and habitat N14 had generally low accuracy values and were frequently confused. Habitat N16 was well identified with UAV data, while it achieved

very low accuracy when WorldView-3 or Google Earth datasets were used.

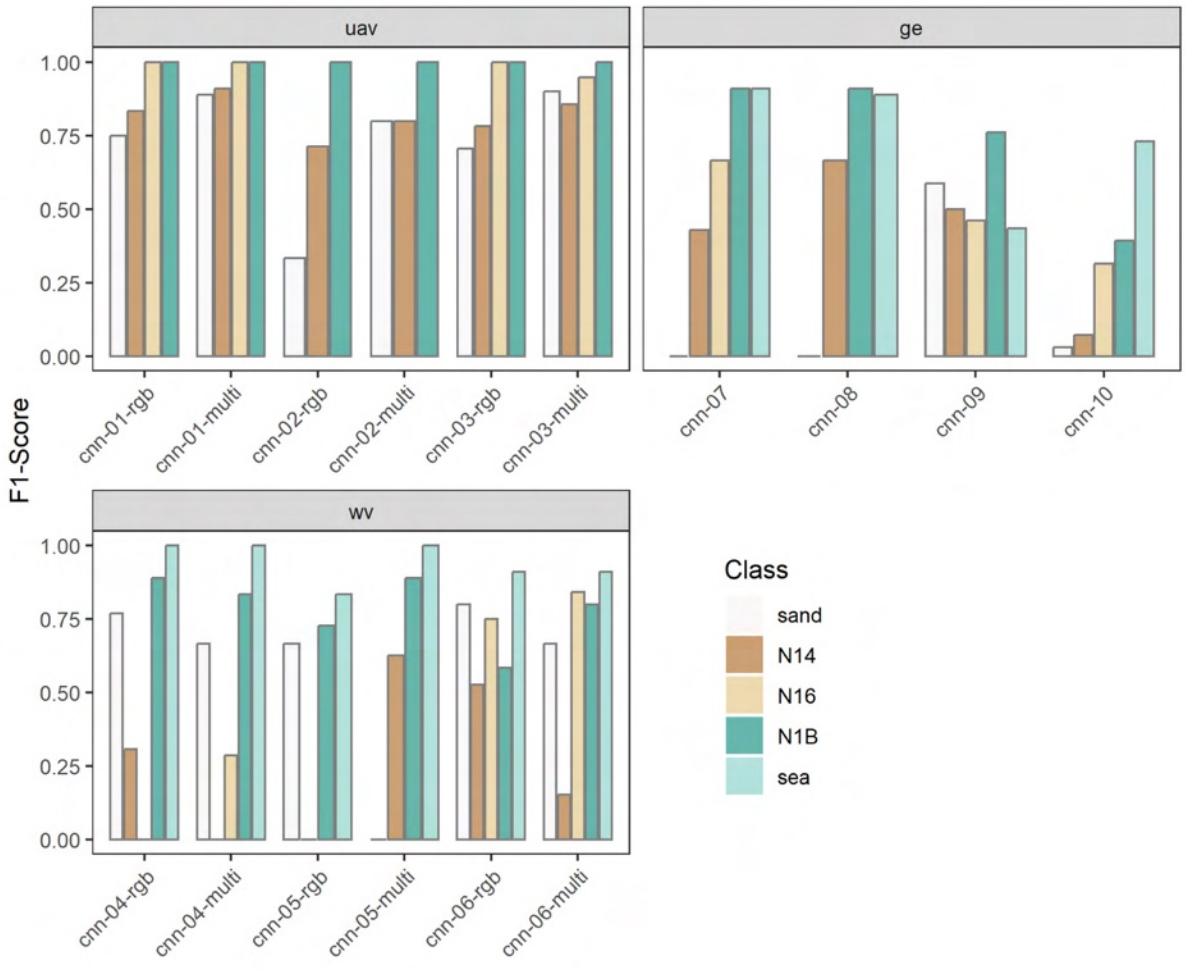


**Fig. 6.** Class-specific accuracy values for the different CNNs trained in this study (see Table 2 for details).

## 4. Discussion

This study advances the understanding of how advanced image analysis methods, particularly Convolutional Neural Networks (CNNs), can be effectively applied to habitat mapping in highly challenging ecosystems such as coastal dunes, which are characterized by strong environmental heterogeneity, small and fragmented vegetation patches, marked temporal dynamics, and often intense human pressure. By assessing the generalization capabilities of CNNs across multiple sites and remote sensing datasets with varying spatial resolutions and spectral content, this study addresses a critical gap between methodological advances in deep learning and their practical applicability for large-scale habitat mapping.

### 4.1. Influence of spatial and spectral resolution on CNN applicability

The maximum level of accuracy achieved here is in line with other studies, which achieved a value of 0.95 using airborne RGB imagery and additional data layers (Lansu et al., 2025), 0.88 using UAV (Pérez-Carabaza et al., 2021), 0.83 using hyperspectral data (Laporte-Fauret et al., 2020), 0.78 using multispectral UAV (Suo et al., 2019), 0.78 combining UAV and environmental predictors (Agrillo et al., 2023).

By comparing the accuracy of habitat maps produced using different spectral datasets, it was possible to better understand which factors mainly affect CNN performance. The first factor is spatial resolution: on average, maps derived from UAV data were the most accurate, reflecting the high detail provided by these types of images. Recent research on CNNs for habitat mapping also highlighted the importance of image spatial resolution aside from the data source, for example with Google Earth images, where accuracy in tree mapping dropped from 0.93 at 0.13 m to 0.74 at 0.65 m (Watanabe et al., 2020), or with UAV images, where accuracy dropped from 0.89 at 0.02 m to 0.62 at 0.32 m (Schiefer et al., 2020).

The contribution of spectral information to mapping accuracy depended on spatial resolution. In general, adding spectral bands improved the results, as observed in other studies (Wolff et al., 2023). For example, near-infrared bands have been demonstrated to improve freshwater recognition on dunes (Lansu et al., 2025). However, the improvement was generally small for UAV imagery. This suggests that at hyperspatial resolutions, spatial context might outweigh spectral information, confirming previous works that emphasize the potential of RGB sensors (Kattenborn et al., 2019).

Interestingly, the largest difference between RGB and multispectral imagery was found for the UAV dataset of pilot site B, while the difference was much smaller for pilot site A. This may be partly explained by differences in sensors used in the two cases: at site A, a single integrated multispectral camera was used, while at site B, RGB and multispectral data were acquired using two separate sensors, potentially introducing inconsistencies between datasets.

A slight difference was observed between single-site models trained on pilot sites A and B, with generally better results for the former. It can reasonably be excluded that this difference is due to the time interval between field data collection and image acquisition. Field surveys were carried out in the same season in the two pilot sites (late spring 2018 for site A, late spring 2024 for site B), so that the phenological phase could not confound the relationship between

species composition and spectral reflectance (Feilhauer & Schmidtlein, 2011). On the other hand, site B is characterized by stronger anthropogenic pressure, which can generally cause problems in habitat assignment (Sarmati et al., 2019).

In terms of class-specific performances, the results align with previous research indicating that habitats characterized by a single dominant species (low $\alpha$- and $\beta$-diversity) are easier to classify using remote sensing, while species-rich habitats (high $\alpha$-and $\beta$-diversity), are more difficult to recognize, as far as the spectral component is considered (Jarocińska et al., 2023).

### 4.2. Multi-site applicability of CNNs

In this work, the generalization capabilities of dune habitat mapping models were tested considering two cases. First, two pilot study areas were analyzed by comparing the results produced by single-site and multi-site models. Subsequently, a test was performed at the national scale. These results could guide the development of a standardized procedure for coastal dune system analysis, as recently done for example for the Bulgarian Black Sea Coast on the basis of UAVs, geological and vegetation surveys (Prodanov et al., 2025).

Results showed relatively good generalization capability of CNNs for the UAV and WorldView-3 datasets, while for Google Earth images the generalization capability was poor. In a study applying CNNs to Google Earth images, Watanabe et al. (2020) found that model transferability was generally poor, and classification performance was strongly related to local conditions. In contrast, Carbonneau, Dugdale, et al. (2020) produced highly transferable models in a study on fluvial scene classification considering multiple sites worldwide, despite radiometric differences within classes among sites caused by differences in vegetation spectral signatures, local geology and different cameras. Good transferability has also been shown in studies exploring tree crown detection, especially when a large and diverse training dataset is used (Weinstein et al., 2020; Schiefer et al., 2020). This is in contrast with the fact that for many classification methods, such as Random Forest, a high heterogeneity in training samples negatively affects classification accuracy (Villoslada et al., 2020).

In the national-scale test, the classification performance was the lowest. Italian coastal dunes are characterized by high heterogeneity in terms of vegetation composition and of dune morphology (ISPRA, 2025a). This ecological heterogeneity is complicated by heterogeneity in the imagery itself, caused by differences in illumination conditions, acquisition dates, sensor

characteristics, which are especially great for Google Earth data and cannot be completely solved by pre-processing procedures (Watanabe et al., 2020). These factors strongly reduce spectral consistency within habitat classes, as also emerged from the ridgeline plots, limiting CNN transferability across sites.

### 4.3. Uncertainties and future steps

A limitation of this work, common to most remote sensing applications, is the limited amount of ground truth data available compared to the millions of images generally used in computer vision for training a neural network from scratch (Ball et al., 2017). Further increasing the training dataset with targeted field sampling could improve the generalization capabilities of CNNs (Weinstein et al., 2020; Schiefer et al., 2020). Moreover, some studies suggest that incorporating pre-trained models could possibly improve results (Rezaee et al., 2018).

Ancillary datasets, such as topographic information, can increase classification accuracy in landcover and habitat mapping (Khatami et al., 2016), also on coastal dunes (Cruz et al., 2023), in particular increasing the differentiation between shrubs and trees (Lansu et al., 2025). In these ecosystems, indeed, vegetation is strongly linked with dune morphology (Bazzichetto et al., 2016). However, these data are currently not available with enough spatial detail and temporal update at the Italian scale, unlike for other cases such as the Netherlands (Lansu et al., 2025), thus they were not included in this work. Some studies have hypothesized that a raster of distance from the sea could be added as an input layer, considering that the sea-inland gradient influences much of the variability in coastal dune vegetation (Tordoni et al., 2018; Torca et al., 2019). However, adding this information has not always proved useful (Lansu et al., 2025), and likely this would also happen in Italy, where coastal dune systems are highly heterogeneous in terms of width (ISPRA, 2025a). Also, spectral diversity metrics, which have been tested in pixel-based approaches to classification (Pafumi et al., 2023), could possibly be used as additional input layers also in CNNs.

In this study, various remote sensing datasets were considered separately, to understand differences among them in terms of applicability. However, these data sources could be integrated in other ways, leveraging the complementary strengths of each (Pettorelli et al., 2025; Álvarez-Martínez et al., 2026). For instance, UAVs can provide training and validation data for unmixing satellite imagery having coarser spatial resolution but higher temporal coverage, as demonstrated for rivers (Carbonneau, Belletti, et al., 2020) and wetlands (Alvarez-

Vanhard et al., 2020). Incorporating multi-temporal information has also been shown to improve habitat separability on coastal dunes. In a study carried out in central Italy using Sentinel-2 images, land cover and vegetation classes showed different seasonal patterns of spectral vegetation indices (Marzialetti et al., 2019) and temporal heterogeneity (Marzialetti et al., 2020). Similarly, multi-temporal UAV imagery acquired during early, mid and late growing seasons improved classification accuracy with respect to uni-temporal images in a study from Ireland (Cruz et al., 2023).

A future step would include the analysis of temporal resilience of the models: depending on the dynamism of the area, a model once trained can be valid for a different amount of time. For example, for fluvial scenes it has been found that a biennial UAV acquisition is sufficient for training CNN models using Sentinel-2 (Carbonneau, Belletti, et al., 2020).

Finally, this work focused on the natural vegetation of coastal dunes, considering the EUNIS habitats described at the European level (Chytrý et al., 2020). However, most dune systems in Italy are highly affected by human activities, and disturbed situations are very common (Prisco et al., 2012). A future step would specifically include non-natural vegetation types and consider also invasive species, in accordance with recent research on the application of remote sensing to monitor invasive plants on coastal dunes (Villalobos Perna et al., 2023).

## 5. Conclusion

This study aimed to test the applicability of CNNs, one of the most promising methods of image analysis based on deep learning, to the mapping of coastal dune habitats over multiple sites. CNNs proved effective in producing accurate habitat maps for these highly challenging ecosystems, which are characterized by high spatial and temporal heterogeneity.

The generalization capability was relatively good for high-resolution data derived from UAV sensors, while it decreased dramatically with Google Earth imagery, making a national-scale application still challenging. Nonetheless, the findings suggest potential improvements, related to broader acquisitions of ground truth data and UAV imagery, or multi-source and multi-temporal data integration, to advance towards the objective of an effective broad-scale monitoring of these fragile ecosystems.

# Synthesis and Perspectives

## Key findings

In this thesis, spatial patterns of plant diversity and habitats on coastal dunes were explored to identify gaps in current conservation efforts and to improve the evidence base for defining conservation priorities, while developing effective and innovative tools for large-scale identification and monitoring of these fragile ecosystems.

The key findings of this thesis strongly highlight the importance of integrating multiple approaches to understand and protect biodiversity (Likens & Lindenmayer, 2012). Field-collected plant community data were crucial for identifying priority sites which mainly contribute to the regional biodiversity (Dubois et al., 2020). Even clearer indications emerged when species identity was considered, distinguishing groups of species with different indicator values (Del Vecchio et al., 2016; Prisco et al., 2016). In contrast, remotely sensed data proved essential for producing effective habitat maps for broader extents, when supported by appropriate ground truth data. The integration of *in situ* data collection and remote sensing is recognized as crucial not only for biodiversity monitoring, but also for gaining a full understanding of plant diversity evolution and distribution, ecosystem resilience, land use change dynamics and their drivers (Cavender-Bares et al., 2022).

A central aspect connected to the integration of multiple approaches is the consideration of scale. The problem of scale is central in ecology: patterns of variability change with the scale of observation, while the ecological processes determining these patterns can operate at different scales (Levin, 1992). Biodiversity itself is scale-dependent since its measure is influenced by the sampling effort and the scale of analysis (Whittaker, 1960, 1972; Chase et al., 2018). The issue of scale, particularly spatial scale, recurs throughout this thesis and shapes both the analytical choices and the interpretation of results. First, the analysis of regional plant diversity partitioned across the spatial scales of analysis (from individual plots to sites and regions) revealed differences in the scale at which ecological processes operate for different species groups. In particular, the distribution of synanthropic and alien species was mainly influenced by processes acting at fine scales (i.e., at the level of single beaches), while the processes shaping typical dune species operated at larger scales, creating different communities

among sites and regions, in accordance with patterns observed in other studies (Tordoni et al., 2018). Local environmental conditions, indeed, can strongly influence invasibility on coastal dunes (Carboni et al., 2011; Trotta et al., 2025). In addition, analyzing plant diversity at different scales ($\alpha$, $\beta$ and $\gamma$) made it possible to identify the best strategy for guiding conservation efforts, i.e. favoring compositionally unique sites rather than simply focusing on species-rich sites (Belote et al., 2021).

Remote sensing analyses further highlighted the importance of scale by showing that the detectability and separability of coastal dune habitats depend strongly on the observation scale. In this context, spatial scale encompasses both the grain size (i.e., pixel size) and the spatial extent (Gamon et al., 2020). This thesis employed remote sensing data with multiple grain sizes, ranging from 2 cm (UAV imagery; Chapter 3 and 4), to 20 cm (aerial imagery; Chapter 3), to 30-40 cm (Google Earth imagery; Chapter 3 and 4), to approximately 2 m (commercial satellite imagery; Chapter 2, 3 and 4), and multiple spatial extents, from a single beach (Chapter 3), to multiple protected areas in the same region (Chapter 2), to a large set of sites distributed along the Italian coastline (Chapter 4). Although the scale of remote observations changed across these cases, ground truth data were based on a consistent plot size (2 m × 2 m), ensuring compatibility across analyses and reflecting a scale that has already been identified as appropriate for coastal dune habitats by previous researchers (Carboni et al., 2011; Sperandii et al., 2018). The multi-scale comparisons revealed that very high-resolution data (such as from UAV), combined with deep learning methods such as CNNs, provided the most accurate representations of coastal dune habitats, while high-resolution imagery from satellites benefited more from fuzzy classification methods, which allow sub-pixel representations, than from the use of CNNs.

The distinctiveness of the multiple plant communities of coastal dunes emerged clearly throughout the research. Species such as *Juniperus macrocarpa*, *Calamagrostis arenaria* subsp. *arundinacea* and *Thinopyrum junceum*, which are characteristic of different communities along the dune zonation (Acosta et al., 2007), were the ones that contributed the most to regional $\beta$-diversity (Chapter 1). Moreover, even the most compositionally unique communities (i.e., those with significant LCBD values) at the regional scale occurred across the entire coastal dune zonation, from annual communities of the drift line to inland dune scrubs. The remote sensing studies (Chapters 2, 3 and 4) further confirmed the presence of distinct communities, although in these cases formal definitions of the communities were

adopted, following the Annex I of Habitats Directive (Council Directive 92/43/EEC) and the EUNIS classification system (Davies & Moss, 1998). Even if these definitions did not allow all sampled plots to be classified, leaving out various mixed plots, the studies revealed the presence of four EUNIS habitats and eight Annex I habitat types.

Coastal dune habitats also varied in terms of vulnerability and detectability from remote sensing data. For instance, the pioneer vegetation of drift lines, characterized by highly specialized species like *Cakile maritima*, *Salsola tragus*, *Convolvulus soldanella* (Prisco et al., 2012), made up many of the unique sites, indicating that it was rare in the region, in accordance with findings by other authors (Bertacchi, 2017; Sperandii et al., 2019; Sarmati et al., 2019) and with its vulnerability to erosion (Bazzichetto et al., 2020) and mechanical cleaning (Attorre et al., 2013). As regards detectability, many factors influenced the accuracy of mapping for a specific habitat: its diversity (i.e., habitats characterized by a single dominant species, with low $\alpha$- and $\beta$-diversity, were easier to map), its vegetation cover (i.e., habitats with higher vegetation cover were easier to map), and growth form of the dominant species (i.e., habitats dominated by taller growth form species were easier to map), in accordance with findings from other studies (Bell et al., 2015; Jarocińska et al., 2023).

Despite these habitat-specific differences, the overall conservation of coastal dunes emerging from the results of this thesis indicates some criticalities. In Tuscany, the most compositionally unique sites corresponded to well-preserved aspects of coastal dune vegetation, suggesting they were exceptions within a generally disturbed landscape. The remote sensing chapters did not directly assess conservation status; nonetheless, anthropogenic pressure emerged as a possible factor complicating habitat mapping in the most disturbed study areas. This situation is in line with the broader scale: over 50% of dune habitats in Europe are reported to be in a bad conservation status, and this value reaches 88% in Italy, with rapidly deteriorating trends (European Environment Agency, 2020; Prisco et al., 2020). In Italy, intense human disturbance affects several regions besides Tuscany, such as Veneto (Bezzi et al., 2018) and Lazio (e.g., Carboni et al., 2009; Malavasi et al., 2013), although some regions, such as Molise, still host large patches of natural dunes (Drius et al., 2019). Similar declines have been documented in Spain (Garcia-Lozano & Pintó, 2018; Gómez-Zotano et al., 2017), and in the eastern Adriatic, especially in Croatia and Montenegro, while relatively good conditions remain in Albania (Šilc et al., 2016) and in the Netherlands, where coastal dunes are highly protected for their crucial role as sea barriers (Keijsers et al., 2015).

## Implications for coastal dune conservation

The findings of this thesis bring out several implications for the conservation of coastal dunes. First, the effectiveness of protection areas should be better investigated, as other studies have suggested (Sperandii et al., 2020). Protected sites hosted a higher richness of typical dune species compared to non-protected sites, suggesting a positive role of protection measures in areas subjected to high anthropogenic pressure. However, the richness of synanthropic and alien species was similar inside and outside protected areas, indicating the ineffectiveness of protection measures in limiting the introduction of synanthropic or alien species from the surroundings (Bazzichetto et al., 2018). This result highlights the importance of managing also the unprotected areas, considering coastal areas as whole ecosystems deeply connected (Cox & Underwood, 2011). Moreover, the fact that unique sites were located along the whole sea-inland gradient suggests that conservation strategies should consider the whole coastal dune zonation instead of focusing on single habitats (Acosta et al., 2009).

These results are particularly relevant in the context of assessing the effectiveness of the Natura 2000 network, which represents the largest conservation network worldwide, but whose effectiveness remains only partially assessed due to limited data availability (European Environment Agency, 2020). Several studies have shown limitations of the network both in representing plant diversity (Dimitrakopoulos et al., 2004; Doxa et al., 2017) and in ensuring its conservation over time (Sperandii et al., 2020), and the results of this thesis further support the need to critically evaluate the contribution of Natura 2000 to dune conservation.

The distinct processes affecting typical dune species versus synanthropic and alien species suggest that monitoring and conservation strategies should account for these differences. This is especially important due to the wide extent of plant invasion and disturbance on coastal dunes (Tordoni et al., 2021).

Finally, the results of this thesis show that, once the appropriate scales and methods of analysis are determined, remote sensing can play an important role in producing accurate maps for monitoring the extent of coastal dune habitats, their conservation status, and thus assessing the effectiveness of the implemented conservation measures and supporting effective management planning (Álvarez-Martínez et al., 2026).

## Future perspectives

The application of multiple methods of investigation and scales of analysis, ranging from the analysis of plant taxonomic diversity at the plot, site, cross-sites and regional scales, to the use of remote sensing data with multiple grain sizes, spatial extents and spectral resolutions for habitat identification, has suggested that the integration of approaches and scales of investigation is crucial for complete understanding and supporting conservation on coastal dunes. However, this integration remains preliminary and could be advanced in future research.

The field-based prioritization approach used in this thesis could integrate remote sensing data for larger-scale applications. In this way, broader-scale analyses could be performed, expanding the study area from a single region for example to the national scale. Moreover, it has been demonstrated that basing the prioritization on all biodiversity components, i.e., also on functional and phylogenetic diversity rather than only on taxonomic diversity, can maximize the protection of ecosystem services and minimize biodiversity loss (Girardello et al., 2019).

Even the use of remote sensing data for habitat mapping could be more integrated. Here, different remote sensing datasets were used separately, carrying out comparisons to determine their appropriateness, mainly in terms of spatial or spectral resolution, for different methods of image analysis. However, the most promising research directions involve the use of multi-source models, integrating sensors with complementary strengths (Pettorelli et al., 2025; Álvarez-Martínez et al., 2026). For this purpose, machine learning, and deep learning in particular, are highly useful since they allow the use of multiple input data with different characteristics.

Among sources of remote sensing data, many others can be explored, such as LiDAR, Synthetic Aperture Radar (SAR), and thermal imagery. For example, SAR systems, which provide structural information unaffected by atmospheric effects, have proved useful for mapping coastal salt marsh habitats (Van Beijma et al., 2014). Hyperspectral data can also produce higher classification accuracy than multispectral images for mapping non-forest Annex I habitats such as meadows, grasslands heaths and mires (Jarocińska et al., 2023). Moreover, innovative sensors launched recently such as PRISMA are producing large amounts of data yet to be explored (Cogliati et al., 2021). In the future also UAV data could become available on large scales, opening new possibilities.

Finally, these approaches can be integrated on the temporal dimension. In this thesis, the temporal aspect emerged multiple times, but it was never completely explored. Multi-temporal models can improve habitat mapping results, by considering the phenological differences between vegetation types (Cruz et al., 2023). Moreover, the coastal dune ecosystem is highly dynamic, thus remote sensing data hold great value given that they could be exploited for performing large-scale monitoring, for measuring the magnitude of change and its rate, for assessing its causes, and even for predicting future scenarios in a context of increasingly dramatic global changes.

# Final remarks

This thesis highlights the importance of integrating multiple approaches and scales to understand and support the monitoring and conservation of coastal dune ecosystems. Field-based analysis of plant diversity patterns revealed that conservation priorities should focus on compositionally unique sites, with typical dune species driving regional $\beta$-diversity. In contrast, remote sensing tools provided robust tools for mapping habitats across larger scales, demonstrating in particular that the most accurate representations can derive from combining very high-resolution imagery with deep learning techniques, while fuzzy classification approaches are more effective for representing dune vegetation patterns from coarser satellite imagery. However, the high heterogeneity in ecological conditions and in data availability still limits broad-scale national applications.

Overall, the findings underscore the importance of preserving the whole sea-inland zonation of coastal dunes, improving the effectiveness of protected areas and choosing the appropriate analytical scale for effective monitoring. Future efforts focusing on multi-source, multi-scale and multi-temporal datasets could expand the analyses to broader spatial extents, supporting the conservation of these highly dynamic and threatened habitats.

# References


Abadi, M., Barham, P., Chen, J., Chen, Z., Davis, A., Dean, J., et al. (2015) TensorFlow: Large-scale machine learning on heterogeneous systems.

Acosta, A., Carranza, M.L., & Izzi, C.F. (2009) Are there habitats that contribute best to plant species diversity in coastal dunes? *Biodiversity and Conservation*, 18(4), 1087–1098. https://doi.org/10.1007/s10531-008-9454-9

Acosta, A.T.R., Di Biase, L., Sarmati, S., Allevato, E., Angiolini, C., Bagella, S., et al. (2025) ReSurveyDunes — a data resource of resurveyed coastal dune vegetation plots in Italy. *Vegetation Ecology and Diversity*, 62, 1–6. https://doi.org/10.3897/ved.139539

Acosta, A., Ercole, S., Stanisci, A., Pillar, V.D.P., & Blasi, C. (2007) Coastal Vegetation Zonation and Dune Morphology in Some Mediterranean Ecosystems. *Journal of Coastal Research*, 236, 1518–1524. https://doi.org/10.2112/05-0589.1

Agrillo, E., Filipponi, F., Salvati, R., Pezzarossa, A., & Casella, L. (2023) Modeling approach for coastal dune habitat detection on coastal ecosystems combining very high-resolution UAV imagery and field survey. *Remote Sensing in Ecology and Conservation*, 9(2), 251–267. https://doi.org/10.1002/rse2.308

Airbus. (2023) Pléiades Neo satellite imagery of Collelungo, 26 April 2023. Google Earth Pro © 2025 Airbus.

Álvarez-Martínez, J.M., Lugonja, T.N., Valdés, A., González Le Barbier, J., Suárez, M.P., Romero, G.H., et al. (2026) Four decades of remote sensing for monitoring terrestrial ecosystems: a global review and future challenges. *Science of Remote Sensing*, 13, 100341. https://doi.org/10.1016/j.srs.2025.100341

Alvarez-Vanhard, E., Houet, T., Mony, C., Lecoq, L., & Corpetti, T. (2020) Can UAVs fill the gap between in situ surveys and satellites for habitat mapping? *Remote Sensing of Environment*, 243, 111780. https://doi.org/10.1016/j.rse.2020.111780

Amici, V. (2011) Dealing with vagueness in complex forest landscapes: A soft classification approach through a niche-based distribution model. *Ecological Informatics*, 6(6), 371–383. https://doi.org/10.1016/j.ecoinf.2011.07.001

Andriolo, U., & Gonçalves, G. (2023) Impacts of a massive beach music festival on a coastal ecosystem — A showcase in Portugal. *Science of The Total Environment*, 861, 160733. https://doi.org/10.1016/j.scitotenv.2022.160733

Angiolini, C., Bonari, G., & Landi, M. (2018) Focal plant species and soil factors in Mediterranean coastal dunes: An undisclosed liaison? *Estuarine, Coastal and Shelf Science*, 211, 248–258. https://doi.org/10.1016/j.ecss.2017.06.001

Angiolini, C., Landi, M., Pieroni, G., Frignani, F., Finoia, M.G., & Gaggi, C. (2013) Soil chemical features as key predictors of plant community occurrence in a Mediterranean coastal

ecosystem. *Estuarine, Coastal and Shelf Science*, 119, 91–100. https://doi.org/10.1016/j.ecss.2012.12.019

Arkema, K.K., Guannel, G., Verutes, G., Wood, S.A., Guerry, A., Ruckelshaus, M., et al. (2013) Coastal habitats shield people and property from sea-level rise and storms. *Nature Climate Change*, 3(10), 913–918. https://doi.org/10.1038/nclimate1944

Attorre, F., Maggini, A., Di Traglia, M., De Sanctis, M., & Vitale, M. (2013) A methodological approach for assessing the effects of disturbance factors on the conservation status of Mediterranean coastal dune systems. *Applied Vegetation Science*, 16(2), 333–342. https://doi.org/10.1111/avsc.12002

Bagnaia, R., Viglietti, S., Laureti, L., Giacanelli, V., Ceralli, D., Bianco, P.M., et al. (2017) Carta della Natura della Regione Campania: Carta degli habitat alla scala 1:25.000.

Ball, J.E., Anderson, D.T., & Chan, C.S. (2017) Comprehensive survey of deep learning in remote sensing: theories, tools, and challenges for the community. *Journal of Applied Remote Sensing*, 11(04), 1. https://doi.org/10.1117/1.JRS.11.042609

Bartolucci, F., Peruzzi, L., Galasso, G., Albano, A., Alessandrini, A., Ardenghi, N.M.G., et al. (2018) An updated checklist of the vascular flora native to Italy. *Plant Biosystems - An International Journal Dealing with all Aspects of Plant Biology*, 152(2), 179–303. https://doi.org/10.1080/11263504.2017.1419996

Bazzichetto, M., Malavasi, M., Acosta, A.T.R., & Carranza, M.L. (2016) How does dune morphology shape coastal EC habitats occurrence? A remote sensing approach using airborne LiDAR on the Mediterranean coast. *Ecological Indicators*, 71, 618–626. https://doi.org/10.1016/j.ecolind.2016.07.044

Bazzichetto, M., Malavasi, M., Bartak, V., Acosta, A.T.R., Rocchini, D., & Carranza, M.L. (2018) Plant invasion risk: A quest for invasive species distribution modelling in managing protected areas. *Ecological Indicators*, 95, 311–319. https://doi.org/10.1016/j.ecolind.2018.07.046

Bazzichetto, M., Sperandii, M.G., Malavasi, M., Carranza, M.L., & Acosta, A.T.R. (2020) Disentangling the effect of coastal erosion and accretion on plant communities of Mediterranean dune ecosystems. *Estuarine, Coastal and Shelf Science*, 241, 106758. https://doi.org/10.1016/j.ecss.2020.106758

Beccari, E., Pérez Carmona, C., Tordoni, E., Petruzzellis, F., Martinucci, D., Casagrande, G., et al. (2024) Plant spectral diversity from high-resolution multispectral imagery detects functional diversity patterns in coastal dune communities. *Journal of Vegetation Science*, 35(2), e13239. https://doi.org/10.1111/jvs.13239

Belcore, E., Latella, M., Piras, M., & Camporeale, C. (2024) Enhancing precision in coastal dunes vegetation mapping: ultra-high resolution hierarchical classification at the individual plant level. *International Journal of Remote Sensing*, 45(13), 4527–4552. https://doi.org/10.1080/01431161.2024.2354135

Bell, G., Neal, S., & Medcalf, K. (2015) Use of remote sensing to produce a habitat map of Norfolk. *Ecological Informatics*, 30, 293–299. https://doi.org/10.1016/j.ecoinf.2015.06.003

Bellard, C., Bertelsmeier, C., Leadley, P., Thuiller, W., & Courchamp, F. (2012) Impacts of climate change on the future of biodiversity. *Ecology Letters*, 15(4), 365–377. https://doi.org/10.1111/j.1461-0248.2011.01736.x

Beloiu, M., Heinzmann, L., Rehush, N., Gessler, A., & Griess, V.C. (2023) Individual Tree-Crown Detection and Species Identification in Heterogeneous Forests Using Aerial RGB Imagery and Deep Learning. *Remote Sensing*, 15(5), 1463. https://doi.org/10.3390/rs15051463

Belote, R.T., Barnett, K., Dietz, M.S., Burkle, L., Jenkins, C.N., Dreiss, L., et al. (2021) Options for prioritizing sites for biodiversity conservation with implications for "30 by 30". *Biological Conservation*, 264, 109378. https://doi.org/10.1016/j.biocon.2021.109378

Bertacchi, A. (2017) Dune habitats of the Migliarino – San Rossore – Massaciuccoli Regional Park (Tuscany – Italy). *Journal of Maps*, 13(2), 322–331. https://doi.org/10.1080/17445647.2017.1302365

Bezzi, A., Pillon, S., Martinucci, D., & Fontolan, G. (2018) Inventory and conservation assessment for the management of coastal dunes, Veneto coasts, Italy. *Journal of Coastal Conservation*, 22(3), 503–518. https://doi.org/10.1007/s11852-017-0580-y

Bhatt, P., & Maclean, A.L. (2023) Comparison of high-resolution NAIP and unmanned aerial vehicle (UAV) imagery for natural vegetation communities classification using machine learning approaches. *GIScience & Remote Sensing*, 60(1), 2177448. https://doi.org/10.1080/15481603.2023.2177448

Biondi, E., Blasi, C., Burrascano, S., Casavecchia, S., Copiz, R., Del Vico, E., et al. (2009) *Italian interpretation Manual of the habitats of the 92/43/ EEC Directive*. Società Botanica Italiana. Ministero dell'Ambiente e della tutela del territorio e del mare, D.P.N.: Rome.

Biondi, E., Casavecchia, S., & Pesaresi, S. (2012) Nitrophilous and ruderal species as indicators of climate change. Case study from the Italian Adriatic coast. *Plant Biosystems*, 146(1), 134–142. https://doi.org/10.1080/11263504.2012.672342

Bonari, G., Padullés Cubino, J., Sarmati, S., Landi, M., Zerbe, S., Marcenò, C., et al. (2021) Ecosystem state assessment after more than 100 years since planting for dune consolidation. *Restoration Ecology*, 29(7), e13435. https://doi.org/10.1111/rec.13435

Brandt, M., Chave, J., Li, S., Fensholt, R., Ciais, P., Wigneron, J.-P., et al. (2025) High-resolution sensors and deep learning models for tree resource monitoring. *Nature Reviews Electrical Engineering*, 2(1), 13–26. https://doi.org/10.1038/s44287-024-00116-8

Breiman, L. (2001) Random Forests. *Machine Learning*, 45(1), 5–32. https://doi.org/10.1023/A:1010933404324

Brownett, J., & Mills, R. (2017) The development and application of remote sensing to monitor sand dune habitats. *Journal of Coastal Conservation*, 21(5), 643–656. https://doi.org/10.1007/s11852-017-0504-x

Bruelheide, H., Dengler, J., Jiménez-Alfaro, B., Purschke, O., Hennekens, S.M., Chytrý, M., et al. (2019) sPlot – A new tool for global vegetation analyses. *Journal of Vegetation Science*, 30(2), 161–186. https://doi.org/10.1111/jvs.12710

Bruelheide, H., Tichý, L., Chytrý, M., & Jansen, F. (2021) Implementing the formal language of the vegetation classification expert systems (ESy) in the statistical computing environment R. *Applied Vegetation Science*, 24(1), e12562. https://doi.org/10.1111/avsc.12562

Cade, B.S., & Noon, B.R. (2003) A gentle introduction to quantile regression for ecologists. *Frontiers in Ecology and the Environment*, 1(8), 412–420. https://doi.org/10.1890/1540-9295(2003)001%5B0412:AGITQR%5D2.0.CO;2

Capogrossi, R., Casella, L., Augello, R., Cardillo, A., & Laureti, L. (2013) Carta della Natura della Regione Lazio: Carte di Valore Ecologico, Sensibilità Ecologica, Pressione Antropica e Fragilità Ambientale scala 1:50.000.

Capogrossi, R., Laureti, L., & Angelini, P. (2013) Carta della Natura della Regione Sardegna: Carta della Natura della Regione Sardegna: Carte di Valore Ecologico, Sensibilità Ecologica, Pressione Antropica e Fragilità Ambientale scala 1:50.000.

Capogrossi, R., Laureti, L., Augello, R., & Bianco, P.M. (2013) Carta della Natura della Regione Veneto: Carte di Valore Ecologico, Sensibilità Ecologica, Pressione Antropica e Fragilità Ambientale scala 1:50.000.

Carboni, M., Carranza, M.L., & Acosta, A. (2009) Assessing conservation status on coastal dunes: A multiscale approach. *Landscape and Urban Planning*, 91(1), 17–25. https://doi.org/10.1016/j.landurbplan.2008.11.004

Carboni, M., Santoro, R., & Acosta, A.T.R. (2010) Are some communities of the coastal dune zonation more susceptible to alien plant invasion? *Journal of Plant Ecology*, 3(2), 139–147. https://doi.org/10.1093/jpe/rtp037

Carboni, M., Santoro, R., & Acosta, A.T.R. (2011) Dealing with scarce data to understand how environmental gradients and propagule pressure shape fine-scale alien distribution patterns on coastal dunes. *Journal of Vegetation Science*, 22(5), 751–765. https://doi.org/10.1111/j.1654-1103.2011.01303.x

Carbonneau, P.E., Belletti, B., Micotti, M., Lastoria, B., Casaioli, M., Mariani, S., et al. (2020) UAV-based training for fully fuzzy classification of Sentinel-2 fluvial scenes. *Earth Surface Processes and Landforms*, 45(13), 3120–3140. https://doi.org/10.1002/esp.4955

Carbonneau, P.E., Dugdale, S.J., Breckon, T.P., Dietrich, J.T., Fonstad, M.A., Miyamoto, H., & Woodget, A.S. (2020) Adopting deep learning methods for airborne RGB fluvial scene classification. *Remote Sensing of Environment*, 251, 112107. https://doi.org/10.1016/j.rse.2020.112107

Cardillo, A., Ceralli, D., Canali, E., Laureti, L., D'Angeli, C., & Augello, R. (2021) Carta della Natura della Regione Emilia-Romagna: Carta degli habitat alla scala 1:25.000.

Carlos-Júnior, L.A., Spencer, M., Neves, D.M., Moulton, T.P., Pires, D. de O., e Castro, C.B., et al. (2019) Rarity and beta diversity assessment as tools for guiding conservation strategies in marine tropical subtidal communities. *Diversity and Distributions*, 25(5), 743–757. https://doi.org/10.1111/ddi.12896

Carmignani, L., Conti, P., Cornamusini, G., & Pirro, A. (2013) Geological map of Tuscany (Italy). *Journal of Maps*, 9(4), 487–497. https://doi.org/10.1080/17445647.2013.820154

Carr, D., Lewin-Koh, N., Maechler, M., & Sarkar, D. (2008) hexbin: Hexagonal Binning Routines 1.28.5. https://doi.org/10.32614/CRAN.package.hexbin

Casella, L., Angelini, P., Bianco, P.M., & Papallo, O. (2019) Carta della Natura della Regione Toscana: Carta degli habitat alla scala 1:50.000.

Cavender-Bares, J., Schneider, F.D., Santos, M.J., Armstrong, A., Carnaval, A., Dahlin, K.M., et al. (2022) Integrating remote sensing with ecology and evolution to advance biodiversity conservation. *Nature Ecology & Evolution*, 6(5), 506–519. https://doi.org/10.1038/s41559-022-01702-5

Celata, F., & Gioia, E. (2024) Resist or retreat? Beach erosion and the climate crisis in Italy: Scenarios, impacts and challenges. *Applied Geography*, 169, 103335. https://doi.org/10.1016/j.apgeog.2024.103335

Ceralli, D. (2021) Carta della Natura della Regione Molise: Carta degli habitat alla scala 1:25.000.

Chase, J.M., McGill, B.J., McGlinn, D.J., May, F., Blowes, S.A., Xiao, X., et al. (2018) Embracing scale-dependence to achieve a deeper understanding of biodiversity and its change across communities. *Ecology Letters*, 21(11), 1737–1751. https://doi.org/10.1111/ele.13151

Chavez, P.S. (1988) An improved dark-object subtraction technique for atmospheric scattering correction of multispectral data. *Remote Sensing of Environment*, 24(3), 459–479. https://doi.org/10.1016/0034-4257(88)90019-3

Chelli, S., Conti, F., & Bracchetti, L. (2022) Diachronic Observations Reveal Different and Scale-Dependent Response of Sand Dune Plants to Seashore Dynamics. *Estuaries and Coasts*, 45(7), 2124–2133. https://doi.org/10.1007/s12237-022-01075-9

Chen, L.-C., Papandreou, G., Kokkinos, I., Murphy, K., & Yuille, A.L. (2018) DeepLab: Semantic Image Segmentation with Deep Convolutional Nets, Atrous Convolution, and Fully Connected CRFs. *IEEE Transactions on Pattern Analysis and Machine Intelligence*, 40(4), 834–848. https://doi.org/10.1109/TPAMI.2017.2699184

Chollet, F. (2015) Keras.

Chytrý, M., Tichý, L., Hennekens, S.M., Knollová, I., Janssen, J.A.M., Rodwell, J.S., et al. (2020) EUNIS Habitat Classification: Expert system, characteristic species combinations and distribution maps of European habitats. *Applied Vegetation Science*, 23(4), 648–675. https://doi.org/10.1111/avsc.12519

Ciccarelli, D., Di Bugno, C., & Peruzzi, L. (2014) Checklist della flora vascolare psammofila della Toscana. *Atti della Società Toscana di Scienze Naturali Residente in Pisa Memorie serie B*, (119), 37–88. https://doi.org/10.2424/ASTSN.M.2014.05

Cini, E., Acosta, A.T.R., Malavasi, M., Sarmati, S., Del Vecchio, S., Ciccarelli, D., & Marzialetti, F. (2025) Long-term dynamics of coastal dune landscapes and habitat diversity: Insights from a quarter century of resurveys in Castelporziano Presidential Estate. *Conservation Science and Practice*, e70101. https://doi.org/10.1111/csp2.70101

Cipriano, C., Noce, S., Mereu, S., & Santini, M. (2025) Algorithms going wild – A review of machine learning techniques for terrestrial ecology. *Ecological Modelling*, 506, 111164. https://doi.org/10.1016/j.ecolmodel.2025.111164

Cogliati, S., Sarti, F., Chiarantini, L., Cosi, M., Lorusso, R., Lopinto, E., et al. (2021) The PRISMA imaging spectroscopy mission: overview and first performance analysis. *Remote Sensing of Environment*, 262, 112499. https://doi.org/10.1016/j.rse.2021.112499

Corbane, C., Lang, S., Pipkins, K., Alleaume, S., Deshayes, M., García Millán, V.E., et al. (2015) Remote sensing for mapping natural habitats and their conservation status – New opportunities and challenges. *International Journal of Applied Earth Observation and Geoinformation*, 37, 7–16. https://doi.org/10.1016/j.jag.2014.11.005

Cox, R.L., & Underwood, E.C. (2011) The Importance of Conserving Biodiversity Outside of Protected Areas in Mediterranean Ecosystems. *PLoS ONE*, 6(1), e14508. https://doi.org/10.1371/journal.pone.0014508

Crameri, F., Shephard, G.E., & Heron, P.J. (2020) The misuse of colour in science communication. *Nature Communications*, 11(1), 5444. https://doi.org/10.1038/s41467-020-19160-7

Cresson, R. (2019) A Framework for Remote Sensing Images Processing Using Deep Learning Techniques. *IEEE Geoscience and Remote Sensing Letters*, 16(1), 25–29. https://doi.org/10.1109/LGRS.2018.2867949

Cresson, R. (2020) *Deep Learning for Remote Sensing Images with Open Source Software*. CRC Press. https://doi.org/10.1201/9781003020851

Cribari-Neto, F., & Zeileis, A. (2010) Beta Regression in *R*. *Journal of Statistical Software*, 34(2). https://doi.org/10.18637/jss.v034.i02

Crist, T.O., Veech, J.A., Gering, J.C., & Summerville, K.S. (2003) Partitioning Species Diversity across Landscapes and Regions: A Hierarchical Analysis of α, β, and γ Diversity. *The American Naturalist*, 162(6), 734–743. https://doi.org/10.1086/378901

Cruz, C., O'Connell, J., McGuinness, K., Martin, J.R., Perrin, P.M., & Connolly, J. (2023) Assessing the effectiveness of UAV data for accurate coastal dune habitat mapping. *European Journal of Remote Sensing*, 56(1), 2191870. https://doi.org/10.1080/22797254.2023.2191870

Cruz, C., Perrin, P.M., Martin, J.R., O'Connell, J., McGuinness, K., & Connolly, J. (2024) Mapping of temperate upland habitats using high-resolution satellite imagery and machine

learning. *Environmental Monitoring and Assessment*, 196(9), 869. https://doi.org/10.1007/s10661-024-12998-0

Davies, C.E., & Moss, D. (1998) *EUNIS Habitats Classification. Final report to the European Topic Centre on Nature Conservation*. European Environment Agency: Copenhagen.

De Cáceres, M., Font, X., & Oliva, F. (2010) The management of vegetation classifications with fuzzy clustering: Fuzzy clustering in vegetation classifications. *Journal of Vegetation Science*, 21(6), 1138–1151. https://doi.org/10.1111/j.1654-1103.2010.01211.x

De Cáceres, M., & Legendre, P. (2009) Associations between species and groups of sites: indices and statistical inference. *Ecology*, 90(12), 3566–3574. https://doi.org/10.1890/08-1823.1

De Giglio, M., Goffo, F., Greggio, N., Merloni, N., Dubbini, M., & Barbarella, M. (2017) Satellite and unmanned aerial vehicle data for the classification of sand dune vegetation. *The International Archives of the Photogrammetry, Remote Sensing and Spatial Information Sciences*, XLII-3/W2, 43–50. https://doi.org/10.5194/isprs-archives-XLII-3-W2-43-2017

De Giglio, M., Greggio, N., Goffo, F., Merloni, N., Dubbini, M., & Barbarella, M. (2019) Comparison of Pixel- and Object-Based Classification Methods of Unmanned Aerial Vehicle Data Applied to Coastal Dune Vegetation Communities: Casal Borsetti Case Study. *Remote Sensing*, 11(12), 1416. https://doi.org/10.3390/rs11121416

De Klerk, H.M., Burgess, N.D., & Visser, V. (2018) Probabilistic description of vegetation ecotones using remote sensing. *Ecological Informatics*, 46, 125–132. https://doi.org/10.1016/j.ecoinf.2018.06.001

Defeo, O., McLachlan, A., Schoeman, D.S., Schlacher, T.A., Dugan, J., Jones, A., et al. (2009) Threats to sandy beach ecosystems: A review. *Estuarine, Coastal and Shelf Science*, 81(1), 1–12. https://doi.org/10.1016/j.ecss.2008.09.022

Del Vecchio, S., Pizzo, L., & Buffa, G. (2015) The response of plant community diversity to alien invasion: evidence from a sand dune time series. *Biodiversity and Conservation*, 24(2), 371–392. https://doi.org/10.1007/s10531-014-0814-3

Del Vecchio, S., Slaviero, A., Fantinato, E., & Buffa, G. (2016) The use of plant community attributes to detect habitat quality in coastal environments. *AoB Plants*, 8, plw040. https://doi.org/10.1093/aobpla/plw040

Delbaere, B.C.W. (1998) *Facts and figures on Europe's biodiversity: State and trends 1998–1999.* European Centre for Nature Conservation.: Tilburg, The Netherlands.

Delbosc, P., Lagrange, I., Rozo, C., Bensettiti, F., Bouzillé, J.-B., Evans, D., et al. (2021) Assessing the conservation status of coastal habitats under Article 17 of the EU Habitats Directive. *Biological Conservation*, 254, 108935. https://doi.org/10.1016/j.biocon.2020.108935

Dimitrakopoulos, P.G., Memtsas, D., & Troumbis, A.Y. (2004) Questioning the effectiveness of the Natura 2000 Special Areas of Conservation strategy: the case of Crete. *Global Ecology and Biogeography*, 13(3), 199–207. https://doi.org/10.1111/j.1466-822X.2004.00086.x

Doxa, A., Albert, C.H., Leriche, A., & Saatkamp, A. (2017) Prioritizing conservation areas for coastal plant diversity under increasing urbanization. *Journal of Environmental Management*, 201, 425–434. https://doi.org/10.1016/j.jenvman.2017.06.021

Dray, S., Bauman, D., Blanchet, G., Borcard, D., Clappe, S., Guénard, G., et al. (2023) adespatial: Multivariate Multiscale Spatial Analysis. R package version 0.3-21, https://CRAN.R-project.org/package=adespatial.

Drius, M., Carranza, M.L., Stanisci, A., & Jones, L. (2016) The role of Italian coastal dunes as carbon sinks and diversity sources. A multi-service perspective. *Applied Geography*, 75, 127–136. https://doi.org/10.1016/j.apgeog.2016.08.007

Drius, M., Jones, L., Marzialetti, F., De Francesco, M.C., Stanisci, A., & Carranza, M.L. (2019) Not just a sandy beach. The multi-service value of Mediterranean coastal dunes. *Science of The Total Environment*, 668, 1139–1155. https://doi.org/10.1016/j.scitotenv.2019.02.364

Dubois, R., Proulx, R., & Pellerin, S. (2020) Ecological uniqueness of plant communities as a conservation criterion in lake-edge wetlands. *Biological Conservation*, 243, 108491. https://doi.org/10.1016/j.biocon.2020.108491

Dudley, K.L., Dennison, P.E., Roth, K.L., Roberts, D.A., & Coates, A.R. (2015) A multi-temporal spectral library approach for mapping vegetation species across spatial and temporal phenological gradients. *Remote Sensing of Environment*, 167, 121–134. https://doi.org/10.1016/j.rse.2015.05.004

Duff, T.J., Bell, T.L., & York, A. (2014) Recognising fuzzy vegetation pattern: the spatial prediction of floristically defined fuzzy communities using species distribution modelling methods. *Journal of Vegetation Science*, 25(2), 323–337. https://doi.org/10.1111/jvs.12092

Dufrêne, M., & Legendre, P. (1997) Species Assemblages and Indicator Species: The Need for a Flexible Asymmetrical Approach. *Ecological Monographs*, 67(3), 345. https://doi.org/10.2307/2963459

Durai, P., Bhaskar, A.S., & Sarunjith, K.J. (2024) Spectral classification of AVIRIS NG hyperspectral data for discriminating coastal foredunes based on vegetation species: a case study from Cuddalore district of Tamil Nadu, South India. *Environmental Earth Sciences*, 83(2). https://doi.org/10.1007/s12665-023-11391-3

Eltner, A., Kaiser, A., Castillo, C., Rock, G., Neugirg, F., & Abellán, A. (2016) Image-based surface reconstruction in geomorphometry – merits, limits and developments. *Earth Surface Dynamics*, 4(2), 359–389. https://doi.org/10.5194/esurf-4-359-2016

Ettritch, G., Bunting, P., Jones, G., & Hardy, A. (2018) Monitoring the coastal zone using earth observation: application of linear spectral unmixing to coastal dune systems in Wales. *Remote Sensing in Ecology and Conservation*, 4(4), 303–319. https://doi.org/10.1002/rse2.79

*EU Biodiversity Strategy for 2030. Bringing nature back into our lives*. (2020) European Commission: Brussels.

Euro+Med. (2006) Euro+Med PlantBase – the information resource for Euro-Mediterranean plant diversity.

European Commission. (2022) COMMISSION STAFF WORKING DOCUMENT IMPACT ASSESSMENT Accompanying the proposal for a Regulation of the European Parliament and of the Council on nature restoration.

European Commission. (2013) *Interpretation Manual of European Union Habitats - EUR28*. Bruxelles.

European Environment Agency. (2014) *Terrestrial habitat mapping in Europe: an overview.* Publications Office: LU.

European Environment Agency. (2020) *State of nature in the EU: results from reporting under the nature directives 2013-2018*. Publications Office: LU.

EUROSTAT. (2021) Census population grid.

Everard, M., Jones, L., & Watts, B. (2010) Have we neglected the societal importance of sand dunes? An ecosystem services perspective. *Aquatic Conservation: Marine and Freshwater Ecosystems*, 20(4), 476–487. https://doi.org/10.1002/aqc.1114

Fanfarillo, E., Maccherini, S., Angiolini, C., de Simone, L., Fiaschi, T., Tassinari, A., et al. (2023) Drivers of diversity of arable plant communities in one of their european conservation hotspots. *Biodiversity and Conservation*, 32(6), 2055–2075. https://doi.org/10.1007/s10531-023-02592-0

Feilhauer, H., & Schmidtlein, S. (2011) On variable relations between vegetation patterns and canopy reflectance. *Ecological Informatics*, 6(2), 83–92. https://doi.org/10.1016/j.ecoinf.2010.12.004

Feilhauer, H., Zlinszky, A., Kania, A., Foody, G.M., Doktor, D., Lausch, A., & Schmidtlein, S. (2021) Let your maps be fuzzy!—Class probabilities and floristic gradients as alternatives to crisp mapping for remote sensing of vegetation. *Remote Sensing in Ecology and Conservation*, 7(2), 292–305. https://doi.org/10.1002/rse2.188

Fenu, G., Carboni, M., Acosta, A.T.R., & Bacchetta, G. (2013) Environmental Factors Influencing Coastal Vegetation Pattern: New Insights from the Mediterranean Basin. *Folia Geobotanica*, 48(4), 493–508. https://doi.org/10.1007/s12224-012-9141-1

Foody, G.M. (1996) Fuzzy modelling of vegetation from remotely sensed imagery. *Ecological Modelling*, 85(1), 3–12. https://doi.org/10.1016/0304-3800(95)00012-7

Foody, G.M. (2009) The impact of imperfect ground reference data on the accuracy of land cover change estimation. *International Journal of Remote Sensing*, 30(12), 3275–3281. https://doi.org/10.1080/01431160902755346

Galasso, G., Conti, F., Peruzzi, L., Ardenghi, N.M.G., Banfi, E., Celesti-Grapow, L., et al. (2018) An updated checklist of the vascular flora alien to Italy. *Plant Biosystems - An International Journal Dealing with all Aspects of Plant Biology*, 152(3), 556–592. https://doi.org/10.1080/11263504.2018.1441197

Gamon, J.A., Wang, R., Gholizadeh, H., Zutta, B., Townsend, P.A., & Cavender-Bares, J. (2020) Consideration of Scale in Remote Sensing of Biodiversity. In: Cavender-Bares, J., Gamon, J.A., & Townsend, P.A. (Eds), *Remote Sensing of Plant Biodiversity*. Springer International Publishing: Cham, pp. 425–447. https://doi.org/10.1007/978-3-030-33157-3_16

Garcia-Lozano, C., & Pintó, J. (2018) Current status and future restoration of coastal dune systems on the Catalan shoreline (Spain, NW Mediterranean Sea). *Journal of Coastal Conservation*, 22(3), 519–532. https://doi.org/10.1007/s11852-017-0518-4

García-Navas, V., Martínez-Núñez, C., Tarifa, R., Molina-Pardo, J.L., Valera, F., Salido, T., et al. (2022) Partitioning beta diversity to untangle mechanisms underlying the assembly of bird communities in Mediterranean olive groves. *Diversity and Distributions*, 28(1), 112–127. https://doi.org/10.1111/ddi.13445

Garnier, S., Ross, N., Rudis, R., Camargo, A.P., Sciaini, M., & Scherer, C. (2023) viridis(Lite) - Colorblind-Friendly Color Maps for R. https://doi.org/10.5281/ZENODO.4679424

GEOSCOPIO. (2022) http://www502.regione.toscana.it/geoscopio/ortofoto.html.

Gering, J.C., Crist, T.O., & Veech, J.A. (2003) Additive Partitioning of Species Diversity across Multiple Spatial Scales: Implications for Regional Conservation of Biodiversity. *Conservation Biology*, 17(2), 488–499. https://doi.org/10.1046/j.1523-1739.2003.01465.x

Gholizadeh, H., Bonari, G., Pafumi, E., Bertacchi, A., Calbi, M., Castagnini, P., et al. (2025) SALTISH: The SALt-affected vegeTatIon dataset of Tuscany coaStal Habitats, central Italy. *Vegetation Ecology and Diversity*, 62, 1–8. https://doi.org/10.3897/ved.144362

Gigante, D., Attorre, F., Venanzoni, R., Acosta, A.T.R., Agrillo, E., Aleffi, M., et al. (2016) A methodological protocol for Annex I Habitats monitoring: the contribution of Vegetation science. *Plant Sociology*, (53 (2)), 77–87. https://doi.org/10.7338/pls2016532/06

Girardello, M., Santangeli, A., Mori, E., Chapman, A., Fattorini, S., Naidoo, R., et al. (2019) Global synergies and trade-offs between multiple dimensions of biodiversity and ecosystem services. *Scientific Reports*, 9(1), 5636. https://doi.org/10.1038/s41598-019-41342-7

Gómez-Zotano, J., Olmedo-Cobo, J.A., & Arias-García, J. (2017) Mediterranean dune vegetation: conservation of a threatened ecosystem in southern Spain. *Geografisk Tidsskrift-Danish Journal of Geography*, 117(1), 36–52. https://doi.org/10.1080/00167223.2016.1267579

Google. (2025) Google Earth Pro.

Gray, C.L., Hill, S.L.L., Newbold, T., Hudson, L.N., Börger, L., Contu, S., et al. (2016) Local biodiversity is higher inside than outside terrestrial protected areas worldwide. *Nature Communications*, 7(1), 12306. https://doi.org/10.1038/ncomms12306

Grizonnet, M., Michel, J., Poughon, V., Inglada, J., Savinaud, M., & Cresson, R. (2017) Orfeo ToolBox: open source processing of remote sensing images. *Open Geospatial Data, Software and Standards*, 2(1), 15. https://doi.org/10.1186/s40965-017-0031-6

Gu, H., Singh, A., & Townsend, P.A. (2015) Detection of gradients of forest composition in an urban area using imaging spectroscopy. *Remote Sensing of Environment*, 167, 168–180. https://doi.org/10.1016/j.rse.2015.06.010

Guirado, E., Tabik, S., Alcaraz-Segura, D., Cabello, J., & Herrera, F. (2017) Deep-learning Versus OBIA for Scattered Shrub Detection with Google Earth Imagery: Ziziphus lotus as Case Study. *Remote Sensing*, 9(12), 1220. https://doi.org/10.3390/rs9121220

Hansen, A.J., & DeFries, R. (2007) Ecological mechanisms linking protected areas to surrounding lands. *Ecological Applications*, 17(4), 974–988. https://doi.org/10.1890/05-1098

Hao, X., Liu, L., Yang, R., Yin, L., Zhang, L., & Li, X. (2023) A Review of Data Augmentation Methods of Remote Sensing Image Target Recognition. *Remote Sensing*, 15(3), 827. https://doi.org/10.3390/rs15030827

Harper, L.M., Lefcheck, J.S., Whippo, R., Jones, M.S., Foltz, Z., & Duffy, J.E. (2022) Blinded by the bright: How species-poor habitats contribute to regional biodiversity across a tropical seascape. *Diversity and Distributions*, 28(11), 2272–2285. https://doi.org/10.1111/ddi.13632

Harris, C.R., Millman, K.J., Van Der Walt, S.J., Gommers, R., Virtanen, P., Cournapeau, D., et al. (2020) Array programming with NumPy. *Nature*, 585(7825), 357–362. https://doi.org/10.1038/s41586-020-2649-2

Heino, J., García Girón, J., Hämäläinen, H., Hellsten, S., Ilmonen, J., Karjalainen, J., et al. (2022) Assessing the conservation priority of freshwater lake sites based on taxonomic, functional and environmental uniqueness. *Diversity and Distributions*, 28(9), 1966–1978. https://doi.org/10.1111/ddi.13598

Heino, J., & Grönroos, M. (2017) Exploring species and site contributions to beta diversity in stream insect assemblages. *Oecologia*, 183(1), 151–160. https://doi.org/10.1007/s00442-016-3754-7

Hesp, P.A. (1991) Ecological processes and plant adaptations on coastal dunes. *Journal of Arid Environments*, 21(2), 165–191. https://doi.org/10.1016/S0140-1963(18)30681-5

Hesselbarth, M.H.K., Sciaini, M., With, K.A., Wiegand, K., & Nowosad, J. (2019) *landscapemetrics*: an open-source *R* tool to calculate landscape metrics. *Ecography*, 42(10), 1648–1657. https://doi.org/10.1111/ecog.04617

Hijmans, R. (2023) raster: Geographic Data Analysis and Modeling. R package version 3.6-26.

Hill, M.J., White, J.C., Biggs, J., Briers, R.A., Gledhill, D., Ledger, M.E., et al. (2021) Local contributions to beta diversity in urban pond networks: Implications for biodiversity conservation and management. *Diversity and Distributions*, 27(5), 887–900. https://doi.org/10.1111/ddi.13239

Holenstein, K., Simonson, W.D., Smith, K.G., Blackburn, T.M., & Charpentier, A. (2021) Non-native Species Surrounding Protected Areas Influence the Community of Non-native Species Within Them. *Frontiers in Ecology and Evolution*, 8, 625137. https://doi.org/10.3389/fevo.2020.625137

Honrado, J., Vicente, J., Lomba, A., Alves, P., Macedo, J.A., Henriques, R., et al. (2010) Fine-scale patterns of vegetation assembly in the monitoring of changes in coastal sand-dune landscapes. *Web Ecology*, 10(1), 1–14. https://doi.org/10.5194/we-10-1-2010

Iacarella, J.C. (2022) Fish zeta diversity responses to human pressures and cumulative effects across a freshwater basin. *Diversity and Distributions*, 28(4), 830–843. https://doi.org/10.1111/ddi.13486

Innangi, M., Di Febbraro, M., Balsi, M., Colonna, G., Finizio, M., Pontieri, F., & Carranza, M.L. (2025) A novel high-resolution eco-functional vegetation mapping of coastal dunes. *Ecological Indicators*, 171, 113157. https://doi.org/10.1016/j.ecolind.2025.113157

Innangi, M., Marzialetti, F., Di Febbraro, M., Acosta, A.T.R., De Simone, W., Frate, L., et al. (2023) Coastal Dune Invaders: Integrative Mapping of Carpobrotus sp. pl. (Aizoaceae) Using UAVs. *Remote Sensing*, 15(2), 503. https://doi.org/10.3390/rs15020503

ISPRA. (2025a) *Dissesto idrogeologico in Italia: pericolosità e indicatori di rischio. Edizione 2024*.

ISPRA. (2025b) *Stato dell'ambiente in Italia 2025, indicatori e analisi*.

Janssen, J.A.M., Rodwell, J.S., Criado, M.S., Gubbay, S., Arts, G.H.P., & Haynes, T. (2016) *European red list of habitats. Part 2, Terrestrial and freshwater habitats.* Publications Office: LU.

Jarocińska, A., Kopeć, D., Niedzielko, J., Wylazłowska, J., Halladin-Dąbrowska, A., Charyton, J., et al. (2023) The utility of airborne hyperspectral and satellite multispectral images in identifying Natura 2000 non-forest habitats for conservation purposes. *Scientific Reports*, 13(1), 4549. https://doi.org/10.1038/s41598-023-31705-6

Juel, A., Ejrnæs, R., Fredshavn, J., & Groom, G. (2013) Integrating field survey and orthophoto information to monitor coastal habitats — A pilot study to develop methods and resolve key issues. *Ecological Informatics*, 14, 48–52. https://doi.org/10.1016/j.ecoinf.2012.11.014

Kamusoko, C. (2019) *Remote Sensing Image Classification in R*. Springer Singapore: Singapore. https://doi.org/10.1007/978-981-13-8012-9

Kattenborn, T., Eichel, J., & Fassnacht, F.E. (2019) Convolutional Neural Networks enable efficient, accurate and fine-grained segmentation of plant species and communities from high-resolution UAV imagery. *Scientific Reports*, 9(1), 17656. https://doi.org/10.1038/s41598-019-53797-9

Keijsers, J.G.S., Giardino, A., Poortinga, A., Mulder, J.P.M., Riksen, M.J.P.M., & Santinelli, G. (2015) Adaptation strategies to maintain dunes as flexible coastal flood defense in The

Netherlands. *Mitigation and Adaptation Strategies for Global Change*, 20(6), 913–928. https://doi.org/10.1007/s11027-014-9579-y

Kerry, R.G., Montalbo, F.J.P., Das, R., Patra, S., Mahapatra, G.P., Maurya, G.K., et al. (2022) An overview of remote monitoring methods in biodiversity conservation. *Environmental Science and Pollution Research*, 29(53), 80179–80221. https://doi.org/10.1007/s11356-022-23242-y

Khatami, R., Mountrakis, G., & Stehman, S.V. (2016) A meta-analysis of remote sensing research on supervised pixel-based land-cover image classification processes: General guidelines for practitioners and future research. *Remote Sensing of Environment*, 177, 89–100. https://doi.org/10.1016/j.rse.2016.02.028

Klemas, V.V. (2015) Coastal and Environmental Remote Sensing from Unmanned Aerial Vehicles: An Overview. *Journal of Coastal Research*, 315, 1260–1267. https://doi.org/10.2112/JCOASTRES-D-15-00005.1

Koenker, R. (1999) quantreg: Quantile Regression 6.1. https://doi.org/10.32614/CRAN.package.quantreg

Koyama, A., & Ide, T. (2020) Coastal habitats across sea-to-inland gradient sustain endangered coastal plants and Hymenoptera in coastal dune ecosystems of Japan. *Biodiversity and Conservation*, 29(14), 4073–4090. https://doi.org/10.1007/s10531-020-02065-8

Kozhoridze, G., Ben-Dor, E., Moudrý, V., & Sternberg, M. (2025) Remote sensing assessment of invasive plant species impacts on microclimate and water stress in mediterranean coastal ecosystems. *Agricultural and Forest Meteorology*, 371, 110606. https://doi.org/10.1016/j.agrformet.2025.110606

Kruse, F.A., Lefkoff, A.B., Boardman, J.W., Heidebrecht, K.B., Shapiro, A.T., Barloon, P.J., & Goetz, A.F.H. (1993) The spectral image processing system (SIPS)—interactive visualization and analysis of imaging spectrometer data. *Remote Sensing of Environment*, 44(2–3), 145–163. https://doi.org/10.1016/0034-4257(93)90013-N

Kuester, M. (2016) Radiometric use of WorldView-3 imagery. DigitalGlobe: Longmont, CO, USA.

Kuhn, M. (2021) caret: Classification and Regression Training. R package version 6.0-90.

Kukkala, A.S., & Moilanen, A. (2013) Core concepts of spatial prioritisation in systematic conservation planning. *Biological Reviews*, 88(2), 443–464. https://doi.org/10.1111/brv.12008

Lalitha, V., & Latha, B. (2022) A review on remote sensing imagery augmentation using deep learning. *Materials Today: Proceedings*, 62, 4772–4778. https://doi.org/10.1016/j.matpr.2022.03.341

Lande, R. (1996) Statistics and Partitioning of Species Diversity, and Similarity among Multiple Communities. *Oikos*, 76(1), 5. https://doi.org/10.2307/3545743

Landi, M., Ricceri, C., & Angiolini, C. (2012) Evaluation of Dune Rehabilitation after 95 Years by Comparison of Vegetation in Disturbed and Natural Sites. *Journal of Coastal Research*, 284, 1130–1141. https://doi.org/10.2112/JCOASTRES-D-11-00056.1

Lansu, E.M., Reijers, V.C., Daniëls, F., James, R., Christianen, M.J.A., & Van Der Heide, T. (2025) Habitat mapping of coastal dunes with deep learning. *Ecological Informatics*, 92, 103444. https://doi.org/10.1016/j.ecoinf.2025.103444

Laporte-Fauret, Q., Lubac, B., Castelle, B., Michalet, R., Marieu, V., Bombrun, L., et al. (2020) Classification of Atlantic Coastal Sand Dune Vegetation Using In Situ, UAV, and Airborne Hyperspectral Data. *Remote Sensing*, 12(14), 2222. https://doi.org/10.3390/rs12142222

Latella, M., Luijendijk, A., Moreno-Rodenas, A.M., & Camporeale, C. (2021) Satellite Image Processing for the Coarse-Scale Investigation of Sandy Coastal Areas. *Remote Sensing*, 13(22), 4613. https://doi.org/10.3390/rs13224613

LeCun, Y., Bengio, Y., & Hinton, G. (2015) Deep learning. *Nature*, 521(7553), 436–444. https://doi.org/10.1038/nature14539

Legendre, P. (2014) Interpreting the replacement and richness difference components of beta diversity: Replacement and richness difference components. *Global Ecology and Biogeography*, 23(11), 1324–1334. https://doi.org/10.1111/geb.12207

Legendre, P., & De Cáceres, M. (2013) Beta diversity as the variance of community data: dissimilarity coefficients and partitioning. *Ecology Letters*, 16(8), 951–963. https://doi.org/10.1111/ele.12141

Leutner, B., Horning, N., Schwalb-Willmann, J., & Mueller, K. (2024) RStoolbox: Remote Sensing Data Analysis. R package version 0.4.0.

Levin, S.A. (1992) The Problem of Pattern and Scale in Ecology: The Robert H. MacArthur Award Lecture. *Ecology*, 73(6), 1943–1967. https://doi.org/10.2307/1941447

Likens, G.E., & Lindenmayer, D.B. (2012) Integrating approaches leads to more effective conservation of biodiversity. *Biodiversity and Conservation*, 21(13), 3323–3341. https://doi.org/10.1007/s10531-012-0364-5

Listiani, I.A., Leloglu, U.M., Zeydanli, U., & Caliskan, B.K. (2022) Mapping Mediterranean maquis formations using Sentinel-2 time-series. *Ecological Informatics*, 71, 101814. https://doi.org/10.1016/j.ecoinf.2022.101814

Lozano, V., Di Febbraro, M., Brundu, G., Carranza, M.L., Alessandrini, A., Ardenghi, N.M.G., et al. (2023) Plant invasion risk inside and outside protected areas: Propagule pressure, abiotic and biotic factors definitively matter. *Science of The Total Environment*, 877, 162993. https://doi.org/10.1016/j.scitotenv.2023.162993

Lucas, N.S., Shanmugam, S., & Barnsley, M. (2002) Sub-pixel habitat mapping of a costal dune ecosystem. *Applied Geography*, 22(3), 253–270. https://doi.org/10.1016/S0143-6228(02)00007-3

Luijendijk, A., Hagenaars, G., Ranasinghe, R., Baart, F., Donchyts, G., & Aarninkhof, S. (2018) The State of the World's Beaches. *Scientific Reports*, 8(1), 6641. https://doi.org/10.1038/s41598-018-24630-6

Mairota, P., Cafarelli, B., Didham, R.K., Lovergine, F.P., Lucas, R.M., Nagendra, H., et al. (2015) Challenges and opportunities in harnessing satellite remote-sensing for biodiversity monitoring. *Ecological Informatics*, 30, 207–214. https://doi.org/10.1016/j.ecoinf.2015.08.006

Malavasi, M. (2020) The map of biodiversity mapping. *Biological Conservation*, 252, 108843. https://doi.org/10.1016/j.biocon.2020.108843

Malavasi, M., Bartak, V., Carranza, M.L., Simova, P., & Acosta, A.T.R. (2018) Landscape pattern and plant biodiversity in Mediterranean coastal dune ecosystems: Do habitat loss and fragmentation really matter? *Journal of Biogeography*, 45(6), 1367–1377. https://doi.org/10.1111/jbi.13215

Malavasi, M., Bazzichetto, M., Komárek, J., Moudrý, V., Rocchini, D., Bagella, S., et al. (2021) Unmanned aerial systems-based monitoring of the eco-geomorphology of coastal dunes through spectral Rao's *Q*. *Applied Vegetation Science*, 24(1), e12567. https://doi.org/10.1111/avsc.12567

Malavasi, M., Santoro, R., Cutini, M., Acosta, A.T.R., & Carranza, M.L. (2016) The impact of human pressure on landscape patterns and plant species richness in Mediterranean coastal dunes. *Plant Biosystems*, 150(1), 73–82. https://doi.org/10.1080/11263504.2014.913730

Malavasi, M., Santoro, R., Cutini, M., Acosta, A.T.R., & Carranza, M.L. (2013) What has happened to coastal dunes in the last half century? A multitemporal coastal landscape analysis in Central Italy. *Landscape and Urban Planning*, 119, 54–63. https://doi.org/10.1016/j.landurbplan.2013.06.012

Mantel, N. (1967) The Detection of Disease Clustering and a Generalized Regression Approach. *Cancer Research*, 27(2), 209–220.

Marcenò, C., Guarino, R., Loidi, J., Herrera, M., Isermann, M., Knollová, I., et al. (2018) Classification of European and Mediterranean coastal dune vegetation. *Applied Vegetation Science*, 21(3), 533–559. https://doi.org/10.1111/avsc.12379

Margules, C.R., & Pressey, R.L. (2000) Systematic conservation planning. *Nature*, 405(6783), 243–253. https://doi.org/10.1038/35012251

Martínez, M.L., Psuty, N.P., & Lubke, R.A. (2008) A Perspective on Coastal Dunes. In: Martínez, M.L. & Psuty, N.P. (Eds), *Coastal Dunes*, Ecological Studies. Springer Berlin Heidelberg: Berlin, Heidelberg, pp. 3–10. https://doi.org/10.1007/978-3-540-74002-5_1

Martín-Gallego, P., Delgado-Fernandez, I., & Marston, C. (2025) The application of satellite remote sensing to coastal dune environments: A systematic review. *Progress in Physical Geography: Earth and Environment*, 03091333251380450. https://doi.org/10.1177/03091333251380450

Marzialetti, F., Di Febbraro, M., Malavasi, M., Giulio, S., Acosta, A.T.R., & Carranza, M.L. (2020) Mapping Coastal Dune Landscape through Spectral Rao's Q Temporal Diversity. *Remote Sensing*, 12(14), 2315. https://doi.org/10.3390/rs12142315

Marzialetti, F., Frate, L., De Simone, W., Frattaroli, A.R., Acosta, A.T.R., & Carranza, M.L. (2021) Unmanned Aerial Vehicle (UAV)-Based Mapping of Acacia saligna Invasion in the Mediterranean Coast. *Remote Sensing*, 13(17), 3361. https://doi.org/10.3390/rs13173361

Marzialetti, F., Giulio, S., Malavasi, M., Sperandii, M.G., Acosta, A.T.R., & Carranza, M.L. (2019) Capturing Coastal Dune Natural Vegetation Types Using a Phenology-Based Mapping Approach: The Potential of Sentinel-2. *Remote Sensing*, 11(12), 1506. https://doi.org/10.3390/rs11121506

Maun, M.A. (2009) *The Biology of Coastal Sand Dunes*. Oxford University Press. https://doi.org/10.1093/oso/9780198570356.001.0001

Maxwell, A.E., Warner, T.A., & Fang, F. (2018) Implementation of machine-learning classification in remote sensing: an applied review. *International Journal of Remote Sensing*, 39(9), 2784–2817. https://doi.org/10.1080/01431161.2018.1433343

Maxwell, A.E., Warner, T.A., & Guillén, L.A. (2021) Accuracy Assessment in Convolutional Neural Network-Based Deep Learning Remote Sensing Studies—Part 1: Literature Review. *Remote Sensing*, 13(13), 2450. https://doi.org/10.3390/rs13132450

Medina Machín, A., Marcello, J., Hernández-Cordero, A.I., Martín Abasolo, J., & Eugenio, F. (2019) Vegetation species mapping in a coastal-dune ecosystem using high resolution satellite imagery. *GIScience & Remote Sensing*, 56(2), 210–232. https://doi.org/10.1080/15481603.2018.1502910

Meerdink, S., Hiatt, D., Flory, S.L., & Zare, A. (2024) Dealing with imperfect data for invasive species detection using multispectral imagery. *Ecological Informatics*, 79, 102432. https://doi.org/10.1016/j.ecoinf.2023.102432

Menicagli, V., Balestri, E., & Lardicci, C. (2019) Exposure of coastal dune vegetation to plastic bag leachates: A neglected impact of plastic litter. *Science of The Total Environment*, 683, 737–748. https://doi.org/10.1016/j.scitotenv.2019.05.245

Mikula, K., Šibíková, M., Ambroz, M., Kollár, M., Ožvat, A.A., Urbán, J., et al. (2021) NaturaSat—A Software Tool for Identification, Monitoring and Evaluation of Habitats by Remote Sensing Techniques. *Remote Sensing*, 13(17), 3381. https://doi.org/10.3390/rs13173381

Naas, A.E., Halvorsen, R., Horvath, P., Wollan, A.K., Bratli, H., Brynildsrud, K., et al. (2023) What explains inconsistencies in field-based ecosystem mapping? *Applied Vegetation Science*, 26(1), e12715. https://doi.org/10.1111/avsc.12715

Nagendra, H. (2001) Using remote sensing to assess biodiversity. *International Journal of Remote Sensing*, 22(12), 2377–2400. https://doi.org/10.1080/01431160117096

Nagendra, H., Lucas, R., Honrado, J.P., Jongman, R.H.G., Tarantino, C., Adamo, M., & Mairota, P. (2013) Remote sensing for conservation monitoring: Assessing protected areas, habitat extent, habitat condition, species diversity, and threats. *Ecological Indicators*, 33, 45–59. https://doi.org/10.1016/j.ecolind.2012.09.014

Nagendra, H., & Rocchini, D. (2008) High resolution satellite imagery for tropical biodiversity studies: the devil is in the detail. *Biodiversity and Conservation*, 17(14), 3431–3442. https://doi.org/10.1007/s10531-008-9479-0

Nawarat, K., Reyns, J., Vousdoukas, M.I., Duong, T.M., Kras, E., & Ranasinghe, R. (2024) Coastal hardening and what it means for the world's sandy beaches. *Nature Communications*, 15(1), 10626. https://doi.org/10.1038/s41467-024-54952-1

Neumann, C., Itzerott, S., Weiss, G., Kleinschmit, B., & Schmidtlein, S. (2016) Mapping multiple plant species abundance patterns - A multiobjective optimization procedure for combining reflectance spectroscopy and species ordination. *Ecological Informatics*, 36, 61–76. https://doi.org/10.1016/j.ecoinf.2016.10.002

Niskanen, A.K.J., Heikkinen, R.K., Väre, H., & Luoto, M. (2017) Drivers of high-latitude plant diversity hotspots and their congruence. *Biological Conservation*, 212, 288–299. https://doi.org/10.1016/j.biocon.2017.06.019

Novoa, A., González, L., Moravcová, L., & Pyšek, P. (2013) Constraints to native plant species establishment in coastal dune communities invaded by Carpobrotus edulis: Implications for restoration. *Biological Conservation*, 164, 1–9. https://doi.org/10.1016/j.biocon.2013.04.008

Oksanen, J., Simpson, G., Blanchet, F., Kindt, R., Legendre, P., Minchin, P., et al. (2022) vegan: Community Ecology Package. R package version 2.6-4.

Orme, C.D.L., Davies, R.G., Burgess, M., Eigenbrod, F., Pickup, N., Olson, V.A., et al. (2005) Global hotspots of species richness are not congruent with endemism or threat. *Nature*, 436(7053), 1016–1019. https://doi.org/10.1038/nature03850

Pafumi, E., Angiolini, C., Bacaro, G., Fanfarillo, E., Fiaschi, T., Rocchini, D., et al. (2025) Fuzzy approaches provide improved spatial detection of coastal dune EU habitats. *Ecological Informatics*, 86, 103059. https://doi.org/10.1016/j.ecoinf.2025.103059

Pafumi, E., Petruzzellis, F., Castello, M., Altobelli, A., Maccherini, S., Rocchini, D., & Bacaro, G. (2023) Using spectral diversity and heterogeneity measures to map habitat mosaics: An example from the Classical Karst. *Applied Vegetation Science*, 26(4), e12762. https://doi.org/10.1111/avsc.12762

Papini, F., Gianguzzi, L., Brullo, S., Bianco, P.M., & Angelini, P. (2008) Carta della Natura della Regione Sicilia: carta degli habitat alla scala 1:50.000.

Perez Rocha, M., Morris, T.J., Cottenie, K., & Schwalb, A.N. (2023) Limitations of beta diversity in conservation site selection. *Ecological Indicators*, 154, 110732. https://doi.org/10.1016/j.ecolind.2023.110732

Pérez-Carabaza, S., Boydell, O., & O'Connell, J. (2021) Habitat classification using convolutional neural networks and multitemporal multispectral aerial imagery. *Journal of Applied Remote Sensing*, 15(04). https://doi.org/10.1117/1.JRS.15.042406

Persson, H.J., Ekström, M., & Ståhl, G. (2022) Quantify and account for field reference errors in forest remote sensing studies. *Remote Sensing of Environment*, 283, 113302. https://doi.org/10.1016/j.rse.2022.113302

Pesaresi, S., Biondi, E., & Casavecchia, S. (2017) Bioclimates of Italy. *Journal of Maps*, 13(2), 955–960. https://doi.org/10.1080/17445647.2017.1413017

Pettorelli, N., Williams, J., Schulte To Bühne, H., & Crowson, M. (2025) Deep learning and satellite remote sensing for biodiversity monitoring and conservation. *Remote Sensing in Ecology and Conservation*, 11(2), 123–132. https://doi.org/10.1002/rse2.415

Pimm, S.L., Jenkins, C.N., Abell, R., Brooks, T.M., Gittleman, J.L., Joppa, L.N., et al. (2014) The biodiversity of species and their rates of extinction, distribution, and protection. *Science*, 344(6187), 1246752. https://doi.org/10.1126/science.1246752

Pinna, M.S., Bacchetta, G., Cogoni, D., & Fenu, G. (2019) Is vegetation an indicator for evaluating the impact of tourism on the conservation status of Mediterranean coastal dunes? *Science of The Total Environment*, 674, 255–263. https://doi.org/10.1016/j.scitotenv.2019.04.120

Portal to the Flora of Italy. (2023). https://dryades.units.it/floritaly/ [Accessed 15 March 2023]

Pressey, R.L., Ferrier, S., Hager, T.C., Woods, C.A., Tully, S.L., & Weinman, K.M. (1996) How well protected are the forests of north-eastern New South Wales? — Analyses of forest environments in relation to formal protection measures, land tenure, and vulnerability to clearing. *Forest Ecology and Management*, 85(1–3), 311–333. https://doi.org/10.1016/S0378-1127(96)03766-8

Prisco, I., Acosta, A.T.R., & Ercole, S. (2012) An overview of the Italian coastal dune EU habitats. *Annali di Botanica*, 2(0), 39–48. https://doi.org/10.4462/annbotrm-9340

Prisco, I., Acosta, A.T.R., & Stanisci, A. (2021) A bridge between tourism and nature conservation: boardwalks effects on coastal dune vegetation. *Journal of Coastal Conservation*, 25(1), 14. https://doi.org/10.1007/s11852-021-00809-4

Prisco, I., Angiolini, C., Assini, S., Buffa, G., Gigante, D., Marcenò, C., et al. (2020) Conservation status of Italian coastal dune habitats in the light of the 4th Monitoring Report (92/43/EEC Habitats Directive). *Plant Sociology*, 57(1), 55–64. https://doi.org/10.3897/pls2020571/05

Prisco, I., Carboni, M., & Acosta, A.T.R. (2013) The Fate of Threatened Coastal Dune Habitats in Italy under Climate Change Scenarios. *PLoS ONE*, 8(7), e68850. https://doi.org/10.1371/journal.pone.0068850

Prisco, I., Stanisci, A., & Acosta, A.T.R. (2016) Mediterranean dunes on the go: Evidence from a short term study on coastal herbaceous vegetation. *Estuarine, Coastal and Shelf Science*, 182, 40–46. https://doi.org/10.1016/j.ecss.2016.09.012

Prodanov, B., Gussev, C., Sopotlieva, D., Valcheva, M., Bekova, R., Baltakova, A., et al. (2025) A standard procedure for dune mapping along the Bulgarian Black Sea coast: an integrated approach combining UAS photogrammetry, geomorphological and phytocoenological surveys. *Frontiers in Marine Science*, 12, 1579724. https://doi.org/10.3389/fmars.2025.1579724

Prudnikova, E., Savin, I., Vindeker, G., Grubina, P., Shishkonakova, E., & Sharychev, D. (2019) Influence of Soil Background on Spectral Reflectance of Winter Wheat Crop Canopy. *Remote Sensing*, 11(16), 1932. https://doi.org/10.3390/rs11161932

QGIS Development Team. (2022) QGIS Geographic Information System.

QGIS Development Team. (2024) QGIS Geographic Information System.

R Core Team. (2023) R: A language and environment for statistical computing. R Foundation for Statistical Computing, Vienna, Austria. URL https://www.R-project.org/.

R Core Team. (2025) R: A language and environment for statistical computing. R Foundation for Statistical Computing, Vienna, Austria. URL https://www.R-project.org/.

Rapinel, S., Clément, B., Magnanon, S., Sellin, V., & Hubert-Moy, L. (2014) Identification and mapping of natural vegetation on a coastal site using a Worldview-2 satellite image. *Journal of Environmental Management*, 144, 236–246. https://doi.org/10.1016/j.jenvman.2014.05.027

Rapinel, S., Mony, C., Lecoq, L., Clément, B., Thomas, A., & Hubert-Moy, L. (2019) Evaluation of Sentinel-2 time-series for mapping floodplain grassland plant communities. *Remote Sensing of Environment*, 223, 115–129. https://doi.org/10.1016/j.rse.2019.01.018

Rapinel, S., Rossignol, N., Hubert-Moy, L., Bouzillé, J., & Bonis, A. (2018) Mapping grassland plant communities using a fuzzy approach to address floristic and spectral uncertainty. *Applied Vegetation Science*, 21(4), 678–693. https://doi.org/10.1111/avsc.12396

Räsänen, A., Juutinen, S., Tuittila, E., Aurela, M., & Virtanen, T. (2019) Comparing ultra-high spatial resolution remote-sensing methods in mapping peatland vegetation. *Journal of Vegetation Science*, 30(5), 1016–1026. https://doi.org/10.1111/jvs.12769

Rasino, M.D.V., Fattorini, S., Sciarretta, A., Colacci, M., Stanisci, A., & Carranza, M.L. (2024) Cross-taxon analysis in the highly threatened Mediterranean dunes reveals consistent diversity patterns in butterfly and plant communities. *Biodiversity and Conservation*, 33(13), 3643–3661. https://doi.org/10.1007/s10531-024-02914-w

Reddy, C.S. (2021) Remote sensing of biodiversity: what to measure and monitor from space to species? *Biodiversity and Conservation*, 30(10), 2617–2631. https://doi.org/10.1007/s10531-021-02216-5

Regione Toscana. (2023) Ortofoto 2023 - Regione Toscana - Base Informativa Territoriale regionale, art. 55 della L.R. 65/2014.

Rezaee, M., Mahdianpari, M., Zhang, Y., & Salehi, B. (2018) Deep Convolutional Neural Network for Complex Wetland Classification Using Optical Remote Sensing Imagery. *IEEE Journal of Selected Topics in Applied Earth Observations and Remote Sensing*, 11(9), 3030–3039. https://doi.org/10.1109/JSTARS.2018.2846178

Richards, J.A. (2013) *Remote Sensing Digital Image Analysis*. Springer Berlin Heidelberg: Berlin, Heidelberg. https://doi.org/10.1007/978-3-642-30062-2

Roberts, D.A., Gardner, M., Church, R., Ustin, S., Scheer, G., & Green, R.O. (1998) Mapping Chaparral in the Santa Monica Mountains Using Multiple Endmember Spectral Mixture Models. *Remote Sensing of Environment*, 65(3), 267–279. https://doi.org/10.1016/S0034-4257(98)00037-6

Roberts, D.A., Yamaguchi, Y., & Lyon, R.J. (1986) *Comparison of various techniques for calibration of AIS data.*

Rocchini, D. (2010) While Boolean sets non-gently rip: A theoretical framework on fuzzy sets for mapping landscape patterns. *Ecological Complexity*, 7(1), 125–129. https://doi.org/10.1016/j.ecocom.2009.08.002

Rocchini, D., Balkenhol, N., Carter, G.A., Foody, G.M., Gillespie, T.W., He, K.S., et al. (2010) Remotely sensed spectral heterogeneity as a proxy of species diversity: Recent advances and open challenges. *Ecological Informatics*, 5(5), 318–329. https://doi.org/10.1016/j.ecoinf.2010.06.001

Rocchini, D., & Cade, B.S. (2008) Quantile Regression Applied to Spectral Distance Decay. *IEEE Geoscience and Remote Sensing Letters*, 5(4), 640–643. https://doi.org/10.1109/LGRS.2008.2001767

Rocchini, D., Chieffallo, L., Torresani, M., & Thouverai, E. (2025) imageRy: Modify and Share Images 0.3.0. https://doi.org/10.32614/CRAN.package.imageRy

Rocchini, D., Foody, G.M., Nagendra, H., Ricotta, C., Anand, M., He, K.S., et al. (2013) Uncertainty in ecosystem mapping by remote sensing. *Computers & Geosciences*, 50, 128–135. https://doi.org/10.1016/j.cageo.2012.05.022

Rocchini, D., & Ricotta, C. (2007) Are landscapes as crisp as we may think? *Ecological Modelling*, 204(3–4), 535–539. https://doi.org/10.1016/j.ecolmodel.2006.12.028

Rodwell, J.S., Evans, D., & Schaminée, J.H.J. (2018) Phytosociological relationships in European Union policy-related habitat classifications. *Rendiconti Lincei. Scienze Fisiche e Naturali*, 29(2), 237–249. https://doi.org/10.1007/s12210-018-0690-y

Ronneberger, O., Fischer, P., & Brox, T. (2015) U-Net: Convolutional Networks for Biomedical Image Segmentation. In: Navab, N., Hornegger, J., Wells, W.M., & Frangi, A.F. (Eds), *Medical Image Computing and Computer-Assisted Intervention – MICCAI 2015*,

Lecture Notes in Computer Science. Springer International Publishing: Cham, pp. 234–241. https://doi.org/10.1007/978-3-319-24574-4_28

Ryan, C., Buckley, H.L., Bishop, C.D., Hinchliffe, G., & Case, B.S. (2025) Quantifying vegetation cover on coastal active dunes using nationwide aerial image analysis. *Remote Sensing in Ecology and Conservation*, 11(1), 40–57. https://doi.org/10.1002/rse2.410

Sada, A., Kinoshita, Y., Shiota, S., & Kiya, H. (2018) Histogram-Based Image Pre-processing for Machine Learning. *2018 IEEE 7th Global Conference on Consumer Electronics (GCCE)*. IEEE: Nara, Japan, pp. 272–275. https://doi.org/10.1109/GCCE.2018.8574654

Santoro, R., Carboni, M., Carranza, M.L., & Acosta, A.T.R. (2012) Focal species diversity patterns can provide diagnostic information on plant invasions. *Journal for Nature Conservation*, 20(2), 85–91. https://doi.org/10.1016/j.jnc.2011.08.003

Santoro, R., Jucker, T., Carboni, M., & Acosta, A.T.R. (2012) Patterns of plant community assembly in invaded and non-invaded communities along a natural environmental gradient. *Journal of Vegetation Science*, 23(3), 483–494. https://doi.org/10.1111/j.1654-1103.2011.01372.x

Santoro, R., Jucker, T., Prisco, I., Carboni, M., Battisti, C., & Acosta, A.T.R. (2012) Effects of Trampling Limitation on Coastal Dune Plant Communities. *Environmental Management*, 49(3), 534–542. https://doi.org/10.1007/s00267-012-9809-6

Sarmati, S., Angiolini, C., Sperandii, M.G., Barták, V., Gennai, M., Acosta, A.T.R., et al. (2025) A complex interplay between natural and anthropogenic factors shapes plant diversity patterns in Mediterranean coastal dunes. *Landscape Ecology*, 40(1), 20. https://doi.org/10.1007/s10980-024-02025-5

Sarmati, S., Bonari, G., & Angiolini, C. (2019) Conservation status of Mediterranean coastal dune habitats: anthropogenic disturbance may hamper habitat assignment. *Rendiconti Lincei. Scienze Fisiche e Naturali*, 30(3), 623–636. https://doi.org/10.1007/s12210-019-00823-7

Schiefer, F., Kattenborn, T., Frick, A., Frey, J., Schall, P., Koch, B., & Schmidtlein, S. (2020) Mapping forest tree species in high resolution UAV-based RGB-imagery by means of convolutional neural networks. *ISPRS Journal of Photogrammetry and Remote Sensing*, 170, 205–215. https://doi.org/10.1016/j.isprsjprs.2020.10.015

Shanmugam, P., Ahn, Y.-H., & Sanjeevi, S. (2006) A comparison of the classification of wetland characteristics by linear spectral mixture modelling and traditional hard classifiers on multispectral remotely sensed imagery in southern India. *Ecological Modelling*, 194(4), 379–394. https://doi.org/10.1016/j.ecolmodel.2005.10.033

Shanmugam, S., Lucas, N., Phipps, P., Richards, A., & Barnsley, M. (2003) Assessment of Remote Sensing Techniques for Habitat Mapping in Coastal Dune Ecosystems. *Journal of Coastal Research*, 19, 64–75.

Šilc, U., Mullaj, A., Alegro, A., Ibraliu, A., Dajić Stevanović, Z., Luković, M., & Stešević, D. (2016) Sand dune vegetation along the eastern Adriatic coast. *Phytocoenologia*, 46(4), 339–355. https://doi.org/10.1127/phyto/2016/0079

Silva, J.P., Toland, J., Eldridge, J., Potter, J., Jones, S., Nottingham, S., et al. (Eds). (2017) *LIFE and coastal habitats*. Publications Office: Luxembourg. https://doi.org/10.2779/180145

Smyth, T.A.G., Wilson, R., Rooney, P., & Yates, K.L. (2022) Extent, accuracy and repeatability of bare sand and vegetation cover in dunes mapped from aerial imagery is highly variable. *Aeolian Research*, 56, 100799. https://doi.org/10.1016/j.aeolia.2022.100799

Socolar, J.B., Gilroy, J.J., Kunin, W.E., & Edwards, D.P. (2016) How Should Beta-Diversity Inform Biodiversity Conservation? *Trends in Ecology & Evolution*, 31(1), 67–80. https://doi.org/10.1016/j.tree.2015.11.005

Sperandii, M.G., Barták, V., & Acosta, A.T.R. (2020) Effectiveness of the Natura 2000 network in conserving Mediterranean coastal dune habitats. *Biological Conservation*, 248, 108689. https://doi.org/10.1016/j.biocon.2020.108689

Sperandii, M.G., Bazzichetto, M., Acosta, A.T.R., Barták, V., & Malavasi, M. (2019) Multiple drivers of plant diversity in coastal dunes: A Mediterranean experience. *Science of The Total Environment*, 652, 1435–1444. https://doi.org/10.1016/j.scitotenv.2018.10.299

Sperandii, M.G., Prisco, I., & Acosta, A.T.R. (2018) Hard times for Italian coastal dunes: insights from a diachronic analysis based on random plots. *Biodiversity and Conservation*, 27(3), 633–646. https://doi.org/10.1007/s10531-017-1454-1

Sperandii, M.G., Prisco, I., Stanisci, A., & Acosta, A.T.R. (2017) RanVegDunes - A random plot database of Italian coastal dunes. *Phytocoenologia*, 47(2), 231–232. https://doi.org/10.1127/phyto/2017/0198

Suo, McGovern, & Gilmer. (2019) Coastal Dune Vegetation Mapping Using a Multispectral Sensor Mounted on an UAS. *Remote Sensing*, 11(15), 1814. https://doi.org/10.3390/rs11151814

Tan, L., Fan, C., Zhang, C., & Zhao, X. (2019) Understanding and protecting forest biodiversity in relation to species and local contributions to beta diversity. *European Journal of Forest Research*, 138(6), 1005–1013. https://doi.org/10.1007/s10342-019-01220-3

Tapia, R., Stein, A., & Bijker, W. (2005) Optimization of sampling schemes for vegetation mapping using fuzzy classification. *Remote Sensing of Environment*, 99(4), 425–433. https://doi.org/10.1016/j.rse.2005.09.013

Thouverai, E., Marcantonio, M., Bacaro, G., Da Re, D., Iannacito, M., Marchetto, E., et al. (2021) Measuring diversity from space: a global view of the free and open source rasterdiv R package under a coding perspective. *Community Ecology*, 22(1), 1–11. https://doi.org/10.1007/s42974-021-00042-x

Timm, B.C., & McGarigal, K. (2012) Fine-scale remotely-sensed cover mapping of coastal dune and salt marsh ecosystems at Cape Cod National Seashore using Random Forests. *Remote Sensing of Environment*, 127, 106–117. https://doi.org/10.1016/j.rse.2012.08.033

Tomaselli, V., Veronico, G., Sciandrello, S., & Blonda, P. (2016) How does the selection of landscape classification schemes affect the spatial pattern of natural landscapes? An assessment

on a coastal wetland site in southern Italy. *Environmental Monitoring and Assessment*, 188(6), 356. https://doi.org/10.1007/s10661-016-5352-x

Torca, M., Campos, J.A., & Herrera, M. (2019) Changes in plant diversity patterns along dune zonation in south Atlantic European coasts. *Estuarine, Coastal and Shelf Science*, 218, 39–47. https://doi.org/10.1016/j.ecss.2018.11.016

Tordoni, E., Bacaro, G., Weigelt, P., Cameletti, M., Janssen, J.A.M., Acosta, A.T.R., et al. (2021) Disentangling native and alien plant diversity in coastal sand dune ecosystems worldwide. *Journal of Vegetation Science*, 32(1), e12861. https://doi.org/10.1111/jvs.12961

Tordoni, E., Napolitano, R., Maccherini, S., Da Re, D., & Bacaro, G. (2018) Ecological drivers of plant diversity patterns in remnants coastal sand dune ecosystems along the northern Adriatic coastline. *Ecological Research*, 33(6), 1157–1168. https://doi.org/10.1007/s11284-018-1629-6

Tordoni, E., Petruzzellis, F., Nardini, A., Savi, T., & Bacaro, G. (2019) Make it simpler: Alien species decrease functional diversity of coastal plant communities. *Journal of Vegetation Science*, 30(3), 498–509. https://doi.org/10.1111/jvs.12734

Torresani, M., Rossi, C., Perrone, M., Hauser, L.T., Féret, J.-B., Moudrý, V., et al. (2024) Reviewing the Spectral Variation Hypothesis: Twenty years in the tumultuous sea of biodiversity estimation by remote sensing. *Ecological Informatics*, 82, 102702. https://doi.org/10.1016/j.ecoinf.2024.102702

Triepke, F.J. (2017) Fuzzy Classification of Vegetation for Ecosystem Mapping. In: Remmel, T.K. & Perera, A.H. (Eds), *Mapping Forest Landscape Patterns*. Springer New York: New York, NY, pp. 63–103. https://doi.org/10.1007/978-1-4939-7331-6_2

Trotta, G., Vuerich, M., Petrussa, E., Asquini, E., Cingano, P., & Boscutti, F. (2025) Capturing plant functional traits in coastal dunes using close-range remote sensing. *Ecological Informatics*, 88, 103159. https://doi.org/10.1016/j.ecoinf.2025.103159

Unberath, I., Vanierschot, L., Somers, B., Van De Kerchove, R., Vanden Borre, J., Unberath, M., & Feilhauer, H. (2019) Remote sensing of coastal vegetation: Dealing with high species turnover by mapping multiple floristic gradients. *Applied Vegetation Science*, 22(4), 534–546. https://doi.org/10.1111/avsc.12446

Valentini, E., Taramelli, A., Filipponi, F., & Giulio, S. (2015) An effective procedure for EUNIS and Natura 2000 habitat type mapping in estuarine ecosystems integrating ecological knowledge and remote sensing analysis. *Ocean & Coastal Management*, 108, 52–64. https://doi.org/10.1016/j.ocecoaman.2014.07.015

Van Beijma, S., Comber, A., & Lamb, A. (2014) Random forest classification of salt marsh vegetation habitats using quad-polarimetric airborne SAR, elevation and optical RS data. *Remote Sensing of Environment*, 149, 118–129. https://doi.org/10.1016/j.rse.2014.04.010

Van Der Biest, K., De Nocker, L., Provoost, S., Boerema, A., Staes, J., & Meire, P. (2017) Dune dynamics safeguard ecosystem services. *Ocean & Coastal Management*, 149, 148–158. https://doi.org/10.1016/j.ocecoaman.2017.10.005

Van Der Biest, K., Meire, P., Schellekens, T., D'hondt, B., Bonte, D., Vanagt, T., & Ysebaert, T. (2020) Aligning biodiversity conservation and ecosystem services in spatial planning: Focus on ecosystem processes. *Science of The Total Environment*, 712, 136350. https://doi.org/10.1016/j.scitotenv.2019.136350

Vanden Borre, J., Paelinckx, D., Mücher, C.A., Kooistra, L., Haest, B., De Blust, G., & Schmidt, A.M. (2011) Integrating remote sensing in Natura 2000 habitat monitoring: Prospects on the way forward. *Journal for Nature Conservation*, 19(2), 116–125. https://doi.org/10.1016/j.jnc.2010.07.003

Villalobos Perna, P., Di Febbraro, M., Carranza, M.L., Marzialetti, F., & Innangi, M. (2023) Remote Sensing and Invasive Plants in Coastal Ecosystems: What We Know So Far and Future Prospects. *Land*, 12(2), 341. https://doi.org/10.3390/land12020341

Villoslada, M., Bergamo, T.F., Ward, R.D., Burnside, N.G., Joyce, C.B., Bunce, R.G.H., & Sepp, K. (2020) Fine scale plant community assessment in coastal meadows using UAV based multispectral data. *Ecological Indicators*, 111, 105979. https://doi.org/10.1016/j.ecolind.2019.105979

Vousdoukas, M.I., Ranasinghe, R., Mentaschi, L., Plomaritis, T.A., Athanasiou, P., Luijendijk, A., & Feyen, L. (2020) Sandy coastlines under threat of erosion. *Nature Climate Change*, 10(3), 260–263. https://doi.org/10.1038/s41558-020-0697-0

Walker, B. (1995) Conserving Biological Diversity through Ecosystem Resilience. *Conservation Biology*, 9(4), 747–752. https://doi.org/10.1046/j.1523-1739.1995.09040747.x

Wang, G., Gertner, G., Xiao, X., Wente, S., & Anderson, A.B. (2001) Appropriate Plot Size and Spatial Resolution for Mapping Multiple Vegetation Types. *Photogrammetric Engineering & Remote Sensing*, 67(5), 575–584.

Wang, Z., Wang, T., Zhang, X., Wang, J., Yang, Y., Sun, Y., et al. (2024) Biodiversity conservation in the context of climate change: Facing challenges and management strategies. *Science of The Total Environment*, 937, 173377. https://doi.org/10.1016/j.scitotenv.2024.173377

Watanabe, S., Sumi, K., & Ise, T. (2020) Identifying the vegetation type in Google Earth images using a convolutional neural network: a case study for Japanese bamboo forests. *BMC Ecology*, 20(1), 65. https://doi.org/10.1186/s12898-020-00331-5

Watson, J.E.M., Darling, E.S., Venter, O., Maron, M., Walston, J., Possingham, H.P., et al. (2016) Bolder science needed now for protected areas: Protected-Area Science Needs. *Conservation Biology*, 30(2), 243–248. https://doi.org/10.1111/cobi.12645

Weinstein, B.G., Marconi, S., Bohlman, S.A., Zare, A., & White, E.P. (2020) Cross-site learning in deep learning RGB tree crown detection. *Ecological Informatics*, 56, 101061. https://doi.org/10.1016/j.ecoinf.2020.101061

Whittaker, R.H. (1972) Evolution and measurement of species diversity. *Taxon*, 21(2–3), 213–251. https://doi.org/10.2307/1218190

Whittaker, R.H. (1960) Vegetation of the Siskiyou Mountains, Oregon and California. *Ecological Monographs*, 30(3), 279–338. https://doi.org/10.2307/1943563

Wiser, S.K., McCarthy, J.K., Bellingham, P.J., Jolly, B., Meiforth, J.J., & Warawara Komiti Kaitiaki. (2022) Integrating plot-based and remotely sensed data to map vegetation types in a New Zealand warm-temperate rainforest. *Applied Vegetation Science*, 25(4), e12695. https://doi.org/10.1111/avsc.12695

Wolff, F., H. M. Kolari, T., Villoslada, M., Tahvanainen, T., Korpelainen, P., A. P. Zamboni, P., & Kumpula, T. (2023) RGB vs. Multispectral imagery: Mapping aapa mire plant communities with UAVs. *Ecological Indicators*, 148, 110140. https://doi.org/10.1016/j.ecolind.2023.110140

Yao, J., Huang, J., Ding, Y., Xu, Y., Xu, H., & Zang, R. (2021) Ecological uniqueness of species assemblages and their determinants in forest communities. *Diversity and Distributions*, 27(3), 454–462. https://doi.org/10.1111/ddi.13205

Zadeh, L.A. (1965) Fuzzy sets. *Information and Control*, 8(3), 338–353. https://doi.org/10.1016/S0019-9958(65)90241-X

Zlinszky, A., & Kania, A. (2016) Will it blend? Visualization and accuracy evaluation of high-resolution fuzzy vegetation maps. *The International Archives of the Photogrammetry, Remote Sensing and Spatial Information Sciences*, XLI-B2, 335–342. https://doi.org/10.5194/isprs-archives-XLI-B2-335-2016

# List of publications

**Core papers related to this thesis published or prepared in the course of the PhD ***

**Pafumi E**, Angiolini C, Sarmati S, Bacaro G, Fanfarillo E, Fiaschi T, Foggi B, Gennai M, Maccherini S (2024) Spatial patterns of coastal dune plant diversity reveal conservation priority hotspots in and out a network of protected areas. *Global Ecology and Conservation* 54, e03085 https://doi.org/10.1016/j.gecco.2024.e03085

**Pafumi E**, Angiolini C, Bacaro G, Fanfarillo E, Fiaschi T, Rocchini D, Sarmati S, Torresani M, Feilhauer H, Maccherini S (2025) Fuzzy approaches provide improved spatial detection of coastal dune EU habitats. *Ecological Informatics* 86, 103059 https://doi.org/10.1016/j.ecoinf.2025.103059

**Pafumi E**, Angiolini C, Bacaro G, de Simone L, Fanfarillo E, Fiaschi T, Rocchini D, Thouverai E, Maccherini S. Pixels and patterns in the sand: decoding coastal dune habitats with multi-resolution CNNs. Under review in *Journal of Vegetation Science*

* All authors agreed that published articles could be used as chapters of this thesis.

**Side papers published in the course of the PhD**

**Pafumi E**, Petruzzellis F, Castello M, Altobelli A, Maccherini S, Rocchini D, Bacaro G (2023) Using spectral diversity and heterogeneity measures to map habitat mosaics: An example from the Classical Karst. *Applied Vegetation Science* 26, e12762. https://doi.org/10.1111/avsc.12762

Fiaschi T, Bonari G, Frignani F, Gizzi G, Landi M, Magrini S, Quilghini G, **Pafumi E**, Scoppola A, Angiolini C (2024) Vascular flora of the isthmus of Feniglia (southern Tuscany, Italy). *Italian Botanist* 17, 77–101. https://doi.org/10.3897/italianbotanist.17.122982

Fanfarillo E, de Simone L, Fiaschi T, Foggi B, Gabellini A, Gennai M, Maccherini S, **Pafumi E**, Tordoni E, Viciani D, Zangari G, Angiolini C (2025) Drivers and patterns of community completeness suggest that Tuscan Fagus sylvatica forests can naturally have a low plant diversity. *Forest Ecosystems* 12, 100276. https://doi.org/10.1016/j.fecs.2024.100276

Acosta ATR, Di Biase L, Sarmati S, Allevato E, Angiolini C, Bagella S, Bazan G, Bertacchi

A, Brancaleoni L, Buffa G, Calbi M, Caria MC, Ciccarelli D, Cutini M, De Francesco MC, De Natale A, Fantinato E, Fiaschi T, Gangale C, Gerdol R, Gianguzzi L, Laface VLA, Maccherini S, Morabito A, Mugnai M, Musarella CM, **Pafumi E**, Santangelo A, Sciandrello S, Siccardi E, Spampinato G, Stanisci A, Strumia S, Viciani D, Del Vecchio S (2025) ReSurveyDunes — a data resource of resurveyed coastal dune vegetation plots in Italy. *Vegetation Ecology and Diversity* 62, 1–6. https://doi.org/10.3897/ved.139539

Gholizadeh H, Bonari G, **Pafumi E**, Bertacchi A, Calbi M, Castagnini P, Ciccarelli D, Fanfarillo E, Ferretti G, Fiaschi T, Foggi B, Gennai M, Lazzaro L, Mugnai M, Sarmati S, Viciani D, Angiolini C, Maccherini S (2025) SALTISH: The SALt-affected vegeTatIon dataset of Tuscany coaStal Habitats, central Italy. *Vegetation Ecology and Diversity* 62, 1–8. https://doi.org/10.3897/ved.144362

Cannucci S, Fanfarillo E, Maccherini S, Bolpagni R, Bonari G, De Simone L, Fiaschi T, Mascia F, **Pafumi E**, Angiolini C (2025) Mediterranean farmland ponds as unique habitats for plant diversity across different pondscapes. *Hydrobiologia*. https://doi.org/10.1007/s10750-025-05884-4

Fanfarillo E, Angiolini C, Capitani C, De Pasquale Picciarelli M, Fedeli R, Fiaschi T, Jepkogei P, **Pafumi E**, Valle B, Maccherini S (2025) Short-Term Effects of Minimum Tillage and Wood Distillate Addition on Plants and Springtails in an Olive Grove. *Environments* 12, 204. https://doi.org/10.3390/environments12060204

Fanfarillo E, Angiolini C, De Simone L, Bacaro G, Castaldini M, Fiaschi T, Mocali S, **Pafumi E**, Vitali F, Maccherini S (2025) Different control strategies of the invasive plant *Arundo donax* L. have taxon-specific effects on above- and belowground biodiversity. *Journal of Environmental Management* 392, 126833. https://doi.org/10.1016/j.jenvman.2025.126833

# Acknowledgements

I am sincerely grateful to my supervisors for their constant support and inspiration: to Simona Maccherini, for welcoming me into the research group and offering countless feedback and opportunities; to Giovanni Bacaro, for motivating me on this journey and guiding me along it; to Duccio Rocchini, for providing valuable support and innumerable research ideas.

I would also like to thank the rest of the group in Siena for these past three years. Thanks to Claudia Angiolini for sharing knowledge and perspectives on dune ecosystems and plants in general. To Emanuele Fanfarillo, for helping me through many doubts and writing challenges with clarity and availability. To Leopoldo de Simone, for the ideas and assistance in all drone matters. To Tiberio Fiaschi, for the support with everything related to species and field activities. To Silvia Cannucci, for the constant exchange and company in all the experiences we shared. Thanks also to everyone else on the third floor who, over time, shared with me ideas, suggestions and projects, or simply chats, dinners and walks: Hamid, Gianmaria, Francesco, Francesco, Hanna, Hannelore, Dario, Emanuele, Martina, Lisa, Mirko, Riccardo, Debora, Diego and all the others.

I am also grateful to the remote sensing group in Prague for the time I spent there: to Vítezslav Moudrý for supervising my stay in the lab; to Michela Perrone, Elena Cini and Elisa Thouverai for their insightful and kind research suggestions and for the moments spent together.

I would also like to thank all the researchers who shared the data that made this thesis possible, including Simona Sarmati, Marco Malavasi and all the other co-authors of the papers related to this thesis.

Finally, thanks to my parents, for supporting me during these three years as in all those before. To Ginevra, for reviewing dozens of emails and drafts and advising me thousands of times. To Paul, for patiently answering my endless programming questions. To my friends in Trieste, for always being ready to see me when I come home. To Carlotta, for the chats through which we supported each other in the ups and downs of the PhD. To Giovanni, for cheering me up in many moments of discouragement and for sharing the passion and curiosity for the natural world that give meaning to this work.

# Appendix

Supplementary materials to Chapter 1

Supplementary materials to Chapter 2

Supplementary materials to Chapter 3

Supplementary materials to Chapter 4

## Supplementary materials to Chapter 1

**Table S1.** List of the species found in the study area, assigned to the dune (D), synanthropic (S) and alien (A) groups.

| Species name | Abbreviation | Species group |
|---|---|---|
| *Achillea maritima* | Ach_mar | D |
| *Ambrosia psilostachya* | Amb_psi | A |
| *Anisantha rigida* | Ani_rig | S |
| *Anisantha rubens* | Ani_rub | S |
| *Anisantha sterilis* | Ani_ste | S |
| *Anisantha tectorum* | Ani_tec | S |
| *Anthemis maritima* | Ant_mar | D |
| *Arbutus unedo* | Arb_une | D |
| *Arenaria serpyllifolia* | Are_ser | S |
| *Arundo donax* | Aru_don | A |
| *Asparagus acutifolius* | Asp_acu | D |
| *Atriplex* sp. | Atr_sp. | |
| *Avena barbata* | Ave_bar | S |
| *Avena fatua* | Ave_fat | A |
| *Avena sterilis* | Ave_ste | A |
| *Blackstonia perfoliata* | Bla_per | |
| *Bolboschoenus maritimus* | Bol_mar | S |
| *Brachypodium distachyon* | Bra_dis | D |
| *Brachypodium sylvaticum* | Bra_syl | S |
| *Cakile maritima* | Cak_mar | D |
| *Calamagrostis arenaria* subsp. *arundinacea* | Cal_aru | D |
| *Campanula rapunculus* | Cam_rap | |
| *Carex flacca* | Car_fla | |
| *Carex* sp. | Car_sp. | |
| *Catapodium balearicum* | Cat_bal | |
| *Catapodium hemipoa* | Cat_hem | D |
| *Centaurea aplolepa* subsp. *subciliata* | Cen_sub | D |
| *Centaurea sphaerocephala* | Cen_sph | D |
| *Centaurium erythraea* | Cen_ery | S |
| *Centaurium maritimum* | Cen_mar | |
| *Cerastium diffusum* subsp. *diffusum* | Cer_dif | |
| *Cerastium glomeratum* | Cer_glo | S |
| *Cerastium* sp. | Cer_sp. | |

| | | |
|---|---|---|
| *Chamaerops humilis* | Cha_hum | |
| *Chenopodium* sp. | Che_sp. | S |
| *Cichorium intybus* | Cic_int | S |
| *Cistus creticus* subsp. *eriocephalus* | Cis_eri | D |
| *Clematis flammula* | Cle_fla | D |
| *Clematis vitalba* | Cle_vit | S |
| *Clinopodium nepeta* | Cli_nep | |
| *Convolvulus soldanella* | Con_sol | D |
| *Convolvulus* sp. | Con_sp. | S |
| *Crepis foetida* | Cre_foe | S |
| *Crepis* sp. | Cre_sp. | S |
| *Crithmum maritimum* | Cri_mar | D |
| *Crucianella maritima* | Cru_mar | D |
| *Cuscuta* sp. | Cus_sp. | |
| *Cutandia maritima* | Cut_mar | D |
| *Cynanchica pyrenaica* subsp. *cynanchica* | Cyn_cyn | D |
| *Cynodon dactylon* | Cyn_dac | S |
| *Cyperus capitatus* | Cyp_cap | D |
| *Dactylis glomerata* | Dac_glo | S |
| *Daphne gnidium* | Dap_gni | D |
| *Daphne sericea* | Dap_ser | D |
| *Daucus pumilus* | Dau_pum | D |
| *Daucus* sp. | Dau_sp. | S |
| *Dittrichia viscosa* | Dit_vis | S |
| *Echinophora spinosa* | Ech_spi | D |
| *Elymus repens* | Ely_rep | S |
| *Equisetum ramosissimum* | Equ_ram | S |
| *Erica multiflora* | Eri_mul | D |
| *Erigeron canadensis* | Eri_can | A |
| *Erigeron sumatrensis* | Eri_sum | A |
| *Eryngium maritimum* | Ery_mar | D |
| *Euphorbia barrelieri* | Eup_bar | D |
| *Euphorbia paralias* | Eup_par | D |
| *Euphorbia peplis* | Eup_pep | D |
| *Euphorbia peplus* | Eup_pep1 | S |
| *Festuca fasciculata* | Fes_fas | D |
| *Fumaria bicolor* | Fum_bic | S |
| *Galatella tripolium* | Gal_tri | D |
| *Galium murale* | Gal_mur | S |
| *Geranium purpureum* | Ger_pur | S |
| *Geranium pusillum* | Ger_pus | S |

| | | |
|---|---|---|
| *Glaucium flavum* | Gla_fla | D |
| *Hedera helix* | Hed_hel | |
| *Hedypnois rhagadioloides* | Hed_rha | S |
| *Helichrysum stoechas* | Hel_sto | D |
| *Hypochaeris achyrophorus* | Hyp_ach | |
| *Hypochaeris glabra* | Hyp_gla | |
| *Hypochaeris radicata* | Hyp_rad | D |
| *Imperata cylindrica* | Imp_cyl | |
| *Jacobaea maritima* | Jac_mar | D |
| *Juncus acutus* | Jun_acu | D |
| *Juncus bufonius* | Jun_buf | S |
| *Juncus inflexus* | Jun_inf | |
| *Juncus tenageia* | Jun_ten | |
| *Juniperus macrocarpa* | Jun_mac | D |
| *Juniperus turbinata* | Jun_tur | D |
| *Lagurus ovatus* | Lag_ova | D |
| *Lamium purpureum* | Lam_pur | S |
| *Lamium* sp. | Lam_sp. | |
| *Limbarda crithmoides* subsp. *longifolia* | Lim_lon | |
| *Limonium multiforme* | Lim_mul | |
| *Linum corymbulosum* | Lin_cor | |
| *Linum* sp. | Lin_sp. | |
| *Linum strictum* | Lin_str | |
| *Linum tenuifolium* | Lin_ten | |
| *Lomelosia rutifolia* | Lom_rut | D |
| *Lonicera implexa* | Lon_imp | D |
| *Lotus cytisoides* | Lot_cyt | D |
| *Lotus hirsutus* | Lot_hir | D |
| *Lysimachia arvensis* | Lys_arv | S |
| *Marcus-kochia ramosissima* | Mar_ram | D |
| *Maresia nana* | Mar_nan | D |
| *Matthiola sinuata* | Mat_sin | D |
| *Medicago littoralis* | Med_lit | D |
| *Medicago lupulina* | Med_lup | S |
| *Medicago marina* | Med_mar | D |
| *Medicago minima* | Med_min | |
| *Medicago rigidula* | Med_rig | S |
| *Medicago* sp. | Med_sp. | S |
| *Mentha suaveolens* subsp. *suaveolens* | Men_sua | |
| *Myosotis arvensis* | Myo_arv | S |
| *Myrtus communis* | Myr_com | D |

| | | |
|---|---|---|
| *Odontites luteus* | Odo_lut | |
| *Oenothera* sp. | Oen_sp. | A |
| *Onobrychis caput-galli* | Ono_cap | |
| *Ononis reclinata* | Ono_rec | |
| *Ononis variegata* | Ono_var | D |
| *Orobanche minor* | Oro_min | S |
| *Orobanche* sp. | Oro_sp. | |
| *Osyris alba* | Osy_alb | |
| *Pancratium maritimum* | Pan_mar | D |
| *Papaver rhoeas* | Pap_rho | S |
| *Parapholis incurva* | Par_inc | D |
| *Paspalum vaginatum* | Pas_vag | A |
| *Petrorhagia prolifera* | Pet_pro | |
| *Phalaris canariensis* | Pha_can | A |
| *Phillyrea angustifolia* | Phi_ang | D |
| *Phleum arenarium* subsp. *caesium* | Phl_cae | D |
| *Phragmites australis* | Phr_aus | |
| *Pinus pinaster* | Pin_pina | D |
| *Pinus pinea* | Pin_pin | A |
| *Pistacia lentiscus* | Pis_len | D |
| *Pittosporum tobira* | Pit_tob | A |
| *Plantago coronopus* | Pla_cor | D |
| *Poa bulbosa* | Poa_bul | |
| *Polycarpon* sp. | Pol_sp. | S |
| *Polygonum maritimum* | Pol_mar | D |
| *Polypogon subspathaceus* | Pol_sub | D |
| *Quercus ilex* | Que_ile | D |
| *Quercus suber* | Que_sub | |
| *Raphanus raphanistrum* | Rap_rap | S |
| *Raphanus* sp. | Rap_sp. | S |
| *Reichardia picroides* | Rei_pic | S |
| *Reseda alba* | Res_alb | S |
| *Rhamnus alaternus* | Rha_ala | D |
| *Rubia peregrina* | Rub_per | D |
| *Rubus ulmifolius* | Rub_ulm | S |
| *Ruscus aculeatus* | Rus_acu | |
| *Sabulina tenuifolia* | Sab_ten | D |
| *Salsola tragus* | Sal_tra | D |
| *Salvia rosmarinus* | Sal_ros | D |
| *Samolus valerandi* | Sam_val | |
| *Schoenus nigricans* | Sch_nig | |

| | | |
|---|---|---|
| *Scirpoides holoschoenus* | Sci_hol | |
| *Seseli tortuosum* | Ses_tor | D |
| *Sherardia arvensis* | She_arv | S |
| *Silene canescens* | Sil_can | D |
| *Silene otites* | Sil_oti | |
| *Silene* sp. | Sil_sp. | |
| *Smilax aspera* | Smi_asp | D |
| *Solanum nigrum* | Sol_nig | S |
| *Solanum* sp. | Sol_sp. | S |
| *Solidago virgaurea* subsp. *litoralis* | Sol_lit | D |
| *Sonchus asper* | Son_asp | S |
| *Sonchus bulbosus* | Son_bul | D |
| *Sonchus oleraceus* | Son_ole | S |
| *Sonchus* sp. | Son_sp. | S |
| *Sporobolus pumilus* | Spo_pum | A |
| *Sporobolus virginicus* | Spo_vir | D |
| *Stachys arvensis* | Sta_arv | S |
| *Stachys major* | Sta_maj | D |
| *Stachys maritima* | Sta_mar | D |
| *Tamarix gallica* | Tam_gal | |
| *Tamarix* sp. | Tam_sp. | |
| *Teucrium capitatum* | Teu_cap | |
| *Teucrium flavum* subsp. *flavum* | Teu_fla | |
| *Thinopyrum junceum* | Thi_jun | D |
| *Trifolium campestre* | Tri_cam | S |
| *Trifolium dubium* | Tri_dub | S |
| *Trifolium* sp. | Tri_sp. | S |
| *Trifolium striatum* | Tri_str | |
| *Tripidium ravennae* | Tri_rav | |
| *Tuberaria guttata* | Tub_gut | D |
| *Urospermum dalechampii* | Uro_dal | S |
| *Verbascum sinuatum* | Ver_sin | S |
| *Vicia bithynica* | Vic_bit | S |
| *Vicia narbonensis* | Vic_nar | |
| *Xanthium orientale* | Xan_ori | A |
| *Yucca gloriosa* | Yuc_glo | A |

**Table S2.** Results of beta regression analysis of LCBD with landscape variables, performed separately for the North (pseudo-$R^2$ = 0.29) and the South (pseudo-$R^2$ = 0.06) of the region.

| | | Estimate | Std. Error | z value | Pr(>\|z\|) |
|---|---|---|---|---|---|
| *North* | | | | | |
| | (Intercept) | -5.59 | 0.02 | -368.28 | < 0.01 |
| | Sea distance | -0.01 | 0.01 | -9.81 | < 0.01 |
| | Slope | -0.01 | 0.01 | -2.71 | < 0.01 |
| | %ART | 0.01 | 0.01 | 2.34 | 0.02 |
| | %WTC | 0.09 | 0.03 | 2.91 | < 0.01 |
| | Distance to ART | 0.01 | 0.01 | 2.96 | < 0.01 |
| *South* | | | | | |
| | (Intercept) | -5.33 | 0.01 | -485.08 | < 0.01 |
| | Slope | -0.01 | 0.01 | -2.21 | 0.03 |
| | Distance to ART | 0.01 | 0.01 | 2.78 | < 0.01 |

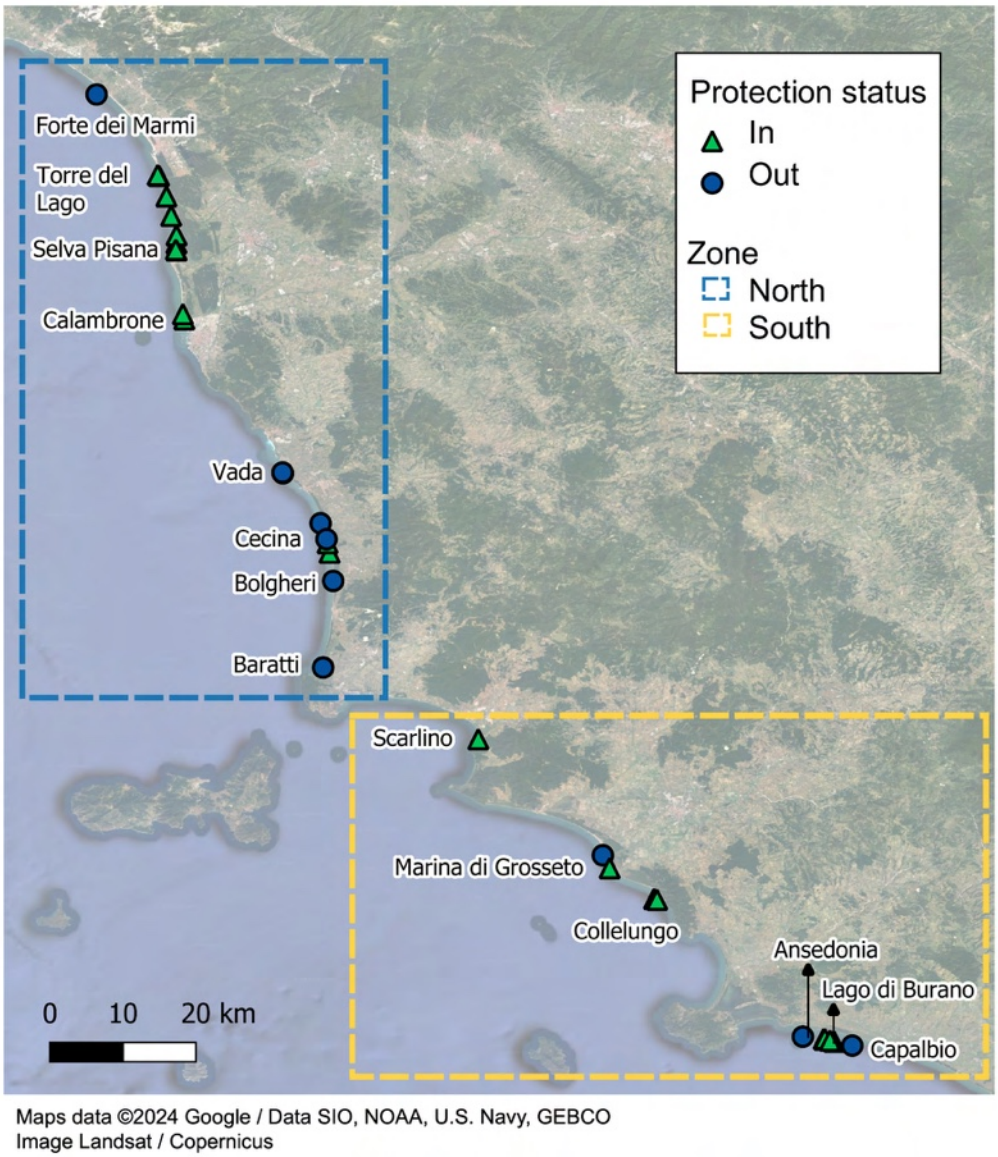


**Fig. S1.** Local Contributions to Beta Diversity for the plots in the study area, computed separately for the North and the South of the region, and colored according to the protection status. Only plots with a significant LCBD value ($p < 0.05$) are shown. Image source: Google Earth 2024. Figure adapted from the published version of Chapter 1 (colors modified).

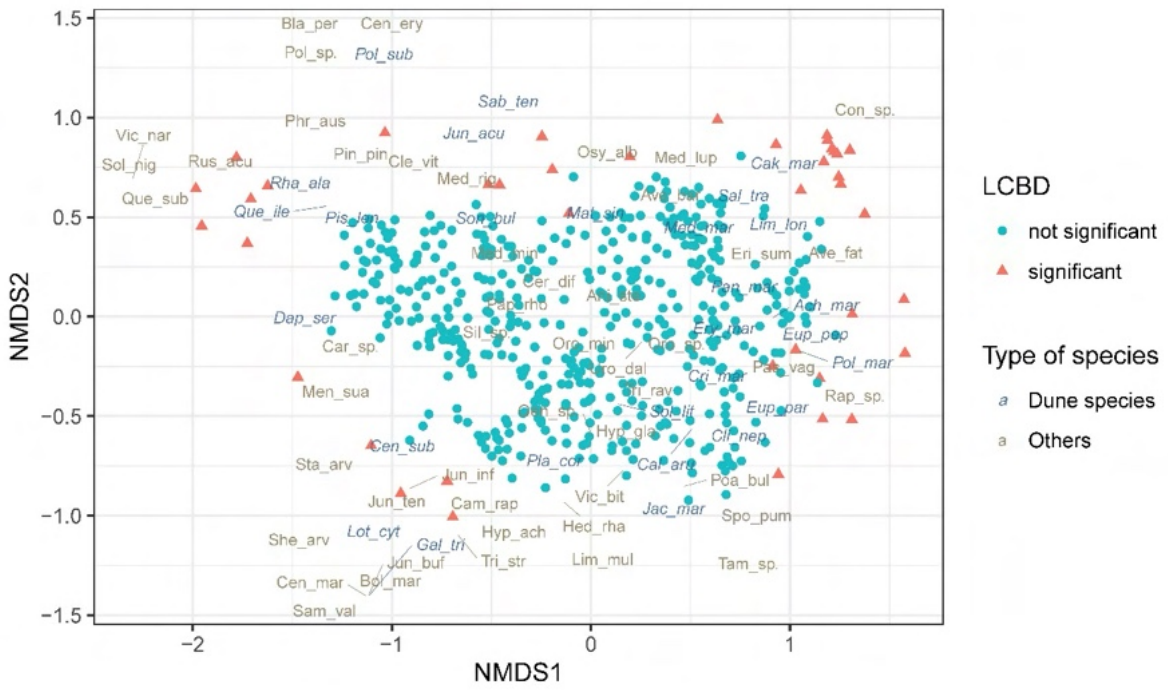


**Fig. S2.** Output of NMDS ordination, derived from Bray-Curtis similarity matrix based on log-transformed species abundances (stress = 0.18). Sites were colored according to the significance of their LCBD values. Site n. 472 was removed from the plot for graphical reasons.

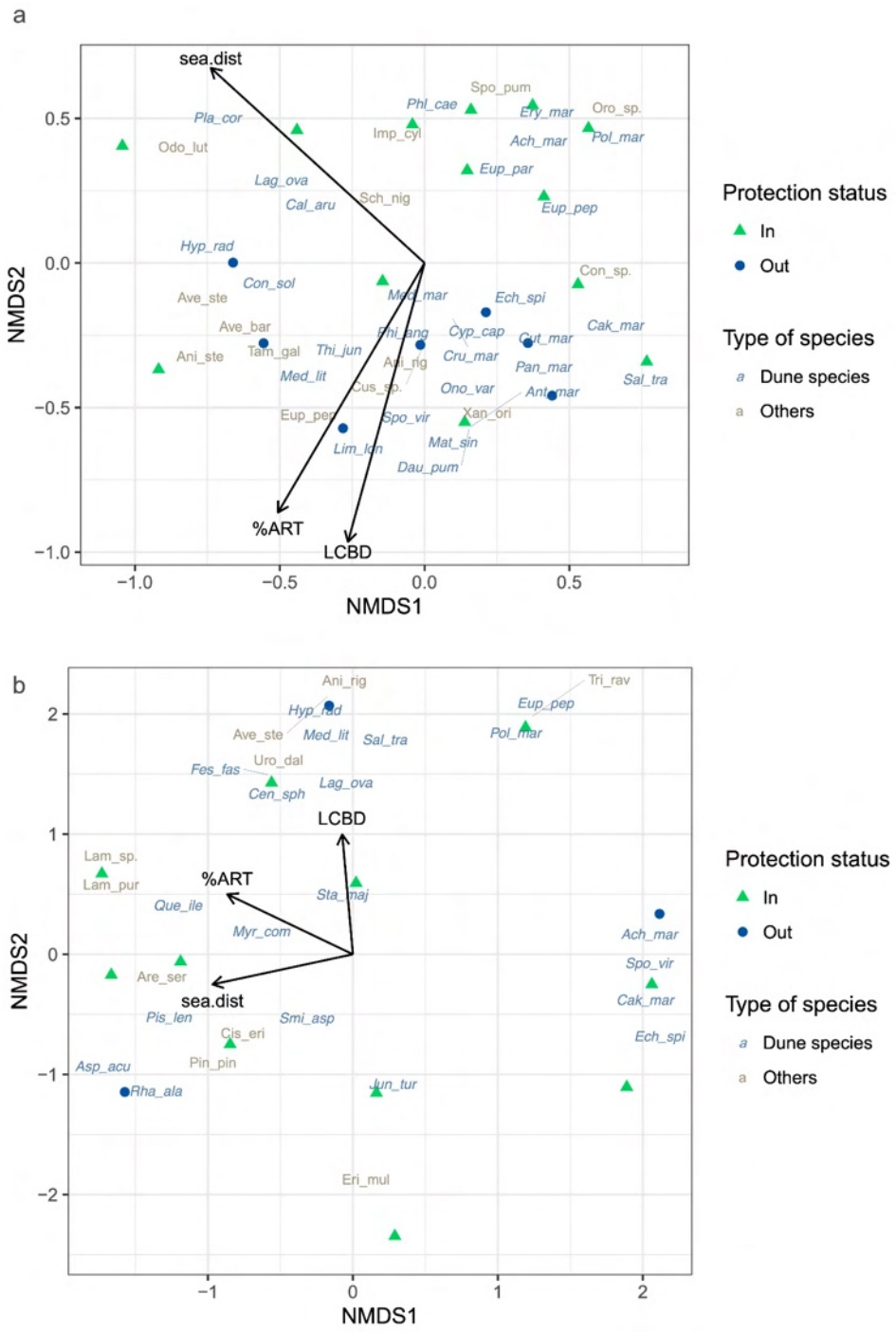


**Fig. S3.** Output of NMDS ordination, derived from Bray-Curtis similarity matrix based on log-transformed species abundances, for the plots with significant LCBD values computed separately for the Northern (a; stress = 0.09) and Southern (b; stress = 0.25) parts of the region. Plots are colored according to the protection status. Species names were abbreviated as reported in Table S1. Figure adapted from the published version of Chapter 1 (colors modified).

## Supplementary materials to Chapter 2

**Table S1.** Indicator species for the Annex I habitats obtained from expert classification.

| Habitat | Indicator Species | IndVal | p value |
|---|---|---|---|
| 1210 | *Salsola tragus* | 0.97 | 0.01** |
| | *Cakile maritima* | 0.94 | 0.01** |
| 2110 | *Thinopyrum junceum* | 0.86 | 0.01** |
| | *Polygonum maritimum* | 0.53 | 0.01* |
| | *Achillea maritima* | 0.48 | 0.04* |
| | *Sporobolus pumilus* | 0.45 | 0.05* |
| 2120 | *Calamagrostis arenaria* subsp. *arundinacea* | 0.99 | 0.01** |
| 2210 | *Helichrysum stoechas* | 0.82 | 0.01* |
| 2230 | *Festuca fasciculata* | 0.82 | 0.01** |
| | *Marcus-kochia ramosissima* | 0.79 | 0.01** |
| | *Lagurus ovatus* | 0.71 | 0.01** |
| | *Cerastium glomeratum* | 0.70 | 0.01** |
| | *Phleum arenarium* subsp. *caesium* | 0.68 | 0.01* |
| | *Medicago littoralis* | 0.58 | 0.02* |
| | *Lomelosia rutifolia* | 0.55 | 0.01* |
| | *Silene canescens* | 0.50 | 0.03* |
| 2250 | *Juniperus macrocarpa* | 1.00 | 0.01** |
| | *Smilax aspera* | 0.67 | 0.01* |
| | *Rubia peregrina* | 0.64 | 0.02* |

**Table S2.** Indicator species for the EUNIS habitats obtained from EUNIS Expert System.

| Habitat | Indicator Species | IndVal | p value |
|---|---|---|---|
| N12 | *Cakile maritima* | 0.95 | 0.01** |
| | *Salsola tragus* | 0.87 | 0.01** |
| | *Euphorbia peplis* | 0.51 | 0.03* |
| N14 | *Calamagrostis arenaria* subsp. *arundinacea* | 0.82 | 0.01** |
| | *Echinophora spinosa* | 0.66 | 0.02* |
| | *Euphorbia paralias* | 0.63 | 0.01** |
| | *Eryngium maritimum* | 0.55 | 0.05* |
| N16 | *Festuca fasciculata* | 0.76 | 0.01** |
| | *Lomelosia rutifolia* | 0.75 | 0.01** |
| | *Cerastium glomeratum* | 0.66 | 0.01** |
| | *Marcus-kochia ramosissima* | 0.58 | 0.01** |
| | *Medicago littoralis* | 0.55 | 0.04* |
| | *Silene canescens* | 0.55 | 0.02* |
| | *Phleum arenarium* subsp. *caesium* | 0.51 | 0.03* |
| N1B | *Juniperus macrocarpa* | 1.00 | 0.01** |
| | *Smilax aspera* | 0.76 | 0.01** |
| | *Rubia peregrina* | 0.76 | 0.01** |
| | *Pinus pinaster* | 0.57 | 0.01** |
| | *Pistacia lentiscus* | 0.56 | 0.01** |
| | *Rubus ulmifolius* | 0.50 | 0.01* |
| | *Brachypodium sylvaticum* | 0.41 | 0.01* |
| | *Quercus ilex* | 0.41 | 0.03* |
| | *Teucrium flavum* subsp. *flavum* | 0.41 | 0.03* |

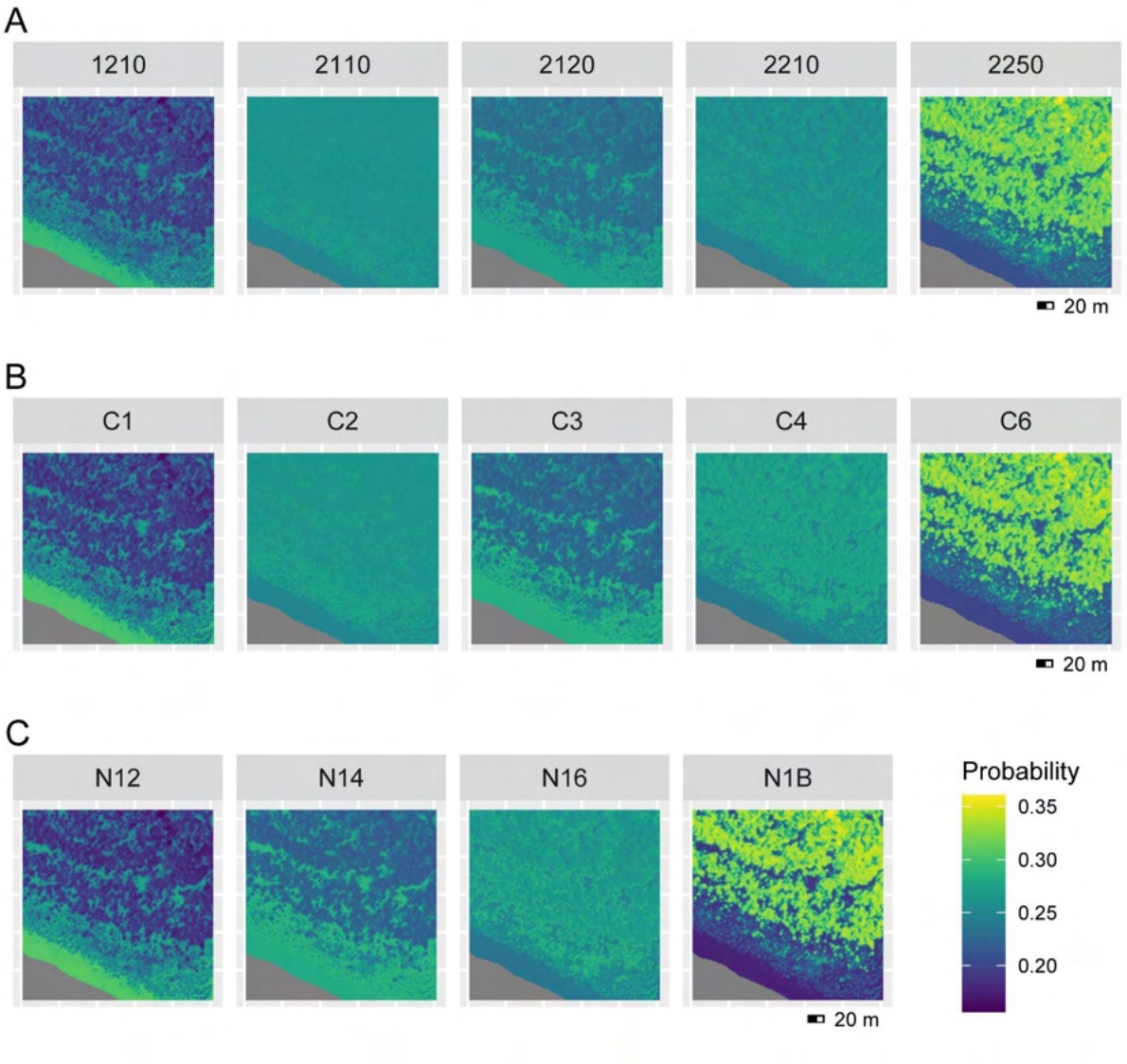


**Fig. S1.** Close-up of the fuzzy Spectral Angle Mapper classified maps in a portion of the Maremma Park. The represented classes correspond to expert-classified Annex I habitats (A), clusters obtained from noise clustering (B), and EUNIS habitats (C).

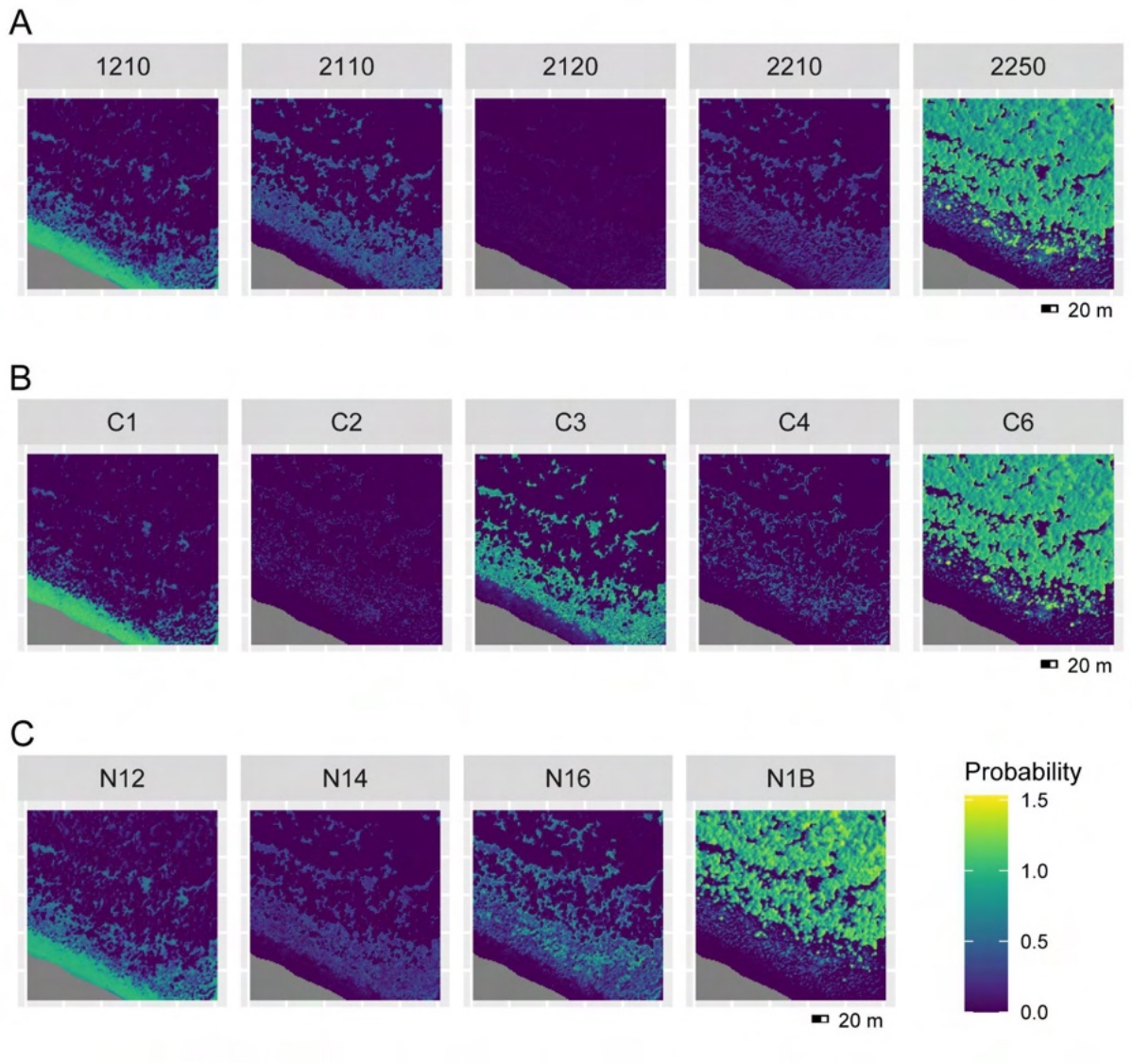


**Fig. S2.** Close-up of the fuzzy Multiple Endmember Spectral Mixture Analysis classified maps in a portion of the Maremma Park. The represented classes correspond to expert-classified Annex I habitats (A), clusters obtained from noise clustering (B), and EUNIS habitats (C).

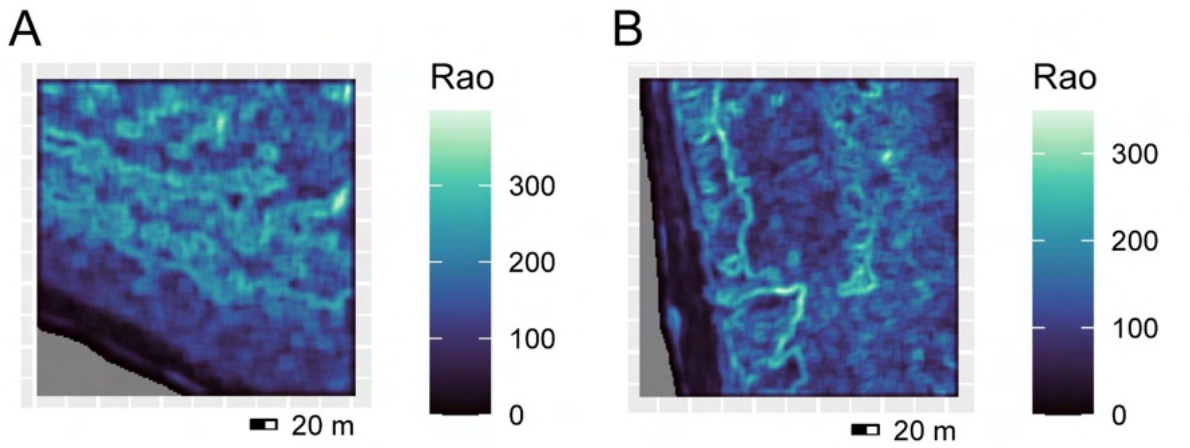


**Fig. S3.** Close-up of two areas: one more heterogeneous in the Maremma Park (A), and the other more homogeneous in the Migliarino-San Rossore-Massaciuccoli Park (B). For each area, a map of spectral Rao heterogeneity (calculated in a moving window of 7 x 7 pixels) is represented.

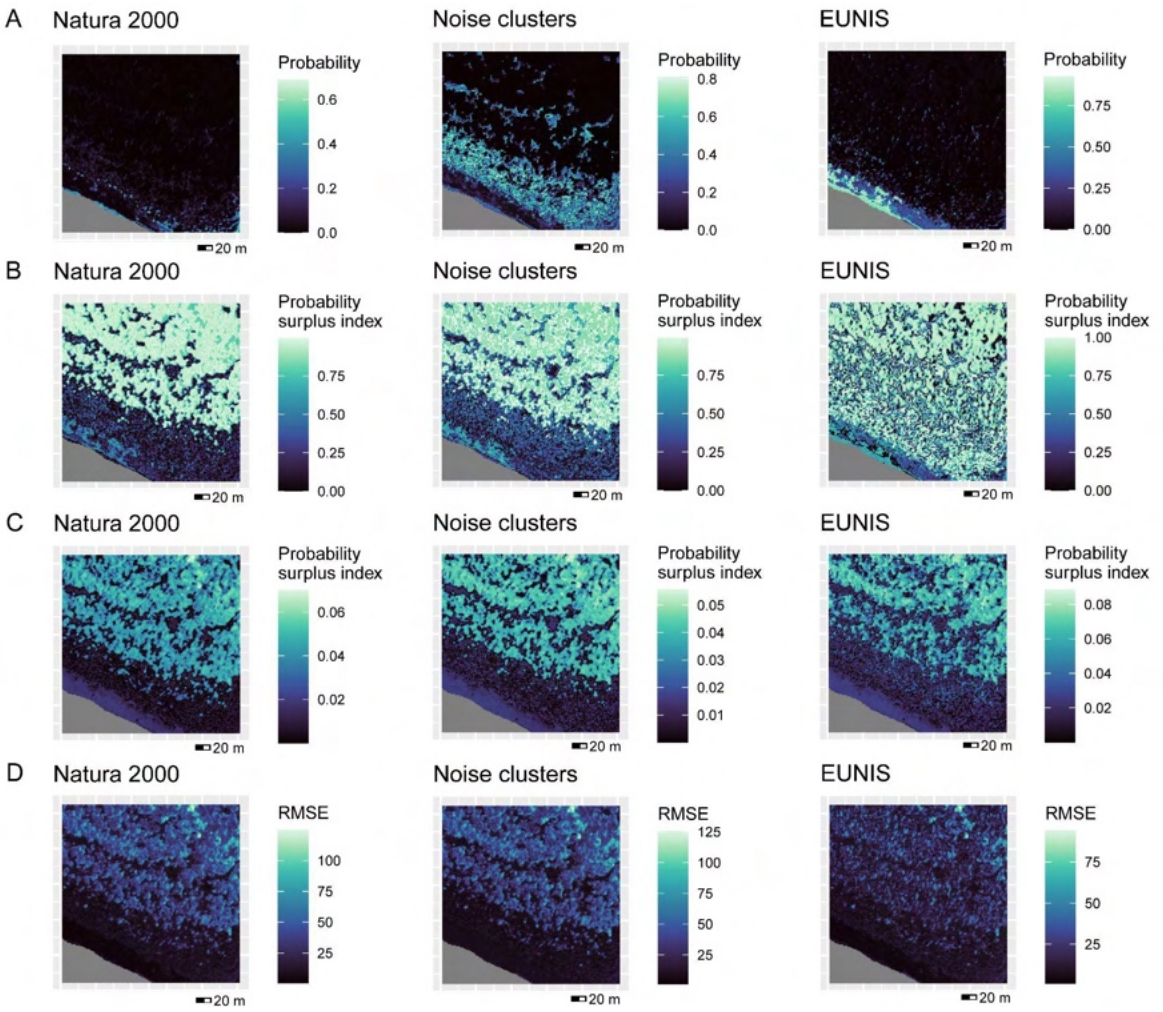


**Fig. S4.** Maps of classification uncertainty for a portion of the Maremma Park (represented in Fig. 6A). Uncertainty was measured as the probability of the dominant class for the crisp Random Forest classification (A), as the probability surplus index for the fuzzy Random Forest classification (B) and the Spectral Angle Mapper (C), and as the Root Mean Square Error (RMSE) for the Multiple Endmember Spectral Mixture Analysis classification (D). The left column displays maps of Annex I habitats, the middle column displays clusters obtained from noise clustering and the right column EUNIS habitats.

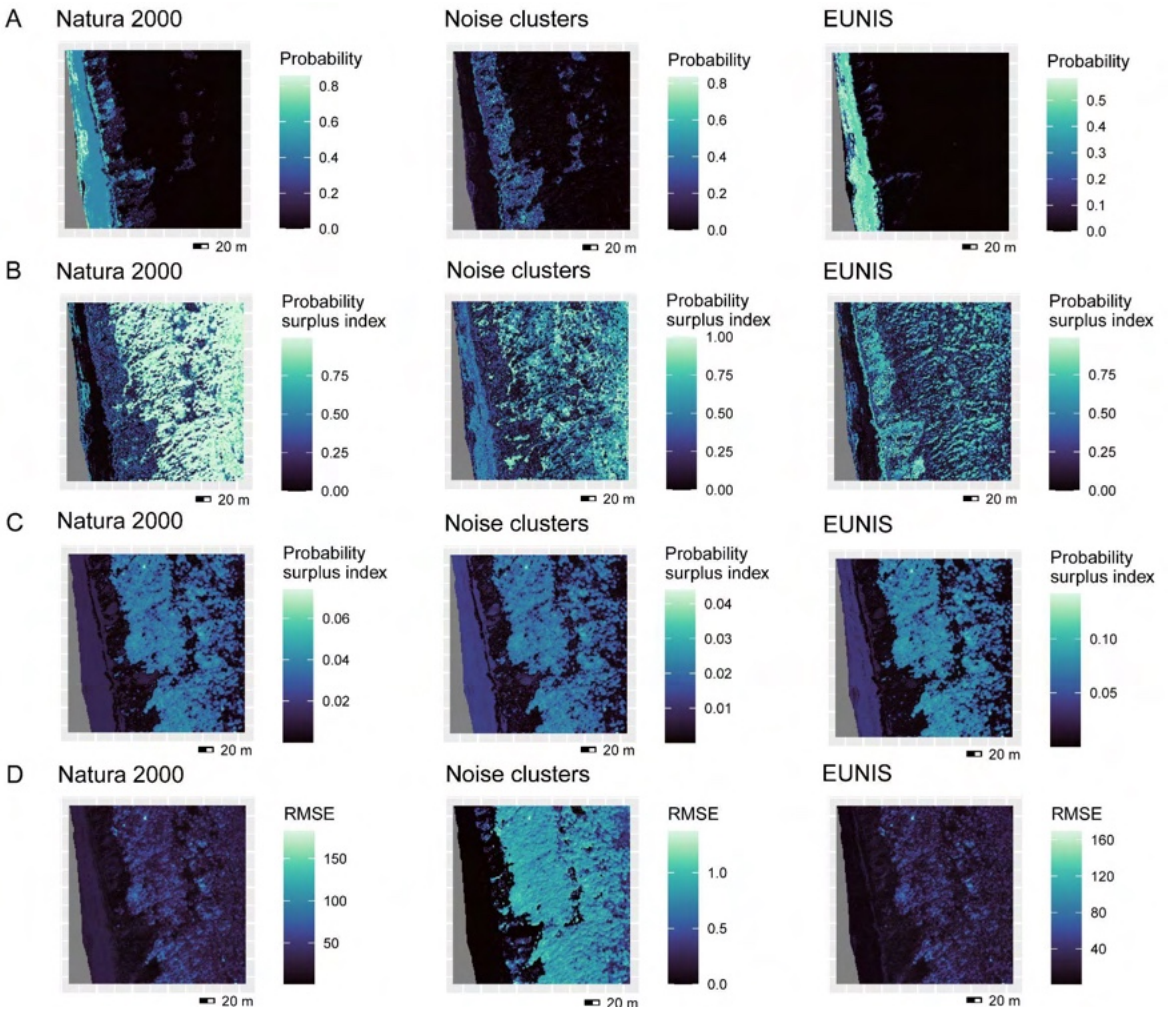


**Fig. S5.** Maps of classification uncertainty for a portion of the Migliarino-San Rossore-Massaciuccoli Park (represented in Fig. 6D). Uncertainty was measured as the probability of the dominant class for the crisp Random Forest classification (A), as the probability surplus index for the fuzzy Random Forest classification (B) and the Spectral Angle Mapper (C), and as the Root Mean Square Error (RMSE) for the Multiple Endmember Spectral Mixture Analysis classification (D). The left column displays maps of Annex I habitats, the middle column displays clusters obtained from noise clustering and the right column EUNIS habitats.

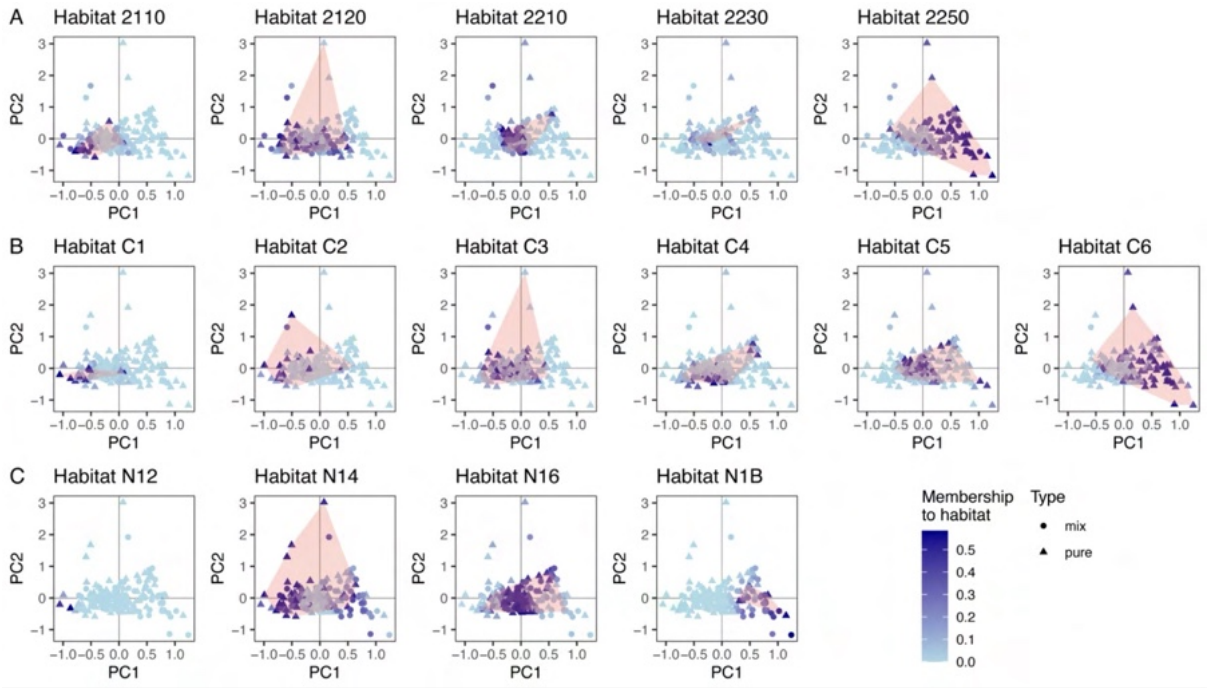


**Fig. S6.** Principal component analysis of the field-sampled plots on coastal dune habitats in the Migliarino-San Rossore-Massaciuccoli Park based on their spectral characteristics. Plots have different shapes depending on their being pure or mixed and are colored according to their probability of membership to each habitat in the Habitats Directive classification (A), noise clustering (B) and EUNIS classification (C). In each biplot, the red polygon indicates plots identified as belonging to the specific habitat according to the habitat classification.

## Supplementary materials to Chapter 3

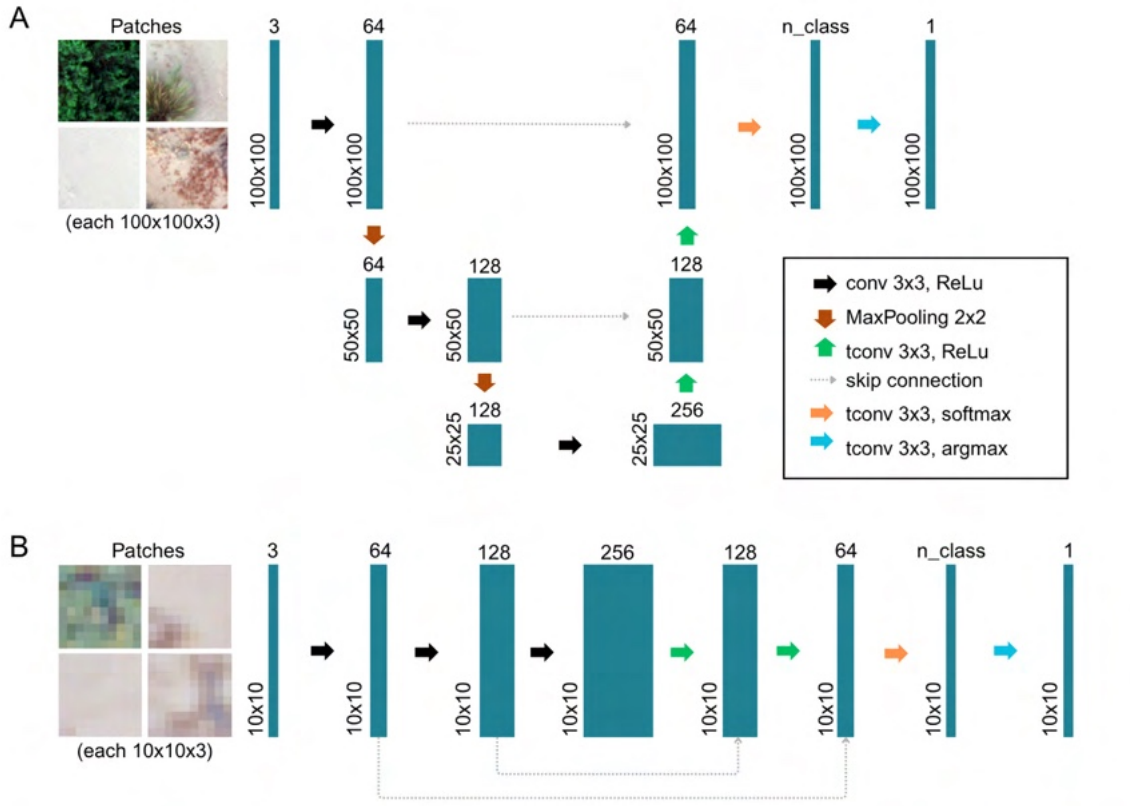


**Fig. S1.** Scheme of the CNN architecture used in this study for the UAV dataset (A) and for the other datasets (B). Reported patch sizes correspond to those used in CNN-01 (A) and CNN-03 (B).

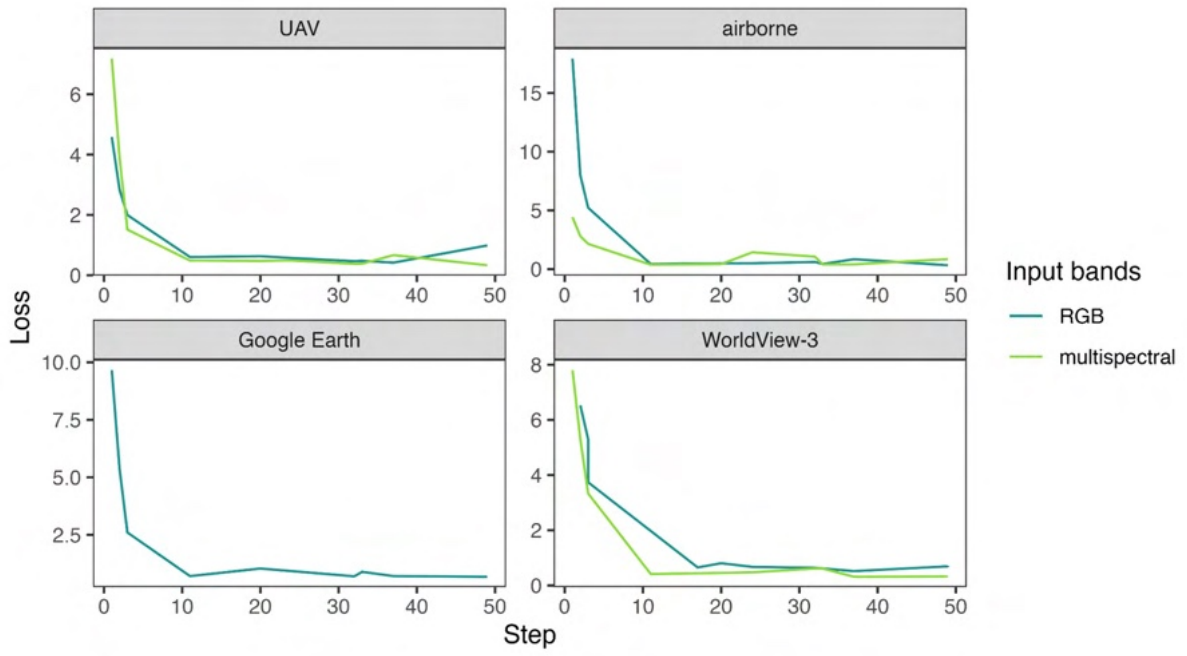


**Fig. S2.** Validation loss of CNN models trained on different datasets across learning epochs.

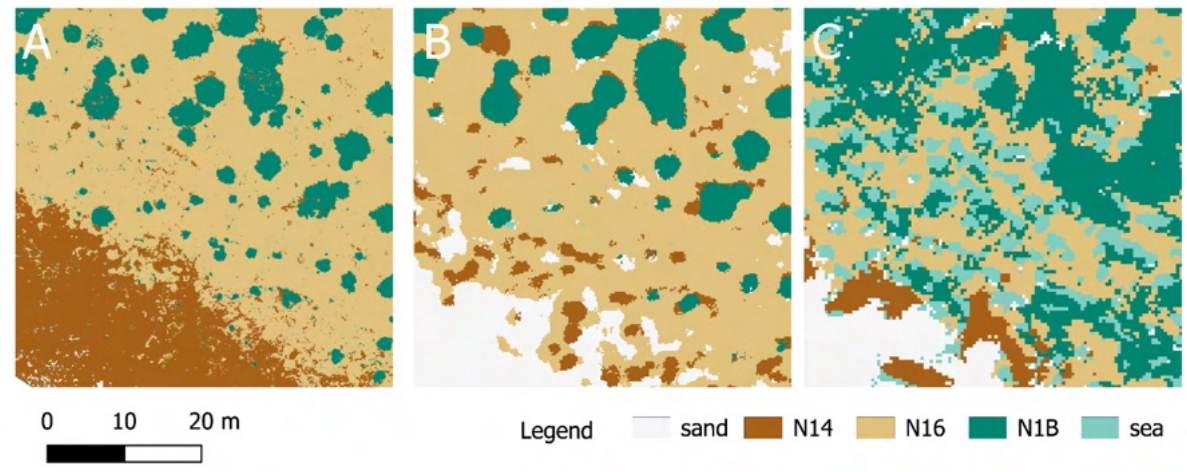


**Fig. S3.** Close-up views of the habitat maps produced through CNN segmentation of multispectral imagery from three datasets: UAV (A), airborne (B), and WorldView-3 (C).

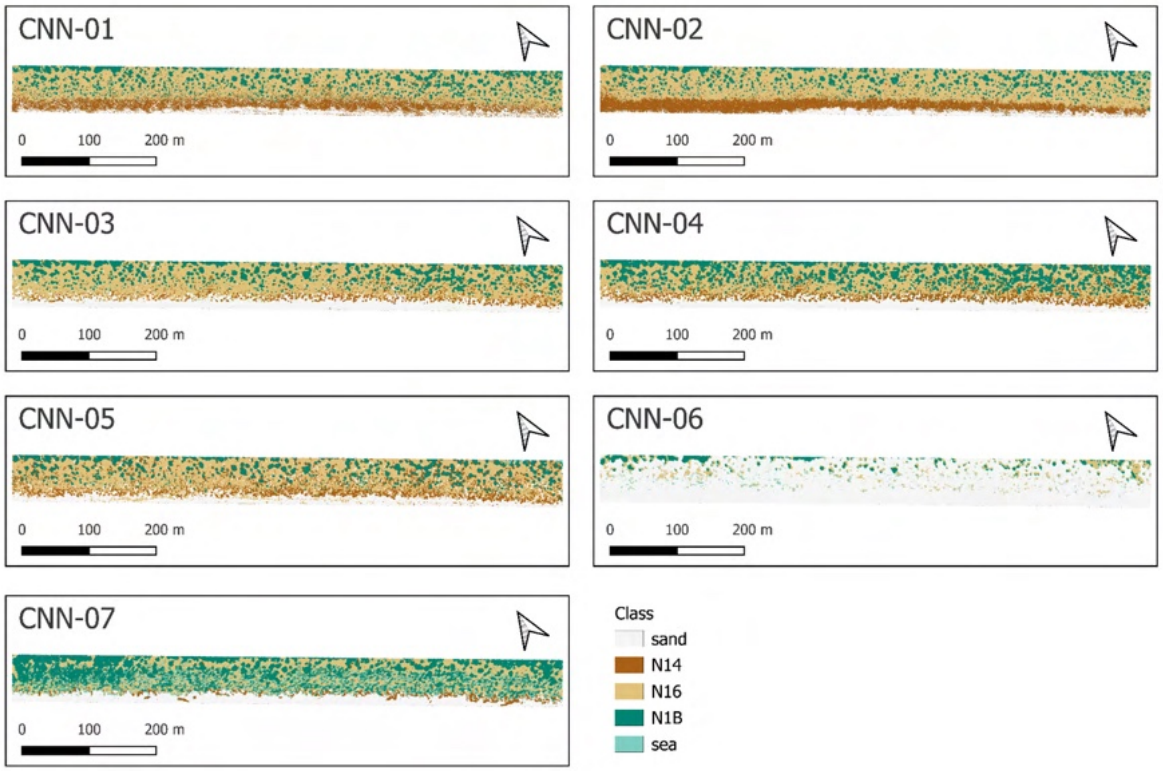


**Fig. S4.** Habitat maps of the whole study area produced from CNN models trained on different datasets.

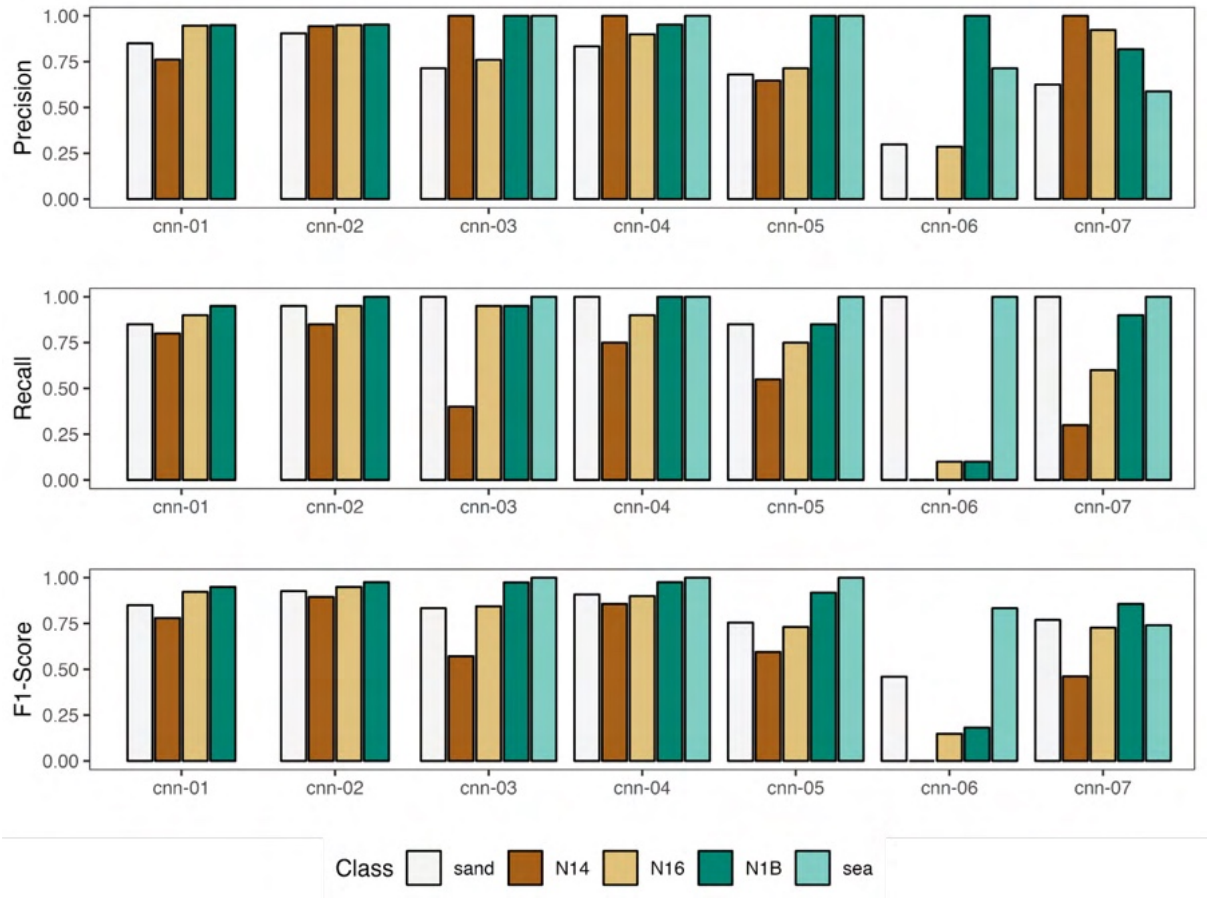


**Fig. S6.** Class-specific accuracy metrics for each CNN model: precision (i.e., proportion of true positives over all classified positives), recall (i.e., proportion of true positives over all actual positives) and F1-score (i.e., harmonic mean of precision and recall).

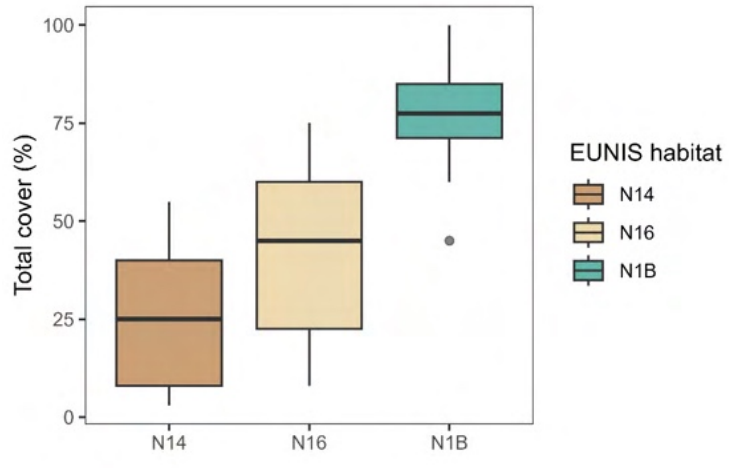

**Fig. S7.** Boxplot of the total vegetation cover recorded in the field-surveyed plots, assigned to three EUNIS habitats: shifting dunes (N14), dune grasslands (N16), and dune scrub (N1B).

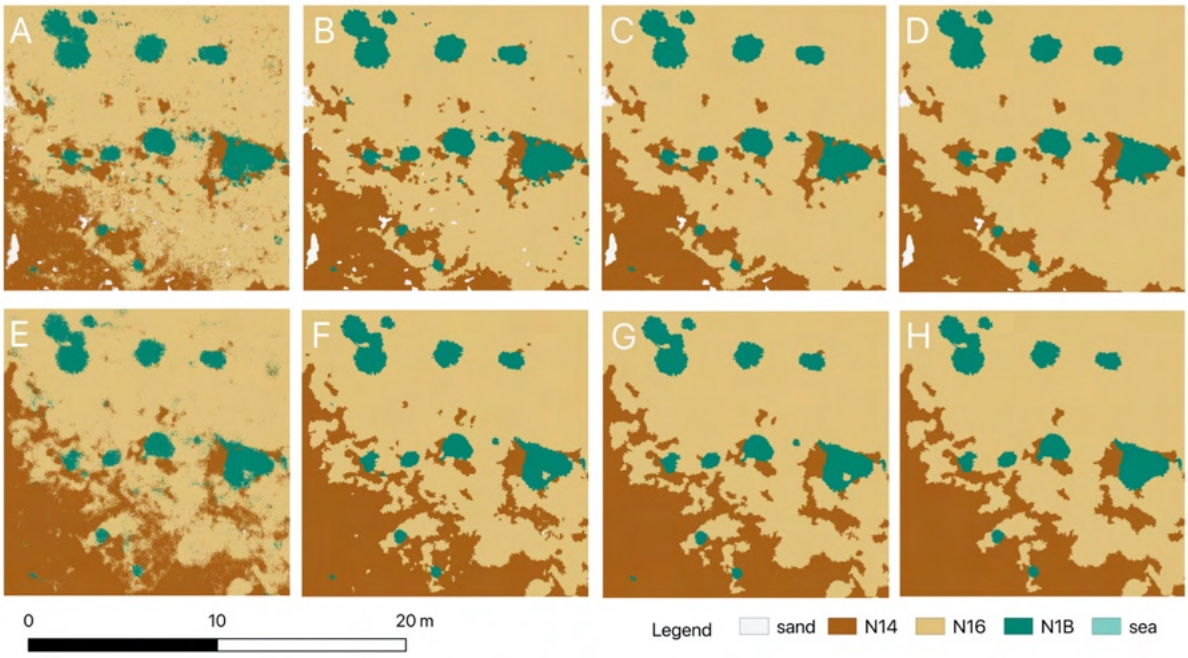


**Fig. S8.** Close-up views of the habitat maps produced from CNN-01 (A-D) and CNN-02 (E-H). The panels represent the output map before (A, E) and after (B-D, F-H) a post-processing step, consisting in the application of a sieve filter removing patches with < 25 pixels (B, F), < 100 pixels (C, G), and < 250 pixels (D, H).

**Table S1.** Confusion matrices for CNN models. Real ground truth classes are reported on the rows, predicted values are reported on the columns. Values on the diagonal represent correct classifications.

**CNN-01**

| | sand | N14 | N16 | N1B |
|---|---|---|---|---|
| sand | 17 | 3 | . | . |
| N14 | 3 | 16 | 1 | . |
| N16 | . | 1 | 18 | 1 |
| N1B | . | 1 | . | 19 |

**CNN-02**

| | sand | N14 | N16 | N1B |
|---|---|---|---|---|
| sand | 17 | 1 | . | . |
| N14 | 2 | 17 | 1 | . |
| N16 | . | . | 19 | 1 |
| N1B | . | . | . | 20 |

**CNN-03**

| | sand | N14 | N16 | N1B | sea |
|---|---|---|---|---|---|
| sand | 20 | . | . | . | . |
| N14 | 7 | 8 | 5 | . | . |
| N16 | 1 | . | 19 | . | . |
| N1B | . | . | 1 | 19 | . |
| sea | . | . | . | . | 20 |

**CNN-04**

| | sand | N14 | N16 | N1B | sea |
|---|---|---|---|---|---|
| sand | 20 | . | . | . | . |
| N14 | 3 | 15 | 2 | . | . |
| N16 | 1 | . | 18 | 1 | . |
| N1B | . | . | . | 20 | . |
| sea | . | . | . | . | 20 |

**CNN-05**

| | sand | N14 | N16 | N1B | sea |
|---|---|---|---|---|---|
| sand | 17 | . | 3 | . | . |
| N14 | 6 | 11 | 3 | . | . |
| N16 | 2 | 3 | 15 | . | . |
| N1B | . | 3 | . | 17 | . |
| sea | . | . | . | . | 20 |

**CNN-06**

| | sand | N14 | N16 | N1B | sea |
|---|---|---|---|---|---|
| sand | 20 | . | . | . | . |
| N14 | 20 | . | . | . | . |
| N16 | 16 | . | 2 | . | 2 |
| N1B | 11 | . | 5 | 2 | 2 |
| sea | . | . | . | . | 10 |

**CNN-07**

| | sand | N14 | N16 | N1B | sea |
|---|---|---|---|---|---|
| sand | 20 | . | . | . | . |
| N14 | 10 | 6 | 1 | . | 3 |
| N16 | . | . | 12 | 4 | 4 |
| N1B | 2 | . | . | 18 | . |
| sea | . | . | . | . | 10 |

**Table S2.** Percentage cover of each class in the maps of the study area produced by the CNN models trained on different datasets.

| CNN | sand (%) | N14 (%) | N16 (%) | N1B (%) | sea (%) |
|---|---|---|---|---|---|
| CNN-01 | 17.76 | 19.79 | 50.19 | 18.24 | - |
| CNN-02 | 10.13 | 24.42 | 47.71 | 17.73 | - |
| CNN-03 | 22.01 | 9.09 | 51.15 | 17.57 | 0.16 |
| CNN-04 | 20.11 | 13.44 | 40.77 | 25.49 | 0.18 |
| CNN-05 | 19.03 | 17.49 | 48.62 | 14.61 | 0.24 |
| CNN-06 | 85.05 | 0.02 | 7.66 | 4.25 | 3.01 |
| CNN-07 | 19.84 | 4.18 | 28.93 | 36.64 | 10.39 |

**Table S3.** Accuracy metrics for habitat maps derived from UAV imagery, before and after applying post-processing sieve filters (25, 100, 250 pixels).

| CNN | sieve | overall accuracy | F1-Score | | | |
|---|---|---|---|---|---|---|
| | | | sand | N14 | N16 | N1B |
| CNN-01 | no | 0.88 | 0.85 | 0.78 | 0.92 | 0.95 |
| | 25 | 0.90 | 0.90 | 0.84 | 0.93 | 0.92 |
| | 100 | 0.90 | 0.90 | 0.84 | 0.93 | 0.92 |
| | 250 | 0.90 | 0.90 | 0.84 | 0.93 | 0.92 |
| CNN-02 | no | 0.94 | 0.93 | 0.89 | 0.95 | 0.98 |
| | 25 | 0.94 | 0.93 | 0.90 | 0.97 | 0.95 |
| | 100 | 0.94 | 0.93 | 0.90 | 0.97 | 0.95 |
| | 250 | 0.94 | 0.93 | 0.92 | 0.95 | 0.95 |

## Supplementary materials to Chapter 4

**Table S1.** List of areas of interest (AOIs), with centroid coordinates and the date of the corresponding image downloaded from Google Earth.

| AOI | Region | Locality | Lat | Lon | Image date |
|---|---|---|---|---|---|
| cam_00 | Campania | Lago Patria | 40.91710 | 14.02529 | 06-06-22 |
| cam_01 | Campania | Licola | 40.85380 | 14.05069 | 09-04-21 |
| cam_02 | Campania | Licola | 40.84560 | 14.05072 | 09-04-21 |
| cam_03 | Campania | Licola | 40.83740 | 14.05071 | 09-04-21 |
| cam_04 | Campania | Licola | 40.82921 | 14.05071 | 09-04-21 |
| cam_05 | Campania | Lago Fusaro | 40.82122 | 14.05071 | 09-04-21 |
| emi_00 | Emilia-Romagna | Bardello | 44.53468 | 12.23689 | 01-06-23 |
| emi_01 | Emilia-Romagna | Lido di Spina | 44.64324 | 12.25721 | 11-06-23 |
| emi_02 | Emilia-Romagna | Lido di Volano | 44.80694 | 12.27630 | 01-06-24 |
| laz_00 | Lazio | Tarquinia-Pescia | 42.37411 | 11.46163 | 02-07-19 |
| laz_01 | Lazio | Tarquinia-Pescia | 42.37050 | 11.47273 | 02-07-19 |
| laz_02 | Lazio | Tarquinia-Pescia | 42.36697 | 11.48375 | 02-07-19 |
| laz_03 | Lazio | Tarquinia-Pescia | 42.31629 | 11.59432 | 02-07-19 |
| laz_04 | Lazio | Tarquinia-Pescia | 42.30908 | 11.60870 | 02-07-19 |
| laz_05 | Lazio | Tarquinia-Pescia | 42.29989 | 11.62544 | 02-07-19 |
| laz_06 | Lazio | Tarquinia-Pescia | 42.28873 | 11.64290 | 02-07-19 |
| laz_07 | Lazio | Lido di Maccarese | 41.87160 | 12.17883 | 26-04-18 |
| laz_08 | Lazio | Coccia di Morto | 41.80409 | 12.21910 | 26-04-18 |
| laz_09 | Lazio | Coccia di Morto | 41.79675 | 12.22254 | 26-04-18 |
| laz_10 | Lazio | Coccia di Morto | 41.78870 | 12.22456 | 26-04-18 |
| laz_11 | Lazio | Coccia di Morto | 41.78112 | 12.22630 | 26-04-18 |
| laz_12 | Lazio | Capocotta (Ostia) | 41.68254 | 12.38170 | 26-04-18 |
| laz_13 | Lazio | Capocotta (Ostia) | 41.67573 | 12.38957 | 26-04-18 |
| laz_14 | Lazio | Capocotta (Ostia) | 41.66890 | 12.39870 | 26-04-18 |
| laz_15 | Lazio | Capocotta (Ostia) | 41.66324 | 12.40842 | 26-04-18 |
| laz_16 | Lazio | Capocotta (Ostia) | 41.65343 | 12.42260 | 26-04-18 |
| laz_17 | Lazio | Tor San Lorenzo | 41.55665 | 12.53331 | 26-04-18 |
| laz_18 | Lazio | Tor San Lorenzo | 41.54562 | 12.54384 | 26-04-18 |
| laz_19 | Lazio | Tor San Lorenzo | 41.52889 | 12.55883 | 26-04-18 |
| laz_20 | Lazio | Tor San Lorenzo | 41.51352 | 12.57308 | 26-04-18 |
| laz_21 | Lazio | Torre Astura | 41.42383 | 12.74239 | 26-04-18 |
| laz_22 | Lazio | Torre Astura | 41.41875 | 12.75268 | 26-04-18 |
| laz_23 | Lazio | Circeo | 41.39775 | 12.89190 | 25-07-19 |
| laz_24 | Lazio | Circeo | 41.39316 | 12.90262 | 25-07-19 |
| laz_25 | Lazio | Circeo | 41.38331 | 12.91954 | 25-07-19 |
| laz_26 | Lazio | Circeo | 41.37439 | 12.93199 | 25-07-19 |
| laz_27 | Lazio | Circeo | 41.35084 | 12.96576 | 25-07-19 |
| laz_28 | Lazio | Circeo | 41.33083 | 12.98627 | 25-07-19 |
| laz_29 | Lazio | Circeo | 41.32358 | 12.99197 | 25-07-19 |

| | | | | | |
|---|---|---|---|---|---|
| laz_30 | Lazio | Circeo | 41.31534 | 12.99977 | 25-07-19 |
| laz_31 | Lazio | Circeo | 41.30434 | 13.00677 | 25-07-19 |
| laz_32 | Lazio | Circeo | 41.29712 | 13.01310 | 25-07-19 |
| laz_33 | Lazio | Circeo | 41.28331 | 13.02012 | 25-07-19 |
| laz_34 | Lazio | Circeo | 41.27593 | 13.02549 | 25-07-19 |
| laz_35 | Lazio | Circeo | 41.26608 | 13.02962 | 25-07-19 |
| laz_36 | Lazio | Circeo | 41.25251 | 13.03602 | 25-07-19 |
| laz_37 | Lazio | Sperlonga | 41.29071 | 13.33931 | 13-06-22 |
| laz_38 | Lazio | Sperlonga | 41.27611 | 13.39272 | 13-06-22 |
| mol_00 | Molise | A Nord di Termoli | 42.03891 | 14.84519 | 12-04-22 |
| mol_01 | Molise | A Nord di Termoli | 42.03456 | 14.85625 | 12-04-22 |
| mol_02 | Molise | A Nord di Termoli | 42.03044 | 14.86660 | 12-04-22 |
| mol_03 | Molise | A Nord di Termoli | 42.02706 | 14.88143 | 12-04-22 |
| mol_04 | Molise | A Nord di Termoli | 42.02172 | 14.89816 | 12-04-22 |
| mol_05 | Molise | A Nord di Termoli | 42.01477 | 14.93828 | 12-04-22 |
| mol_06 | Molise | A Nord di Termoli | 42.01106 | 14.95788 | 12-04-22 |
| mol_07 | Molise | A Sud di Termoli | 41.99100 | 15.00570 | 29-06-16 |
| mol_08 | Molise | A Sud di Termoli | 41.96608 | 15.04562 | 29-06-16 |
| mol_09 | Molise | A Sud di Termoli | 41.94695 | 15.07098 | 29-06-16 |
| mol_10 | Molise | A Sud di Termoli | 41.93646 | 15.09104 | 29-06-16 |
| mol_11 | Molise | A Sud di Termoli | 41.93318 | 15.10170 | 29-06-16 |
| mol_12 | Molise | A Sud di Termoli | 41.93026 | 15.11964 | 29-06-16 |
| mol_13 | Molise | A Sud di Termoli | 41.92667 | 15.13317 | 29-06-16 |
| sar_00 | Sardegna | Sa Mesa Longa | 40.04751 | 8.40075 | 14-05-22 |
| sar_01 | Sardegna | Sa Rocca Tunda | 40.04324 | 8.41052 | 14-05-22 |
| sar_02 | Sardegna | Sa Rocca Tunda | 40.04324 | 8.42196 | 14-05-22 |
| sar_03 | Sardegna | Platamona | 40.81848 | 8.47421 | 28-04-22 |
| sar_04 | Sardegna | Platamona | 40.81996 | 8.50067 | 28-04-22 |
| sar_05 | Sardegna | Platamona | 40.82991 | 8.55913 | 28-04-22 |
| sar_06 | Sardegna | Platamona | 40.83217 | 8.56995 | 28-04-22 |
| sar_07 | Sardegna | Capo Testa | 41.23669 | 9.16166 | 11-05-22 |
| sar_08 | Sardegna | Spiaggia del Liscia | 41.19253 | 9.31562 | 03-07-23 |
| sar_09 | Sardegna | La Maddalena | 41.24350 | 9.39981 | 21-02-24 |
| sic_00 | Sicilia | Capo Feto | 37.65911 | 12.52855 | 24-02-25 |
| sic_01 | Sicilia | Puzziteddu | 37.56159 | 12.67949 | 01-02-23 |
| sic_02 | Sicilia | Foce Belice | 37.58494 | 12.85936 | 28-03-24 |
| sic_03 | Sicilia | Porto Palo | 37.57621 | 12.91221 | 18-10-23 |
| sic_04 | Sicilia | Vittoria | 37.57618 | 12.92231 | 18-10-23 |
| sic_05 | Sicilia | Roccazzelle | 37.09546 | 14.16021 | 18-01-24 |
| sic_06 | Sicilia | Passo Marinaro | 36.85921 | 14.46313 | 03-03-22 |
| sic_07 | Sicilia | Punta Braccetto | 36.82711 | 14.45935 | 03-03-22 |
| sic_15 | Sicilia | Simeto | 37.34771 | 15.09135 | 22-05-22 |
| sic_16 | Sicilia | Simeto | 37.37932 | 15.08745 | 02-03-22 |
| sic_17 | Sicilia | Simeto | 37.38706 | 15.08736 | 02-02-24 |
| sic_18 | Sicilia | Simeto | 37.39921 | 15.08717 | 02-02-24 |
| sic_19 | Sicilia | Simeto | 37.41092 | 15.08761 | 12-03-21 |
| sic_20 | Sicilia | Simeto | 37.41854 | 15.08767 | 02-02-24 |
| sic_21 | Sicilia | Simeto | 37.43025 | 15.08748 | 02-02-24 |

| | | | | | |
|---|---|---|---|---|---|
| sic_22 | Sicilia | Simeto | 37.44022 | 15.08730 | 02-02-24 |
| tos_00 | Toscana | Collelungo | 42.63581 | 11.07292 | 26-04-23 |
| tos_02 | Toscana | Torre del Lago | 43.84409 | 10.24844 | 13-06-19 |
| tos_03 | Toscana | Torre del Lago | 43.83605 | 10.25120 | 13-06-19 |
| tos_04 | Toscana | Torre del Lago | 43.82804 | 10.25470 | 13-06-19 |
| tos_05 | Toscana | Torre del Lago | 43.82062 | 10.25920 | 13-06-19 |
| tos_06 | Toscana | Torre del Lago | 43.81259 | 10.26219 | 13-06-19 |
| tos_07 | Toscana | Selva Pisana | 43.80476 | 10.26451 | 13-06-19 |
| tos_08 | Toscana | Selva Pisana | 43.79651 | 10.26701 | 13-06-19 |
| tos_09 | Toscana | Selva Pisana | 43.78844 | 10.26862 | 13-06-19 |
| tos_10 | Toscana | Selva Pisana | 43.77559 | 10.27139 | 13-06-19 |
| tos_11 | Toscana | Selva Pisana | 43.76692 | 10.27280 | 13-06-19 |
| tos_12 | Toscana | Selva Pisana | 43.73925 | 10.27964 | 13-06-19 |
| tos_13 | Toscana | Selva Pisana | 43.73054 | 10.27887 | 13-06-19 |
| tos_14 | Toscana | Selva Pisana | 43.72243 | 10.28088 | 13-06-19 |
| tos_15 | Toscana | Selva Pisana | 43.71441 | 10.28091 | 13-06-19 |
| tos_16 | Toscana | Calambrone | 43.60986 | 10.29179 | 13-06-19 |
| tos_17 | Toscana | Calambrone | 43.60270 | 10.29406 | 13-06-19 |
| tos_18 | Toscana | Calambrone | 43.59467 | 10.29601 | 13-06-19 |
| tos_19 | Toscana | Rosignano | 43.37876 | 10.43809 | 13-06-19 |
| tos_20 | Toscana | Rosignano | 43.37005 | 10.44353 | 13-06-19 |
| tos_21 | Toscana | Vada | 43.34191 | 10.45676 | 13-06-19 |
| tos_22 | Toscana | Cecina | 43.25978 | 10.51898 | 05-04-22 |
| tos_23 | Toscana | Marina di Bibbona | 43.23999 | 10.52838 | 05-04-22 |
| tos_24 | Toscana | Marina di Bibbona | 43.23118 | 10.53023 | 05-04-22 |
| tos_25 | Toscana | Bolgheri | 43.21932 | 10.53388 | 05-04-22 |
| tos_26 | Toscana | Bolgheri | 43.21061 | 10.53431 | 05-04-22 |
| tos_27 | Toscana | Bolgheri | 43.20226 | 10.53543 | 05-04-22 |
| tos_28 | Toscana | Bolgheri | 43.19199 | 10.54014 | 05-04-22 |
| tos_29 | Toscana | Castagneto Carducci | 43.18326 | 10.54015 | 05-04-22 |
| tos_30 | Toscana | Castagneto Carducci | 43.17462 | 10.54014 | 05-04-22 |
| tos_31 | Toscana | Castagneto Carducci | 43.16607 | 10.54016 | 05-04-22 |
| tos_32 | Toscana | San Vincenzo | 43.15323 | 10.54234 | 05-04-22 |
| tos_33 | Toscana | San Vincenzo | 43.14467 | 10.54223 | 05-04-22 |
| tos_34 | Toscana | San Vincenzo | 43.13636 | 10.54237 | 05-04-22 |
| tos_35 | Toscana | Rimigliano | 43.04860 | 10.53060 | 05-04-22 |
| tos_36 | Toscana | Rimigliano | 43.03101 | 10.52581 | 05-04-22 |
| tos_37 | Toscana | Rimigliano | 43.02225 | 10.52353 | 05-04-22 |
| tos_41 | Toscana | Sterpaia | 42.95039 | 10.67988 | 01-04-20 |
| tos_42 | Toscana | Sterpaia | 42.94896 | 10.69129 | 01-04-20 |
| tos_43 | Toscana | Follonica | 42.93434 | 10.72881 | 01-04-20 |
| tos_58 | Toscana | Parco Maremma | 42.64501 | 11.04840 | 26-04-23 |
| tos_59 | Toscana | Parco Maremma | 42.64123 | 11.06004 | 26-04-23 |
| tos_60 | Toscana | Parco Maremma | 42.63040 | 11.08422 | 10-04-22 |
| tos_61 | Toscana | Giannella | 42.47067 | 11.18975 | 10-04-22 |
| tos_62 | Toscana | Giannella | 42.46182 | 11.18535 | 10-04-22 |
| tos_63 | Toscana | Giannella | 42.45298 | 11.18063 | 10-04-22 |
| tos_64 | Toscana | Giannella | 42.43776 | 11.16695 | 10-04-22 |

| | | | | | |
|---|---|---|---|---|---|
| tos_65 | Toscana | Feniglia | 42.41299 | 11.21620 | 29-04-22 |
| tos_66 | Toscana | Feniglia | 42.41769 | 11.22785 | 29-04-22 |
| tos_67 | Toscana | Feniglia | 42.42080 | 11.23950 | 29-04-22 |
| tos_68 | Toscana | Feniglia | 42.42279 | 11.25120 | 29-04-22 |
| tos_69 | Toscana | Feniglia | 42.42278 | 11.26284 | 29-04-22 |
| tos_70 | Toscana | Feniglia | 42.41952 | 11.27446 | 29-04-22 |
| tos_71 | Toscana | Capalbio | 42.40863 | 11.30728 | 02-07-19 |
| tos_72 | Toscana | Capalbio | 42.40546 | 11.32409 | 02-07-19 |
| tos_73 | Toscana | Capalbio | 42.40397 | 11.34101 | 02-07-19 |
| tos_74 | Toscana | Burano | 42.40191 | 11.35257 | 02-07-19 |
| tos_75 | Toscana | Burano | 42.39965 | 11.36422 | 02-07-19 |
| tos_76 | Toscana | Burano | 42.39820 | 11.37580 | 02-07-19 |
| tos_77 | Toscana | Burano | 42.39524 | 11.38728 | 02-07-19 |
| tos_78 | Toscana | Burano | 42.39029 | 11.40621 | 02-07-19 |
| tos_79 | Toscana | Burano | 42.38387 | 11.43037 | 02-07-19 |
| tos_80 | Toscana | Burano | 42.38119 | 11.44119 | 02-07-19 |
| ven_00 | Veneto | Brussa | 45.61642 | 12.92618 | 26-06-17 |
| ven_01 | Veneto | Brussa | 45.61921 | 12.93717 | 26-06-17 |
| ven_02 | Veneto | Brussa | 45.62168 | 12.94801 | 26-06-17 |
| ven_03 | Veneto | Brussa | 45.62377 | 12.95909 | 26-06-17 |
| ven_04 | Veneto | Capalonga | 45.62764 | 12.98392 | 26-06-17 |
| ven_05 | Veneto | Ca' Savio | 45.44013 | 12.45333 | 29-07-21 |
| ven_06 | Veneto | Barricata | 44.85722 | 12.47231 | 01-06-24 |
| ven_07 | Veneto | Barricata | 44.86707 | 12.47764 | 01-06-24 |
| ven_09 | Veneto | Rosolina | 45.09824 | 12.33284 | 26-07-23 |

**Table S2.** Summary accuracy metrics: overall accuracy (OA), Kappa, average precision (AP), average recall (AR) and average F1-Score (AF).

| CNN | Site | OA | Kappa | AP | AR | AF |
|---|---|---|---|---|---|---|
| cnn-01-rgb | A | 0.90 | 0.87 | 0.90 | 0.90 | 0.90 |
| cnn-01-multi | A | 0.95 | 0.93 | 0.96 | 0.95 | 0.95 |
| cnn-02-rgb | B | 0.73 | 0.60 | 0.85 | 0.73 | 0.68 |
| cnn-02-multi | B | 0.87 | 0.80 | 0.87 | 0.87 | 0.87 |
| cnn-03-rgb | AB | 0.86 | 0.81 | 0.89 | 0.88 | 0.87 |
| cnn-03-multi | AB | 0.91 | 0.88 | 0.93 | 0.93 | 0.93 |
| cnn-04-rgb | A | 0.64 | 0.55 | 0.58 | 0.64 | 0.59 |
| cnn-04-multi | A | 0.64 | 0.55 | 0.54 | 0.64 | 0.56 |
| cnn-05-rgb | B | 0.65 | 0.53 | 0.49 | 0.65 | 0.56 |
| cnn-05-multi | B | 0.70 | 0.60 | 0.61 | 0.70 | 0.63 |
| cnn-06-rgb | AB | 0.69 | 0.61 | 0.74 | 0.72 | 0.71 |
| cnn-06-multi | AB | 0.69 | 0.61 | 0.68 | 0.72 | 0.67 |
| cnn-07 | A | 0.64 | 0.55 | 0.55 | 0.64 | 0.58 |
| cnn-08 | B | 0.70 | 0.60 | 0.58 | 0.70 | 0.62 |
| cnn-09 | AB | 0.56 | 0.46 | 0.68 | 0.60 | 0.55 |
| cnn-09 | Ita | 0.38 | 0.22 | 0.36 | 0.41 | 0.31 |

**Table S3.** Class-specific accuracy metrics.

| CNN | Site | Class | Precision | Recall | F1-Score |
|---|---|---|---|---|---|
| 01-rgb | A | sand | 1.00 | 0.60 | 0.75 |
| | | N14 | 0.71 | 1.00 | 0.83 |
| | | N16 | 1.00 | 1.00 | 1.00 |
| | | N1B | 1.00 | 1.00 | 1.00 |
| 01-multi | A | sand | 1.00 | 0.80 | 0.89 |
| | | N14 | 0.83 | 1.00 | 0.91 |
| | | N16 | 1.00 | 1.00 | 1.00 |
| | | N1B | 1.00 | 1.00 | 1.00 |
| 02-rgb | B | sand | 1.00 | 0.20 | 0.33 |
| | | N14 | 0.56 | 1.00 | 0.71 |
| | | N1B | 1.00 | 1.00 | 1.00 |
| 02-multi | B | sand | 0.80 | 0.80 | 0.80 |
| | | N14 | 0.80 | 0.80 | 0.80 |
| | | N1B | 1.00 | 1.00 | 1.00 |
| 03-rgb | AB | sand | 0.86 | 0.60 | 0.71 |
| | | N14 | 0.69 | 0.90 | 0.78 |
| | | N16 | 1.00 | 1.00 | 1.00 |
| | | N1B | 1.00 | 1.00 | 1.00 |
| 03-multi | AB | sand | 0.90 | 0.90 | 0.90 |
| | | N14 | 0.82 | 0.90 | 0.86 |
| | | N16 | 1.00 | 0.90 | 0.95 |
| | | N1B | 1.00 | 1.00 | 1.00 |
| 04-rgb | A | sand | 0.63 | 1.00 | 0.77 |
| | | N14 | 0.25 | 0.40 | 0.31 |
| | | N16 | 0.00 | 0.00 | 0.00 |
| | | N1B | 1.00 | 0.80 | 0.89 |
| | | sea | 1.00 | 1.00 | 1.00 |
| 04-multi | A | sand | 0.50 | 1.00 | 0.67 |
| | | N14 | 0.00 | 0.00 | 0.00 |
| | | N16 | 0.50 | 0.20 | 0.29 |
| | | N1B | 0.71 | 1.00 | 0.83 |
| | | sea | 1.00 | 1.00 | 1.00 |
| 05-rgb | B | sand | 0.57 | 0.80 | 0.67 |
| | | N14 | 0.00 | 0.00 | 0.00 |
| | | N1B | 0.67 | 0.80 | 0.73 |
| | | sea | 0.71 | 1.00 | 0.83 |
| 05-multi | B | sand | 0.00 | 0.00 | 0.00 |
| | | N14 | 0.45 | 1.00 | 0.63 |
| | | N1B | 1.00 | 0.80 | 0.89 |
| | | sea | 1.00 | 1.00 | 1.00 |

| | | | | | |
|---|---|---|---|---|---|
| 06-rgb | AB | sand | 0.80 | 0.80 | 0.80 |
| | | N14 | 0.56 | 0.50 | 0.53 |
| | | N16 | 1.00 | 0.60 | 0.75 |
| | | N1B | 0.50 | 0.70 | 0.58 |
| | | sea | 0.83 | 1.00 | 0.91 |
| 06-multi | AB | sand | 0.53 | 0.90 | 0.67 |
| | | N14 | 0.33 | 0.10 | 0.15 |
| | | N16 | 0.89 | 0.80 | 0.84 |
| | | N1B | 0.80 | 0.80 | 0.80 |
| | | sea | 0.83 | 1.00 | 0.91 |
| 07 | A | sand | 0.00 | 0.00 | 0.00 |
| | | N14 | 0.33 | 0.60 | 0.43 |
| | | N16 | 0.75 | 0.60 | 0.67 |
| | | N1B | 0.83 | 1.00 | 0.91 |
| | | sea | 0.83 | 1.00 | 0.91 |
| 08 | B | sand | 0.00 | 0.00 | 0.00 |
| | | N14 | 0.50 | 1.00 | 0.67 |
| | | N1B | 0.83 | 1.00 | 0.91 |
| | | sea | 1.00 | 0.80 | 0.89 |
| 09 | AB | sand | 0.71 | 0.50 | 0.59 |
| | | N14 | 0.67 | 0.40 | 0.50 |
| | | N16 | 1.00 | 0.30 | 0.46 |
| | | N1B | 0.73 | 0.80 | 0.76 |
| | | sea | 0.28 | 1.00 | 0.43 |
| 10 | Ita | sand | 0.33 | 0.02 | 0.03 |
| | | N14 | 0.25 | 0.04 | 0.07 |
| | | N16 | 0.32 | 0.31 | 0.31 |
| | | N1B | 0.26 | 0.82 | 0.39 |
| | | sea | 0.64 | 0.86 | 0.73 |